

**Faculty of Science & Engineering
WA School of Mines: Minerals, Energy and Chemical
Engineering**

**A Novel Mobility Control Technique in Miscible Gas
Injection Using Direct Gas Thickening in High Pressure
and Temperature Reservoir**

Nasser Mohammed Al Hinai

**This thesis is presented for the degree of
Doctor of Philosophy**

Curtin University

January 2019

Declaration

To the best of my knowledge and belief this thesis contains no material previously published by any other person except where due acknowledgment has been made.

This thesis contains no material which has been accepted for the award of any other degree or diploma in any university.

Signature:  (Nasser Al Hinai)

Date: 25th of January 2019

Copyright

I warrant that I have obtained, where necessary, permission from the copyright owners to use any third-party copyright material reproduced in the thesis (e.g. questionnaires, artwork, unpublished letters), or to use any of my own published work (e.g. journal articles) in which the copyright is held by another party (e.g. publisher, co-author).

Signature:

A handwritten signature in Arabic script, enclosed in an oval. The signature appears to be 'Nasser Al Hinai'.

(Nasser Al Hinai)

Date: 25th of January 2019

Dedication

I would like to dedicate this thesis to my beloved parents, who have been my source of inspiration and gave me strength and self-confident to reach my goals, who continually provide their moral, spiritual, emotional, and financial support.

To my beloved wife and my children for their greatest support and patience

To my brothers, sisters, relatives, and friends who shared their words of advice, support and encouragement to finish this thesis.

To his Majesty Sultan Qaboos, building Oman renaissance.

Acknowledgements

I would like to express my sincere gratitude to my respected main **supervisor Associate Professor Ali Saeedi** and co-supervisor **Dr. Colin Wood** (Commonwealth Scientific and Industrial Research Organisation, CSIRO) for their continuous supports of my Ph.D study and related research, for their patience, motivation, and immense knowledge. The knowledge, insights and thoughtful suggestions they brought to me truly contribute to the completion of this research. Their guidance helped me in all the time of research and writing of this thesis. It is a great honour and privilege for me to do my PhD under their supervision which has opened up a new horizon of opportunity in front me to enhance the quality and applicability of my research. I feel very fortunate to have their company during my PhD journey.

I also express my deepest appreciation and grateful to Dr. Mathews Myer from CSIRO for very interesting technical discussions, insightful comments and encouragement but also for the hard questions which encouraged me to widen my research from various perspectives. Besides that, I would like to thank him for giving me access to the CSIRO laboratory and research facilities. Without his valuable support it would not have been possible to continue with this research.

I would like to acknowledge the support provided by the Petroleum Development Oman (PDO) and Ministry of Oil and Gas (MOG) in Oman. They provided reservoir and fluid data for Field A and the scholarship and financial support throughout my PhD. My sincere thanks goes to Abdullah Al Hadhrami, Abdullah Al Riyami, Raul Valadez, Fakhriya Al Shuaibi, Ralf Schulz from PDO for their support for collecting data , their affirmative input, expert recommendations, and simulation helps and supports. I would also like to thank Dr. Seyed Ali Mousavi from Research Institute of Petroleum Industry (RIPI) for his assistance and cooperation.

During this work I have companied with many wonderful colleagues in Petroleum Engineering Discipline at Curtin University for whom I have great regard, and I wish to extend my warmest thanks to all those who have offered help, friendship, and technical support during my work in this project. I am also very grateful to Mr. Bob Webb (Laboratory Technical Officer) for his generous support including laboratory management and procuring of the materials used in this research.

Last but not the least, I wish to express my deepest gratitude to family members: my parents, brothers and sisters for their encouragement, prayers, and support throughout my study in Australia. I wish also to express my sincere appreciation and acknowledgement to my wife Noura for her unconditional love, support, understanding and being on my side even at the most challenging situations during the tenure of my study. To my beloved daughters Eynas and Reemas and my son Ahmed, I would like to express my thanks for being such good children always cheering me up.

List of Publications

Published Article Papers:

1. **Al Hinai, N.M.**, A. Saeedi, C.D. Wood, R.Valdez, and L. Esteban, *Experimental Study of Miscible Thickened Natural Gas Injection for Enhanced Oil Recovery*. Energy & Fuels, 2017. 31(5): p. 4951-4965.
2. **Al Hinai, N.M.**, A. Saeedi, C.D. Wood, M. Myers, R. Valdez, A.K. Sooud, and A. Sari, *Experimental Evaluations of Polymeric Solubility and Thickeners for Supercritical CO₂ at High Temperatures for Enhanced Oil Recovery*. Energy & Fuels, 2018. 32(2): p. 1600-1611.
3. **Al Hinai, N.M.**, A. Saeedi, C.D. Wood, M. Myers, R. Valdez, Q. Xie, and F. Jin, *New Approach to Alternating Thickened–Unthickened Gas Flooding for Enhanced Oil Recovery*. Industrial & Engineering Chemistry Research, 2018. 57(43): p. 14637-14647.

Under Review Article Paper:

1. **Al Hinai, N.M.**, M. Myers, Seyed. Ali, C.D. Wood, R. Valdez, F. Jin, Q. Xie, and A. Saeedi, *Effects of Oligomers Dissolved in CO₂ or Associated Gas on IFT and Miscibility Pressure with a Gas-light Crude Oil System*. Journal of the Taiwan Institute of Chemical Engineers (under review).

Conference Paper:

1. **Al Hinai, N.M.**, A. Saeedi, C.D. Wood, and R. Valdez, *A Numerical Study of Using Polymers to Improve the Gas Flooding in the Harweel Cluster*, in *SPE Reservoir Characterisation and Simulation Conference and Exhibition*. 2017, Society of Petroleum Engineers: Abu Dhabi, UAE

Book Chapter:

1. **Al Hinai, N.M.**, A. Saeedi, M. Myers, C.D. Wood. Direct gas thickeners. Laura Romero (Ed.) *Enhanced Oil Recovery Processes - New Technologies*. IntechOpen. (under review)

Executive Summary

Miscible Gas injection (MGI) is an effective enhanced oil recovery (EOR) method used worldwide often for light oil recovery. In the petroleum industry, many MGI processes typically involve injection of an associated gas (AG) mixture or CO₂, which have both been recognised as excellent candidates for such processes. However, in general, the viscosity of a typical injected gas at reservoir condition is significantly lower than that of the resident crude oil leading to an unfavourable mobility ratio and low volumetric sweep efficiency. In addition, reservoir heterogeneity tends to further worsen the situation by, for example, promoting gas channeling through high permeability layers, leading to a low oil recovery. Several techniques that have been proposed in the literature to counteract the negative effects of such challenges during an MGI process, including water alternating gas flooding (WAG), foam flooding, and direct gas thickening.

For many years, direct gas thickening has been recognised as a game changing technology to improve volumetric sweep efficiency for MGI projects. However, to date, the viability of this method with technically feasible thickeners has not been verified at the field-scale due to a combination of potential issues such as high costs and potential environmental complications. In addressing some of these issues, two main objectives were set for this study: 1) identifying viable, commercial, and safe gas thickeners that are capable of increasing the viscosity of an AG and CO₂ at high temperature conditions. 2) explore a technique to lower the volume of thickeners utilised during field-scale applications as an attempt to improve the economic feasibility of the technique. The primary focus of this study has been on an oilfield (Field A) located in the Harweel cluster in southern Oman.

In this study, extensive experimental and simulation evolutions have been carried out to predict the potential benefits of adding a thickener to the injected gas in Field A and to identify, and test chemical additives that can be dissolved in either CO₂ or field's AG mixture to form a thickened gaseous phase to be used as the injection fluid during MGI. A mechanistic simulation study performed for Field A indicates that an increase from 0.1 to 0.16 cP (3.3 to 5.3 fold) in the viscosity of the injected gas (AG mixture or CO₂) would be adequate to improve gas mobility favourably and enhance sweep efficiency. In an ensuing laboratory study, the suitability of a library of commercially

available polymers/oligomers capable of thickening the AG mixture and CO₂ at a high pressure and temperature (55 MPa and 377 K, respectively) was assessed using a parallel gravimetric extraction technique combined with cloud point pressure measurements. Then, the viscosity of the AG mixture and CO₂ thickened with the identified soluble polymeric candidates was measured in a capillary viscometer at reservoir conditions. For the AG mixture, three additives were found to be completely or partially soluble including poly(1-decene) (P-1-D), poly(methyl hydro siloxane) (PMHS), and poly(dimethylsiloxane) (PDMS). Among the three candidate additives, P-1-D was found to be completely soluble in the AG mixture in the concentration range of 1.5–9 wt%. The viscosity of the P-1-D-thickened AG mixture increased by 2–7.4 times compared with that of the unthickened AG mixture at 358–377 K. For CO₂, four additives of ((P-1-D), poly(ethyl vinyl ether) (PVEE), poly(iso-butyl vinyl ether) (Piso-BVE), and (PDMS)) were found to be completely soluble. Given the relatively low in-situ viscosity of oil in Field A (0.23 cP), P-1-D was deemed as an effective thickener for the AG mixture, while for CO₂ both of P-1-D and PVEE could be considered suitable. Piso-BVE was not considered effective because despite its solubility it did not change the CO₂ viscosity above 358 K (55 MPa) when used at a concentration of 1.5 wt%.

In the next step, reservoir condition core flooding experiments were performed to examine the performance of continuous thickened AG as well as alternating injection of thickened AG (TAG) or thickened CO₂ (TCO₂) with unthickened AG at the laboratory-scale. Twelve experiments were conducted using different injection schemes (i.e., continuous unthickened, continuous thickened, and alternating thickened–unthickened). These tests demonstrated that continuous thickened-AG mixture flooding would delay gas breakthrough and result in 8–15% additional oil recovery. In addition, it was found that the alternating injection of TAG or TCO₂ with unthickened AG mixture may yield additional recoveries close (5-12%) to those obtained with continuous thickened AG mixture injection. Such an outcome helps to reduce the consumption of thickening agents noticeably resulting in reduced operational costs and improved economic viability of the direct gas thickening method.

Finally, the phase behaviour of P-1-D and PVEE in the two gas solvents (CO₂ and AG mixtures) was examined. In addition, a qualitative assessment was made of the effect of the dissolution of these oligomers in CO₂ and AG mixture on the equilibrium IFT

and miscibility pressures using the vanishing interfacial tension (VIT) technique. The cloud point pressure measurements revealed that the P-1-D-thickened CO₂ would exhibit a UCST (upper critical solution temperature) trend while P-1-D-thickened AG mixture would follow a LCST (lower critical solution temperature) behaviour. The solubility of P-1-D in CO₂ is a function of enthalpy and in AG mixture a function of entropy. The solubility of PVEE is entropically driven through the molecular interactions between ether oxygen atom in PVEE and the carbon atom in CO₂. Moreover, the dissolution of P-1-D and/or PVEE in CO₂ resulted in a slight reduction in the IFTs and miscibility of the light oil/CO₂ system. The plasticization effects of dissolved gas in P-1-D and the dissolution of P-1-D in the AG mixture can cause an increase in the IFTs and miscibility pressures of the light oil/AG mixture.

Table of Contents

Declaration	ii
Copyright	iii
Dedication	iv
Acknowledgements	v
List of Publications	vii
Executive Summary	viii
Table of Contents	xi
List of Figures	xiii
List of Tables.....	xviii
Abbreviations.....	Error! Bookmark not defined.
Chapter 1. Introduction and Background	1
1.1 Enhanced Oil Recovery	1
1.2 Miscible Gas Injection (MGI).....	3
1.3 Challenges Associated with MGI Process.....	7
1.4 Gas Mobility Control Techniques	15
1.5 Research Objectives	34
Chapter 2. Literature Review: Previous Attempts at Thickening Gases	39
2.1 Direct Carbon Dioxide Thickeners	39
2.2 Hydrocarbon Gas Thickeners	58
Chapter 3. Numerical Study of Using Polymer to Improve the Gas Flooding in the Harweel Cluster*	67
3.1 Introduction.....	67
3.2 Numerical Model	69
3.3 Fluids PVT Model.....	72
3.4 Results and Discussion.....	72
3.5 Summary and Conclusions	84
Chapter 4. Experimental Study of Miscible Thickened Natural Gas Injection for Enhanced Oil Recovery*	86
4.1 Introduction.....	86
4.2 Experimental Methodology	91

4.3	Results and Discussions	102
4.4	Summary and Conclusions	116
Chapter 5. Experimental Evaluations of Polymeric Solubility and Thickeners for Supercritical CO₂ at High Temperature for Enhanced Oil Recovery*		
		118
5.1	Introduction.....	118
5.2	Experimental Methodology	123
5.3	Results and Discussions	130
5.4	Summary and Conclusions	140
Chapter 6. A New Approach of Alternating Thickened-Unthickened Gas Flooding for Enhanced oil Recovery*		
		143
6.1	Introduction.....	143
6.2	Experimental Methodology	147
6.3	Results and Discussions	151
6.4	Summary and Conclusion.....	164
Chapter 7. Effects of Oligomers Dissolved in CO₂ or Associated Gas on IFT and Miscibility Pressure with a Gas-light Crude Oil System*		
		166
7.1	Introduction.....	166
7.2	Experimental Methodology	169
7.3	Results and Discussions	173
7.4	Summary and Conclusion.....	187
Chapter 8. Conclusions and Recommendations		
		189
8.1	Conclusions.....	189
8.2	Recommendations for future work.....	193
Appendices		196
References		217

List of Figures

Figure 1.1 Worldwide EOR projects contribute to global oil production.[6]	2
Figure 1.2 The contribution of current EOR projects implemented in Oman oil fields.[7].....	3
Figure 1.3 Development of miscibility of injected CO ₂ in oil.[19]	4
Figure 1.4 Geological cross-section of the carbonate stringers (left) and an aerial overview of Harweel Fields in southern Oman (right).[34]	6
Figure 1.5 Effect of viscous fingering on the development of areal sweep efficiency against time (t) in a quarter of a 5-spot flood pattern during gas flooding, A) an unstable displacement with poor macroscopic sweep, B) A stable displacement good with macroscopic sweep, ⊗) An injection well and O) A production well.[40].....	8
Figure 1.6 Areal sweep efficiency as a function of mobility ratio and pore volumes of displacing phase injected for an MGI process.[40].....	10
Figure 1.7 Viscous fingering growth for different mobility ratio and injected pore volume.[40].....	11
Figure 1.8 A) Reservoir heterogeneity due to permeability variation versus depth in Field A located in South of Oman, B) Example effect of possible gravity segregation on vertical sweep efficiency.	13
Figure 1.9 A typical WAG injection process as an EOR method that involves the injection of gas and water alternatively into an oil reservoir.....	16
Figure 1.10 A micro-pore illustration of foam flow and gas trapping in the porous media. The cross-hatched spaces represent the solid grains, and the dotted spaces indicate the wetting liquid.[60, 117].....	24
Figure 1.11 X-ray CT scan images for (A) a CO ₂ miscible flood (Blue) in a core saturated with oil (red) and residual brine (yellow) and (B) CO ₂ -foam flooding (blue) in a core saturated with oil (red) and a surfactant solution (yellow).[72, 127]	24
Figure 1.12 (A) A high interfacial tension results in large capillary force, which prevents the oil drop from crossing through the downstream pore throat, (B) Ultra-low interfacial tension leads to near zero capillary force, which allows the oil drop to flow through the pore throat and be produced.[59].....	25
Figure 1.13 Simplified illustration of a thickened gas flooding	29
Figure 2.1 High/low molecular weight polymeric thickener tested in CO ₂ with/without co-solvent.[172].....	41
Figure 2.2 The viscosity enhancements of PFOA in CO ₂ at different pressures and concentrations and temperature of 323 K.[190]	46

Figure 2.3 The effect of temperature on the relative viscosity of polyFAST in CO ₂ solution at 34 MPa.[191].....	48
Figure 2.4 Association mechanism of tributyltin fluoride.[210].....	51
Figure 2.5 Molecular structure of a non-fluorous bisures.[219].....	53
Figure 2.6 Molecular structure of a fluorinated twin-tailed surfactant as a CO ₂ thickener.[203].....	54
Figure 2.7 General Molecular structure of small molecules Cyclic Amide and Urea Based.[227].....	55
Figure 2.8 Association mechanism of tributyltin fluoride.[71].....	62
Figure 2.9 Association mechanism of HAD2EH molecules.[71].....	63
Figure 2.10 Molecular structure of Phosphate di/mono-ester, Phosphonic acid ester and dialkyl phosphinic acid.[71].....	64
Figure 2.11 Chelation mechanism and micellar structure of phosphate ester/metal ion complex.[246].....	65
Figure 3.1 Geological cross-section of the carbonate stringers (left) and an aerial overview of Harweel Fields in southern Oman (right).....	67
Figure 3.2 3D reservoir model showing the permeability distribution.....	71
Figure 3.3 The oil viscosity reductions with addition of different gas compositions into oil at 55MPa and 377 K.....	73
Figure 3.4 The oil density changes with addition of different gas compositions into oil at 55MPa and 377 K.....	75
Figure 3.5 The swelling factor changes with addition of different gas compositions into oil at 55 MPa and 377 K.....	76
Figure 3.6 Oil recovery profiles for different unthickened gas floods.....	77
Figure 3.7 Oil recovery factor and GOR for different unthickened gas floods.....	78
Figure 3.8 Effect of thickened AG2 mixture on the vertical oil sweep efficiency.....	80
Figure 3.9 Effect of AG2 viscosity enhancement on the oil recovery profiles and production GOR development.....	81
Figure 3.10 Oil recovery profiles and production GOR for 0.1 cP viscosity thickened gas floods.....	83
Figure 3.11 Oil recovery profiles and production GOR for 0.16 cP viscosity thickened gas floods.....	83
Figure 3.12 Oil recovery profiles and production GOR for 0.25 cP viscosity thickened gas floods.....	84
Figure 4.1 Schematic diagram of gravimetric extraction equipment used for rapid measurement of polymers solubility in AG mixture.....	95
Figure 4.2 Schematic diagram of experimental setup used for cloud point pressure measurements.....	96

Figure 4.3 Schematic of Capillary Viscometer used for viscosity measurements (55 MPa and 377 K).	98
Figure 4.4 Schematic diagram of the core-flood setup.	101
Figure 4.5 Extracted weight % in the AG mixture for a library the 32 polymers/oligomers at 55 MPa and 377 K. The name of the polymers/oligomers whose numbers are presented on the horizontal axis can be found in Table 4.1.	103
Figure 4.6 Measured cloud point pressures for three polymers at 1.5wt% in the AG mixture at different temperatures.	106
Figure 4.7 Measured cloud point pressures for PMHS at 1.5 wt% in the AG mixture containing different percentages of CO ₂ at different temperatures.	107
Figure 4.8 Measured cloud point pressures for P-1-D at 1.5 wt% in the AG mixture containing different percentages of CO ₂ at different temperatures.	107
Figure 4.9 Measured cloud point pressures for P-1-D at different concentrations and temperatures.	109
Figure 4.10 Measured P-1-D-thickened AG gas viscosity at different P-1-D concentrations, temperatures, and pressures.	110
Figure 4.11 Relative viscosity μ_{sol}/μ_{AG} at different P-1-D concentrations, temperatures, and pressures.	111
Figure 4.12 Measured oil recovery factor versus 3.6 of total injected pore volume of AG mixture or P-1-D-thickend AG solution at flow rate 0.4 cm ³ .min ⁻¹ , reservoir temperature 377 K, and pressure 55 MPa.	115
Figure 4.13 Measured total oil recovery factor versus 9 of total injected pore volume of AG mixture or P-1-D-thickend AG solution at flow rate 0.4 cm ³ .min ⁻¹ , reservoir temperature 377 K, and pressure 55 MPa.	116
Figure 5.1 Schematic diagram of gravimetric extraction equipment used for rapid measurement of polymers/oligomers solubility in AG mixture.	127
Figure 5.2 Schematic diagram of experimental setup used for cloud point pressure measurements.	128
Figure 5.3 Schematic of the capillary viscometer used for viscosity measurements (50-55 MPa and 329-377 K).	130
Figure 5.4 Extracted weight % in scCO ₂ for the library of the 26 polymers/oligomers at 41, 48 and 55 MPa and 377 K. The name of the polymers/oligomers whose numbers are presented on the horizontal axis are defined provided in Table 5.1.	132
Figure 5.5 Compare cloud point pressures between PVEE and Piso-BVE at different concentrations and temperatures.	135

Figure 5.6 Measured cloud point pressures for P-1-D at different concentrations and temperatures.	136
Figure 5.7 Relative viscosity μ_{sol}/μ_{CO_2} at different PVEE concentrations, temperatures and pressures.	137
Figure 5.8 Relative viscosity μ_{sol}/μ_{CO_2} at different PISO-BVE concentrations, temperatures and pressures.	138
Figure 5.9 Relative viscosity μ_{sol}/μ_{CO_2} at different P-1-D concentrations, temperatures and pressures.	139
Figure 6.1 Measured P-1-D-thickened AG and CO ₂ solution viscosities at different P-1-D concentrations, temperatures (377 K), and pressures (50-55MPa) from a capillary viscometer (0.01-15,000 cP).[288, 332].....	146
Figure 6.2 Schematic diagram of the core-flood setup.	149
Figure 6.3 Fracture visualisation in composite core plugs sample and CT scan.....	149
Figure 6.4 Measured oil recovery profiles for the four injection schemes of continuous unthickened AG flooding, continuous thickened AG flooding, thickened AG alternating AG flooding (TAG-A-AG) (ratio: 1:2), and thickened CO ₂ alternating AG flooding (TCO ₂ -A-AG) (ratio: 1:2) in non-fractured composite sample, all conducted at 377 K and 53 MPa.	154
Figure 6.5 Graphical representation of the injection patterns and measured ultimate oil recovery factors for different injection schemes and different TAGR in non-fractured core plugs.	154
Figure 6.6 Measured oil recovery profiles for the four injection schemes of continuous unthicken AG flooding, continuous thickened AG flooding and thickened AG alternating AG flooding (TAG-A-AG) (ratios: 1:2, 1:3 and 1:5) in non-fractured composite sample, all conducted at 377 K and 53 MPa.	156
Figure 6.7 Measured oil recovery profiles for the four injection schemes of continuous unthicken AG flooding, continuous thickened AG flooding, thickened AG alternating AG flooding (TAG-A-AG) (ratio: 1:2), and thickened CO ₂ alternating AG flooding (TCO ₂ -A-AG) (ratio: 1:2) in a fractured composite sample, all conducted at 377 K and 53 MPa.....	158
Figure 6.8 Comparison of measured ultimate oil recovery factors at different injection schemes and different TAGR in fractured core plugs.....	159
Figure 6.9 Collected oil produced in graduated cylinders from core-flooding tests in fractured core plugs: A, TCO ₂ -A-AG (1:2); and B, TAG-A-AG (1:2). The fluorescence color changes of residual oil in the last cylinder is dark brown in alternating TCO ₂ flooding and yellow color in TAG alternating flooding.....	159

Figure 6.10 Measured oil recovery profiles for the four injection schemes of continuous unthickened AG flooding, continuous thickened AG flooding, and thickened AG alternating AG flooding (TAG-A-AG) (ratios: 1:2, 1:3 and 1:5) in a fractured composite sample, all conducted at 377 K and 53 MPa.	161
Figure 6.11 Measured oil recovery profiles for continuous TAG and continuous unthickened AG floods in non-fractured and fractured core plugs, all conducted at 377 K and 53 MPa.	162
Figure 6.12 Measured total oil recovery factor versus 8.3 of total injected pore volume of TAG-A-AG and TCO ₂ -A-AG in non-fractured and fractured core plugs at a flow rate of 0.4 cm ³ .min ⁻¹ , reservoir temperature of 377 K, and pressure of 53 MPa.	163
Figure 7.1 Light oil measured density at 377K and different pressures.	171
Figure 7.2 Schematic diagram of the experimental setup used for IFT measurements.....	173
Figure 7.3 Measured cloud point pressures for P-1-D at different concentrations and temperatures in CO ₂ .[332].....	175
Figure 7.4 Measured cloud point pressures for P-1-D at different concentrations and temperatures in AG mixture.[288].....	175
Figure 7.5 Measured cloud point pressures for P-1-D at 1.5wt% concentration in the AG mixture containing different percentages of CO ₂ at different temperatures.[288, 332].....	176
Figure 7.6 Measured IFTs and miscibility pressures (MMP and P _{max}) for light oil/AG mixture system and light oil/CO ₂ system at different equilibrium pressures at constant temperature (377 K).....	179
Figure 7.7 Measured IFTs for the light oil/P-1-D-thickened CO ₂ system and light oil/CO ₂ system at different equilibrium pressures and constant temperature (377 K).	182
Figure 7.8 Measured IFTs for the light oil/PVEE-CO ₂ system and light oil-CO ₂ system at different equilibrium pressures and constant temperature (377 K).....	182
Figure 7.9 Measured IFTs for light crude oil/P-1-D-AG system and light crude oil-AG mixture system at different equilibrium pressures, different P-1-D concentrations (and constant temperature (377 K).	184
Figure 7.10 Solubility parameters of light oil, P-1-D, CO ₂ , AG rich, AG, AG lean, methane, ethane and Propane at different pressures and temperature of 377 K.	186
Figure 7.11 Photographs showing the evolution of the dissolved gas from P-1-D during pressure release after its exposure to the AG mixture at temperature of 377 K and three pressures of 3.44 MPa (A), 6.89 MPa (B) and 20.68 MPa (C).	187

List of Tables

Table 2.1 Review of small molecules compounds solubility in CO ₂ and their thickening capability results	57
Table 2.2 Summary of small molecules compounds solubility in NGL components and thickening capability results	66
Table 3.1 Composition of various injection gases studied.....	71
Table 3.2 Reservoir and fluid properties.....	71
Table 4.1 Library of polymers/oligomers used in parallel gravimetric extraction experiments.....	92
Table 4.2 Compositional analysis results of Field A dead oil in mole percentage	93
Table 4.3 Summary of the Core-Flooding Experiment Data (377 K and 55MPa). K: permeability; ϕ : porosity; $S_{w,irr}$: irreducible water saturation; S_{oi} : oil saturation; RF_{AG} : AG recovery factor; $RF_{thick'd AG}$: thickened AG recovery factor; and RF_{total} : total recovery factor.....	113
Table 5.1 The library of polymers and oligomers used in parallel gravimetric extraction experiments.....	125
Table 5.2 Classification of polymers/oligomers based on extraction ability in scCO ₂	131
Table 5.3 The measured viscosities for pure CO ₂ and CO ₂ thickened using different concentrations of PVEE, PISO-BVE and P-1-D at different pressures and temperature (377 K).	140
Table 6.1 Compositional analysis results of Field A dead oil in mole percentage	147
Table 6.2 Details of the 6 core-flooding test performed in each composite core plugs setups.....	150
Table 6.3 Summary of the core-flooding experiments conducted on non-fractured core plugs (377 K and 53 MPa). K, Permeability; ϕ , Porosity; $S_{oil,max}$, oil saturation upon the achievement of irreducible water; Injected TAGR, injected thickened ratio; BT, breakthrough in pore volume; and RF_{total} , ultimate oil recovery factor.....	152
Table 6.4 Summary of the core-flooding experiment conducted on fractured core plugs (377 K and 53 MPa) for fractured core plugs. K, Permeability; ϕ , Porosity; $S_{oil,max}$, Oil saturation upon the achievement of irreducible water; injected TAGR, injected thickened ratio; BT, breakthrough in pore volume; and RF_{total} , ultimate oil recovery Factor.....	160
Table 7.1 Compositional analysis results of Field A dead oil in mole percentage	170

Nomenclature

Abbreviations

AG	associated gas
ADSA	axisymmetric drop shape analysis
BT	breakthrough
BPR	back pressure regulator
CO ₂	carbon dioxide
scCO ₂	supercritical carbon dioxide
DRA	drag-reducing agent
CDC	continual dissolution capacity
EOS	equation of state
EOR	enhanced oil recovery
FCM	first-contact miscibility
GPC	gel permeation chromatography
GOR	gas oil ratio
H ₂ S	hydrogen sulphide
HAD2EH	hydroxyaluminum di-2ethylhexanoate
HTGE	high throughput gravimetric extraction
IOR	improved recovery methods
IFT	interfacial tension
LCST	lower critical solution temperature
MGI	miscible gas injection
ME	Middle East
MMP	minimum miscibility pressure
MCM	multi-contact miscibility
NGL	natural gas liquids
NIST	National Institute of Standards and Technology
OOIP	original oil in place
PVAc	polyvinyl acetate
polyFAST	fluoroacrylate-styrene copolymers
P-1-D	poly(1-decene)
PVME	poly(vinyl methyl ether)

PVEE	poly(vinyl ethyl ether)
PDMS	poly(dimethylsiloxane)
PMHS	poly(methyl hydro siloxane)
PVA	poly(vinyl alcohol)
PAO	poly alfa-olefin
Piso-BVE	poly(isobutyl vinyl ether)
PVAc-co-VA	poly(vinyl acetate-co-vinyl alcohol)
PFOA	poly(1-,1-, dihydroperfluorooctyl acrylate)
polyBOVA	Poly(benzoyl co-vinyl acetate)
PR_EOS	Peng-Robinson equation of state
PDO	Petroleum Development Oman
SCF	supercritical fluid
TBTF	tributyltin fluoride
TDS	total dissolved solids
TAG-A-AG	thickened AG alternating AG
TCO ₂ -A-AG	thickened CO ₂ alternating AG flooding
TAG	thickened AG
TAGR	thickened AG ratio
UCST	upper critical solution temperature
VIT	vanishing interfacial tension
WAG	water alternating gas

Uints

bpd	barrels per day
m	meter
mm	millimeter
cm	centimeter
m ³	cubic meter
MPa	miga Pascal
K	kelvin
Kg.m ⁻³	kilogram per cubic meter
cP	centipoises
g.L ⁻¹	gram per leter

g. cm^{-3}	Gram per cubic centri meter
ppm	part per million
API	american petroleum institute
m^3/day	cubic meter per day
mN/m	milli Newtin per meter
bar	bar
g.m^{-3}	gram per cubic meter
PV	Pore volume
$\text{cm}^3.\text{min}^{-1}$	cubic centimeter per minute
$\text{cc}.\text{min}^{-1}$	cubic centimeter per minute
$\text{m}^3.\text{s}^{-1}$	cubic meter per second
mol%	mole percent
vol%	volume percent
wt%	weight percent

Symbole

$\Delta\rho$	density difference
G	gravitational acceleration
L	length of the porous medium
K	absolute permeability
K_i	effective permeability
K_e	equivalent permeability
Mw	Molecular weight
M	mobility ratio
N_g	gravity number
N_c	capillary number
PV	pore volume
P_{\max}	first contact miscibility pressure
ΔP	pressure drop along the porous medium
Q	Fluid flow rate
RF	recovery factor
VI	viscosity index

μ_i	effective viscosity
μ_{oil}	oil viscosity
μ_{gas}	gas viscosity
λ_i	mobility of a fluid
ρ_o	oil density
ρ_g	gas density
Σ	interfacial tension between the two fluids
Θ	contact angle.

Chapter 1. Introduction and Background

1.1 Enhanced Oil Recovery

Over the past few decades, the rate of the new substantial oil discoveries has been on the decline. As a result nowadays, many oil companies are trying to maximise oil production from their existing reserves and maintain oil flowrates at or above the economic level through production optimisation and the use of enhanced oil recovery (EOR) techniques.[1] Enhanced oil recovery refers to the methods of increasing or maintaining the ability of oil to flow through interconnected pores towards the production wells by changing the physical and/or chemical properties of the in-situ fluid-rock system. Presently, the average recovery factor (RF) from mature oilfields under the primary and secondary recovery is only 20 to 40%.[2] Given the earlier mentioned lack of substantial new discoveries, increasing the RF from matures fields has become important to meet the growing energy demand in the years to come.

During the life cycle of an oil field, the oil extraction may occur typically in three recovery stages of primary, secondary, and tertiary (i.e. EOR). Essentially, the petroleum product is produced from the reservoir initially by the natural reservoir energy such as the solution gas drive, gas cap drive and aquifer influx.[3] This is often termed as primary recovery, where the first wells drilled in the field are able to produce the oil from the reservoir without any intervention. In this stage primarily, the pressure gradient between the reservoir and surface controls the hydrocarbon flow into the well and then to surface. Over time, the reservoir pressure may decline reducing the pressure at the bottomhole which may then become closer to the hydrostatic head of the fluid column in a production well reducing the oil flowrate achievable from the well. Subsequently, secondary recovery methods may be applied, for example, by injecting water or gas via injection wells into the reservoir to maintain the reservoir pressure and eliminate or minimise the previously observed decline in oil flow. This type of recovery methods has its own technical and economic limitations as may be determined by the cost and availability of injection fluids and/or the issues that may arise during the development of the in-situ flooding. For instance, in both water and gas flooding, the difference in fluid properties between the displacing fluid and to be displaced in-situ oil can result in unstable displacement, leading to a large oil volume

left behind due to poor displacement efficiency and early breakthrough. Therefore, the application of such techniques may typically add up to only 40-50% of eventual oil recovery.

When the oil in a reservoir can no longer be produced by natural reservoir pressure (i.e. primary recovery), or by water or gas injection (i.e. secondary, improved recovery methods (IOR), or pressure maintenance), EOR techniques may be considered. In general, as briefly referred to earlier, EOR techniques aim to stimulate oil flow by overcoming the physical, chemical and geologic factors that inhibit the production of the remaining hydrocarbons.[4] One of the most widely implemented EOR processes today is thermal recovery, which involves heating the oil bearing interval with steam or hot water to reduce the oil viscosity. Miscible Gas injection (MGI) is another most widely used approach today, which is carried out by the injection of a high-pressure gas, such as carbon dioxide or hydrocarbon gas, to sweep an additional oil towards the wellbores by employing a number of in-situ mechanisms such as oil viscosity and IFT reductions. Chemical agents dissolved in water and injected into the reservoir can also improve the displacement properties during a water flood. Currently, various EOR projects executed around the world, as shown in Figure 1.1, account for only 4.5% (3 million barrels per day (bpd)) of the total world oil production (75 million bpd). However, further application of these technologies has the potential to increase oil recovery from existing fields and new discoveries and alleviate oil supply shortage in the future.[5, 6]

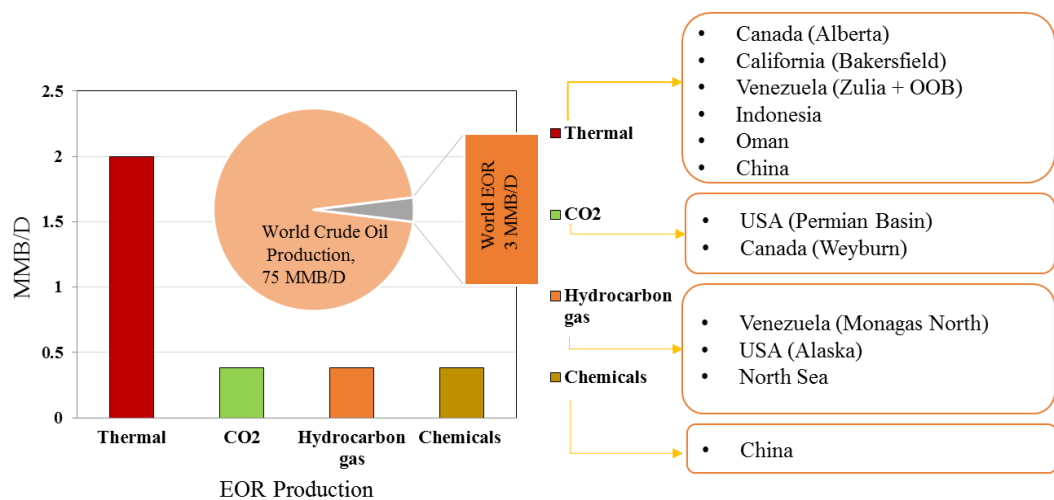


Figure 1.1 Worldwide EOR projects contribute to global oil production.[6]

The application of EOR techniques in Oman may be considered as a successful example of how such techniques may be used to boost oil production and achieve substantial enhancements in recovery. Over the past decade, a number of EOR projects in the Middle East (ME) have been executed. Among the ME countries, Oman leads the way mainly owing to its declining overall oil production rate[7] which has seen EOR to become a major strategy to meet target oil production from its existing fields.[8] In 2007, this country’s oil production declined to an average of 700,000 bpd. However, with the aid of EOR methods, the field operators have been able to increase the country’s overall oil production to its current level of nearly 1 million bpd. Miscible gas injection is one of the EOR technique used in the country. The largest fields produced using EOR techniques in Oman and the indicative contributions made by such techniques in each field are depicted in Figure 1.2. The daily oil production rate from these Fields with implanting EOR techniques varies between 40 to 80 thousand bpd (Mbpd). While without EOR it was 3 to 45 Mbpd making such techniques the key driver of Oman’s oil production nowadays.[9]

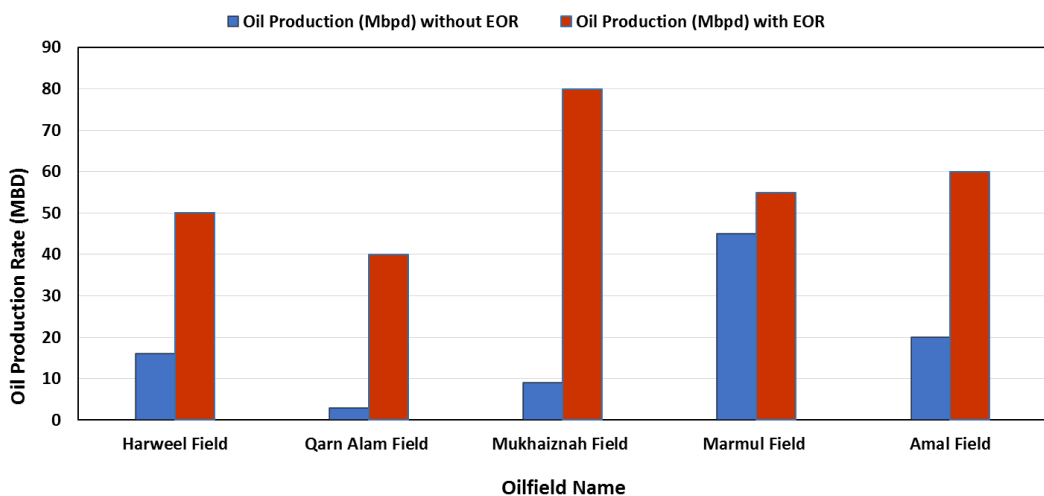
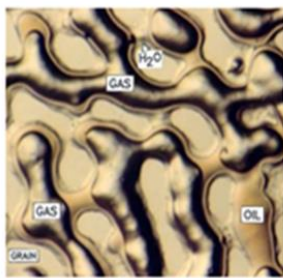


Figure 1.2 The contribution of current EOR projects implemented in Oman oil fields.[7]

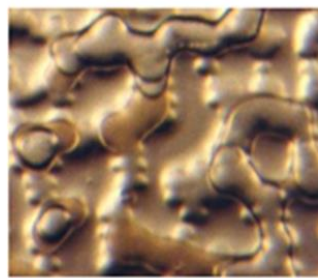
1.2 Miscible Gas Injection (MGI)

The MGI is one of the most effective EOR methods used to enhance the production of light crude oil in the petroleum industry.[10] This method is PVT driven in which the injected gas (CO₂, Associated Gas (AG), or Natural Gas Liquids (NGL)), in addition to helping with pressure maintenance, would mix with and alter the properties of the in-situ oil allowing the otherwise trapped oil to become mobile and easily

displaced.[11, 12] During the miscible gas flooding, the injected gas would become miscible with the reservoir oil at or above the minimum miscibility pressure (MMP) of the reservoir oil (Figure 1.3). By definition, the MMP is the pressure at which the mass transfer and molecular interactions between the gas and oil intensify forcing the physical and chemical properties of the two phases to converge.[13, 14] In other words, upon reaching MMP, the gas acts as a solvent for the oil towards forming a single fluid phase (liquid) in the reservoir with the potential of effectively reducing the saturation of the remaining oil to near zero under ideal conditions.[4] During this process, the improved displacement efficiency of the flood is realised via three main mechanisms including substantial reduction in IFT (i.e. elimination of the interface between the two fluids and reduction of capillary pressure to zero), reduction of oil viscosity, and oil swelling.[15, 16] The value of MMP depends on the reservoir temperature as well as the compositions of the injected gas and in-situ oil.[17, 18]



Stage-1: Immiscible CO₂ in oil at 6.89 MPa and 315 K



Stage-2: Miscibility developed between oil and CO₂ at 9.38 MPa and 315 K, the displacement appears to be above MMP



Stage-3: CO₂ has developed miscibility with oil at 17.2 MPa and 315 K (above MMP). The miscible fluid is very dilute (light) flowing in the pore channels

Figure 1.3 Development of miscibility of injected CO₂ in oil.[19]

In general, the miscibility process of the crude oil-gas system may occur through two paths of multi-contact miscibility (MCM) and first-contact miscibility (FCM).[20] The MCM would take place if the in-situ pressure is equal to MMP which as discussed previously, is a critical property to be taken into account for designing an MGI process.[21] The MCM may develop gradually via a number of processes including vaporising gas drive, condensing gas drive and a combination of the two drives.[14] On the other hand, when the reservoir pressure is adequately high and well above MMP, FCM would take place in which the injected gas would develop miscibility with the in-situ oil at all proportions as soon as they are brought in contact. Since FCM

would only occur at high enough pressures, depending on the type of injectant used, achieving this type of miscibility could be challenging.

The type of the injected gas used for MGI depends on the gas availability and reservoir conditions[2] with the common gases used around the world being CO₂, hydrocarbon gas mixture (AG, NGL), flue gas and N₂. [20, 22] Carbon Dioxide, which has been most widely used in the United State, Canada, and China, [23] can achieve miscibility at relatively low pressures (when compared to other gases) and has a relatively high density (can be similar to oil). The latter can help to reduce the severity of gravity segregation and override which can negatively affect the sweep efficiency. The use of this gas for flooding can also help to reduce the global level of CO₂ emissions. However, some of the main challenges for a successful CO₂ flooding in general are the availability of CO₂ and corrosion in wells and surface facilities which can result in considerable cost increases, in particular, for remotely located fields.

In the Middle East, the available CO₂ supply is limited to industrial sources[24] which, when combined with the earlier mentioned issues associated with using this gas, has made its wide application limited. However, the hydrocarbon gas injection could be considered for MGI processes more widely for which the produced AG is usually readily available from the field itself or those close by. On the other hand, as mentioned earlier, unlike CO₂, conducting MGI using AG, depending on the gas composition, requires a relatively high pressure to achieve miscibility. To date, there have been three MGI projects (at either pilot- or field-scale) in the Middle East as reported in the literature.[25] Two of the projects involve miscible CO₂ injection and the other utilises AG injection. The Rumaitha Field in Abu Dhabi was the first pilot miscible CO₂ injection implemented in the region.[25-28] The second pilot CO₂-EOR project has been implemented in Minagish Oolite Reservoir in west Kuwait.[29] The third project has been implemented in Field A located in the Harwell Cluster in southern Oman in which the field's AG mixture (CH₄ enriched with light and heavy hydrocarbon fractions found in natural gas as well as considerable amounts of sour gases (3-5 mol % H₂S and 10-25 mol % CO₂)) is used for re-injection.[30, 31] As will be discussed in further details later, improving the MGI process in this field is a main focus of the current study.

Harweel Fields consist of a cluster reservoirs deep within the tight carbonate oil-bearing rocks in the south of Oman in the Petroleum Development Oman (PDO) concession area, as shown in Figure 1.4. The figure also presents a geological cross-section of the carbonate stringers, as encased in the Ara salt, and the general geological setting of the area. The fields are expected to make a significant contribution to the Sultanate's oil production over the coming 30 years. The reservoir rocks in these fields are more than half a billion years old (where the hydrocarbon deposits are among the oldest in the world) located at a depth of about 5 kilometers, making them PDO's deepest producing oil fields.[32, 33] As indicated earlier, the MGI in Field A, located in the cluster, has already begun in which the source of the injection gas is the Field's AG.[30] The produced AG mixture is reinjected into the reservoir at high pressures of up to 55 MPa during which the injected gas develops miscibility with the in-situ oil under the reservoir's high temperature (up to 377 K). The reservoir contains a light crude oil with a typical gravity of 42°API and a viscosity of 0.23 cP at reservoir conditions. It was initially estimated that up to 47% of the Field's original oil in place (OOIP) could be recovered with the MGI process.[32] However, it has been realised since then that the presumed RF might not be eventually achievable due to the technical and operational challenges faced in this field e.g. premature gas breakthrough and high degree of reservoir heterogeneity. As mentioned earlier, this research will be mainly focusing on addressing some of the technical challenges experienced during MGI in Field A and similar fields by proposing and testing a novel mobility control technique applicable to such a high pressure and temperature environment.

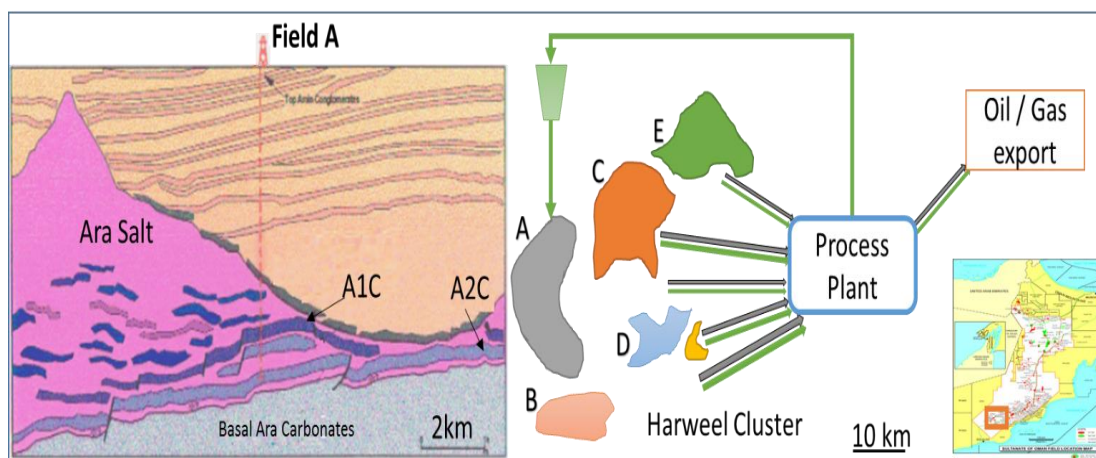


Figure 1.4 Geological cross-section of the carbonate stringers (left) and an aerial overview of Harweel Fields in southern Oman (right).[34]

1.3 Challenges Associated with MGI Process

As with other EOR techniques, MGI can be economically expensive and technically challenging to implement.[35] For example, even when the injection gas is readily available on site (e.g. associated gas), gas processing , handling and compression as part of the expected gas recycling scheme can be costly.[2, 36] Full lifecycle economics of a gas injection project, therefore, must be taken into account to justify its implementation. In addition, as an example, a technical challenge in achieving a profitable MGI is the instability of the oil displacement process in the reservoir mainly due to the expected unfavourable mobility ratio and possible gravity segregation whose effects may be intensified by the level of reservoir heterogeneity.

From a more general technical perspective, the efficiency of an MGI is controlled by the collective effects of several physical forces acting on the displacement front. These forces include the viscous forces that stem from viscosity contrast in the flood, gravity forces caused by fluid-fluid density differences, dispersive forces driven by the fluid concentration gradients and, finally, the capillary forces that have roots in the IFT between any immiscible fluids. The large differences in fluid viscosities can cause viscous fingers at the displacement front. If the vertical permeability in the reservoir is quite high, a pronounced density difference can cause gravity segregation. Both of the above have the potential to leave a large amount of oil unswept. The capillary and dispersive forces tend to enhance the fluid mixing but do not often overwhelm the viscous fingering.[37, 38] Therefore, the gravity and viscosity forces are the essential forces driving the instability of the oil displacement process during MGI.[39] Provided in the following two subsections are further details about the underlying mechanisms behind these two forces and how they may interfere with the performance of an MGI process. Possible mitigation strategies to lessen their effects will be outlined and adequately discussed in later sections of this chapter.

1.3.1 Viscous Fingering

When a fluid is injected into a reservoir to displace another, there is almost never a collective perfect piston-like displacement across the entire reservoir interval. Especially in a gas flood, unstable displacement due to viscous fingering can lead to uneven or poor sweep, as depicted in Figure 1.5.[40] Viscous fingering is generally defined as a hydrodynamic instability that occurs between two fluids of differing

mobility/viscosity in the porous media that could lead to reduced sweep efficiency and early breakthrough.[39, 41, 42] The terms mobility, mobility ratio and that in a gas flood mobility ratio may be interchangeably used with viscosity ratio would be defined and discussed shortly. In MGI, there are several parameters that affect the viscous instability at the fluid-fluid interface including fluid viscosities, degree of miscibility, gas dissolution and exsolution, and reservoir heterogeneity.[39, 42-44] However, the viscosity contrast and permeability heterogeneity are the two that mainly control the dynamics of the fingering phenomenon.[37, 45] The importance of mobility/viscosity ratio may be further realised after defining the mobility ratio (M) as a widely used criterion to characterise and determine the occurrence and possible effects of viscous fingering.

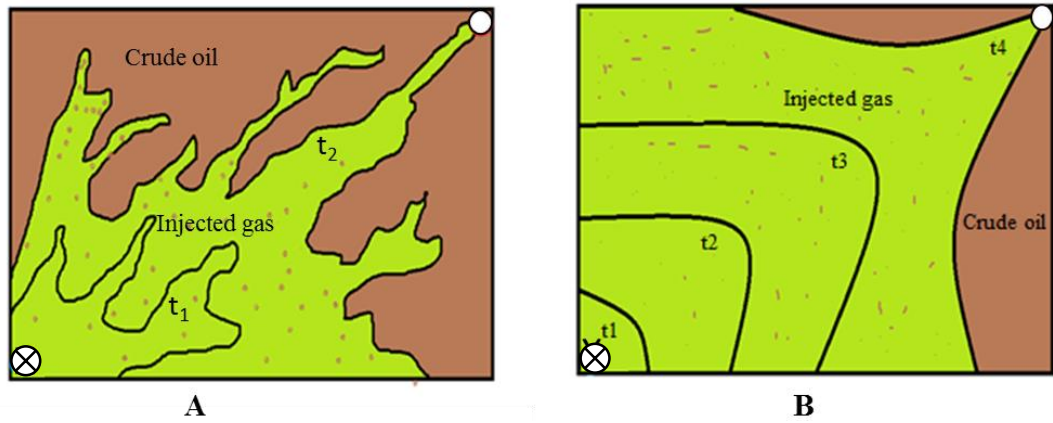


Figure 1.5 Effect of viscous fingering on the development of areal sweep efficiency against time (t) in a quarter of a 5-spot flood pattern during gas flooding, A) an unstable displacement with poor macroscopic sweep, B) A stable displacement good with macroscopic sweep, (⊗) An injection well and (○) A production well.[40]

As indicated by Equation 1.1, the mobility of a fluid (λ_i) in a porous medium may be defined as the ratio of effective permeability (K_i) and effective viscosity (μ_i) experienced by the fluid while flowing in the medium,[40, 46, 47]

$$\lambda_i = \frac{K_i}{\mu_i} \quad \text{Eq 1. 1}$$

Subsequently, for any fluid-fluid displacement, such as an MGI, the mobility ratio (M) can be simply defined as the mobility of the displacing fluid over that of the displaced

fluid.[40, 47] For instance, Equation 1.2 defines M for an MGI process where gas displaces the in-situ oil.

$$M = \frac{\lambda_{\text{gas}}}{\lambda_{\text{oil}}} = \frac{K_{\text{gas}}/\mu_{\text{gas}}}{K_{\text{oil}}/\mu_{\text{oil}}} \quad \text{Eq 1. 2}$$

Where, μ_{oil} and μ_{gas} are the oil and injected gas viscosities, respectively. For a miscible displacement, where the gas solvent may displace the oil at irreducible water saturation and the effective permeability to both fluids may be considered to be the similar, Equation 1.2 may be reduced to Equation 1.3.[40] Furthermore, during gas flooding, due to the large viscosity contrast between the gas and the in-situ oil, viscosity ratio may be considered adequate for qualitative evaluation of viscous instability in the flood.[40, 45, 48] Therefore, for the purpose of qualitatively characterising the effect of viscous fingering on the performance of an MGI process, the viscosity ratio may be used interchangeably with the mobility ratio.[40]

$$M = \frac{\mu_{\text{oil}}}{\mu_{\text{gas}}} \quad \text{Eq 1. 3}$$

During its development, the severity of viscous fingering increases with increase in the mobility/viscosity ratio of the fluid system. If M is larger than unity, the displacement becomes unstable resulting in the development of viscous fingers. Therefore, to achieve a stable displacement, where possible, the viscosity of the displacing fluid may be increased or its effective permeability reduced until the value of M approaches unity or less. For instance, if the injected gas viscosity is increased, the gas mobility may be suppressed. Hence, the severity of the viscous fingering and the chance of developing premature breakthrough can be reduced, resulting in improved displacement efficiency. Figure 1.6 demonstrates the effect of mobility ratio on the area sweep efficiency of an MGI process as reported by Habermann et al.[40] As can be seen from the figure, when $M = 1$, the ultimate areal sweep reaches as high as 99%, however, if M increases to 38.2, the areal sweep would decrease by more than 20%. The physical development of viscous fingers as the mobility ratio changes for the cases presented in Figure 1.6 is demonstrated by the diagrams included in

Figure 1.7. As can be seen in this figure, the displacement is characterised as stable if the value of M is one or lower. The effect of M as demonstrated through the above sweep values and Figures 1.6 and 1.7 was for a homogenous porous system. The presence of permeability heterogeneity would also make considerable contribution towards initiating and development of viscous fingering.[41] A high permeability layer would present a preferential flow path for the fingering of the injected gas causing early gas breakthrough and a low overall oil recovery factor.[28, 29][49]

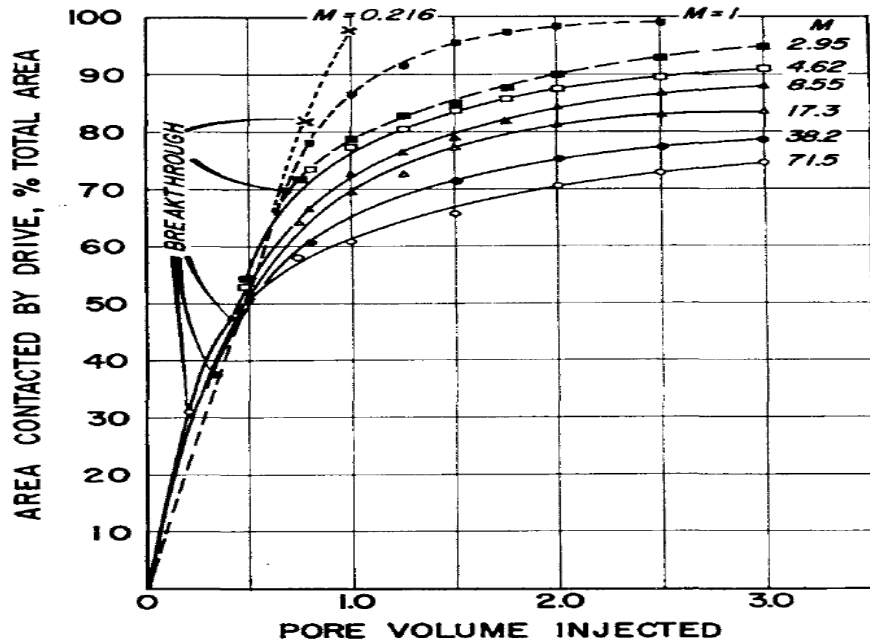


Figure 1.6 Areal sweep efficiency as a function of mobility ratio and pore volumes of displacing phase injected for an MGI process.[40]

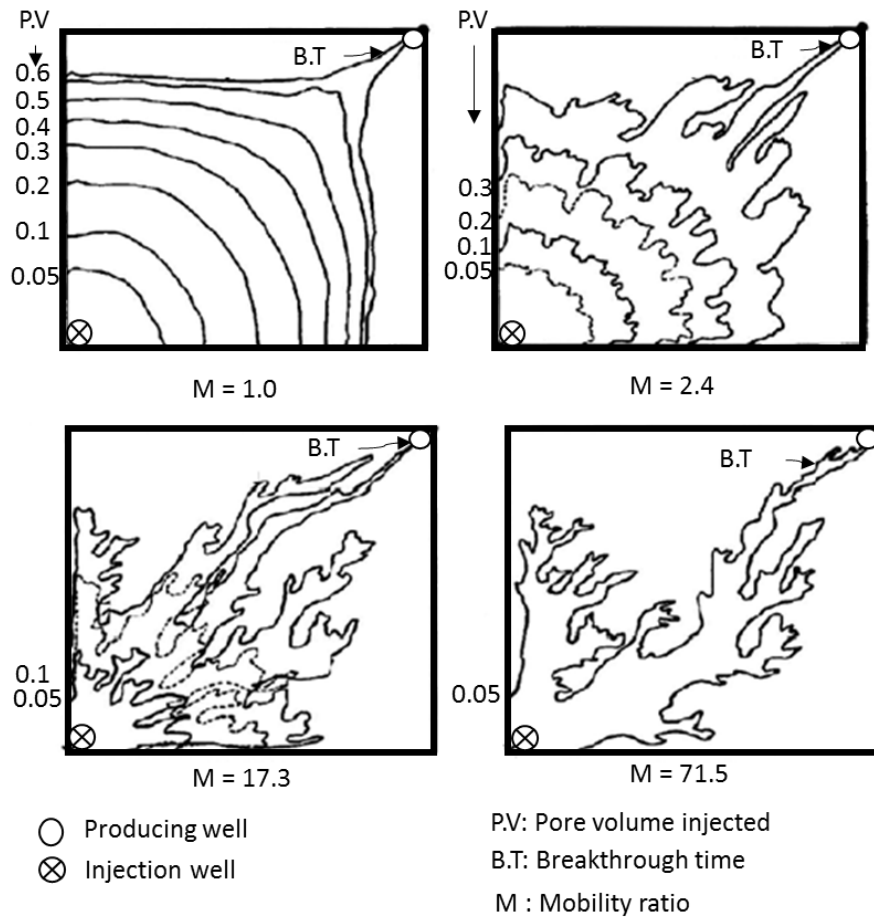


Figure 1.7 Viscous fingering growth for different mobility ratio and injected pore volume.[40]

1.3.2 Gravity Segregation

As indicated earlier, another possible major technical challenge faced by an MGI process that influences the vertical sweep efficiency is the gravity segregation or gravity override. The injected gas (such as CO₂ or hydrocarbon gas) is usually less dense than the in-situ oil which may lead the injected gas to flow upwards, rather than lateral, forming a gravity tongue.[49, 50] Such a behaviour, similar to unfavourable mobility ratio, would result in early gas breakthrough and reduced vertical sweep efficiency in horizontal MGI processes as depicted in Figure 1.8. The effect of gravitational force on an MGI process has been studied by Moissis et al.[51] using numerical simulation. They found two dimensionless parameters of relevance, the dimensional density difference ($\Delta\rho$):

$$\Delta\rho = \frac{\rho_o - \rho_g}{\rho_g} \quad \text{Eq 1. 4}$$

and the dimensionless gravity number (N_g):

$$N_g = \frac{(\rho_o - \rho_g)gK_e}{q\mu_o} \quad \text{Eq 1. 5}$$

where N_g represents the ratio of gravity forces to viscous forces, ρ_o and ρ_g are the oil and gas densities, respectively, K_e is equivalent permeability, μ_o is the oil viscosity, q is the flow rate of the less viscous fluid in the porous medium of interest and g is the gravitational acceleration. The simulation results obtained by Moïssis et al.[51] show that the gravity force does not influence viscous fingering growth at small N_g values indicating the dominance of the viscous forces under such a condition.[51] As N_g increases to larger values, the gravity force begins to influence the growth rate of viscous fingering in the upper part of the porous medium. For sufficiently large N_g values, gravity override completely dominates the displacement where, even though the viscous fingering can still occur near the gravity tongue, it is suppressed in the bottom part leaving this part of the porous medium completely unswept. Overall, as may be expected, with increase in N_g the gas breakthrough occurs earlier reducing the overall oil recovery.[51]

Further interplay between the gravity and viscous forces towards controlling the efficiency of a gas flood may be deduced by further scrutiny of Equation 1.5. Controlled by the magnitude of N_g , the effect of the gravitational force is expected to be even larger at high flood viscous ratios because the gravity to viscous forces ratio is inversely proportional to the viscosity of the fluid available in the porous medium. At the beginning of the flood, as defined by Equation 1.5, this ratio is equal to N_g . However, as the displacement proceeds and more of the less viscous gas enters the porous medium at constant flow rate, the gravity to viscous forces ratio begins to increase resulting in more severe gravity override. Such an effect would be more pronounced in the case of floods characterised by a high viscosity ratio.[51]

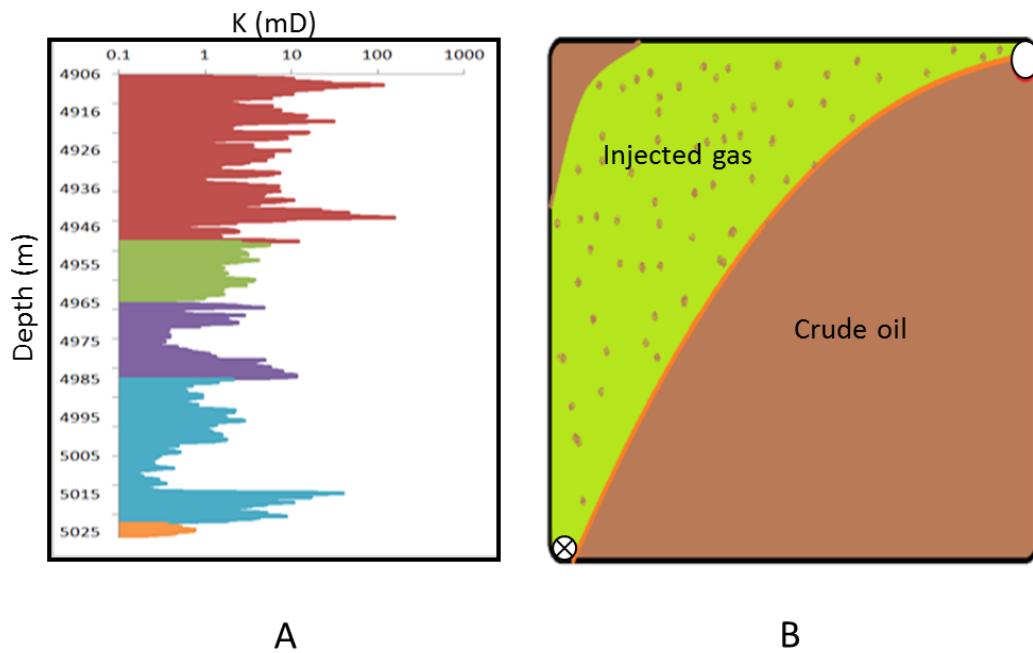


Figure 1.8 A) Reservoir heterogeneity due to permeability variation versus depth in Field A located in South of Oman, B) Example effect of possible gravity segregation on vertical sweep efficiency.

Scott et al.[50] have suggested to combat the gravity segregation by adjusting the density of the miscible gas injected as part of an MGI. For example, the pressure within the formation can be maintained high enough so that the density of the injected fluid approaches that of the reservoir oil. However, for measurable outcomes in general, the density of the miscible fluid should be maintained within about 10 percent of the density of the to be displaced in-situ oil.[50] Furthermore, this technique may be proven difficult and impractical if large injection volumes are required to maintain the reservoir pressure. Scott et al.[50] have also indicated that the density adjustment may be obtained by injecting carbon dioxide or intermediate natural gas fractions (C_2H_6 , C_3H_8 , and C_4H_{10}). Carbon dioxide in its supercritical state is capable of exhibiting a density greater than that of the reservoir oil.[50] However, hydrocarbon gases alone may not normally achieve a density equal or close to that of the resident crude oil under typical reservoir conditions therefore, severe gravity override could still occur. Another technique to increase the density of injected gas is the use of chemical additives, however to date suitable and viable chemical additives to be used for this purpose are yet to be developed.[52] As suggested in the literature, the mitigation of the gravity segregation can be possibly achieved by mobility or conformance control.[52]

1.3.3 Statement of Problem

As mentioned before, Field A in south Oman (Figure 1.4) has been the subject of a viable MGI process since 2004 during which the Field's AG mixture has been reinjected into the reservoir at high pressure (up to 55 MPa) and high temperature (up to 377 K) where it would develop miscibility with the in-situ oil. As outlined earlier, the Field's AG contains CH₄ enriched with light and heavy hydrocarbon fractions typically found in natural gas as well as considerable amounts of carbon dioxide at 10–25 mol% and H₂S at 3-5 mol%.[30, 31] It was believed initially that with the miscible AG injection, an estimated 47% of the Field's OOIP could be recovered.[32] However, even though the Field contains a light oil (42°API) with a relatively low viscosity (0.23 cP), technical and operational challenges such as early gas breakthrough and low sweep efficiency have prevented the ongoing MGI process from realising its full potential. In addition, the permeability variation in the Field is quite high (0.1-100 mD) negatively impacting on the development of the MGI process. As can be seen from Figure 1.8, higher permeability zones (10-100 mD) are located in the upper and lower sections of the reservoir leaving the middle sections with mostly sub-mD permeabilities. In general, in Field A, the presence of high permeability zones that present preferential flow paths for the gas leads to uneven oil displacement leaving substantial amounts of oil behind in the low and intermediate permeability zones sandwiched in the middle. This is one of the main reason behind the observed early gas breakthrough in some production wells.

Given the description provided above, the two suspected major challenges faced by the MGI process in Field A may include gravity override and unfavourable mobility ratio caused by, respectively, the density and viscosity contrasts between the injected AG and the displaced oil. Both of the above factors in conjunction with the Field's heterogeneity could result in the early breakthrough of the injection gas and poor volumetric sweep, reducing the overall efficiency of the MGI development. As mentioned earlier, some of the production wells in the Field have already experienced an early gas breakthrough, leading to their high production GOR and declining oil production. With respect to the suspected gravity override, there is not considerable density contrast between the injected AG and the displaced oil (400-600 kg/m³ and 639 kg/m³, respectively). That is due to the presence of CO₂ and H₂S in the injected gas composition that dope the injection gas towards having a high density. Hence, the

gravity override may not be a primary problem in this Field. Therefore, the MGI may not benefit from any special treatments (e.g., chemical additives) to increase its density. However, the injected AG has a relatively low in-situ viscosity (0.01 to 0.03 cP) compared with that of the oil (0.23 cP). Therefore, the high viscosity contrast in combination with the effect of reservoir heterogeneity present the major challenge to be possibly addressed using a suitable remedial technique that would be both technically and economically viable.

Although the problem at hand has been stated in the context of Field A, given the relatively high pressure (up to 55 MPa), high temperature (up to 377 K), and high salinity (275,000 ppm) of this field, any technique and methodology developed in this research work can be potentially applied to reservoirs with similar harsh subsurface conditions where viscous fingering and severe channelling of the injected gas may hamper the development of an MGI process. In fact an extensive literature survey has revealed the lack of past research work relevant to such conditions.

1.4 Gas Mobility Control Techniques

As mentioned above, the major challenge with the ongoing AG flooding in Field A is the unfavourable mobility ratio. This challenge can be addressed by the implementation of several approaches as proposed in the literature (although mainly for CO₂ flooding) including water alternating gas flooding (WAG),[53-55] foam flooding,[56-62] and increasing the gas viscosity using the addition of polymers as thickening agents.[52, 63-71] The common main objective of these approaches would be to control the gas mobility effectively and, as a result, increase the sweep efficiency of the gas flooding.[72] Further technical details about each of the above mentioned techniques are provided in the upcoming subsections of this chapter.

1.4.1 WAG Process

As an EOR method, the WAG process is defined as the injection of a gas (e.g. CO₂ or hydrocarbon gases) and water alternately into an oil bearing formation (Figure 1.9). The WAG injection scheme was initially proposed by Claudle and Dyes in 1958[55] to improve sweep efficiency during gas flooding. Their study showed that this injection scheme would result in the reduction of the relative permeability to the gas phase and suppress its mobility. In other words, the WAG would improve the sweep

efficiency of the injected gas by using water to control the gas mobility and stabilise the displacement front. In general, depending on the MMP of the in-situ oil, this technique can be classified into the two categories of miscible and immiscible WAG displacements[73] however, as reported in the literature, the majority (79%) of the historical WAG field applications fall into the miscible category.[74, 75] In some recent field applications, in an injection scheme similar to WAG, the produced gas has been reinjected through water injection wells to improve the oil recovery and help to provide pressure maintenance.[76] The majority of the WAG injection projects are found onshore (88 %), and few others are reported to have been implemented in an offshore environment (12%).[75]

In general, there are a number of factors affecting the performance of the WAG process including the degree of reservoir heterogeneity, in-situ fluid properties, injection technique, miscibility conditions and other WAG parameters such as the individual gas and water slug sizes and their size ratio (WAG ratio), number of injection cycles and injection rates.[77-79] Similar to other EOR processes, the WAG flooding has a number of advantages and disadvantages that will be presented and discussed below.

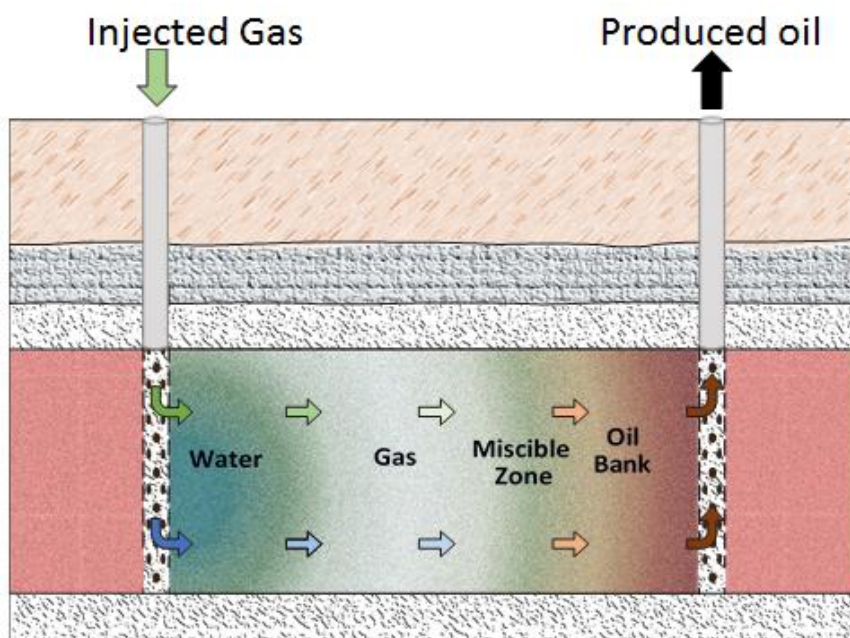


Figure 1.9 A typical WAG injection process as an EOR method that involves the injection of gas and water alternatively into an oil reservoir.

1.4.1.1 The Mechanisms and Factors Influencing WAG Flooding

During WAG injection, the improved recovery is not often achieved through modifying the fluid properties of each of the injected phases, it rather tends to combine the advantages of each of the continuous gas or continuous water floods through creating a synergism between the in-situ flow properties of the two phases if injected on their own. Overall, when WAG injection is applied in an oil reservoir, it may yield favourable outcomes through several mechanisms.[80] Firstly, the injection process may help to maintain the reservoir pressure above the MMP of the oil resulting the achievement of the more desirable miscible flood. Secondly, the injected gas mobility is reduced by suppressing the gas relative permeability in any existing preferential flow channels. This is achieved by the increase in water saturation in these zones and therefore reduction in gas saturation suppressing the possibility of gas channelling and viscous fingering.[52, 81, 82] Thirdly, in the case of a miscible flood, the excellent microscopic displacement efficiency of the miscible gas flooding is put into use across a larger portion of the reservoir by the mobility control and conformance control provided by the water phase, leading to higher oil recovery. Lastly, compared with a continuous gas injection process (e.g. continuous MGI) the WAG flooding decreases the amount of the gas needed for injection leading to possible improvement in the economics of the overall flooding process. Considering the collective advantages mentioned here, the WAG injection process may become a viable option for some fields around the world.

Laboratory experiments have been used to study the effect of various parameters such as WAG slug size and WAG ratio (tapering), number of WAG cycle and injection flow rate on the performance of WAG.[53, 54, 73, 83-89] In general, these parameters show strong effects on the oil recovery trends of a WAG injection. It has been found that, in general, decreasing slug size and WAG ratio, and increasing the number of WAG cycles would lead to a higher oil recovery.[53, 80] However, the optimum WAG ratio often depends on the wettability of reservoir rock, in-situ fluid properties and the type of gas being used as well as economic evaluations.[53] The optimum WAG ratio is considered as a key parameter for the successful implementation of a WAG injection process. A high WAG ratio may lead to an excessive water injection into the reservoir giving rise to the water blocking effect where the water phase would surround the trapped oil in low permeable zones and reduce accessibility by the injected gas decreasing the overall oil recovery. On the other hand, if the ratio is too low, the

conformance control of the WAG flood would be lost and the injected gas would penetrate through the reservoir very fast under the effect of unfavourable mobility ratio and lead to early breakthrough. Overall, the experimental results have demonstrated that the WAG process may help to suppress viscous fingering and lead to increased oil recovery in gas flooding.[74, 75]

1.4.1.2 Challenges of WAG Flooding

The WAG injection has been successfully applied in several oilfields worldwide demonstrating that it could result in considerable incremental oil recovery at the field-scale (5-10% of OIIP).[90] However, some published literature also indicate that some of the field-scale WAG processes have not reached their expected target recovery factors, especially in naturally fractured, highly permeable, and highly heterogeneous reservoirs.[75] Furthermore, the field-scale implementation of this technique has also helped to identify a number of challenges that may be faced by the field operators. Such challenges are presented and discussed below by first dividing them into the two categories of operational challenges versus those of subsurface reservoir related.

Operational Issues: A numbers of operational related issues have been reported in the literature including:[74, 75, 90]

- **Reduced Injectivity:** The ability to inject the required amounts of gas and water through the injection wells is critical towards achieving the desirable WAG performance. Reduced injectivity can result in a pressure reduction in the reservoir, which may impact on, for example, miscibility, performance of the displacement and the eventual production yield. This issue may be caused by changes in the phase relative permeabilities and/or near wellbore formation damage. In general, the field trials have shown that the reduced injectivity may be experienced for the water injection rather than the gas injection stage during the alternating injection of the two phase.[75, 90]
- **Corrosion:** Corrosion problems have been reported in many projects that have involved WAG injection. Often such issues have been encountered because the pre-existing injection and production facilities were not initially designed to handle the WAG injection process. Six fields are reported to have experienced corrosion problems, mainly on the injection facilities. The

existing case studies indicate that in most cases, such problems could be adequately addressed by using corrosion resistant materials in the manufacture of equipment, coating the flow-lines, and chemical treatments.[75, 90]

- ***Asphaltene, Scale and Hydrate Formation:*** Asphaltene and scale precipitation and hydrate formation are among other problems that have been experienced in various WAG field trials. These problems would lead to production disturbance and even flowlines blockage which may increase the operating costs of a WAG process. Three fields (East Vacuum, Wertz Tensleep, Mitsue) have experienced asphaltene precipitation, and two fields (Ekofisk and Wasson Denver) have reported the formation of hydrate in the injection wells due to the low temperature in the injectors or cold weather at the wellhead. Some of these problems could be resolved by chemical treatments.[75, 90]

Subsurface Reservoir Issues: Besides the operational problems discussed above, there are also a number of issues related specifically to the subsurface and fluid flow in the bulk of the reservoir presenting challenges for the WAG implementation:

- ***Premature Gas Breakthrough:*** Unexpected early gas breakthrough has been reported in several WAG field applications despite the fact that WAG is often implemented to combat this issue in particular. The main cause for this problem has often been inadequate characterisation of the reservoir, poor design of the WAG process or limitations imposed by the existing versus required infrastructure (e.g. limited number of injection/production wells). Regardless of the cause, early gas breakthrough would often occur due to gas channeling through highly permeable layers or gravity override.[91, 92] The early gas breakthrough leads to loss of reservoir pressure and lost miscibility in a miscible WAG project.[93, 94] As reported in the literature, five oil fields (University Block 9, Juravlevsko-Stepanovskoye, Lick Creek, Caroline, and Snorre) have experienced this problem because of gas channeling.[93, 95-98] Unfortunately, this problem is hard to resolve as once occurred, its root causes (as mentioned at the beginning of this paragraph) are difficult to address. However, adequate reservoir characterisation before

the implementation of this mobility control technique can be helpful in avoiding unexpected early gas breakthrough.[75]

- **Oil Trapping:** Several studies have demonstrated the occurrence of oil trapping by water in the WAG flooding.[99-102] This phenomenon is also referred to as water blocking.[102] During the WAG injection, the injected mobile water traps/encases the residual oil which then becomes difficult for the gas phase to access and mobilise. Therefore a high residual oil saturation may be left behind in the reservoir even after WAG flooding. It has been determined that rock wettability and WAG ratio can strongly affect the oil trapping with being more severe in the case of water-wet rock formations or high WAG ratios.[80, 99, 100, 103]
- **High Water Production:** The injection of large amounts of the water into the reservoir (i.e. high WAG ratio) can cause high water saturation[104] leading to excessive water production and, hence, reduced oil recovery.[105] In addition, the excessive water production would require additional water treatment capacity that brings about additional costs impacting on the project economics.[103]

1.4.2 Gas Foam Flooding Process

1.4.2.1 Gas-Foam Generation and Foaming Agents

Gas-foam injection is another approach to combat the conformance and mobility limitations encountered in an MGI process. Furthermore, this technique may also bring about some of the advantages of the chemical EOR due to the chemical additives required for foam stabilisation and generally better foam generation. The foam flooding was first introduced by Bond and Halbrook in 1958 to show that the foam generated by the injection of an aqueous surfactant solution and miscible/immiscible gas could increase sweep efficiency.[106] With the favourable results obtained from the above study in the subsequent years, it was proposed to use foam injection as a means of gas mobility control. However, the concept did not become widely known and immediately adopted due to the lack of understanding of mobility control mechanisms behind the foam flooding.[107]

In the context of fluid flow in porous media, a foam is generally defined as a gas-liquid mixture where the liquid phase exists as a continuous wetting phase in the rock, whereas all or parts of the gas form the discontinuous phase surrounded by a thin liquid film or Lamellae.[60] According to the literature, the research conducted in the area of gas foam flooding mostly relate to CO₂-EOR because the required chemicals are much easier to dissolve in CO₂ towards the generation of a CO₂ foam at reservoir conditions.[72] A gas foam may be stabilised by the addition of effective surfactants, which contain a hydrophobic and hydrophilic segment.[72] Surfactants then can be either water-soluble or CO₂ soluble.[60, 108, 109] The selection of surfactant depends on the reservoir conditions. If the reservoir condition is suitable for a surfactant to be soluble in the injected gas, then injection of water with the surfactant can be eliminated.[110] Numerous CO₂ soluble surfactants have been experimentally identified.[56, 109, 110] For example, the hydrocarbon-based ethoxylates surfactant has been suggested by Scheivelbein et al. as a CO₂ foam agent instead of using a water-soluble surfactant.[110] The other reported surfactant products include Tergitol TMN-6, oligo (vinyl acetate), poly(ethylene glycol) 2,6,8-trimethyl-4-nonyl ethers, and ethoxylated amine surfactant.[111-115] For miscible hydrocarbon gas flooding, only water-soluble surfactants can be used as the foaming agent because no effective surfactant directly soluble in hydrocarbon gases for gas-foam generation has been reported in the literature.[57] Nine water soluble surfactants have been identified for foam generation with hydrocarbon solvents, including Alkanolamides, Amine oxides, Betaine derivatives, Ethoxylated and propoxylated alcohols and alkylphenols, Ethoxylated and propoxylated fatty acids, Ethoxylated fatty amines, Fatty acid esters, Fluorocarbon-based surfactants, and Sulfate and Sulfonate derivatives.[57] As the temperature increases, most of the water-soluble surfactants become less soluble in water. Therefore, it may be necessary to evaluate the surfactant solubility in either CO₂ or water for application in high-temperature reservoirs.[72, 116]

The foam used for gas foam flooding may be generated in several ways as discussed in the literature. It may be formed within the target porous media by alternating injection or co-injection of a suitable surfactant and gas (CO₂ or hydrocarbon gas mixture). In the case of CO₂ foam flooding, the foam can be formed when a surfactant is dissolved into CO₂ (usually in supercritical state) and then injected into the porous media, without requiring the injection of a liquid slug.[59] The foam can also be

generated at the wellhead by the simultaneous injection of the gas and surfactant solution. Then, as the foam leaves the wellbore, it could be re-formed and strengthened as it enters the micropores of the reservoir rock.[72]

As a gas foam enters a rock formation, it would need to propagate through the entire formation suppressing the high gas mobility for the whole duration of the flood. However, the injected foam is not often thermodynamically stable under in-situ conditions, and, therefore, the two-phase foam system may collapse with time. On the other hand, as mentioned earlier, the passage of the fluids through the porous rock formation could result in the regeneration of the foam due to shearing effects applied by the micron sized tortuous pores and pore channels.[117] Therefore, in order to have an effective foam for mobility control, the rate of in-situ foam generation would need to be equal to or greater than the rate of its decay.[72] In general, the foam propagation at the large reservoir scale and the foam stability are the main challenges faced by the gas foam flooding technique.

1.4.2.2 Main Mechanisms of Gas-Foam Flooding

A gas-foam may be used as part of an EOR scheme for two purposes.[57] Firstly, it can be designed to reduce the gas mobility to a level that is comparable to or even less than that of the displaced oil so that the gas viscous fingering and channeling can be effectively suppressed. Thereby the areal sweep efficiency could be improved considerably. However, it is worth noting that the reduction level in the foam mobility has to be optimised and controlled to avoid the prohibitive pressure drop in the reservoir caused by extremely low foam mobility. Therefore as a compromise, a weak and modest foam may be generated by varying the surfactant concentration in a gas-foam injection.[118] The second possible purpose of using a gas-foam is for conformance control or blocking of a thief gas channel to divert the injection fluids away from it and into other unswept lower permeability oil-rich zones to mobilise the otherwise bypassed oil.[72, 109] Typically, this can be achieved by the alternating injection of an aqueous solution with a high concentration of a surfactant.[57] The high concentration of surfactant then generates a strong foam that would flow in the highly permeable or thief zone[118] resulting in the diversion of the gas flow into the lower permeability zones.

The enhanced recovery of a gas foam injection is usually achieved through a number of different mechanisms as summarised and briefly discussed below.

- ***Stabilising the Displacement Front:*** The efficiency of a fluid-fluid displacement in a porous medium is in general controlled by the three gravity, viscous and capillary forces.[60, 119] Therefore, the manipulation of these forces can result in enhanced recovery. Concerning the application of a gas foam during a gas flooding process such as MGI, the mobility control and, therefore, stabilisation of the flood front may be achieved by the higher viscosity and reduced relative permeability of the gas-foam both relative to the case of injecting the gas on its own. Typically, these effects may be achieved through two mechanisms.[60] The first mechanism is related to the movement and re-arrangement of bubbles due to the local gradient in the surfactant concentration and, therefore, the interfacial tension. The surfactant movement within the liquid film (Lamellae) lowers the surface tension between the two phases (liquid and gas) that slows down the bubble motion and causes an increase in the gas phase effective viscosity.[120-122] The second mechanism that reduces the gas-foam mobility is gas trapping.[123, 124] As the foam injected and/or formed in a porous medium, as also indicated earlier, it prefers to flow through highly permeable and porous zones, while the low permeability areas with small pores remain occupied by the wetting phase,[125] (Figure 1.10). Thus, the gas bubbles may enter and become trapped in the intermediate size pores, where a large fraction of foam bubbles are immobilised due to the high enough capillary pressure.[59] Nguyen et al.[126] found that the amount of trapped gas in this form is governed by several factors, such as the foam texture, pore geometry, and pressure gradients. The blocked intermediate size pores decrease the pore volume available for the gas-foam to flow through, thus the reduced relative permeability and suppressed gas-foam mobility.[60]

A gas foam can help to combat gravity segregation too.[60] Figure 1.11 demonstrates the effectiveness of a CO₂ foam towards stabilising the displacement front in the X-ray CT scanned core-flooding experiments conducted by Wellington and Vinegar.[127] As can be seen from the left hand side images, the researchers found that CO₂ injection alone would lead to the

formation of a gravity tongue whereas, the right hand side images show that the CO₂-foam injection prevented the gravity and viscous instabilities towards the uniform displacement of the in-situ oil.

Overall, based on the discussion presented so far, a gas foam would not change the gas phase density but exhibit its effectiveness by suppressing the gravity and viscous forces, leading to stabilisation of the displacement front.

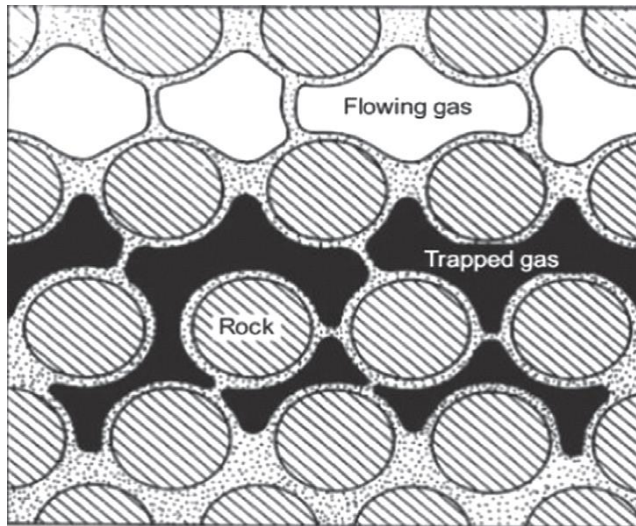


Figure 1.10 A micro-pore illustration of foam flow and gas trapping in the porous media. The cross-hatched spaces represent the solid grains, and the dotted spaces indicate the wetting liquid.[60, 117]

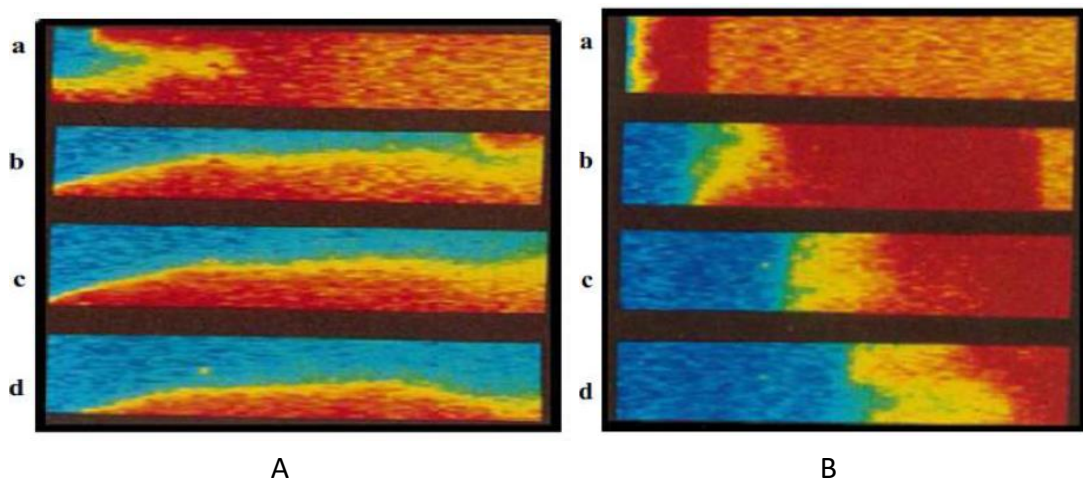


Figure 1.11 X-ray CT scan images for (A) a CO₂ miscible flood (Blue) in a core saturated with oil (red) and residual brine (yellow) and (B) CO₂-foam flooding (blue) in a core saturated with oil (red) and a surfactant solution (yellow).[72, 127]

- **Reducing the Capillary Force:** Capillary pressure is usually held responsible for the bulk of the entrapped oil (often non-wetting phase) in rock formations. That is why Zhang et al.[128] point out that the removal of the trapped crude from a reservoir rock needs ultra-low interfacial tension through an emulsification mechanism. The capillary number as set out in Equation 1.6 defines the ratio between viscous and capillary forces acting on a displacement. The lower the interfacial tension (low capillary forces), the higher the capillary number and, therefore, the more dominant would be the viscous forces resulting in higher recoveries.

$$N_c = \frac{K\Delta P}{\sigma L \cos\theta} \quad \text{Eq 1. 6}$$

where: N_c : capillary number, dimensionless, K : absolute permeability of the porous medium, ΔP : pressure drop along the porous medium, σ : the interfacial tension between the two fluids, L : length of the porous medium, and θ : contact angle.

Once during foam injection, the surfactant in the injected slugs proceeds through the porous rock, different interactions occur at oil, foam and rock interface[129] leading to ultra-reduction of the interfacial tension between the oil and water resulting in the formation of an oil-in-water emulsion. Accordingly, the capillary force reduces to near zero allowing the emulsion to move through the pore throats (Figure 1.12) resulting in enhanced recovery.[60]

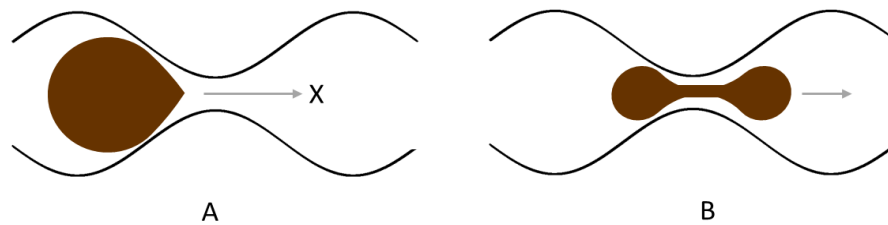


Figure 1.12 (A) A high interfacial tension results in large capillary force, which prevents the oil drop from crossing through the downstream pore throat, (B) Ultra-low interfacial tension leads to near zero capillary force, which allows the oil drop to flow through the pore throat and be produced.[59]

- ***Altering the Rock Wettability:*** The wettability of a porous rock formation is an essential factor to be taken into account in its characterisation because of its impact on the bond between oil and rock, the multiphase flow behaviour and distribution of fluid saturations in the reservoir.[108] Wettability alteration may occur in the foam flooding process due to the interactions between the surfactants used and the rock surface.[59] According to Equation 1.6, the capillary number can also be increased by changing the contact angle, which means altering the rock wettability. As mentioned before, increasing the capillary number can result in low residual oil.[59] The importance of wettability alteration is not often considered in both experimental and simulation work, because of the erroneous assumption that all rocks remain water-wet during foam injection and it is difficult to quantify the reservoir wettability in a meaningful and repeatable manner.[130] Although Rai and Bernard et al.[131] do not agree that wettability may change due to a foaming agent, in a number of other studies, wettability alteration due the surfactant adsorption has been reported to change porous rocks from oil-wet to water-wet.[131-133]

Overall, the foam injection process can enhance the oil recovery by mobility control in combination with ultra-low IFT and possible alteration of the rock wettability due to the presence of surfactant in the foam.

1.4.2.3 Challenges and Field Application for Gas-Foam EOR

The application of the gas-foam process in oil fields for mobility control has shown to be technically and economically challenging. This is because the effectiveness of a gas foam flooding highly depends on several parameters such as oil type, oil and water saturation, brine salinity and pH, surfactant formulation and concentration, reservoir heterogeneity, capillary pressure and gas flow rate.[134, 135] For example, a high oil saturation and low water saturation in the presence of light oil may cause the foam to decay and collapse.[136] As a consequence, before applying a foam EOR process, it is extremely important to gain a comprehensive understanding of the physical aspects of the process and how the foam may flow and behave once injected through a porous rock formation. The two main broad technical and operational difficulties in applying foam-EOR at the large field scale are described below.

- Foam Stability and Propagation:*** According to the numerous studies conducted to date, it may be difficult to achieve a stable and reliable foam generation under the harsh reservoir condition (high temperature and high salinity) often encountered and also control the propagation of the foam over large distances in the reservoir scale. Under high salinity and high temperature, the gas-foam cannot be stabilised with the surfactant, because under such conditions the surfactant solubility in water or CO₂ would be reduced resulting in its precipitation onto the rock surface.[115, 137] In addition, with the loss of the surfactant, the necessary ultra-low IFT may not be achievable.[138, 139] The level of oil and water saturations are other parameters that affect foam stability. Mayberry et al.[140] examined the foam strength at different oil and water saturations. Their experimental results indicate that the apparent foam viscosity is significantly reduced at oil saturations greater or lower than a critical oil saturation. The presence of the oil in the formation has a strong effect on the foam rupture, and breakdown due to the interactions occurring between the foam lamellae and the oil phase.[141] Law et al.[142] also found that foam is degraded if the oil saturation exceeds critical foaming oil saturation of the surfactant. It is also shown that the light and less viscous oils are more destructive to foam stability than heavy oils.[136] Moreover, the reservoir water saturation is crucial for the foam stability. When a foam is injected at water saturations below a critical value, which corresponds to a limiting capillary pressure, the foam may begin to coalesce and dry out. It should be noted that below the critical water saturation and above the critical oil saturation the foam is eliminated.[56, 136]
- Scale up from Pilot to Full Field Application:*** There have been several CO₂-foam trials performed since 1990 mainly in the United States.[143-145] Some of these, such as that performed in Joffre Viking oil field, were unsuccessful, because of the foam propagation control failure.[146] On the other hand, a few of the pilot tests have been successful, including that conducted in the Rock Creek Field[147] and Northward-Estes Field. In Northward-Estes Field, it was observed that the foam injection led to reduced CO₂ injectivity by 40 to 85%.[143] Several other pilot studies were conducted using CO₂-foam in East Vacuum Grayberg/San Andreas Unit[148] and SACROC Field in West

Texas,[149, 150] all of which proved that CO₂ mobility could be reduced and oil production increased. However, a transition from pilot-scale to a wider field application have not been implemented due to various challenges such as issues associated with chemical supply and transportation, processing and separation of the produced fluids, offshore supply and also safety concern.[151-154]

1.4.3 Direct Gas Thickeners

The use of direct gas thickeners is another method that brings together the combined possible advantages of using chemical additives and MGI. This technique has been recognised as a “game-changing technology” for mobility control, which was first reported in late 1960.[68, 69, 72, 155] Since then, the interest in synthesising and designing affordable gas thickeners has been carrying on steadily. However, until now the term “gas thickener” has been used in laboratory investigations only and its effectiveness has not yet been verified in any field-scale applications around the world. In general, this technique involves increasing the injected gas viscosity by directly adding chemicals that exhibit good solubility in common supercritical fluids (SCF) used for EOR such as CO₂ or hydrocarbon solvents. Chemicals that may increase the viscosity of a SCF include entrainers, conventional oligomers and polymers and small associating compounds.[156] In an ideal situation, chemical compounds need to be readily soluble in the dense CO₂ or hydrocarbons solvents and insoluble in both crude oil and brine at reservoir conditions.[52] It should be noted that the thickening level of the gas is not expected to affect its injectivity because this solution would exhibit a shear-thinning behaviour near the wellbore which facilitates the mobility of the thickened gas in this area but the mobility ratio of the gas flood would be improved in the bulk of the rock formation leading to enhanced recovery (Figure 1.13). In addition, the thickened gas would uniformly flow into different zones, allowing the gas to also mobilise the trapped oil in the low permeable zones. In other words, this technique can be applied as a way of improving the flood conformance and mobility control as illustrated in Figure 1.13.

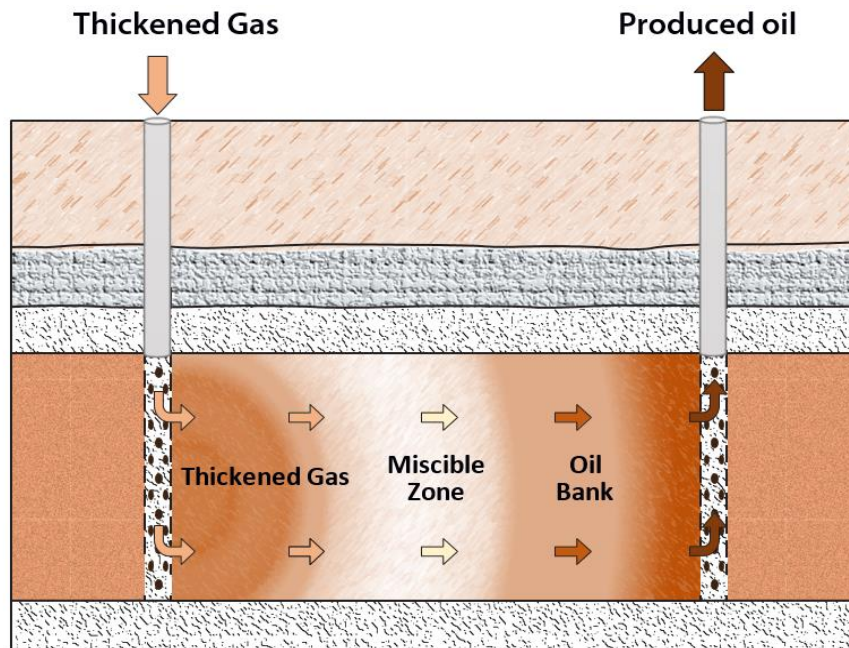


Figure 1.13 Simplified illustration of a thickened gas flooding

Two fundamental strategies have been introduced in the literature to increase the injected gas viscosity:[157]

- Direct Dissolution of Polymers:*** In this strategy, a gas thickener is typically a synthesised or identified polymer or oligomer that promotes attractive interactions and dissolution with gas molecules. However, it has been recognised that the use of polymers with extraordinary molecular weight for the above purpose would be quite challenging since most of the SCF fluids are very stable and weak solvents due to the very low dielectric constant, no dipole momentum and sometimes low density. The intermolecular attractions between the polymer molecules are typically strong enough at ambient temperature so that even stirring them would be insufficient to attain dissolution. Therefore, they may only dissolve in a gas solvent at elevated pressure and temperature because such conditions give rise to the intermolecular forces between the solvent-polymer segments, or solvent-solvent or polymer segment-segment pairs in the solution given by difference on the free volume between the polymer and gas solvent and the free energy.[158] In addition, heat may be required too weaken intermolecular interactions between the polymer molecules (e.g. hydrogen bond).[158] Another approach for obtaining high solubility of the polymer in solvents is to

introduce associating or functional groups in the polymer's molecular chains, for example to become CO₂ philic, and therefore assist the polymer dissolution in the solvent.[159, 160] Some examples of the associated polymers include polyvinyl acetate (PVAc), oligo (3-acetoxy oxetane), poly [(1-O-(vinyl-2, 3, 4, 6-tetra-O-acetyl-β-D-glucopyranoside))] and amorphous polylactic acid.[161, 162] Once the molecules of the polymer are dissolved in the solvent, the intermolecular/intramolecular association may occur which would result in an increased solution viscosity. Some of the polymers can increase the solvent viscosity significantly by simply changing the thickener concentration or by twining their molecular structure like a hair between different polymer chains.[163]

- ***Dissolution of Small Molecules (Self-Assembling and Associating Compound)***: The second strategy is focusing on the design of small molecules material that contain a self-assembling and associating compound to form a viscosity-enhancing supramolecular network structure in the solution. Such a material contains an associating group composed of a solvent philic segment that facilitates dissolution and one or more solvent-phobic segments that would induce the intramolecular association with neighboring molecules, thereby molecular association establishing a viscosity enhancement for the solution, but its impact on viscosity could be minimal.[72] The small molecules thickeners have shown little success to thicken CO₂ and light alkane solvents primarily because these are regarded as weak solvents for the ionic and polar associating compounds that are commonly composed into the small molecules thickeners.[71, 157]

Overall, a polymeric or small molecules compound thickener capable of dissolving into CO₂ or light hydrocarbon solvents has to be identified to increase the solution viscosity under typical field conditions. The ideal chemical additives are those that can effectively increase the viscosity of the injected gas very close to that of the crude oil. Furthermore, a viscosified gas used for EOR has to be transparent and single phase rather than opaque viscous solution in order to be capable of flowing through micro-pore throats in rock formations.[157] A viscosified gas with the above described desirable characteristics used for an MGI process can suppress the gas mobility in the reservoir reducing the severity of viscous fingering and the chance of developing

premature gas breakthrough and high production gas oil ratio (GOR). As a result, the sweep efficiency would be improved for the gas flood. Various studies conducted over the past several decades have resulted in successful laboratory-scale progress in thickening of CO₂ and NGL (natural gas liquefied). The successful CO₂ thickeners include the fluoroacrylate-styrene copolymer polyFAST and poly(dimethylsiloxane)-toluene solutions.[160] These two thickeners have been found to be capable of increasing the CO₂ viscosity by approximately 10 and 4 fold, respectively, at dilute concentrations.[160] A drag-reducing agent (DRA) poly(α -olefin) was presented as the most significant thickener that can increase the viscosity of the NGL.[164] A detailed review of all the previous attempts made to synthesise and/or identify the polymeric and small molecules material suitable for thickening CO₂ and light hydrocarbon solvents will be presented in Chapter 2.

1.4.3.1 Challenges and Opportunity for Gas Thickeners

The use of gas thickeners has the potential to eliminate many of the earlier mentioned challenges and difficulties associated with WAG and gas-foam injections. However, the discovery of inexpensive polymers or small molecules materials soluble in CO₂ or alkane solvents has so far been a major challenge. Furthermore, the performance of none of the identified or synthesised thickeners has been verified in even a field pilot test yet.

In general, the following challenges have hindered the identification of effective thickeners that could be used for a gas flood:

- **Thickener Solubility:** The attainment of adequate solubility has been the primary obstacle in finding viable thickeners because most of the designed and identified polymers for the CO₂ and hydrocarbon gases exhibit extremely low solubility unless a large volume of a co-solvent (e.g., 10-15 wt% toluene) is added. The reason behind this problem is that CO₂ and alkane gases are poor solvents for extremely high molecular weight, polar and ionic associated groups that are composed in small molecules thickeners. The alkane gases (methane and ethane) do not have dipole or quadruple moments, so the dispersion interactions are dominant with these solvents. Thereby, alkane gases would not be suitable SCF solvents unless the density of these solvents is increased considerably by increasing the system pressure.

Unlike alkane gases, CO₂ has a substantial quadrupole moment that induces quadruple interaction as the temperature is low.[158] In addition, CO₂ acts as a Lewis acid for the polymers containing oxygen.[165] In general, as mentioned before, a polymeric CO₂ thickener needs to contain a CO₂-philic function group that facilitates the polymer solubility and CO₂-phobic function group that promotes intermolecular associations to enhance the viscosity.[166] To date, solubility remains a key major challenge in the identification of an inexpensive thickener for CO₂ and hydrocarbon solvents.

- ***Cost and environmental persistence:*** The high price and environmental issues are other challenges that impede the use of the identified or developed thickeners to date in field applications. In fact, most of such thickeners are unaffordable and/or unavailable in large enough quantities. The requirement of an organic co-solvent to obtain the necessary dissolution levels further adds to the cost. Moreover, some of the developed thickeners, such as fluoroacrylate-styrene copolymers (polyFAST) and semi-fluorinated trialkyltin fluorides, are fluorinated compounds that contain Fluorine. These thickeners have been identified as the best thickeners for CO₂ and NGL, respectively. However, the Fluorine in these thickeners would bring about potential negative effects on the environment making them unsuitable for EOR applications.[52, 72, 157, 160]

1.4.4 Mobility control: Field A

Overall, from the discussions presented so far, it is clear that each of the proposed mobility control methods, as applicable to an MGI process, has its own challenges and deficiencies. The possible field-scale implementation of each method often depends primarily on the in-situ conditions and specific characteristics of the field of interest. The objective of this section of the chapter is to present an evaluation of the applicability of each of the techniques discussed earlier in Field A given its specific conditions and characteristics.

- ***WAG Technique:*** As mentioned earlier, in field applications, the WAG process has been applied successfully in a number of oil fields around the world.[74, 75] A total of 72 field-scale miscible and immiscible WAG

projects were reviewed by Skauge et al. that have utilised hydrocarbon or non-hydrocarbon gases. Majority of these projects have been successful resulting in incremental oil recoveries in the range of 5-10% of OIIP. For successful projects, the WAG process consistently yielded better oil recovery than that could be achieved with continuous gas injection even though, often, a large amount of oil (35-65 % of OIIP) would still be left behind.[52] Some of reviewed projects have also been unsuccessful due to operational and/or reservoir related difficulties such as gas gravity segregation, extreme reservoir heterogeneity, excessive water production, corrosion, scale and/or hydrate formation, etc.[74] In the case of Field A, in-situ water saturation is very low (<10%) and, therefore, the field surface facilities and well completions are not designed to inject or handle large amounts of water. Therefore, the WAG strategy is not the best choice to implement in this field.

- ***Gas Foam Technique:*** It was previously discussed that the gas foam injection process has been tried at the pilot-scale in some fields in the US and Canada. However, this technique has never been performed in any field in the Middle East due to the difficulties of finding a suitable surfactant (water soluble) or due to the harsh reservoir conditions encountered including high salinity and high temperature. Although there have been a number of laboratory-scale studies done to date evaluating the application of the technique under conditions encountered in this region. For example, in a recent study conducted by Sumaiti et al.[56, 111], the foamability and mobility of CO₂-ethoxylated amine in carbonate cores was investigated at a salinity of 220,000 ppm and a temperature of 393 K. The foamability of Ethomeen (C₁₂) and apparent foam viscosity increase were confirmed at these conditions. In addition, CO₂-foam core flooding obtained 8.89% of additional oil recovery. However, the availability of CO₂ is very limited in the Middle East. Concerning Field A, the reservoir presents a harsh environment with a formation brine salinity of 275,000 ppm and a reservoir temperature of 377 K with low in-situ water saturation and a very light oil (42°API). It is extremely difficult to find a surfactant, especially water-soluble, that can work under these conditions. For the CO₂-foam process, there is a lack of adequate CO₂ availability in Oman. As a result, it is expected that achieving

adequate foam stability would be a major challenge to implement a gas-foam process in Field A.

- ***Direct Thickened Technique:*** As discussed earlier, several laboratory-scale studies have been conducted to date to find and/or develop direct thickeners for CO₂ and NGL. However, the cost and environmental issues associated with these thickeners have prevented their application outside the laboratory.[167] In addition, none of the identified thickeners (non-fluorous), as presented in the literature, have been tested for their performance at high temperatures (<373 K) or evaluated specifically as direct thickeners for an AG mixture. As outlined earlier, this technique has several distinct advantages compared to the other two mobility/conformance control techniques of WAG and gas-foam injection. Firstly, a screened thickener additive would be thermodynamically stable and chemically inert (with no or minimal interaction with reservoir sediments), making it ideal for application in harsh reservoir conditions (i.e., high formation salinity and temperature). Secondly, the gas viscosity increase achievable by a thickener does not depend on rock characteristics, properties and saturations of other fluids in the reservoir and injection flow rates. Thirdly, it eliminates the need for water co-injection which minimises the chance of excessive water production and treatment requirements substantially and eliminates the water blocking effect too. Lastly, it has been demonstrated at the laboratory-scale that this technique can increase the sweep efficiency considerably because of delayed gas breakthrough and improved gas mobility. Hence, it is believed that CO₂ or AG mixture thickening may be the only viable technique for Field A to counteract unfavourable mobility conditions present in the Field and further enhance the oil recovery of the current ongoing MGI.

1.5 Research Objectives

The main objective of this research is to identify, and test chemical additives that can be dissolved in either CO₂ or hydrocarbon gases enriched with CO₂ to form a thickened gaseous phase in high pressure and temperature reservoirs. This thickened gaseous phase could then be used as the injection fluid during MGI to mitigate the

unstable displacement in the reservoir. In other words, the thickened gas would help to control the gas mobility and possible channeling through any existing high-permeability streaks in the reservoir and eventually lead to improved sweep efficiency. Furthermore, this research aims to develop and test the applicability of the alternating thickened-unthickened gas injection as a novel technique that has a real potential to address the economic issues associated with the direct gas thickening technique. What is more, this study would examine the effectiveness of any identified chemical additive and the above alternating injection approach in the context of the complexities surrounding oil production from Field A in southern Oman.

The followings outline the specific objectives perused in conducting different phases of this research:

- Identifying any chemical additives (low/high molecular weight polymers) that can be dissolved in an AG mixture enriched with CO₂ (60 mol% methane, 6 mol% ethane, 6 mol% propane and 25 mol% CO₂) or pure CO₂, this would be accomplished by using a parallel gravimetric extraction method and cloud point pressure measurements.
- Examining a possible viscosity enhancement for the identified highly soluble additives in the AG mixture and CO₂, to form a viable thickened gas solution, using a capillary viscometer at different temperatures, pressures, and concentrations.
- Evaluating the potential and effectiveness of the thickened gas injection to improve the oil sweep efficiency by conducting reservoir condition core flooding experiments and numerical simulation using a box model. The results of this numerical simulation work could also help in deciding the level of thickening necessary to achieve measurable enhancement in the recovery.
- Developing a novel approach that can lower the volume of thickeners utilised by implementing an alternating thickened-unthickened gas injection scheme, with the performance to be determined by carrying out extensive core flooding experiments.

- A qualitative assessment of the effect of dissolved polymers in CO₂ and AG mixture on the equilibrium IFT and miscibility pressures of the gas-crude oil system using the vanishing interfacial tension (VIT) technique.

1.5.1 Thesis Organisation

As also evident from the discussions presented so far in this chapter, this thesis presents and discusses the results of a coupled experimental and numerical simulation approach to evaluate the performance of thickened AG and thickened CO₂ injection at high temperatures in an MGI process. It is organised in eight chapters to cover the introduction and background, literature review, results and discussion (five chapters), and conclusions and recommendations for future work. Provided below is a short description of the contents of all eight chapters presented according to the way they appear in the thesis from the beginning to the end.

Chapter 1- Introduction and Background—At the highest level, this chapter may be divided into four consecutive sections. The initial part provides a broad introduction and background to the EOR techniques used worldwide as well as those implemented in Oman oil fields and briefly discusses their critical importance. The second part covers the technical details of the MGI process and the potential problems and challenges associated with it, while the third part focuses mainly on the common techniques used to control gas mobility during gas flooding including MGI. The impediments and challenges for wide application of the mobility control techniques and a statement of the problem addressed by this research are also presented in this part. The last section of this chapter presents the objectives of the current study and thesis organisation.

Chapter 2- Literature reviewer: Previous Attempts at Thickening Gases — This chapter presents a comprehensive review of previously developed and/or identified polymeric and small molecule thickeners to increase the viscosity of injected gases. The first part of this chapter covers the previous attempts made to thicken CO₂, while the second part describes those relevant to hydrocarbon gas components (ethane, propane, and butane). The reviewed literature cover the studies aimed at controlling the gas mobility during EOR gas floods as well as those focused on enhancing productivity in tight reservoirs via hydraulic fracturing.

Chapter 3- *A Numerical Study of Using Polymers to Improve the Gas Flooding in the Harweel Cluster, SPE-185999-MS*—This chapter presents the details of a mechanistic or box model numerical simulation study, which was performed to assess the potential benefits of adding polymers to the injected gas for mobility control. Considering the composition of the AG in Field A, this study gives a preliminary evaluation of the level of viscosity enhancement required to improve the gas mobility favourably towards further enhancement in oil recovery in Field A.

Chapter 4- *Experimental Study of Miscible Thickened Natural Gas Injection for Enhanced Oil Recovery, Energy & Fuels 31, no. 5 (2017): 4951-4965*— This Chapter assesses the suitability of a library of polymers and oligomers to thicken AG as a means of mobility control. Firstly, the solubility of the polymers and oligomers in an AG mixture were determined using a parallel gravimetric extraction technique combined with cloud point pressure measurements. Then, the achievable viscosity enhancements by the identified soluble candidates in the AG mixture was measured in a capillary viscometer at reservoir conditions. Furthermore, core flooding experiments were performed to examine the effectiveness of the thickened AG gas mixture to enhance oil recovery under reservoir conditions.

Chapter 5- *Experimental Evaluations of Polymeric Solubility and Thickeners for Supercritical CO₂ at High Temperature for Enhanced Oil Recovery, Energy & Fuels 32, no. 2 (2018): 1600-1611* — This chapter presents the solubility and thickening results of a library of commercially available polymers/oligomers to thicken CO₂ at a high temperature.

Chapter 6- *A New Approach to Alternating Thickened-Unthickened gas Flooding for Enhanced oil Recovery, Industrial & Engineering Chemistry Research 57, no. 43 (2018): 14637-14647* — This chapter covers the details of a new alternating injection approach developed in this study that can lower the volume of thickeners required during field-scale application of a thickened gas flood. It presents and discusses the results of a detailed core flooding program conducted to evaluate the performance alternating thickened-unthickened gas injection (similar to water-alternating-gas (WAG)) as compared with a continuous thickened/unthickened gas injection.

Chapter 7- *Effects of Oligomers Dissolved in CO₂ or Associated Gas on IFT and Miscibility Pressure with a Gas-light Crude Oil System, Journal of the Taiwan*

Institute of Chemical Engineers (2019): under review – This chapter examines the phase behaviour of poly (1-decene) (P-1-D) in the AG mixture and CO₂ and the phase behaviour of poly (ethyl vinyl ether) (PVEE) in CO₂. In addition, the chapter evaluates the effect of dissolved oligomers in CO₂ and AG mixture on the equilibrium IFT and miscibility pressures using the vanishing interfacial tension (VIT) technique.

Chapter 8- Conclusions and Recommendations – This chapter presents a summary of the research program, and then based on the experimental and numerical simulation results, provides a list of its key conclusions. It also provides a few recommendations for future research to be conducted in the same area.

Chapter 2. Literature Reviewer: Previous Attempts at Thickening Gases

Over the past 50 years, several research groups have attempted to increase the viscosity of gas-solvents for two purposes. The first purpose is to reduce the gas mobility and improve conformance control for miscible gas injection (MGI). By simply increasing the injected gas viscosity, gas mobility will be reduced and as a result the sweep efficiency and oil recovery would be improved. The second purpose is to thicken a supercritical fracturing fluid that is used to enhance well productivity in a tight reservoir.[157, 168, 169] This is a particularly useful technique for reservoirs that are sensitive to the typical water-based fluids used for fracturing. Increasing the viscosity is shown to result in a more effective fracturing fluid.[168] In addition, at high pressures, a viscous fluid would be able to propagate wider fractures by improving the transport of proppant particles and reducing the leak-off of gas into the faces of the fracture.[168-170]

In previous studies about direct gas thickening, the majority of efforts were centred on identifying CO₂ and NGL (i.e. ethane, propane, and butane) thickeners. These attempts were based on polymeric and small molecules candidates as will be reviewed and highlighted in this chapter. The mechanisms behind the thickening of any solvent depend on polymer coil expansion, association, entanglement, aggregation (depend on the polymer molecular weight distributions), self-assembly and indirectly through polymer molecules effect on nearby solvent molecules.[171]

2.1 Direct Carbon Dioxide Thickeners

2.1.1 Polymeric Thickeners

Use of a polymer thickener is one fundamental strategy for increasing CO₂ viscosity [157] and the main advantages are that the thickening process can enhance CO₂ viscosity over a wide range of temperatures and improve sweep efficiency across the reservoir formation.[52] Although high molecular weight (Mw) polymers (Mw >10⁶) are effective viscosity enhancers at dilute concentrations, it is extremely challenging to dissolve ultra-high molecular weight in dense CO₂ at reservoir conditions.[52, 72]

In the literature, several polymers ($M_w 10^3-10^6$) have been designed and identified that can be dissolved and thicken supercritical CO_2 . [168] However, the pressure required for the dissolution of these polymers is very high in the range of 68.95-275.79 MPa, which is significantly higher than the typical reservoir pressures for CO_2 flooding (MMP, 10.3-27.6 MPa). [168]

The earliest attempts at viscosity enhancers for dense CO_2 were with oil-soluble polymers (e.g., non-polar organic polymers) because CO_2 is known to be a non-polar solvent capable of dissolving certain hydrocarbons and other small molecules quite well. [52, 172] Therefore, it was expected that oil-soluble polymers would be a more likely candidate to dissolve in supercritical CO_2 compared to water-soluble polymers. Heller et al. identified 18 hydrocarbon-type polymers that exhibited encouraging solubility (0.22 to 10 g/liter) in CO_2 at pressures of 11.7-21.4 MPa and temperatures of 293-331 K. [64, 66, 173-177] Although several polymers showed a slight increase in CO_2 viscosity, none of the studied polymers were capable of enhancing the viscosity of CO_2 significantly to a useful level. This is attributed to low solubility in CO_2 leading to a random polymer coil structure that is not efficient at increasing viscosity significantly. Furthermore, the molecular weight of the polymers found to be soluble in CO_2 were very low. For example, a 1 wt% solution of low molecular weight atactic poly(methyl oxirane) ($M_w 408$) exhibited slight solubility in CO_2 and increased its viscosity by approximately 25% at 301-306 K and 13.7-17.9 MPa. [66] These initial efforts were followed by subsequent attempts to maximise the entropy of mixing between the CO_2 and polymers by using disordered polymers with irregularity in multiple components and side chains that varied in chain length. [64] Thereby, focus was put on poly(α -olefins), such as poly(1-hexene), poly(1-pentene) and poly(1-decene) (P-1-D). Although some achievements were made with some of the evaluated polymers, none of these amorphous polymers were considered to be effective thickeners primarily due to their low solubility in CO_2 . In general, it is concluded that the molecular weight of the polymers had to be fairly low ($M_w > 1000$) and thus less effective at enhance viscosity to achieve the significant measure of solubility in CO_2 . [52] Typically, high and ultra-high molecular weight polymers are used as effective thickeners. In 2012, Zhang et al. reported that less than 1 wt% solutions of two oligomers (i.e. P-1-D and poly(vinyl ethyl ether)(PVVE)) (Figure 2.1) could increase the viscosity of CO_2 by 13-14 fold at 329 K. [178] Previous research groups

Other researchers have attempted to use entrainers (co-solvents) to improve the solubility of polymers in CO₂[181] and as such increase the CO₂ viscosity as well as increase the solubility of crude oil components in the CO₂ rich phase.[182] These entrainers are relatively low molecular weight non-polar or polar organic compounds which include alcohols, glycols, ethoxylated alcohols and hydrocarbons.[182] Chullick's patent claimed that addition of alcohol and glycol would promote the solubility of polymers in CO₂. [181] The rationale is that polar entrainers improve the polarizability of CO₂, which may act in a similar manner to a surfactant in the water/oil system, while non-polar entrainers may function as mutual solvents in a polymer/CO₂ system.[181] Therefore, the addition of entrainers to a supercritical fluid (SCF) leads to increase in the solvent power of SCF.[182] Furthermore, a NIPER (National Institute for Petroleum and Energy Research) group evaluated the use the entrainers (without polymer) as CO₂ thickeners.[182] They reported substantial increase of CO₂ viscosity with high concentration of entrainers in CO₂. For example, 13 mol% of isooctane and 44 mol% of 2-ethylhexanol increased viscosity of CO₂ by 243% and 1565%, respectively. However, at dilute concentration of entrainers in CO₂, the viscosity enhancement was subtle. For example, 2 mole% of 2-ethylhexanol resulted in 24 % of CO₂ viscosity enhancement.[182] In another patent, a treating fluid was used to increase the viscosity of CO₂ solution. This treating fluid is formed by solubilising a polymer or copolymer of dimethylacrylamide (0.25-2.5 wt%) in the substantially anhydrous liquid which was crosslinked by a metal ion source (0.01-2 wt% of titanium, zirconium, and/or aluminium). The substantially anhydrous fluid/polymer and CO₂ solutions formed a single phase and viscosified fluid (13 to 30 cP) at temperatures of 338-377 K and pressures of 6.89-12 MPa).[183] Although these are significant increase in CO₂ viscosity, the amount of entrainers added is extremely higher.[52]

A group of researchers at the University of Wyoming attempted at in-situ polymerization of CO₂ soluble alkene monomers, including ethylene, octane and decene.[67] They found that polymerized monomers could be miscible in CO₂ at tested conditions (306 K and 17.9 MPa). However, the polymers did not form stable solutions and formed solid precipitates over time. As a result, no viscosity enhancement was observed. In an attempt to obtain a very high molecular weight polymeric thickener for CO₂, researchers at Chevron [63, 184, 185] have assessed candidates that exhibited

Hildebrand solubility parameters of less than $7 \text{ (cal/cc)}^{0.5}$ which is closer to the CO_2 solubility parameter at reservoir conditions (327 K and 17.2 MPa), which is approximately $6 \text{ (cal/cc)}^{0.5}$. [186] Furthermore, they found it beneficial if the polymer candidates contained electron donor atoms such as oxygen, nitrogen and sulfur that are capable of interacting favourably with the carbon atom (i.e. an electron acceptor) within the CO_2 molecules. Electron donor functional groups used in this study included ethers, sulfones, siloxanes, thioethers, silyethers, esters, carbonyls, dialkylamides and tertiary amines. The researchers concluded that such functional groups associated within polymers would enhance the solubility of the polymers to some extent through specific interaction with CO_2 . However, fully dissolution of such polymers in CO_2 could not be attained without the addition of toluene as a co-solvent. [184]

High molecular weight polydimethylsiloxane (PDMS, Mw 135,000) (Figure 2.1) was initially tested by Heller et al. [66] for solubility in CO_2 . They found that 0.03 wt% of PDMS could dissolve in CO_2 at 298 K and 18.9 MPa. However, at this dilute concentration PDMS did not appreciably enhance CO_2 viscosity. Furthermore, others attempted to increase the PDMS concentrations in CO_2 , but the solubility of PDMS in CO_2 could not be attained without substantial addition of toluene as a co-solvent. Therefore, it was determined that very high molecular weight PDMS (Mw 197,000 and $7.3 \text{ (cal/cc)}^{0.5}$) could effectively thicken CO_2 only if a toluene co-solvent (10-20%) was added into the solution. [63] For example, addition of 20 wt% toluene co-solvent enabled up to 4 wt% of PDMS to be dissolved in CO_2 , resulting in a 30-fold of CO_2 viscosity enhancement. [63] This viscosity enhancement was compared only with pure CO_2 viscosity, but it was not compared against toluene/ CO_2 viscosity, because it was expected that toluene addition into CO_2 may not contribute directly to the CO_2 viscosity enhancement and it only improves the solubility of polymer in CO_2 . However, their core flooding experiment results showed that CO_2 /toluene flood gives higher oil recovery than pure CO_2 flood. This attributes to that toluene is a strong solvent which causes a higher oil swelling and oil viscosity reduction. It was also found the viscous solution (20 wt% toluene, 4 wt% of PDMS, and 76 wt% of CO_2) can significantly reduce gas mobility, increase oil recovery (10-20%) and delay the breakthrough in porous media. In another study a group of researchers from Texas A&M University added an organic co-solvent (e.g., toluene) into CO_2 -philic polymeric thickeners (PDMS and poly(vinyl acetate) (PVAc)) during core-flooding experiments

in order to enhance the solubility in CO₂. [187, 188] They prepared solutions of PDMS (5 wt% with a Mw of 260,000) and PVAc (5 wt% with a Mw of 170,000) with a range of toluene concentrations (10-20 wt%) added as a co-solvent. In addition, PVEE was used at the concentration of 0.8 wt% in CO₂ without the addition of a co-solvent, as this polymer has the ability to dissolve in CO₂ without a co-solvent. [188] Their results proved that PDMS and PVAc with the addition of toluene could improve the gas mobility, accelerated the oil recovery (5-10% with PDMS and 4-9 % with PVAc) and delay CO₂ breakthrough. These results were consistent with the finding of Chevron researchers that 4 wt% PDMS was soluble and could thicken CO₂ with the presence of a co-solvent. In other words, both groups found that PDMS and PVAc are both to be CO₂-philic and effective thickeners with the use of substantial amounts of a co-solvent. PVEE (Mw 3800) at low concentration (0.8 wt%) did not show any increase in viscosity or improvement in CO₂ mobility and oil recovery. [188] This means that the PVEE may not be able to increase the CO₂ viscosity at this concentration which further confirms that the thickening level reported by Zhang et.al is higher than expected.

A group of researchers at the New Mexico Petroleum Recovery Research Centre (PRRC) proposed another route towards high-performance thickeners by introducing an associating group at each end of the polymer chains. [177] These polymers with terminal ionic groups (linear, difunctional and telechelic ionomers) were thought to be effective thickeners in non-polar solvents as the ionic groups in each chain could aggregate into multiple ion pairs causing interaction between separate chains. They incorporated sulfonate groups onto the ends of polyisobutylene and although the polyisobutylene is soluble in CO₂ at a concentration of 0.4 wt%, the sulfonated ionomer was only partially dissolved in CO₂ as CO₂ is a weak solvent for this ionic group. In a recent publication, O'Brien et al. [167] used a similar route proposed by PRRC group. The difference between two studies is that PRRC group used associated group in the polymer chain that forms aggregation interactions with CO₂ while the associated group proposed by O'Brien forms self-assembly and association interactions via hydrogen bond (donor-acceptor), π - π stacking, and dipole-dipole. Therefore, the strategy used by O'Brien group could be used to explore oligomeric molecules. So, they synthesised a series of aromatic-amide terminated PDMS oligomers (i.e. low molecular weight polymers) to maximise the entropic

characteristics for oligomeric species interacting with CO₂ by choosing a solute with high free volume and flexible chains. In addition, the aromatic moieties promotes the formation of supramolecular structure between the low molecular weight oligomers. Amide and amide-aromatic further enhance this interaction and induce self-assembly through strong hydrogen bond donor-acceptor interactions. The researchers found that amide-terminated-PDMS oligomers with simple aromatic groups and incorporation of electron-deficient aromatic groups onto these amides (i.e. 4-nitrobenzamide, biphenyl-4-carboxamide and anthraquinone-2-carboxamide) did not show any significant impact on CO₂ viscosity at a concentration of 1 wt% due to the inefficient associating group in these compounds with CO₂. However, they achieved promising results with anthraquinone-2-carboxamide (AQCA) as an end group where it was found to be a gelator of hexane at concentration of 15 wt% and at concentrations of 5-10 wt% in hexane, a significant increase in viscosity was observed. However, this behaviour did not extend to other similar compounds based on either biphenyl-4-carboxamide or 4-nitrobenzamide end groups. Therefore, they attempted to improve the intermolecular association with the AQCA end group by utilising branched anthraquinone amides, where the number of AQCA end groups per molecule can be increased. It was found that branched anthraquinone amides were insoluble in CO₂ at concentrations of 1 wt%. However, it was soluble in CO₂ when hexane as co-solvent was added. Hence, this branched compound can be a useful thickener in the presence of substantial amount of hexane as co-solvent. For example, at a temperature and pressure of 348 K and 34.5 MPa, respectively, a transparent solution composed of 13.3% branched anthraquinone-amide functionalised oligomers, 26.7% hexane and 60% CO₂ was found to have a viscosity 3 times greater than that of a CO₂/hexane mixture without a thickener. Given the low viscosity enhancement (3 fold) and high concentration of this compound and the co-solvent required, this compound was not considered to be economical and practical for CO₂ flooding. The associating small molecules compounds would be further discussed in the next section of this chapter. Overall, all studies found that high/low molecular weight PDMS polymers were more CO₂-philic than hydrocarbon-based polymers,[189] although they were not capable of viscosifying CO₂ without the use of substantial amounts of a co-solvent. However, the high cost of PDMS polymer/oligomer and high concentration of co-solvent required make the field application for this polymer impractical.[52, 72, 157]

DeSimone research group[190] was arguably among the first to report on a high molecular weight polymer-based CO₂ thickener capable of increasing viscosity without the need of a co-solvent. They found that 3.4 wt/v% of either poly(1-,1-, dihydroperfluorooctyl acrylate (PFOA)) (Figure 2.1) or polyfluoroacrylate (PFA, Mw 1,400,000) could be dissolved in CO₂ and remarkably increase the viscosity of CO₂ by a factor of 2.5 at a pressure of 31 MPa and temperature of 323 K. Figure 2.2 shows the increase in CO₂ viscosity resulted from the dissolution of 3.7 wt/v% and 6.7 wt/v% of PFOA at 323K. This is the first example of high Mw polymers that can be dissolved in CO₂ and significantly thicken CO₂ in the absence of a co-solvent. To date, PFOA is still recognised as the most soluble polymer in CO₂ and among the most effective thickeners of CO₂. Unfortunately, PFOA is a fluoropolymer type, which makes it relatively expensive. Furthermore, fluorinated polymers have environmental concerns and there is a high potential risk that PFOA is a suspected carcinogen.[161] Therefore, if the cost and environmental constraints are considered, PFOA is not practical for field application in CO₂ flooding.[157]

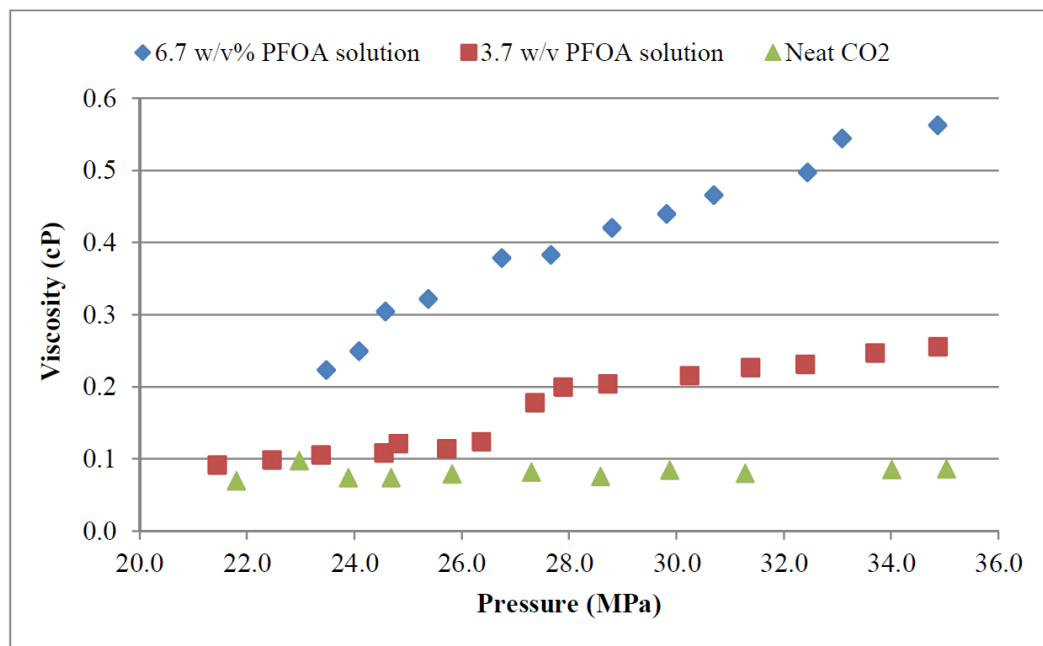


Figure 2.2 The viscosity enhancements of PFOA in CO₂ at different pressures and concentrations and temperature of 323 K.[190]

To limit these negative aspects of fluorinated polymers and potentially make them viable, Enick and Beckman and others co-workers at the University of Pittsburgh have tried to reduce the amount of fluorinated polymers needed without affecting its

performance.[156, 170, 191] They prepared a copolymer based on a perfluoropolyacrylate and associative group which engages strongly in intermolecular interactions, in order to promote an increase in CO₂ viscosity. This copolymer is composed of 71-79 mol% of fluoroacrylate monomer (1-,1-,2-,2-tetrahydro heptaecfluorodecylacrylate) and 21-29 mol% of styrene-associative group (polyfluoroacrylate styrene or polyFAST) (Figure 2.1). The fluoroacrylate monomer is highly CO₂-philic and facilitates polyFAST solubility in CO₂. The associating styrene group is a mildly CO₂ phobic monomer that promotes intermolecular interactions and improves viscosity enhancement through supramolecular interactions. This copolymer was found to be soluble in CO₂ at pressure and temperature conditions close to those used in CO₂-EOR.[156] However, the solubility was found to decrease with an increase in the styrene content.[170] For instance, the cloud point pressure of 1 wt% of 29 mol% styrene-71 mol% fluoroacrylate copolymer and 35 mol% styrene-71 mol% fluoroacrylate copolymer in CO₂ at 297 K are 12 MPa and 16.2 MPa, respectively. Furthermore, it was also found to significantly increase CO₂ viscosity at dilute concentrations of polyFAST. As it can be seen in Figure 2.3, 0.5 wt% and 1 wt% of polyFAST in CO₂ at 298 K are able to increase the viscosity of CO₂ by 1.5 and 2.3 fold, respectively.[156] Although polyFAST is the most effective polymeric thickener for CO₂ at dilute concentration in the absence of a co-solvent. Comparing to PFOA results, this copolymer was successful to reduce concentration by 73 % to achieve the same viscosity improvement (2.3 fold) at 323K and 34 MPa. However, It was not practical to be used for CO₂-EOR application due to the cost of the copolymer (roughly \$132 per kg) and lack of its availability in large quantities.[157] In addition, this copolymer contains a large amount of fluorine, which is environmentally and biologically persistent.[188]

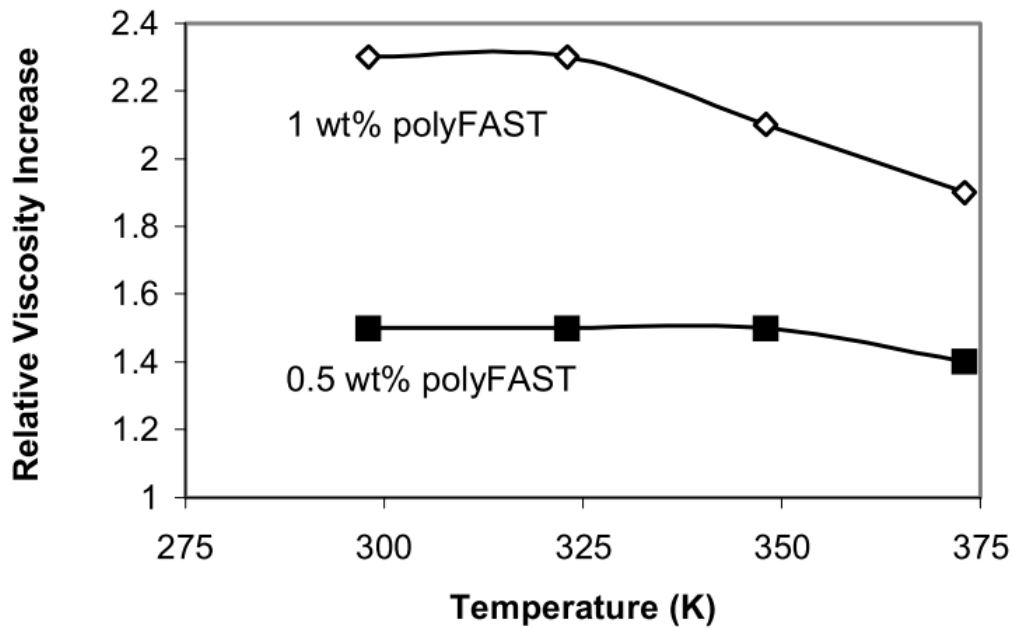


Figure 2.3 The effect of temperature on the relative viscosity of polyFAST in CO₂ solution at 34 MPa.[191]

Another promising strategy to obtain effective CO₂ thickeners was introduced to avoid the aforementioned environmental and economic concerns associated with fluorinated and silicone-based polymers. Several researchers have focused on the synthesis and design of non-fluorinated oligomers and polymers. Tapriyal et al.[162] found that PVAc is the second most CO₂ soluble polymer among non-fluorinated polymers with PDMS being the most soluble. However, the dissolution of high Mw PVAc in CO₂ requires a very high pressure. In addition, no measureable viscosity increase was observed with 1-2 wt% of PVAc (Mw 11000) in CO₂ at 298 K and 64 MPa. Furthermore, Enick and co-workers[162] designed a non-fluorinated version of PFOA in the hopes of finding a thickener candidate that is cheap, environmentally friendly and capable of increasing CO₂ viscosity at low concentration. Therefore, they developed new copolymers based on an oxygenated hydrocarbon polymer (making it CO₂-philic) and an associating group (or CO₂-phobic) to enhance viscosity. Some of the attractive oxygenated hydrocarbon monomers include vinyl acetate, alkyl vinyl ether, carbonyl, and sugar acetate functional groups.[165, 192-197] Oxygenated hydrocarbon monomers containing functional groups with one or more oxygen atoms can induce thermodynamic interactions with CO₂. These oxygen atoms are electropositive while the carbon atoms in CO₂ are electronegative, which facilitates

Lewis acid-base interactions. In addition, the hydrogen bond in the polymer backbone or side chain having increased the positive charge ($H^{\delta+}O$) acts Lewis acids toward electron the oxygen atoms in CO_2 .^[165] As mentioned above, PVAc is among the most CO_2 -philic of high MW oxygenated hydrocarbon polymers.^[197] Therefore, Enick and co-workers replaced the fluoroacrylates in polyFAST with vinyl acetate monomers in order to reduce the cost and design non-fluorous copolymer for CO_2 solubility, while the styrene group was replaced with a benzoyl group for intermolecular association and also to simplify the synthesis as styrene cannot be polymerised with vinyl acetate monomer due to the large reactivity ratios difference.^[162] They synthesised a 5% benzoyl-95% vinyl acetate copolymer or polyBOVA (Mw 7840). A modest increase in CO_2 viscosity of 40-80% at a concentration of a 1 and 2 wt% was observed; however, high pressure was required (64 MPa) to attain the dissolution of this copolymer in CO_2 at 298 K.

2.1.2 Small Molecules Self-Associating Thickeners

An alternate strategy to increase the viscosity of CO_2 is to employ self-associating low molecular weight compounds as thickeners. In order to differentiate between this class of compounds and co-solvents, these compounds as summarised in Chapter 1 as well are associating and self-assembling compounds that contain a solvent-philic group and a solvent-phobic segment while a co-solvent is a non-associated compound composed solely of a solvent-philic segment.^[72] Therefore, the small molecules compounds do not have the requisite molecular weight to substantially increase the gas viscosity, because the molecules in this compound have capability to associate and form a supramolecular network for CO_2 viscosity-enhancing.^[157] In general, these compounds contain functional groups with both CO_2 -philic segments that promotes dissolution and CO_2 -phobic moieties that induce intermolecular association.^[198] Therefore, the various associations between neighboring molecules within the CO_2 matrix lead to viscosity enhancement.^[157] Furthermore, the self-assembly of these molecules in solution can be characterised via a dramatic viscosity change or small angle neutron scattering (SANS), FT-IR, circular dichroism, x-ray diffraction, electron microscopy or differential scanning calorimetry.^[199-207] To date, small associating molecules have yielded little success in thickening CO_2 because CO_2 is a poor solvent for the ionic and polar associating groups, which are inherently

necessary to increase viscosity using small molecule compounds.[172] Based on the previous attempts, the small molecules used to thicken CO₂ are mainly classified as follows.

2.1.2.1 Trialkyltin Fluorides and Semi-Fluorinated Trialkyltin Fluorides

Heller and co-workers studied a series of trialkyltin fluorides compounds as light alkane and CO₂ thickeners.[174, 176, 198] These compounds show a moderate increase in CO₂ viscosity via the formation of intermolecular association between the tin and fluorine atoms in the solution. Figure 2.4 shows the association of tributyltin fluoride molecules. Trialkyltin fluoride forms a long linear transient polymeric chain through intermolecular association between the tin atom and fluorine atom of neighbouring molecules. In fact, the tin atom is slightly electropositive which interacts with the electronegative fluorine atom to form an intermolecular Sn-F association, as can be seen in Figure 2.4. While the hydrocarbon arms branching from the tin atom enhance the free volume which facilitates the solubility in CO₂. [166] Apparently, these molecular structures form linear and associating structures in which the alkyl arms stabilise the aggregation, while the tin atoms in each molecule associate with the fluorine atoms in adjacent neighbour molecule. [166] Although there was some success with tributyltin fluoride or other trialkyltin fluorides in thickening light alkane components, these compounds were insoluble in CO₂ and ineffective as thickeners, even with the addition of pentane as a co-solvent. [208, 209] Later on, Shi et al. [166] synthesised semi-fluorinated trialkyltin fluorides and fluorinated telechelic ionomers to prepare a solution containing both CO₂-philic fluorinated groups to enhance the solubility and CO₂-phobic associating group to promote intramolecular association for viscosity enhancement. Both ionomers were soluble in CO₂ at 2-4 wt% without requiring the addition of a co-solvent. Their results indicated that both ionomers were capable of increasing the viscosity of CO₂ by 2-3 fold over a concentration range of 2-4 wt%. For example, at 4 wt% of tri(2-perfluorobutyl ethyl) tin fluoride in CO₂, the viscosity increased 3 times at 298 K and 16.5 MPa. This viscosity increase was found to be much less than expected because the side-chain fluorine atoms on the Sn-F associations were disrupted. This is attributed to the fluorine atom at the end alkyl arms competing with the fluorine atom attached to the tin atom caused by the electronegativity differences between these chain-end fluorines and those adjacent to

the tin. Hence, the disruption the of fluorinated alkyl chains is responsible for the viscosity increase.[166] Overall, given the necessary high concentrations of the ionomers required and their high costs, these fluorinate oligomers are not considered viable thickeners for field application.[52, 157, 166]

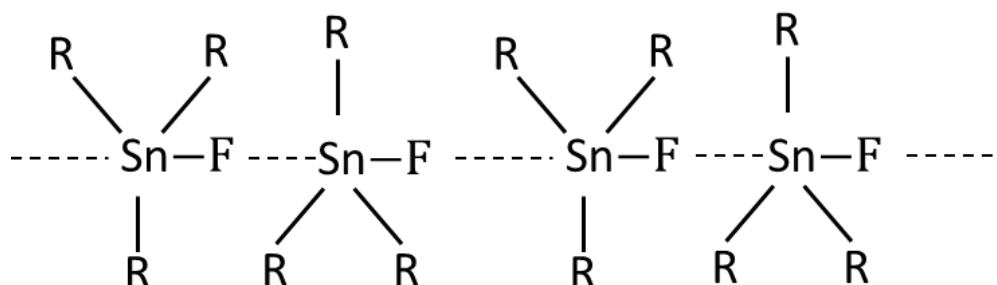


Figure 2.4 Association mechanism of tributyltin fluoride.[210]

2.1.2.2 Fluorinated and Non-Fluorous Hydroxyaluminum Disoaps

Hydroxyaluminum disoaps were developed to thicken gasoline which was used to make napalm which was an infamous weapon type used in World War II.[211-213] These molecules are an aluminium-based soap with two carboxylic acid groups linked to the aluminium atom.[214] A small amount of hydroxyaluminum disoap added to low viscosity gasoline transforms it to a thick and extremely viscous fluid referred as napalm. In an analogous manner, these compounds were studied to determine their solubility in CO₂ and quantify their ability to thicken CO₂. Enick and co-workers synthesised a series of hydroxyaluminum disoaps.[65] Unfortunately, none of the hydroxyaluminum disoaps were soluble in CO₂. Similar to the results with trialkyl tin compounds summarised above, unpublished results by Enick showed that the solubility of some of these compounds in CO₂ could be enhanced either by fluorinating the alkyl arms or using highly branched alkyl chains.[157] However, this trial has not been successful in fully dissolving the hydroxyaluminum disoaps in CO₂. [157] Another attempt to thicken CO₂ was done by heating a mixture of CO₂ and metallic stearate powders.[215] Metal stearates are salts which are produced from the reaction of stearic acid and metal oxide. When dissolved in hydrocarbon-based oils usually with the assistance of heat to break up strong intermolecular forces, the viscosity is enhanced when the solution cools down. This same approach was attempted with CO₂; however, this was unsuccessful as they are insoluble even with the assistance of heat.

2.1.2.3 Semi-Fluorinated Alkanes

Iezzi and co-workers[216] made an early attempt to thicken CO₂ by using semi-fluorinated alkanes. They designed a series of linear diblock alkane compounds (F(CF₂)_n (CH₂)_m H) which contained two immiscible segments forced to interact via a covalent carbon-carbon bond. It is found this compound can gel organic liquid (e.g. decane and octane) through the formation of micro-fibrillar network if the solution is heated and then leave it to cool down. After the solution (CO₂ and semi-fluorinated alkane) cools, the semi-fluorinated compounds form a covalent cross-link between molecules, high porosity and micro-fibrillar networks that can gel the dense CO₂. The fluorinated segments stack with other adjacent fluorinated segments (analogous to hydrocarbon segments) to form the fibres network.[72, 208] However, the gel solution is not suitable for gas mobility control due to its phase behaviour where the viscous solution could not flow through a porous medium and retained at the surface of the rock. This solution may be applicable for conformance control to block fractures or high permeable zones.

2.1.2.4 Hydroxystearic Acid

Heller and co-workers[217] proposed a small organic compound, known as 12-hydroxystearic acid (HAS). This compound (H₃C(CH₂)₅ CHOH(CH₂)₁₀COOH), had previously been used to gel hydrocarbon and chlorinated solvents. However, the essential assessment results indicated that the HAS was insoluble in CO₂ unless a significant amount of a co-solvent (i.e. ethanol) was added. For instance, the addition of 15 wt% of ethanol co-solvent enabled a solubility of up to 3 wt% of HAS in CO₂ resulting in a nearly 100-fold increase in viscosity in the temperature range of 300-307 K. As the temperatures decrease, the solution exhibits a slight viscosity increase. In addition, the presence of micro-fibers in the gel solution forms an opaque solution that would probably impede the fluid flow in the reservoir formation.

2.1.2.5 Fluorinated and Non-Fluorinated Bis-Ureas

A group of researchers at Yale University and the University of Pittsburgh developed a series of small molecules compounds associated with either one or two urea groups.[218] The urea groups in these compounds induce self-assembly interactions via a hydrogen bond, thereby these interactions form macromolecular

associations that can enhance the viscosity of the CO₂ rich solution. Out of the twelve compounds tested, four fluorinated bis-urea compounds were highly soluble in CO₂ without needing heat and capable of improving the CO₂ viscosity by 3-5 fold at 5 wt% of bis-urea at 298 K and 31 MPa. In the hopes of obtaining a non-fluorous bis-urea, Paik et al.[219] attempted to incorporate the CO₂-philic groups (hydrocarbon, carbonyl and ether groups) into the molecular structure of the bis-urea as illustrated in Figure 2.5. However, their assessment results revealed that after forming a transparent solution, micro-fibres began to form slowly due to the molecules undergoing self-assembly and precipitating out of solution. Therefore, these compounds cannot be considered for EOR applications.

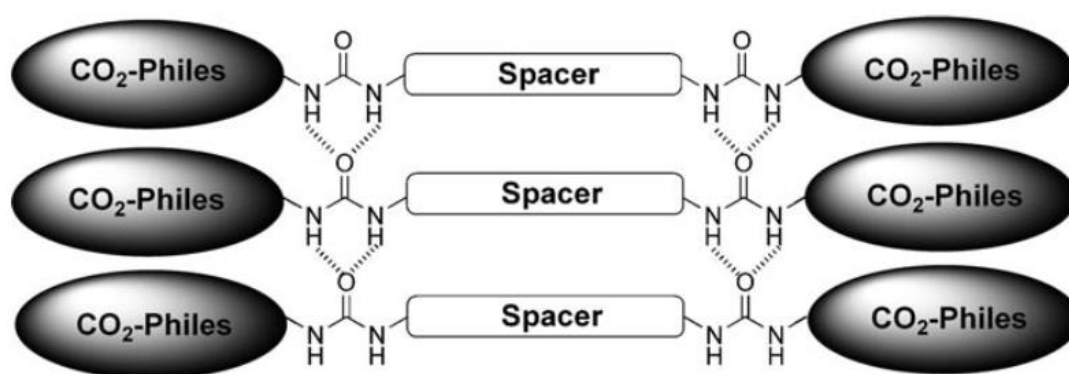


Figure 2.5 Molecular structure of a non-fluorous bisures.[219]

2.1.2.6 Surfactants with Twin and Divalent Metal Cations

Eastoe and co-workers designed semi-fluorinated surfactants based on a previous study that used aerosol-OT (AOT) based water-in-oil micro-emulsions in cyclohexane solvent.[203, 220, 221] The molecular structure of these surfactants are illustrated in Figure 2.6 and were soluble in CO₂. They form rodlike micelles that enhanced CO₂ viscosity with the addition of a small amount of water. The purpose of adding water into the solution is to form a stable microemulsion in the presence of AOT surfactant and also promote an aggregate shape change of surfactant from spheroid (non-viscous) to rod shape (viscous) which significantly contributes to the viscosity enhancement of the solution. Two di-chain perfluorinated sulfosuccinate surfactants (nickel bis-nonofluoropentane sulfosuccinate (Ni-diHCF₄) and sodium pentadecfluoro-5-dodecyl sulfate (NaF₇H₄)) yielded the greatest viscosity increase among the compounds assessed. These surfactants have been modified in such way that can form rod-like micelles to promote the viscosity enhancement and also soluble in CO₂. This was

achieved by the exchange of Na^+ ions with Ni^{2+} or Co^{2+} to drive a sphere-to-rod transition as it is shown in Figure 2.6.[203, 222] Furthermore, a di-chain perfluorinated AOT-analogue is known to stabilise microemulsions of water in CO_2 . [223-226] A high-pressure small angle neutron scattering (SANS) confirmed the solubility of both surfactant in CO_2 and formation of rod-like micelles. At 298 K and 40 MPa, both surfactants (0.05 mol dm^{-3}) with 10-12.5 moles of water per mole of surfactant achieved a transparent solution in CO_2 . [203, 222] At 298 K, 35 MPa, 6 wt% of (Ni-dihCF_4) and 10 moles of water per mole of surfactant added into CO_2 resulted in viscosity enhancements of up to 1.5 fold [203] and 4.4 wt% of NaF_7H_4 with 12.5 moles of water per mole of surfactant, caused a 2 fold increase in viscosity at 313 K and 40 MPa. [222] However, these surfactants required a very high pressure to attain a single phase and high concentrations of 5 to 7 wt% were necessary to achieve a significant viscosity increase. Therefore, these thickeners would not be suitable for field applications as both need a relatively high concentration of these expensive surfactants.

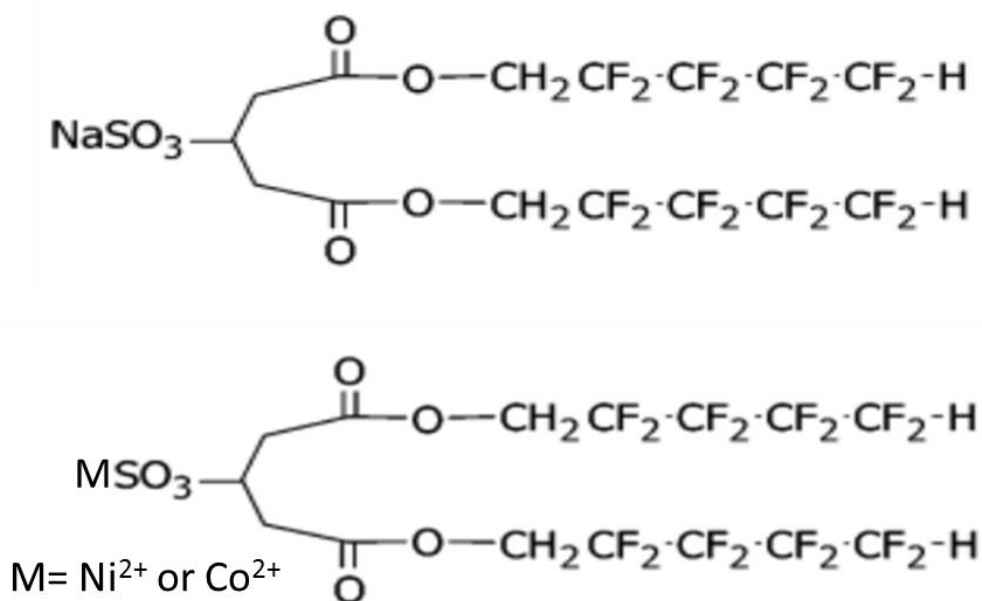


Figure 2.6 Molecular structure of a fluorinated twin-tailed surfactant as a CO_2 thickener. [203]

2.1.2.7 Cyclic and Aromatic Amide and Urea Based

Most of the successful associating small molecules compounds as CO_2 thickeners that have been described above, are fluorinated or semi-fluorinated materials. These

fluorinated materials are both expensive, and environmentally persistent due to the fluorine contents and high concentrations (3-5 wt%) required for use as a CO₂-EOR thickener.[227] Therefore, in a recent publication, Doherty et al.[227] synthesised and examined a series of cyclic and aromatic amide and urea compounds as non-fluorous small-molecules thickeners for dense CO₂ and organic liquids. They designed the molecular structure of the compounds as shown in Figure 2.7. These compounds contain cyclic or aromatic core molecules (e.g. cyclohexane or benzene) which are mildly CO₂-phobic to promote intermolecular interactions. These core ring groups are combined with associating or linking groups (labelled as 'X') which are typically either amide, urea or ester groups to establish the intermolecular interaction for viscosity enhancement. In addition, these linking groups also facilitate the connection of CO₂-philic segments (siloxane or heavily acetylated) to cyclic or aromatic core molecules to improve dissolution in CO₂. It has been found that after heating and cooling the mixture these compounds were capable of thickening organic liquids such as hexane and toluene. Researchers have found branched benzene trisurea (propyltris(trimethylsiloxy)silane-functionalised benzene trisurea and trisurea compounds functionalised with varying proportions of propyltris(trimethylsiloxy)silane and propyl poly(dimethylsiloxane)-butyl groups) to be soluble in dense CO₂ and capable of thickening CO₂ (3–300 fold) at remarkably low concentrations (0.5–2 wt% in the presence of hexane as a co-solvent at high concentrations (18–48 wt%)).[157, 172] A 300 fold viscosity increase is too large and definitely not suitable for EOR purpose. In addition, the high concentration of required co-solvent at low concentration of the additive, the associated high costs and environmental concerns severely limit the applicability of this approach.

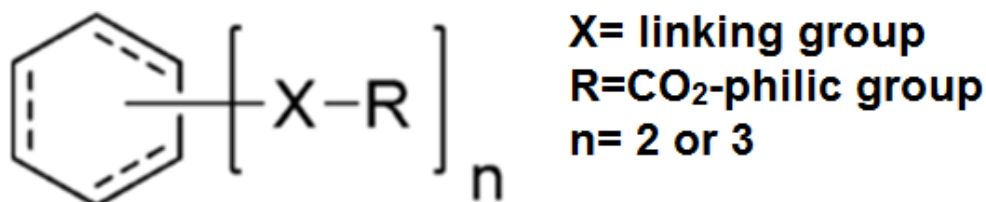


Figure 2.7 General Molecular structure of small molecules Cyclic Amide and Urea Based.[227]

2.1.2.8 Thickening CO₂- Summary

In summary, despite over 50 years of extensive work in developing and identifying both fluorinated and non-fluorinated polymers or copolymers and small molecules compounds, none of these additive materials may be considered as a viable thickener for field application.[52] In fact, the design of an affordable CO₂ thickener that can increase the CO₂ viscosity at dilute concentrations (less than 1 wt%) is highly challenging due to the low solubility of the additives in CO₂. From the above review on the efforts made towards thickening CO₂, the following conclusions may be drawn:

- Three polymeric candidates (PDMS, polyFAST and PFOA) are known as the best and most successful CO₂ thickener candidates for CO₂ mobility and conformance control at the lab-scale.[52, 168, 228] However, due to a combination of either costs, necessity for a high concentration, environment concerns or reservoir condition, none of these polymers can be considered viable for CO₂ flooding in Field A. Therefore, in this study the focus would be on the identification of cheap and readily available non-fluorinated polymers.
- There are several small molecules compounds identified as CO₂ thickeners as it can be seen in Table 2.1, including semi-fluorinated trialkyltin fluorides, fluorinated bis-ureas, di-chain perfluorinated sulfosuccinate surfactants, and branched benzene trisurea. In general, these compounds are capable of increasing the CO₂ viscosity between 1.5 to 300 fold at lower temperatures (298- 313 K). However, most of these materials are fluorinated and can improve the viscosity only at high concentrations (2-10 wt%). In addition, the small molecules compounds are low softening temperature compounds and cannot work at typical reservoir conditions due to the diminishing of the intermolecular associations at high temperature.[157] Therefore, this work would not focus on identifying small molecules compounds for thickening CO₂.

Table 2.1 Review of small molecules compounds solubility in CO₂ and their thickening capability results

Small molecules compound	Concentration in CO ₂	Cosolvent	Soluble in CO ₂ observations	CO ₂ viscosity increased at 298-313 K	Reference
trialkyltin fluoride	0.13 wt%	pentane (39 w%)	insoluble	No viscosity increased	[208]
semi-fluorinated trialkyltin fluorides and fluorinated telechelic ionomers	2-4 wt%	No cosolvent	soluble	2-3 fold	[166]
hydroxyaluminum disoaps	-	-	insoluble	No	[65]
fluorinated hydroxyaluminum disoaps	-	-	partially soluble	NO	[157]
metallic stearate powders	-	-	insoluble	No	[65, 215]
semi-fluorinated alkanes	5-20 wt%	No cosolvent	soluble	gel solution	[216]
hydroxystearic acid	3 wt%	ethanol (15 wt%)	soluble	100 fold (gel solution)	[217]
fluorinated bis-ureas	5 wt%	No cosolvent	soluble	3-5 fold	[218]
non-fluorous bis-ureas	1 wt%	No cosolvent	soluble (opaque solution)	No viscosity measured	[219]
sodium pentadecfluoro-5-dodecyl sulfate (NaF7H4)	4.4 wt% NaF7H4 10 mol of water/mol of surfactant	No cosolvent	soluble	2 fold	[222]
nickel bis-nonofluoropentane sulfosuccinate (Ni-diHCF4)	6 wt% Ni-diHCF4 10 mol of water/mol of surfactant	No cosolvent	soluble	1.5 fold	[203]
branched benzene trisurea	0.5-2 wt%	hexanes (18-48.4 wt%)	soluble	3-300 fold	[227]

2.2 Hydrocarbon Gas Thickeners

2.2.1 Polymeric Thickeners

As discussed so far, most of the research regarding gas thickening agents have focused solely on CO₂ because it is the most common injected fluid for MGI projects in the United States, Canada and elsewhere.[229, 230] In addition, CO₂ is a slightly more powerful solvent than short chained alkane gases in dissolving polymers due to the structural symmetry of CO₂ resulting in a substantial quadrupole moment (Q_i) and being a dense solvent at modest pressure and temperature, which can magnify the quadrupole interaction by scale inversely with the molar volume to the 5/6 power ($Q_i^* = Q_i \cdot V_i^{-5/6}$).[158] Despite these characteristics, CO₂ is still considered a weak solvent when compared to most organic solvents. However, there have been a few attempts at identifying the polymeric thickeners for pure light hydrocarbon gases.[68, 69, 155] In the late 1960s, several registered patents reported the initial attempts made at thickening light alkane gases. Henderson et al.[155] made the first attempt to thicken the buffer hydrocarbon by using three polymers including poly methyl laurylate, polybutadiene and poly(alkyl styrene). These polymers at a concentration of 0.25 vol% are capable of improving the viscosity of light hydrocarbon gases by about 0.1%. Subsequently, Dauben and co-workers examined polyisobutylene polymer (PIB, Mw 130,000) in a rich condensate mixture containing 75 vol% propane and 25 vol% heptane rich. They claimed to achieve a 2-5 fold viscosity increase at a concentration of 0.25 wt% of PIB.[69] However, none of patented work reported the details of the method used to measure the viscosity of the solutions examined.

Subsequent attempts by Heller et al. to identify polymeric thickeners for LPG and CO₂[64] found that various poly α -olefin polymers (PAO) based on n-pentene, n-hexene and n-decene could be used. These polymers were found to be quite soluble in n-butane at a temperature of 298 K and pressure of 8.2 MPa; however, their solubility in CO₂ was much more limited at a temperature of 305 K and pressure of 17.2 MPa. At 1-2.2 wt% of these polymers in n-butane an approximately 5-fold viscosity enhancement was achieved. In a recent publication, Dhuwe et al. assessed the solubility and viscosity enhancing property of high and ultra-high molecular weight polymers in NGL (i.e. a mixture of ethane, propane and butane).[164, 231] Polymers that have been studied in their study included ultra-high molecular weight drag

reducing agent (DRA) poly- α -olefin (Mw 20,000,000) and high molecular weight PDMS (Mw 980,000) and PIB (Mw 130,000). Ultra-high molecular weight DRA poly- α -olefin is commonly used in the oil export pipelines to suppress the energy dissipations near the pipe wall resulted from the turbulent flow at high flow rates. This polymer has been found not to change the fluid properties (e.g viscosity) at dilute concentrations used for this application. Dhuwe et al.[231] found it to be sufficiently soluble in NGL with significant amounts of hexane added as a co-solvent. For example, at 0.5 wt% of DRA polymer and 24.5 wt% hexane in propane or butane, the cloud point pressures at temperatures of 333 K found be equal to 3.07 MPa and 0.77 MPa, respectively. However, it requires very high pressure to attain solubility in ethane (46.95 MPa) at the same concentrations. At 0.5 wt% of DRA polymer and 24.5 wt% of hexane, the viscosity of ethane and propane could be improved by 3-9 fold, while 23-30 fold enhancement was obtained in butane. The reason for greater increase in butane viscosity obtained with DRA polymer is that butane has greater solvent strength to expand the polymer coil and swell the DRA polymer than propane and ethane.[164, 231]

Furthermore, they have also tested the solubility of high molecular weight PIB and PDMS in NGL components. PIB was found to be insoluble in ethane, propane, and butane at temperatures of 298-353 K and high pressure, while PDMS was soluble in all NGL constituents without a co-solvent added.[164, 231] In propane and butane, PDMS was soluble at pressures close to vapour pressures of propane and butane, while in ethane, it required high pressure (much greater than its vapour pressure) to attain solubility. For example, at 333 K and 2 wt% of PDMS in ethane, propane and butane, the cloud point pressures were obtained to be equal to 18 MPa, 2.56 MPa and 0.92 MPa, respectively. Furthermore, they found PDMS to be an effective thickener in propane and butane, but ineffective thickener in ethane. For example the concentration of 2 wt% PDMS achieved viscosity increases of 1.2 fold in ethane, 2 fold in propane and 4 fold in butane at 333 K. It was also found to be a better thickener at high pressure (62 MPa). Overall, high molecular weight PDMS was not found to be a viable thickener of NGL for EOR applications.[231]

In comparison to the results obtained by Heller et al. for 2.2 wt% of PAO (poly(1-pentene), poly (1-hexene), and P-1-D) in butane at 298 K, DRA increases butane viscosity substantially at even lower concentration (0.5 wt%). This is because DRA

has extremely higher molecular weight and also a relatively high concentration of hexane was added. Although PDMS has a higher molecular weight (Mw 980,000), it resulted in a lower relative viscosity (4 fold) than that obtained by low molecular weight PAO (5 fold). The reason behind this difference is that increase in gas viscosity does not only depend on the molecular weight of the additive, there are other factors that can influence the viscosity-enhancing ability of an additive, such as the nature of additives and the solvent, concentration of additives, the molecular weight distribution of the additives and intermolecular interaction between the additives and solvent.[232, 233] These chemical additives (PDMS and PAO) have different chemical structures. PAO has a carbon-carbon backbone with atactic molecular structure of mostly uniform head-to-tail connections with some head-to-head type connections in the structure.[234] On the other hand, PDMS has silicone-oxygen backbone and more flexible molecules than P-1-D molecules. Hence, PDMS can have lower steric hindrance and greater bond angle (143° vs 110° for C-C-C) to rotate around the Si-O bond.[235] Furthermore, the effect of molecular structure and polymer molecular weight on viscosity has been studied by Zolper et al.[235] who found that similar viscosity can be obtained for different molecular mass. For example, the viscosity of PAO at 1000 g/mol is equivalent to the viscosity of PDMS at around 10,000 g/mol. This was attributed to the additional attractive intermolecular forces between the polymers with increasing branch which leads PAO to having higher viscosity indices than PDMS. Therefore, the effect of PAO on butane viscosity could be attributed to the structure of the polymer. These effects could be more pronounced in improving the solvent viscosity than molecular weight for PAO.

2.2.2 Small Molecules Self-Associating Thickeners

Similarly to studies for CO₂, low molecular weight self-associating compounds have been studied as thickening agents of light alkane gases for gas mobility control and hydraulic fracturing purposes.[70, 71, 164, 210] Ideally, the small molecules compounds need two processes to attain dissolution and viscosity enhancement.[70, 71] The first is a high pressure heating cycle, which disrupts the intermolecular association to enhance the dissolution. The second process is the cooling cycle to establish the intermolecular association necessary for viscosity enhancement. However, some of the small molecules compounds do not require this two-step process

to attain dissolution and viscosity enhancement in NGL.[71] The previous studies on the application of the small molecules compounds in light alkane gases are discussed and reviewed below.

2.2.2.1 Trialkyltin Fluorides

Dunn and Oldfield first reported on the use of tri-n-butyl tin fluoride (TBTF) as a direct thickener of non-polar solvents including carbon tetrachloride and n-propane.[236] Figure 2.8 illustrates the association mechanism of tributyltin fluoride where a linear polymeric chain of penta-coordinate tin atoms linked by fluorine atoms. It is in the form of a white powder with melting point 544 K.[70, 71] The three butyl arms attached to the tin atom enhances the solubility of TBTF in a hydrocarbon solvent, while the intermolecular association form between the tin and fluorine atoms induces the viscosity-enhancing. It has been found that TBTF is soluble in organic liquids and light alkane under stirring process for several minutes without requiring a heating and cooling cycle.[71] TBTF is also found to be an effective thickener for the intermediate hydrocarbon components. Dandge et al.[210] found TBTF to be capable of improving the viscosity of propane and butane. For instance, at concentrations of 0.13-0.15 wt% at 298 K, it increased the viscosity of these components by 2-10 fold at 8.3 MPa. In addition, they also found that TBTF was only partially soluble in ethane and with no viscosity change measurable.[210] Later on, Enick and co-workers confirmed the ability of TBTF to thicken propane and butane liquids at 298 K and concentrations of 0.2-5 wt%.[208] Furthermore, other trialkyltin fluorides have also been tested in hydrocarbon solvents. Tripropyltin fluoride (TPTF) was not dissolved in propane and butane, because propyl arms are too short to induce the dissolution of TPTF in these solvents.[237] Therefore, it confirmed that the solubility of trialkyltin fluoride in n-alkane increases as the number of carbon atoms in n-alkyl arms (R) increases.[210] However, at equivalent mass concentration, TBTF in n-hexane or n-butane has shown to outperform in viscosity enhancement compared with other solvents.[210] For example, at a concentration of 10 g/L and 310 K, TBTF increases the viscosity of n-hexane by 750 fold (from 0.265 cP to 196 cP), while the tetrachloroethylene viscosity is enhanced by 380 fold (124.45 cP).[210]

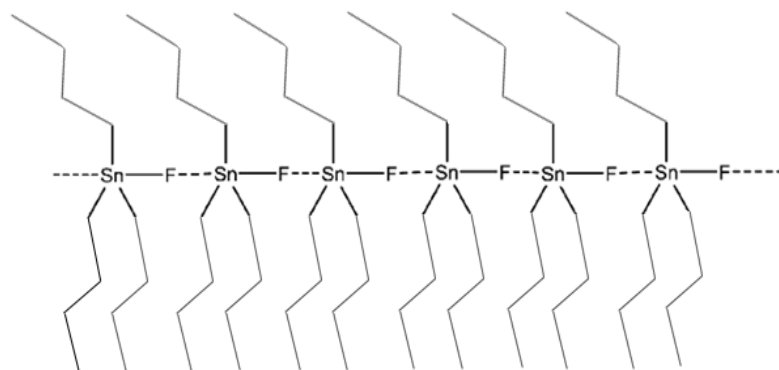


Figure 2.8 Association mechanism of tributyltin fluoride.[71]

A recent study has tested the solubility and viscosity enhancement ability for dilute concentrations (> 1 wt%) of TBTF in ethane, propane, and butane at high pressures (38-64 MPa) and high temperatures (298-373 K).[70, 71, 164] TBTF was found to be soluble in propane and butane at above vapour pressure of these components, while in ethane, it required pressures much higher than ethane vapour pressure. In addition, it was found that the relative viscosity of TBTF in NGL components increases slightly with increasing pressure at all temperatures and TBTF concentrations. Increasing the pressure does not affect the self-assembly of the supramolecular structure, it only affects the solvent strength which has a less significant effect on the solution viscosity. Furthermore, as temperature increases, the intermolecular association between the tin and fluoride molecules diminish, leading to a significant decrease in the viscosity-enhancement in all light alkane components. For example, with 1wt% concentration of TBTF in ethane at 298K, and 62 MPa, the achieved relative viscosity is 90, and it drops to 75 at 313 K. The relative viscosity significantly drops further to 20, 6 and 1.5 at 333, 353 and 373K, respectively.[164]

2.2.2.2 Hydroxyaluminum Di-2-Ethyl Hexanoate (HAD2EH)

As mentioned earlier, hydroxyaluminum disoap (often called napalm) was invented in World War II in order to gel and weaponise an organic liquid (gasoline).[211-213] A mixture of aluminium disoap and gasoline liquid was heated to high temperatures to promote its dissolution by dismantling the intermolecular associations between the aluminium disoap. Then it cooled down to allow self-assembly of the disoap molecules, whereby the viscosity of the solution is enhanced significantly.[70, 71] Enick and co-workers[65] studied a single aluminum salt,

referred to as hydroxylaluminum di-2-ethylhexanoate (HAD2EH). Figure 2.9 depicted the association mechanism of HAD2EH. They found HAD2EH to exhibit a remarkable solubility in light hydrocarbon gases such as propane and butane and also capable of thickening these components at dilute concentrations. For example, At 293 K, HAD2EH concentrations of 0.2-1 wt% were capable of increasing the viscosity of the solution by 10-100 fold as tested in a high pressure falling ball cylinder viscometer. However, the solution formed was not transparent and hazy, due to a portion of the HAD2EH molecules forming solid fibres in both liquid propane and butane at high pressures.

Dhuwe et al.[71, 164] examined HAD2EH again in all of the NGL constituents (i.e. ethane, propane, and butane) individually under a range of pressures (34-62 MPa) and temperatures (298-273 K). HAD2EH was found to be soluble in propane and butane while insoluble in ethane. At the temperature of 298 K, HAD2EH was insoluble in all light alkanes, requiring heating to 373 K at high pressure and stirring to attain dissolution and then cooling down to a temperature above 313 K for the solution remained in a single phase. When the solution cooled down to a temperature of 298 K, HAD2EH precipitated in both propane and ethane. Accordingly, it has been found that HAD2EH is an effective thickener in butane and propane at temperatures as low as 313 K. For example, at a concentration of 0.5 wt% HAD2EH and temperatures of 333-373 K, butane viscosity increases by 15-19 fold, while propane is thickened by 2-3 fold.[71, 164]

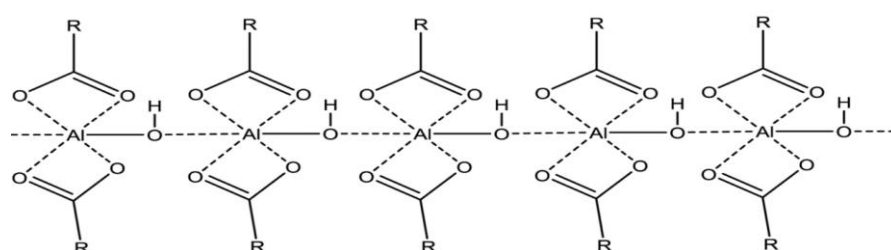


Figure 2.9 Association mechanism of HAD2EH molecules.[71]

2.2.2.3 Crosslinked Phosphate Esters

These are several reports available on the attempts made to gel light hydrocarbon gas (LPG) using phosphorous-based esters crosslinked with polyvalent metal ions (Figure 2.10) for dry hydraulic fracturing applications.[238-242] These techniques used phosphate mono/di-esters linked to alkyl tails. Typically, a hydrocarbon liquid

agent solution is formed by combining two low viscosity liquid reactants (i.e. a solution containing the phosphate ester and one containing a polyvalent metal ion crosslinking agent) together in the fluid that is being thickened. It has been found that the two low viscosity liquids quickly dissolve in the fluid (e.g. light alkane) without needing a heating/cooling cycle. The polyvalent metal ion bounds more tightly with phosphate esters than the ligand which leads the phosphate ester to quickly chelate with metal ion and form long micellar and a supramolecular structure as shown in Figure 2.11. If this long micellar structure remains soluble in the solvent, then it can significantly improve the solution viscosity. Rapid dissolution of phosphate esters system in the solvent and the rapid kinetics of viscosity-enhancement could make these attractive for use with NGL in an EOR project.[70, 71]

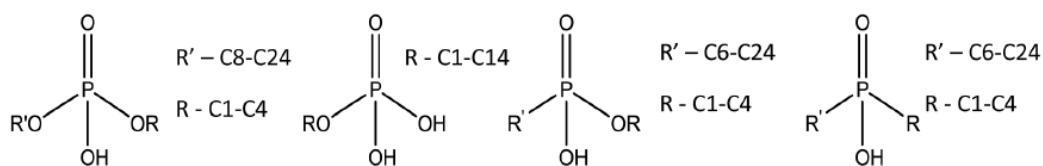


Figure 2.10 Molecular structure of Phosphate di/mono-ester, Phosphonic acid ester and dialkyl phosphinic acid.[71]

There are a few studies reporting that oil-soluble phosphate mono/di-esters, dialkyl phosphinic acids or alkyl phosphonic acid ester crosslinked with polyvalent metal ions including Fe^{3+} , Mg^{2+} , Al^{3+} , Zn^{2+} , and Ti^{4+} can increase the viscosity of hydrocarbon oils (e.g. diesel and kerosene) by 2-100 fold at concentrations of 0.2-2.5 wt%.[240, 241, 243] Furthermore, it has been reported that phosphate-based esters could be used as a gel agent for CO_2 and hydrocarbon liquid mixtures.[244, 245] In recent publications,[70, 71, 164] Lee and Dhuwe et al. studied the mixture of crosslinked phosphate esters (phosphate ester (HGA 70-C6) and cross linker (HGA 65)) with NGL components (ethane, propane and butane) at a range of temperatures (298–373 K) and pressures (13.8-62 MPa). They found that phosphate ester and the crosslinked solution are soluble in ethane, propane, and butane at concentrations of 0.25-1wt% and temperatures of 298-333 K. However, the cross-linked solution was not a transparent phase and instead was slightly hazy due to small droplets suspended in the solution. This mixture (phosphate ester + crosslinker) achieved a modest viscosity increase in ethane; while greater increases occurred in propane and butane. For example at the concentration of 1 wt% at 333 K and 20.68 MPa, the viscosity of ethane increased by a

factor of 1.45 fold and by 2.6 and 3.2 fold with propane and butane, respectively. As the mixture cannot form a single phase in the NGL components due to the suspension of very small droplets in the solution, its suitability for injection into porous media is limited.[70]

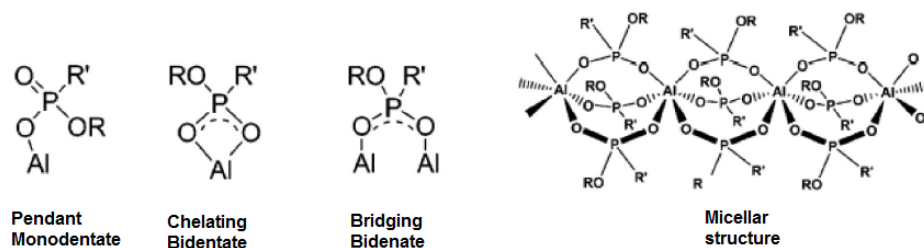


Figure 2.11 Chelation mechanism and micellar structure of phosphate ester/metal ion complex.[246]

2.2.3 Thickening of Hydrocarbon Gases-Summary

Although the previous works mainly focused on the identifying CO₂ thickeners, there are a few studies that have reported the NGL components being thickened separately with polymer candidates and/or small molecules compounds. Based on the above review on work done towards thickening hydrocarbon gases, the following conclusions may be drawn:

- Three polymer candidates were found to be effective thickeners in NGL components including DRA polymer, PDMS, and PAO oligomer. These thickeners are much more effective for thickening butane and less effective for propane and ethane. DRA polymer is a more promising thickener (3 to 23 fold) at dilute concentrations over temperatures of 298-333K, while PDMS and PAO show moderate viscosity enhancements (1.2 to 5 fold) over the same temperatures. However, these thickeners have not been verified at temperature above 373 K.
- As summarised in Table 2.2, three small molecules compounds (TBTF, HAD2EH, and CPE) have been reported as effective thickeners for pure light alkane components at moderate temperatures (313-333 K), however phase behaviour, environment issues (fluorine content) impede for these materials to be used for EOR projects. For example, CPE does not form a single phase in NGL, and TBTF contains fluorine substances. In addition, these compounds exhibit solubility in ethane at high pressure. As the methane and CO₂ are the main components in AG,

the dissolution of these materials in AG mixture would face much difficulty in comparison with ethane. Therefore, the small molecules compounds examination is excluded from this work.

Overall, none of the above reviewed polymeric candidates have been assessed by other researchers as a thickener specifically for an AG mixture containing primarily methane, ethane, propane and CO₂. In the literature, the available data about thickening of an AG mixture are very scarce. Therefore, to date these polymeric materials have not been used as a thickener for a field's AG mixture which is subjected to miscible gas flooding. Hence, this work is going to focus mainly in identifying and examining non-fluorous polymeric thickeners for AG and CO₂ at a viscosity level close to Field A oil viscosity under its specific in-situ conditions.

Table 2.2 Summary of small molecules compounds solubility in NGL components and thickening capability results

Small molecules compound	Concentration in NGL components	Co-solvent	Soluble in NGL observations			Relative viscosity at 333K			Ref.
			C ₂ H ₆	C ₃ H ₈	C ₄ H ₁₀	C ₂ H ₆	C ₃ H ₈	C ₄ H ₁₀	
tri-n-butyl tin fluoride	1 wt%	No	yes	yes	yes	1.5-4 fold	40 fold	60 fold	[70]
hydroxyaluminum di-2-ethyl hexanoate (HAD2EH)	0.5-1 wt%	No	No	yes	yes	No	10 fold	14 fold	[70]
crosslinked phosphate esters (HGA 70-C6)+ HGA 65	0.25-1 wt%	No	yes	yes	yes	1.45 fold	2.6 fold	3.5 fold	[70]

Chapter 3. Numerical Study of Using Polymer to Improve the Gas Flooding in the Harweel Cluster*

3.1 Introduction

The Harweel Cluster consists of several deep reservoirs with tight carbonate oil-bearing rocks in the south of Oman. Field A is one of the Harweel cluster reservoirs as shown in Figure 3.1. The sediments in the field are more than half a billion years old with the hydrocarbon deposits among the oldest in the world, from a depth of roughly 5 kilometres, making it the deepest producing oil field in Oman.[30, 32] Right from the discovery, miscible gas injection (MGI) was identified as the best enhanced recovery process for the field. The gas mixture used for MGI contains mainly methane enriched with light hydrocarbons and acid gases. With this MGI process, it is estimated that up to 47% of the original oil in place (OOIP) can be recovered.[32]

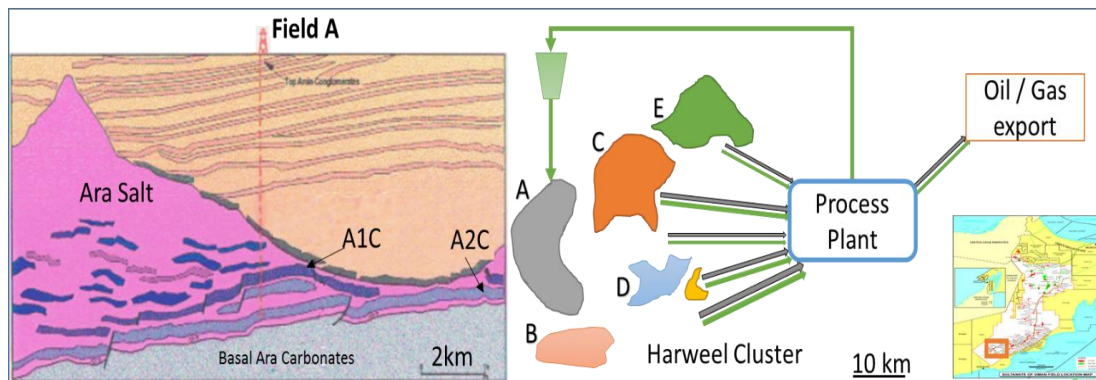


Figure 3.1 Geological cross-section of the carbonate stringers (left) and an aerial overview of Harweel Fields in southern Oman (right).

In general, the relatively low viscosity and density of the injected gas present challenges for MGI projects.[35, 52] The high viscosity and density contrast of the in-situ fluid system would lead to an unfavourable mobility ratio and gravity override, respectively, both of which tend to lower the volumetric sweep efficiency during flooding.[119] In the case of Field A, since the reservoir oil is light (42°API), there is not much density contrast between the injected gas and the displaced oil ($400\text{-}600\text{ kg.m}^{-3}$ and 639 kg.m^{-3} , respectively).[32] The presence of CO_2 and H_2S in the injected

gas composition (15-25 mol% and 3 mol%, respectively) also helps to increase the gas density.[31] Hence, the gravity segregation is not expected to be the primary problem in this field. However, the in-situ viscosity of the AG (0.01-0.03 cP) is much lower compared with that of the oil (0.23 cP). This would result in early gas breakthrough (BT), poor volumetric sweep and reduced overall efficiency of the MGI. In fact, early gas breakthrough has already been experienced in some production wells in Field A. Such a challenge may be addressed by the implementation of several methods proposed in and described in the literature. The common objective of the proposed techniques is to effectively control the gas mobility and, as a result, increase the sweep efficiency of the gas flooding.[52] The most commonly used or proposed methods include Water Alternatives Gas flooding (WAG),[53, 54] entrainment of the gas into a foam during foam flooding,[57, 58, 61, 62] and increasing the gas viscosity by adding polymers as thickening agents to the gas.[52, 66] During the WAG process, the gas mobility is suppressed by injecting water and gas alternately using a single to five cycles.[89, 247] With regards to field applications, the CO₂-WAG flooding has proven to be effective resulting in incremental oil recoveries of around 5-10% of the OOIP.[247] However, very often, a large amount of the residual oil is still left behind after the completion of the WAG injection because of the operational difficulties and challenges associated with this method including the gravity segregation and water blocking due to the excessive water injected into the oil reservoir.[54, 89] Therefore, the WAG strategy may not be the best choice for Field A, where water saturation is already very low and facilities are not designed to inject or handle water.

The application of foaming agents has also been studied as a way of conformance control in miscible flooding.[57] However, applying foams for mobility control has shown to be technically and economically challenging because of the difficulties associated with controlling its propagation over large distances in the reservoir and that large volumes of foam are required.[59] In addition, the majority of the foaming agents are of no use in high salinity reservoirs due to the inability of the surfactants to reduce the interfacial tension (IFT) to the required ultra-low values.[59]

To overcome the above limitations associated with WAG and foam flooding, another technique has been introduced which brings together the advantages of both chemical and miscible gas EOR methods. Introduced for the first time about 45 years ago, the application of thickener agents, such as small/high molecular weight

polymers, has been proposed to directly thicken the injection gas during gas flooding.[66] By increasing the injection gas viscosity, the gas mobility can be suppressed. Hence, the severity of the viscous fingering (i.e. instability in displacement front) and the chance of developing pre-mature breakthrough can be reduced and the microscopic displacement efficiency of an MGI can put into use across a larger portion of the reservoir. Among the techniques used to improve the mobility ratio of a gas flood, a direct thickening of the AG mixture by using additive polymers may be the best method to increase sweep efficiency in Field A. Specific challenges for Field A are the high salinity of the formation water (275,000 ppm) and low water saturation in the reservoir. The AG in Field A contains 15-25 mol% of CO₂. The presence of CO₂, high pressure (55 MPa) and high temperature (377 K) are considered as positive factors as they may make the identification of suitable soluble polymers in the AG mixture easier. There are a number of previously completed studies investigating polymer solubility in CO₂[158] whose results can be used as a guide in choosing suitable thickeners for this field.

In this study, we used the compositional simulator CMG-GEM and the associated PVT module CMG-WinProp to evaluate the potential benefits of adding polymers to the injected gas to increase its viscosity. A box model has been built based on the typical geological & petrophysical characteristics and includes the light oil fluid description & properties in Field A. Considering the composition of the AG of Field A, we have examined a number of different gas compositions to cover a range of hydrocarbon gas and CO₂ mixtures. Also, we have evaluated the direct effect of the different gas compositions on the oil properties during the flood which, besides the viscosity improvement of the thickened gas, can influence the ultimate oil recovery. The simulation runs have indicated a positive response with regards to the oil recovery.

3.2 Numerical Model

A 3D geological box model has been generated based on the typical geological characteristics, fluid properties, and production and injection data of Field A (Figure 3.2). The reservoir heterogeneities are captured in the model based on the reservoir permeability and porosity distribution as reflected in the available log data. The zones with higher permeability are located in the upper and lower sections of the reservoir. The horizontal permeability of these zones is in the range of 10-100 mD

compared with the permeability of middle zones which falls in the range of a 0.1-10 mD. The position of high permeability zones leads to unstable oil displacement where the injected gas passes through them leaving behind the oil in low and intermediate permeable zones as sandwiched between the high permeability zones. The numerical model dimensions are 30m × 30m × 79m in X, Y and Z directions, respectively, with a grid size of 14m in the X and Y directions. The thickness of the grid blocks in the Z direction is 1.53m. Since the reservoir does not contain an aquifer, the entire thickness (120.87m) of the model is considered as the pay zone. Figure 3.2 shows the permeability distribution in the box model constructed. A direct line drive pattern flood was set up for the injection and production wells. The bottom-hole pressure and production/injection rates were used as constraints for the operation of the wells. A maximum bottom-hole pressure of 55 MPa and an injection flowrate of 1MMm³/day were set for the injection wells. A minimum bottom-hole pressure of 40 MPa (the minimum miscible pressure or MMP) and a production flowrate 800 m³/day were set for each production well.

Table 3.1 presents the composition of various injection gas mixtures considered during the simulation study including the use of NGL and pure CO₂ as two possibilities. The injected gas viscosity is modified from its original value in the fluid PVT WinProp model. As mentioned earlier, the simulation work was conducted with different levels of gas viscosity increases and included the oil viscosity and density reductions and oil swelling effects caused by the dissolution of gas into the oil during the flood. Some basic reservoir fluid and rock properties used to construct the simulation model are provided in Table 3.2.

Permeability Z mD

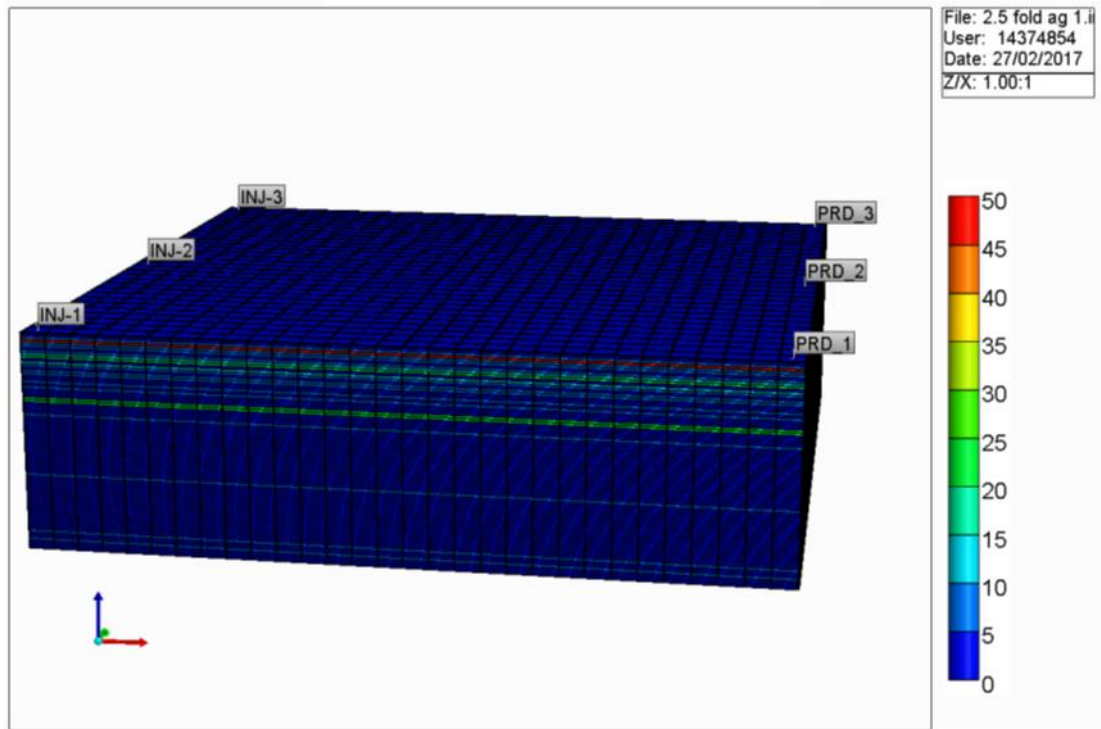


Figure 3.2 3D reservoir model showing the permeability distribution.

Table 3.1 Composition of various injection gases studied.

Component	AG1	AG2	AG3	NGL	CO ₂
	mol. fraction	mol. fraction	mol. fraction	mol. fraction	mol. fraction
CO ₂	0.05	0.25	0.5	0	1
H ₂ S	0.03	0.02	0.02	0	0
C ₁ H ₄	0.7	0.6	0.4	0	0
C ₂ H ₆	0.15	0.08	0.05	0.45	0
C ₃ H ₈	0.07	0.05	0.03	0.3	0
C ₄ H ₁₀	0	0	0	0.25	0
Total	1	1	1	1	1

Table 3.2 Reservoir and fluid properties

Reservoir Size (m)	420 × 420 × 316
Number of grid blocks	71100
Reservoir depth (m)	4574
reservoir pressure (MPa)	55
reservoir temperature (°C)	104
Porosity (frac.)	0.033 to 0.169
Permeability (mD)	5 to 50
oil density (kg.m ⁻³)	639
oil viscosity (cP)	0.24

3.3 Fluids PVT Model

As mentioned earlier, to accurately model the fluid characteristics of Field A, the CMG's PVT WinProp module was used. First, the saturation pressure for the components up to the residue of C₃₆₊ was matched with the experimental saturation pressure by altering the equation of state (EOS) parameters for the C₃₆₊ component. Then, the 36 components were lumped into 8 pseudo components and tuned the Peng-Robinson Equation of State (PR_EOS) parameters to match the simulation data with the experimentally measured field fluid properties data (saturation pressure, viscosity, density, API and gas oil ratio (GOR)). At the end, all simulation parameters were matched as closely as possible to the experimental data. For instance, the bubble point pressure was calculated in the PVT model to be 33.41 MPa while experimentally measured value is 33.40 MPa at the reservoir temperature of 377 K. As mentioned before, we also modelled the oil swelling and viscosity change due to the dissolution of different gas mixtures. The PR_EOS in WinProp was used to model such changes in the oil viscosity, density and the saturation pressure (the amount of swelling) at 55 MPa and 377 K.

3.4 Results and Discussion

3.4.1 Effects of Different Dissolved Gas Compositions on Oil Properties

3.4.1.1 Oil Viscosity Reduction

The oil viscosity reduction is one of the miscible gas injection (MGI) mechanisms that can be achieved by gas solubility into the in-situ oil. Such a mechanism would improve the oil mobility resulting in enhanced oil recovery. In this study, the effect of the dissolution of the Field A's AG enriched by CO₂, pure CO₂ and NGL on the oil viscosity was examined in PVT WinProp. While the oil viscosity reduction was indeed observed, the reduction level was found to vary with change in the composition of the injection gas. Figure 3.3 shows the behaviour of the oil viscosity with the change in the amount of dissolved gas into the oil at the reservoir pressure and temperature of 55 MPa and 377 K, respectively. The AG without CO₂ has a greater effect on the viscosity. Also, NGL showed higher effect on the viscosity only at 10 mol% and 80 mol% dissolutions and between these two values the viscosity reduction level is less than AG (without CO₂) and AG enriched by CO₂. This observation is likely due to the

dissolution of light hydrocarbon fractions in the oil. The presence of CO₂ in the AG mixture, on the other hand, leads to a smaller reduction in the oil viscosity than AG without CO₂. For example, at the reservoir pressure of 55 MPa, when 30 mol% of AG with 25 mol% CO₂ content is dissolved into the oil, the viscosity is reduced to 0.134 cP, but when the CO₂ content is raised to 50 mol%, with the same amount of gas dissolved, the oil viscosity is reduced to 0.14cP. In addition, as the dissolved gas content in the oil increases, the bubble point pressure shifts towards higher values due to the changing oil composition. Above the saturation pressure, the oil viscosity keeps reducing as the dissolved gas content increases. However, as the system pressure exceeds the saturation pressure, the oil viscosity starts to increase due to the light gas components leaving the oil resulting in increase in the mol% of the heavier components. This behaviour is evident from some of the data plotted in the Figure 3.3. As can be seen from the figure, the viscosity of the oil increases, for example, after exceeding 60 mol% of AG (CO₂ 25 mol%) in the oil and 70 mol% for other gas mixtures. In summary, if the effect of oil viscosity reduction is evaluated on its own, it is expected that thickened hydrocarbon gases would result in greater impact than thickened CO₂ in Field A.

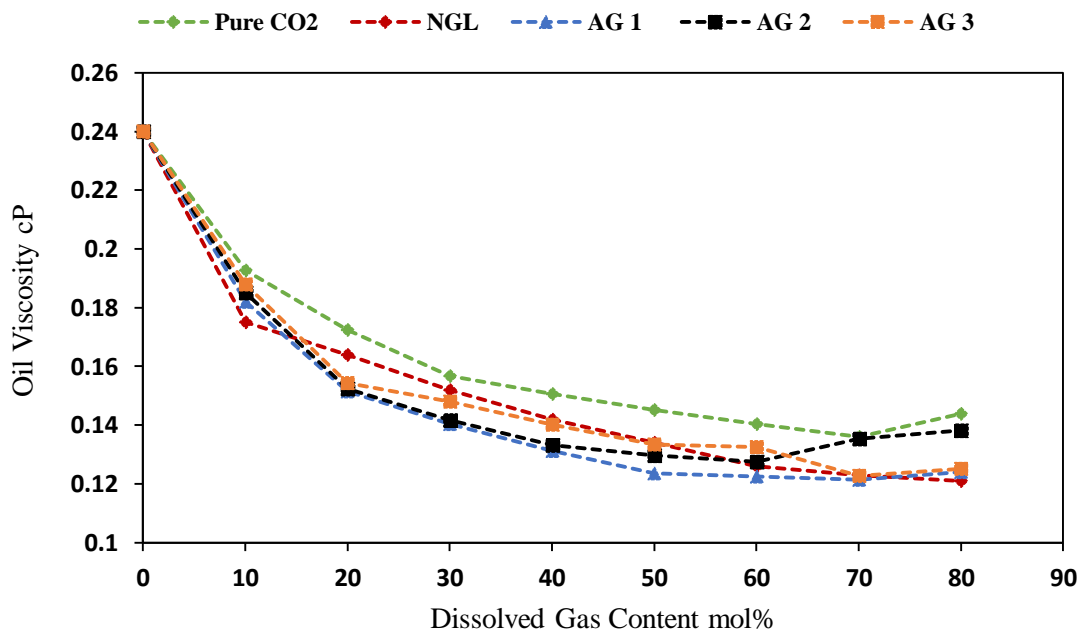


Figure 3.3 The oil viscosity reductions with addition of different gas compositions into oil at 55MPa and 377 K.

3.4.1.2 Effects on Oil Density

The effects of the AG composition on the oil density was also examined at reservoir conditions. Different gas compositions change the oil density differently as their content in the oil varies (Figure 3.4). For pure CO₂, there is a substantial increase in the oil density as its content in the oil increases. This behaviour is very likely because, being in supercritical state, the CO₂ density is higher than that of the oil (light oil from Field A), making the oil denser. The density of in-situ oil and CO₂ at Field A's reservoir conditions are 641 kg.m⁻³ and 832 kg.m⁻³, respectively. In addition, an increase of single-phase fluid density may induce further molecular interactions, which has resulted from strong intermolecular Coulombic interactions or dipole/quadrupole interactions between CO₂ and hydrocarbon molecules.[248] The CO₂ molecules exhibit a significant quadrupole moment; however, it does not have a permanent dipole moment which differs from non-polar molecules such as ethane and propane that have neither a dipole nor a quadrupole moment. The strong quadrupole moment could result in a thermodynamic intermolecular interactions that have a significant effect on mixtures studied here. Several investigators have calculated and reported the thermodynamic effects of gas dissolution in the crude oil on the overall properties of the fluid system.[249-251] Generally, the CO₂ dissolution in oil has more effect on the density of light oils than heavy oils.[252] Overall, the injection of the pure denser CO₂ phase into a reservoir containing light oil may result in gravity override and early breakthrough.

As can be seen from Figure 3.4, the addition of gases other than CO₂ into the oil at reservoir conditions causes the oil density to decrease. However, as the CO₂ concentration in the AG increases, the amount of decrease in the oil density seems to become less pronounced. Such an effect is likely due to the fact that the densities of AG (without CO₂) and NGL (286 kg.m⁻³ and 596 kg.m⁻³, respectively) are lower than that of the oil (641 kg.m⁻³) as opposed to the CO₂ density (832 kg.m⁻³) which is greater than that of oil. A 40 mol% of gas dissolved in the oil at 55 MPa and 377 K lowers the oil density from 641 to 598 kg.m⁻³ (Figure 3.4).

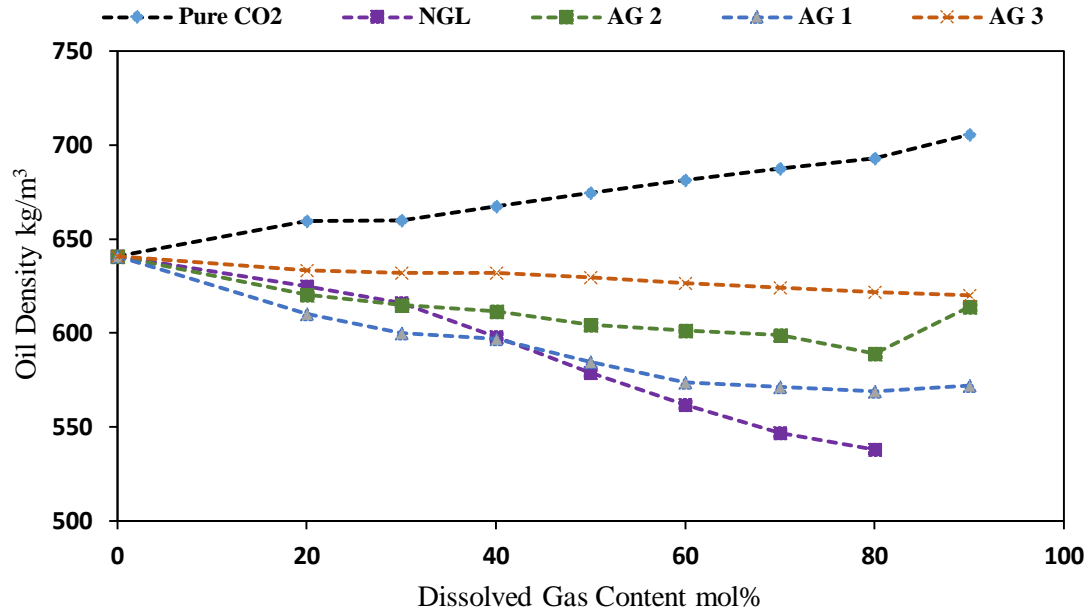


Figure 3.4 The oil density changes with addition of different gas compositions into oil at 55MPa and 377 K.

Overall, the presence of CO₂ in the AG is expected to increase the injected gas density and cause a small decrease in the oil density, resulting in an insignificant difference between the densities of the injected gas and the displaced oil. Therefore, considering the effect of CO₂ on the densities of the injected AG and oil in isolation, presence of CO₂ can potentially suppress the gravity override effect in the reservoir and improved the oil recovery by slightly delaying the gas breakthrough in the unthickened gas flood.

3.4.1.3 Oil Swelling Effects

When the injected gas comes in contact with the oil in a low permeability zone (with low initial recovery) it causes the oil to swell and become less viscous, improving the oil mobility. The swelling would also improve the oil relative permeability by increasing its saturation in the pore space. Therefore, the swelling of the oil helps to displace the oil out of the pores and flow towards the production wells. The degree of the swelling depends on the injected gas compositions, oil composition, as well as the reservoir pressure and temperature.[16, 253] The swelling factor for different gas compositions dissolved into Field A's light oil has been determined using numerical simulation at reservoir conditions. As shown in Figure 3.5, the injection of NGL and AG enriched with CO₂ leads to a higher swelling factor than pure CO₂. By the

continuous dissolution of gas into oil, the swelling factor increases due to the relative volume increase (expansion) at high saturation pressure. It is observed that the CO₂ injection in Field A leads to a significant increase in the saturation pressure of the crude oil which may affect the EOR process (miscibility pressure). Therefore, the swelling factor for CO₂ injection cannot be measured in the model as more CO₂ is added into the oil. However, many studies have reported that CO₂ injection leads to higher swelling factor and lower saturation pressure.[253-255] In this study, Field A oil shows different swelling effects for different gases which is consistent with the results obtained by Bon et al.[250, 256] This result is obtained due to the high solubility of the hydrocarbon gas mixture (alkane) in the light oil at high pressure, leading to the acceleration of the swelling and viscosity reduction process. Thus, the NGL and natural gas (AG) tend to have higher swelling and oil viscosity reduction effects. Such effects, if considered in isolation, may lead to a higher oil recovery in Field A.

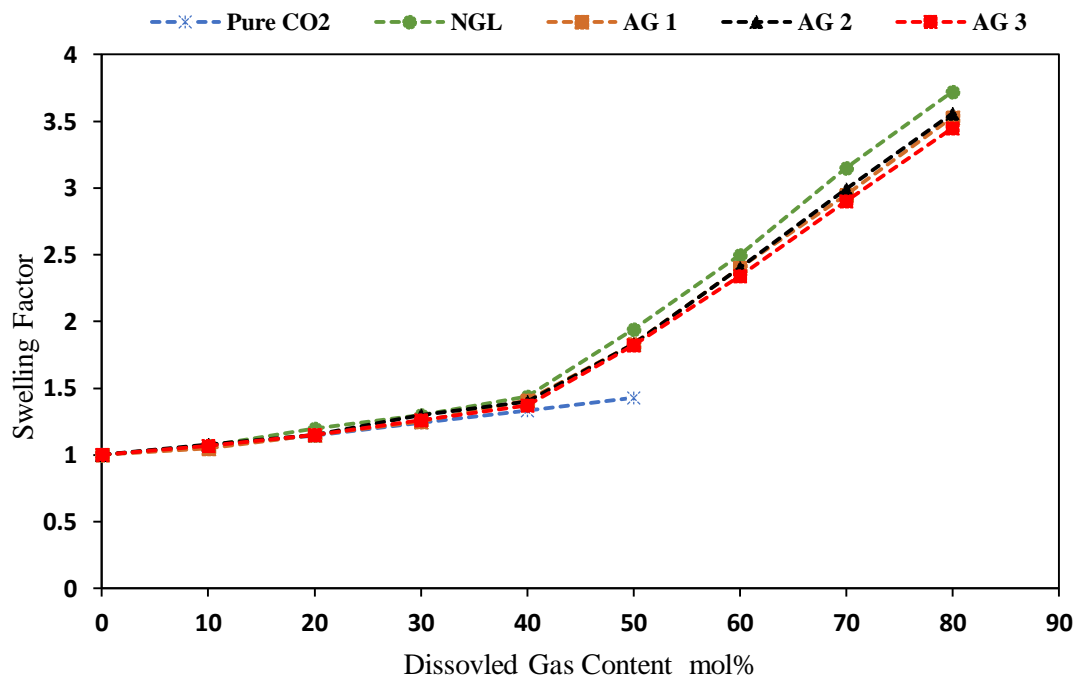


Figure 3.5 The swelling factor changes with addition of different gas compositions into oil at 55 MPa and 377 K.

3.4.2 Unthickened Gas Flood

Continuous gas flooding (not thickened) was simulated with different gas compositions using the GEM module of the CMG software. The model includes pure

CO₂, NGL, and AG enriched with CO₂. Figure 3.6 shows the oil recovery profiles for different gas injection scenarios. The simulation results indicate that NGL injection has the highest cumulative oil recovery among the gases examined, reaching 77.6% oil recovery in 20 years. Such an effect could be due to NGL's large swelling effect (relative to CO₂) and being more miscible than the other injectants. Figure 3.6 also shows that both cases of CO₂-enriched AG injections yield the lowest ultimate oil recovery factors among all. During the early injection period (<10 years), the recovery factor for the CO₂-enriched AG flood is higher than that of the pure CO₂ flood. However, after the first 10 years, the three gases exhibit lower recovery curves, which occurs after a significant increase of production GOR (Figure 3.7).

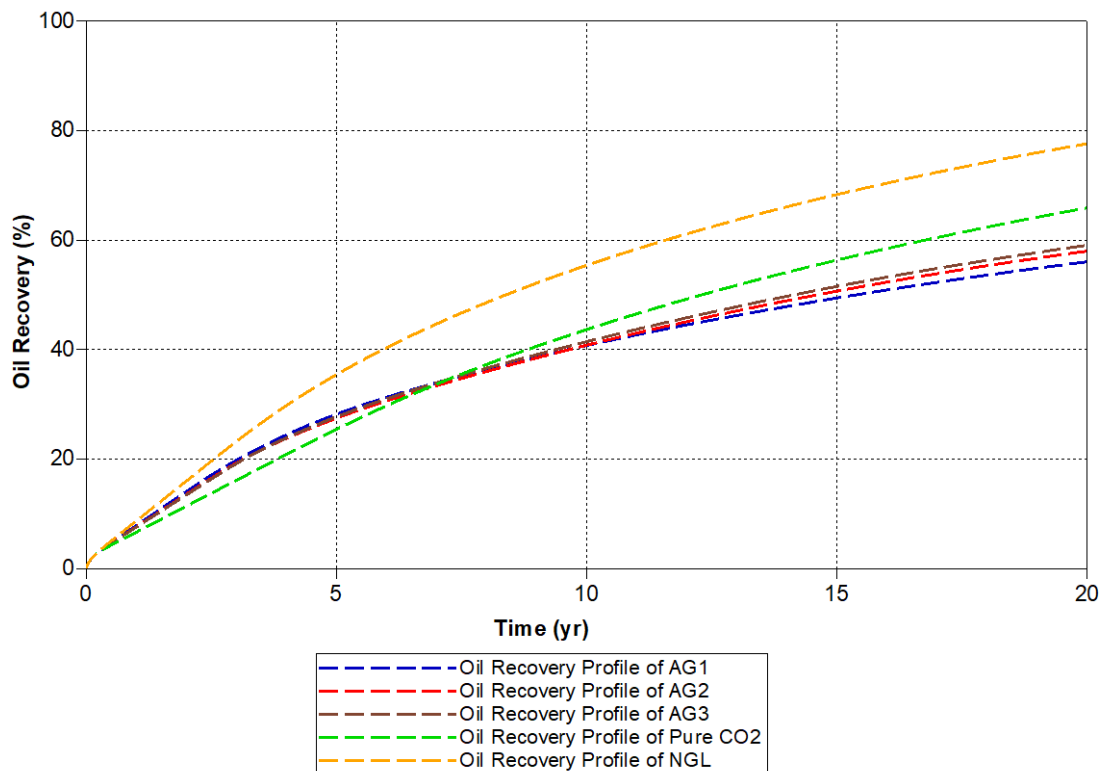


Figure 3.6 Oil recovery profiles for different unthickened gas floods.

Figure 3.7 shows the evolution of the GOR for all five unthickened gas injection scenarios mentioned above. As can be seen, the oil recovery of all AG floods begins to slow down fast with earlier gas breakthrough and increase in the production GOR. As shown in Figure 3.7, after three years of AG flooding, the GOR increases significantly. This sharp increase is due to gas channeling dominating over the earlier discussed mechanisms of oil swelling and oil viscosity reduction. Such behaviour

causes the oil recovery for AG mixture to be lower than those of the pure CO₂ and NGL. The gas breakthrough in the cases of the NGL and CO₂ floods is delayed by about 1 and 2 years, respectively. Overall, as evident from the trends in Figure 3.7, the GOR values for these two gases are also lower than those of the AG floods due to higher viscosity of the NGL and pure CO₂ (0.09 cP and 0.06 cP, respectively) compared with those of the AG mixtures which is well correlated with improved sweep efficiency during the gas flooding process.

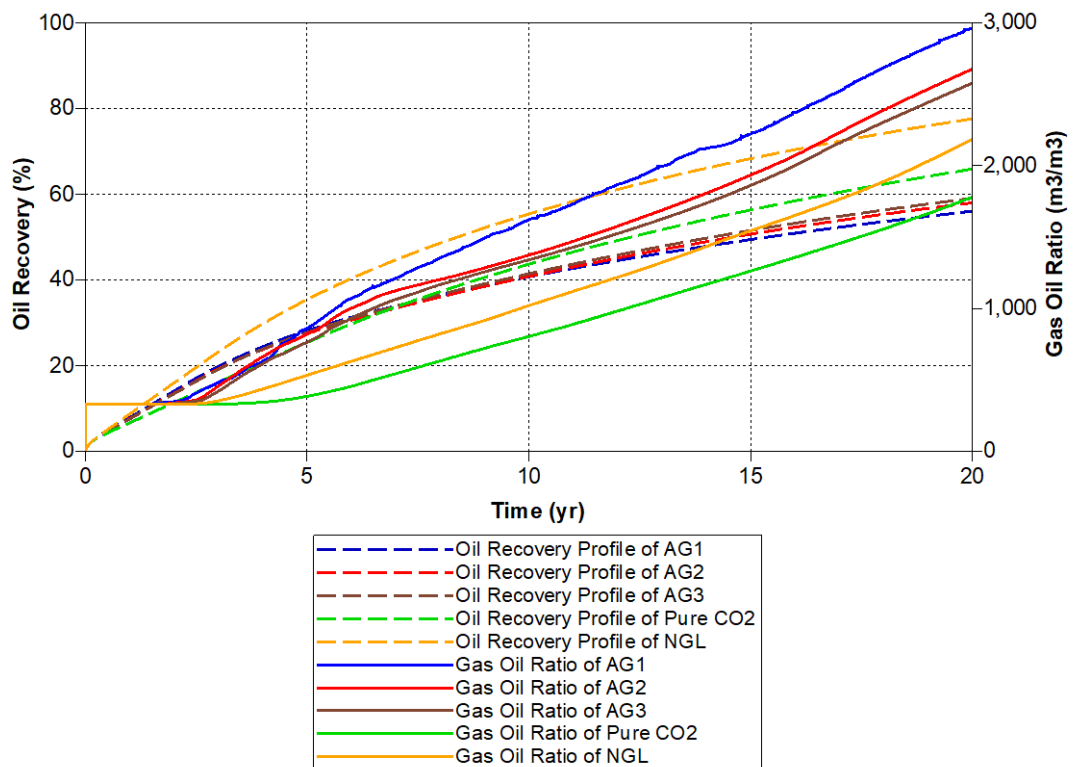


Figure 3.7 Oil recovery factor and GOR for different unthickened gas floods.

3.4.3 Thickened Gas Floods

In this part of the work, the benefits of adding polymers into the Field A's AG and other gas mixtures were evaluated using compositional simulation. To do so, the impact of gas viscosity on oil recovery and gas breakthrough times was investigated by increasing the gas viscosity 2.5 to 6.25 fold. The effect of viscosity change was introduced into the GEM model by manipulating the viscosity of the gas mixtures in WinProp model. In CMG, the reservoir fluid viscosity can be computed during the simulation runs using different correlations such as Jossi, Stiel and Thodos, Hering-Zipperer, Yoon-Thodos, Pedersen and Modified Pedersen. The injected gas viscosity

can be modified in the fluid PVT WinProp model without affecting the other fluid properties (oil and solution gas viscosities). The viscosities of injected AG mixtures and CO₂ in WinProp model were matched at different level of gas viscosity increases (e.g. 0.1 cP, 0.16 cP and 0.25 cP) at pressures of 50-55 MPa and temperature of 377 K. These viscosity data for each injected gas were increased individually by regressing the viscosity parameters for EOS sets.

3.4.3.1 Effect of Thickening Level

For simplicity, the effect of different levels of viscosity enhancement has been discussed for AG2 (Field A's AG enriched with 25 mol% CO₂) only. However, the same discussion and similar conclusions made can be presented for all other gases examined in this work. Figure 3.8 illustrates a visual comparison of the vertical sweep between unthickened (left) and thickened (right) gas floods 4 years after the commencement of AG2 (AG with 25% CO₂) injection for the cases of 2.5, 4 and 6.25 fold gas viscosity enhancement. As can be seen, for the case of the unthickened gas injection, severe viscous fingering and gas channeling occurs in the high permeability zones at the top and bottom sections of the model. This behaviour results in unstable displacement and early gas breakthrough. However, the viscous fingering is largely suppressed as the injected gas viscosity is increased, delaying the gas breakthrough and improving the sweep efficiency. Figure 3.9 shows the effect of viscosity enhancement (2.5, 4 and 6.25 fold increase in gas viscosity) on the oil recovery profile and production GOR development when AG2 is injected at an injection rate of 1MMm³/day. The results show that, as one may expect, higher oil recovery and lower GOR can be achieved by the thickened gas injection. A comparison of the ultimate oil recovery factors shows that, depending on the level of viscosity enhancement, the thickened AG2 flood yields oil recovery factors from 72 to 79%, while the unthickened AG2 flood recovers about 58% of the OOIP. The improved recovery and suppressed GOR profiles are mainly due to the delayed gas breakthrough when a thickened gas is injected. The unthickened AG2 breakthrough occurs after around 3 years from the onset of gas injection, corresponding to an oil recovery of 18%. As the AG2 viscosity is increased, the gas breakthrough is delayed by 1 year for 2.5-fold (0.1 cP) and 2 years for 4-fold (0.16 cP) and 6.25-fold (0.25cP) corresponding to oil recoveries of 25% and 30%, respectively. It is also worth noting that while a 2.5 fold gas viscosity

enhancement results in a relatively large incremental oil recovery, further viscosity enhancements (4 and 6.25 folds) result in smaller further incremental recovery.

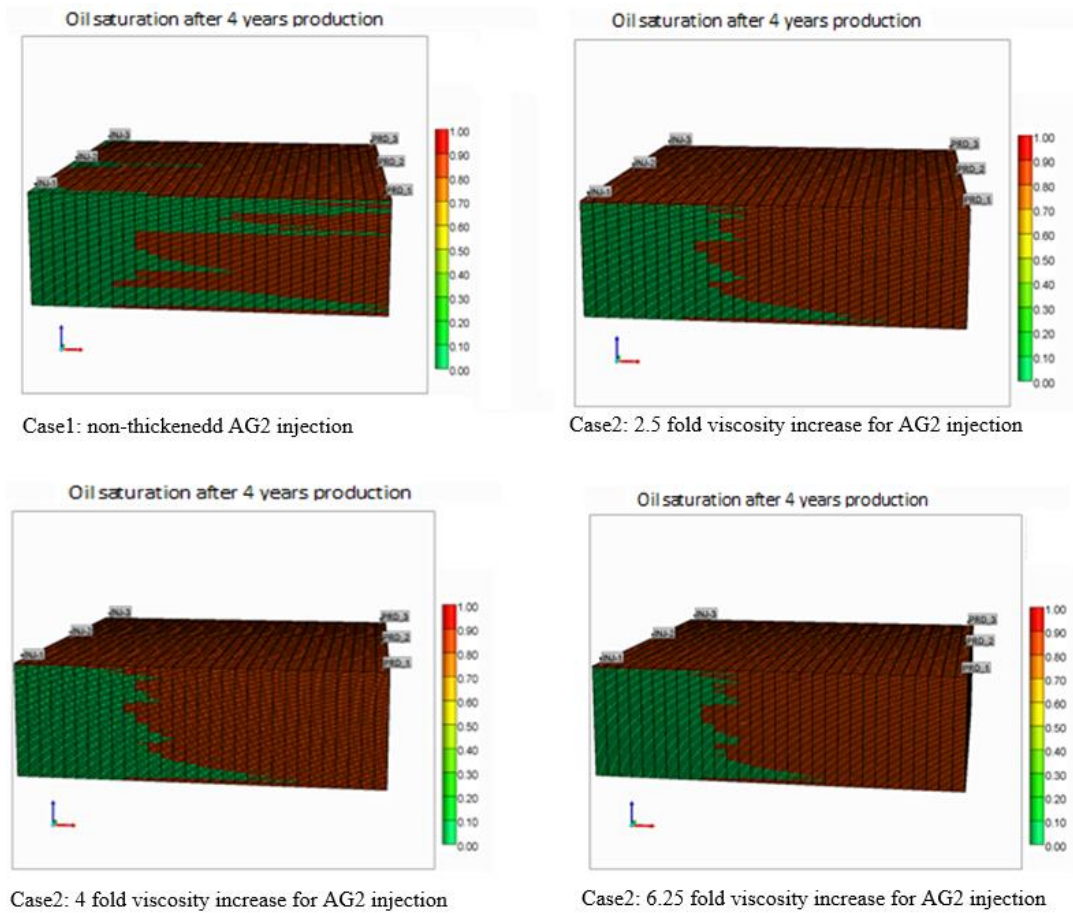


Figure 3.8 Effect of thickened AG2 mixture on the vertical oil sweep efficiency.

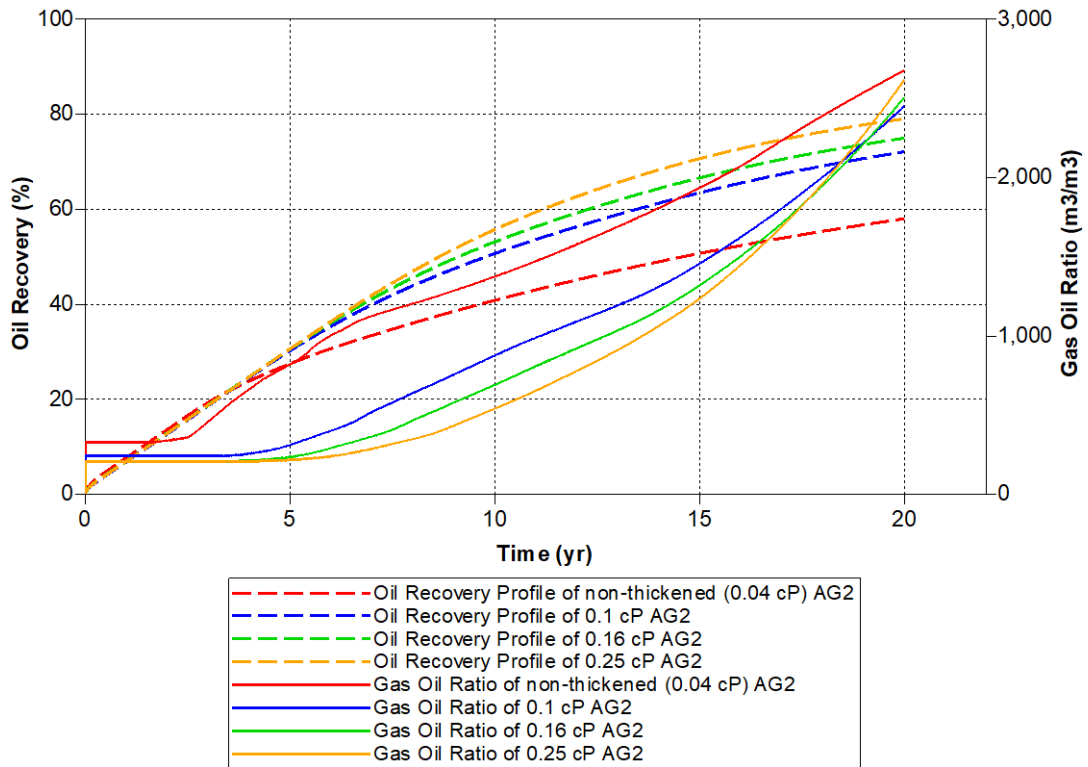


Figure 3.9 Effect of AG2 viscosity enhancement on the oil recovery profiles and production GOR development.

3.4.3.2 Effect of Oil Viscosity Reduction and Swelling

As mentioned earlier, the reduction of oil viscosity and oil swelling are two main factors which control oil recovery enhancement during MGI. Also, as discussed, the oil viscosity reduction and swelling factor vary with changing the amount and composition of the gas dissolved in the oil. Figures 3.10 to 3.12 show the oil recovery profiles and production GOR development for different AG mixtures enriched with CO₂, pure CO₂ and NGL for the cases of 0.1 cP, 0.16 cP and 0.25 cP increase in the injection gas viscosity, respectively. As expected, the oil recovery for the case of NGL injection is consistently higher than other thickened injected gases across all three thickening levels (0.1 cP, 0.16 cP and 0.25cP). This observation can be attributed to the fact that the thickened NGL has the greatest reducing effect on the oil viscosity and causes the highest oil swelling. At 0.16 cP viscosity increase (Figure 3.11), the ultimate oil recovery for the thickened NGL flood is 82.7%, while for the pure CO₂ flood is 72%. The lower recovery with pure CO₂ is because CO₂ is less effective at lowering oil viscosity and oil swelling. For the AG mixtures enriched with CO₂, the oil recovery is high and comparable to the recoveries obtained from thickened pure CO₂ flood. It is also evident from Figures 3.10 to 3.12 that oil recovery increases with

decreasing the CO₂ content in the AG mixtures. For the AG enriched with 50 mol% CO₂ the oil recovery is 73% compared to 76 % for the AG without CO₂ content (Figure 3.11). Similar results have also been obtained by Bon et al.[250] They reported that oil recovery by the injection of methane enriched with C₃₊ was higher than that of pure CO₂.

As discussed earlier in details for the case of AG2 injection, gas breakthrough is delayed for all gas injection scenarios when they are thickened. This delay results in lower overall production GOR in the first 20 years of the gas injection. However, after 8 years and once gas breakthrough occurs, the GOR increases significantly. The development of GOR versus time varies from one injection gas to another (Figures 3.10 to 3.12). The thickened pure CO₂ injection has the lowest overall GOR regardless of the level of thickening while the CO₂-enriched AG floods exhibit the highest overall GOR values. This is because the continual dissolution capacity (CDC) of the gases in oil varies from one gas mixture to another. After breakthrough, the CDC of a gas in oil is reduced, leading to an increase in the production GOR. Pure CO₂ has a higher CDC than the light hydrocarbon gases which results in an increase in the initial gas content of the oil. The CDC for the light hydrocarbon gases is lower which leads to higher GOR in the case of natural gas injection.[255] However, the effect described above does not affect the oil recovery because the oil viscosity reduction and oil swelling effects dominate the oil enhanced recovery process during the flooding.

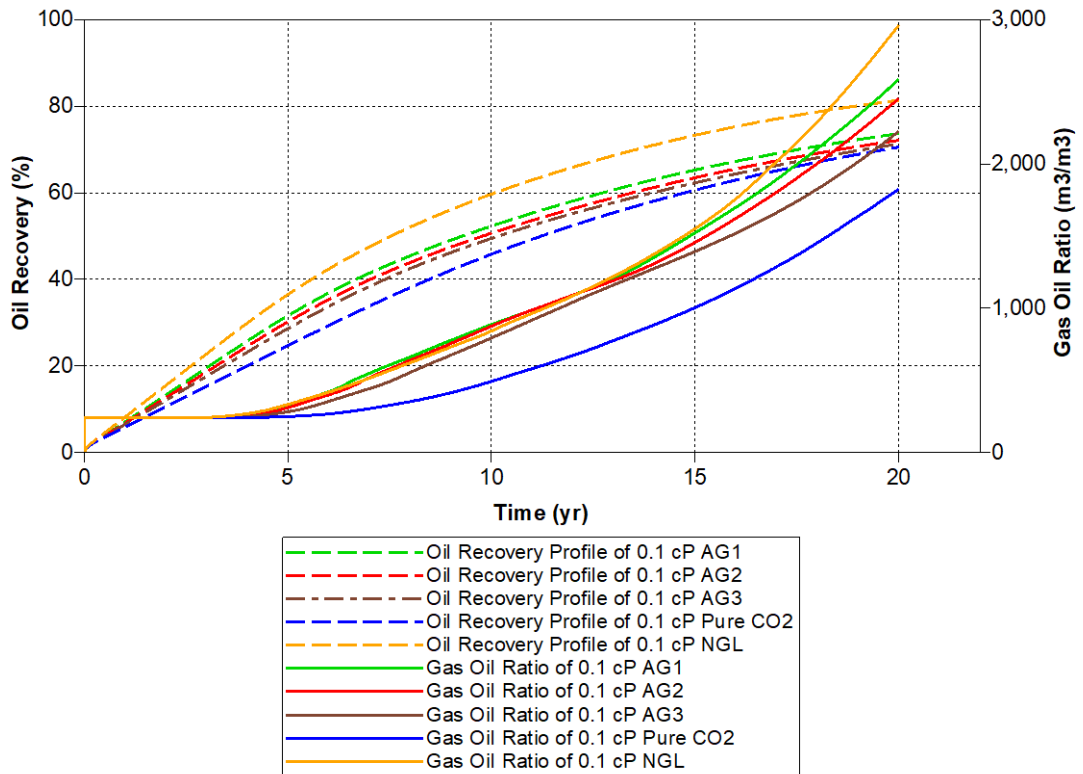


Figure 3.10 Oil recovery profiles and production GOR for 0.1 cP viscosity thickened gas floods.

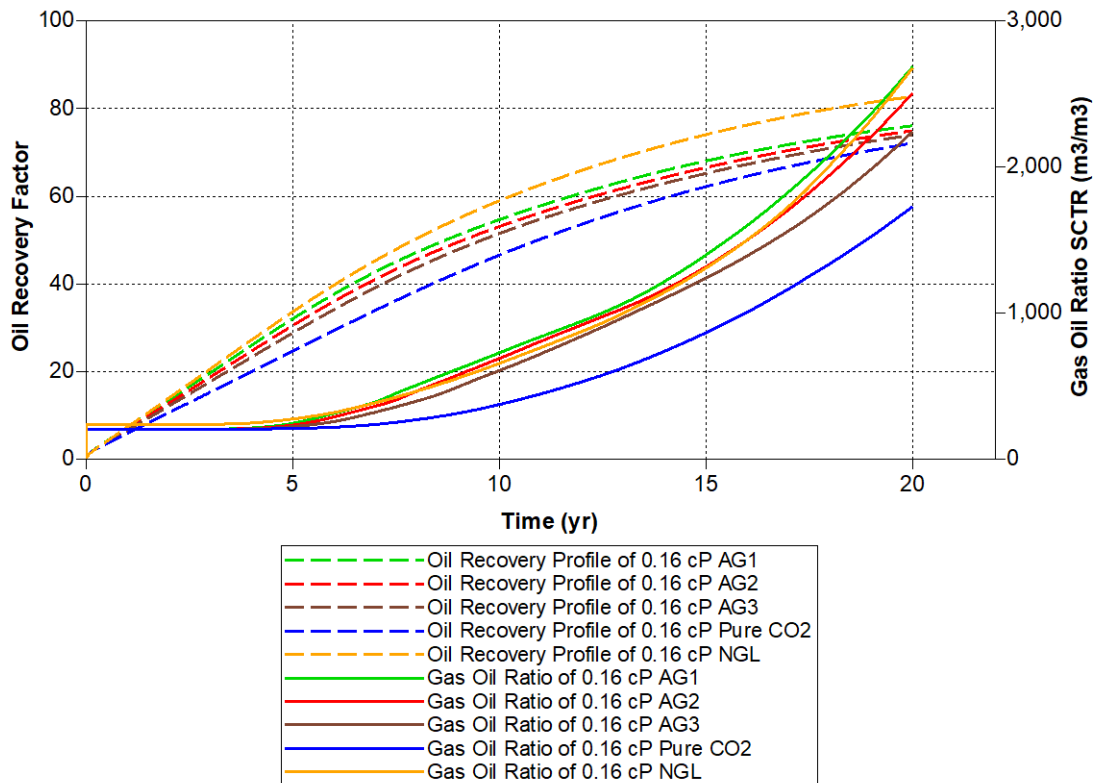


Figure 3.11 Oil recovery profiles and production GOR for 0.16 cP viscosity thickened gas floods.

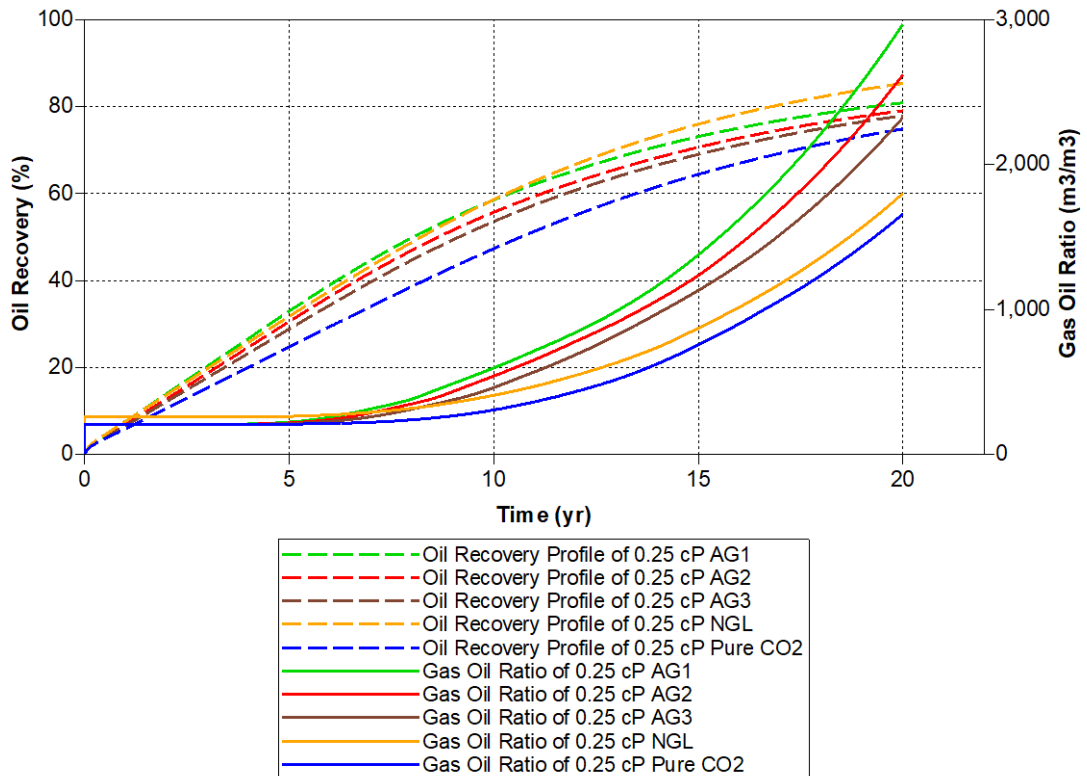


Figure 3.12 Oil recovery profiles and production GOR for 0.25 cP viscosity thickened gas floods.

3.5 Summary and Conclusions

The potential of different unthickened and thickened gas mixtures to enhance oil recovery under miscible conditions in Field A with a heterogeneous geological setting and a light oil was evaluated using a box model in the CMG-GEM simulator. The effect of different dissolution levels of various gas mixtures in the in-situ oil towards changing its properties were determined and taken into account using the CMG-WinProp PVT module. The following specific conclusions can be drawn from the outcomes of this simulation work:

- While a progressively higher reduction in oil viscosity can be obtained with an incremental increase in the dissolution of an injection gas in the oil, the presence of CO₂ in the AG mixture lowers the ability of the gas mixture to reduce the oil viscosity. Also, the oil viscosity reduction with natural gas dissolution is much more pronounced than that of pure CO₂.
- The dissolution of the light hydrocarbon gases into the oil leads to a decrease in the oil density. However the presence of CO₂ in the AG increases the injected

gas density and makes the gas mixture to be less effective in decreasing the oil density. Such an outcome results in a minimal difference between the densities of the injected gas and the light oil of Field A.

- Injection of a light hydrocarbon gas (C₁-C₄) has a higher swelling factor than pure CO₂ and methane enriched with CO₂.
- By adding viscosifying agents to the AG, NGL and CO₂ used for miscible gas flooding in Field A, the ultimate oil recovery factor can be increased significantly. The gas breakthrough can also be delayed reducing production GOR.
- The outcome of the simulation work demonstrate the advantages of thickening natural gas and NGL over CO₂ for improving the gas flood efficiency in a light oil reservoir such as Field A.

Chapter 4. Experimental Study of Miscible Thickened Natural Gas Injection for Enhanced Oil Recovery*

4.1 Introduction

Enhanced oil recovery (EOR) is an important field development step when oil in a reservoir can no longer be produced by natural drive mechanisms of the reservoir (primary recovery) or by water or immiscible gas injection (secondary or improved recovery).[1, 10, 257, 258] The aim of EOR techniques is to stimulate oil flow by overcoming the physical, chemical, and/or geologic factors that inhibit the production of the remaining oil in the reservoir.[4] Hydrocarbon-miscible gas injection (MGI) is considered as a tertiary recovery process that can increase the oil recovery by achieving miscibility between the injected gas and reservoir oil. The resulting gas/oil mixture can then be displaced more easily through the reservoir rock and swept to producing wells resulting in improved recovery.[11] As with other EOR techniques, MGI can be challenging and expensive.[35] For instance, treating and handling the gas as part of a gas recycling scheme can be expensive due to the separation, dehydration, and compression costs; and further impacted by concentration and quantities of gas to be handled. In addition, unfavourable mobility ratio (less viscous gas displacing more viscous oil) is a major subsurface factor that can reduce the sweep efficiency when applying this EOR technique.

In the Middle East, a number of MGI projects are currently being undertaken in carbonate reservoirs in which the injected AG often contains acid gases.[7, 35, 259] Field A, located in the Harweel cluster in southern Oman, has been recognised as a viable MGI candidate. The MGI in this field has already commenced where the source of the injection gas is the field's AG.[30] The AG mixture is reinjected into the reservoir at high pressure (up to 55 MPa) where it becomes miscible with the oil during the displacement at the relatively high reservoir temperature of up to 377 K. The AG in Field A contains CH₄ enriched with light and heavy hydrocarbon fractions found in natural gas and a significant amount of carbon dioxide at 10 – 25 mol%.[30] The reservoir contains a light crude oil with a gravity of 42° API and a viscosity of 0.23 cP

at reservoir conditions. With miscible AG injection, it is estimated that up to 47% of the original oil in place (OOIP) can be recovered.[32] However, even though the Field A oil is light and exhibits low viscosity, the viscosity and density contrast between the injection gas and reservoir oil presents technical challenges for the MGI process.

The major challenges faced by MGI in Field A may include gravity override caused by the density difference between the injected gas and the reservoir fluids and the unfavourable mobility ratio caused by the low in-situ viscosity of the injected gas (0.01 to 0.03 cP) compared with that of the oil (0.23 cP). Gravity override and unfavourable mobility ratio can result in early breakthrough (BT) of the injection gas and poor volumetric sweep, reducing the overall efficiency of the MGI development and preventing it from realising its full potential.[260] In fact, early gas breakthrough has already been experienced in some production wells in Field A. These challenges can be overcome by the implementation of several approaches that have been proposed in the literature, mainly for CO₂ flooding. The main objective of such approaches would be to effectively control the gas mobility and as a result increase the sweep efficiency of the gas flooding.[52] The most commonly used or proposed methods include water alternating gas flooding (WAG),[53, 54] entrainment of the gas into a foam during foam flooding,[57, 58, 61, 62] and increasing the gas viscosity by adding polymers as thickening agents to the gas.[52, 66] During the WAG process, the gas mobility is suppressed by alternating water and gas injection using a single to five cycles.[89, 247] In field applications, the CO₂-WAG flooding has proven to be effective resulting in incremental oil recovery of 5-10% of the OOIP.[247] However, very often, a large amount of residual oil is still left behind after the completion of WAG injection because of operational difficulties and challenges associated with this method, such as gravity segregation and water blocking due to the excessive water injected into the oil reservoir.[54, 89, 178, 258] Therefore, the WAG strategy may not be the best choice for Field A where water saturation is already very low and facilities are not designed to inject or handle water.

The application of foaming agents has also been studied as a way of conformance control in miscible flooding.[57] However, applying foams for mobility control has been shown to be technically and economically challenging because of the difficulties associated with controlling its propagation over large distances in the reservoir and that large volumes of a foam are required.[59] In addition, the majority of the foaming

agents are of no use in high salinity reservoirs due to the inability of the surfactants to reduce the interfacial tension (IFT) to the required ultralow values.[59]

To overcome the above limitations associated with WAG and foam flooding, another technique has been introduced which brings together the advantages of both chemical and miscible gas EOR methods. Introduced for the first time about 45 years ago, the application of thickener agents, such as small/high molecular weight polymers, has been proposed to directly thicken the injection gas used during gas flooding.[66] By increasing the injected gas viscosity, the gas mobility can be suppressed. Hence, the severity of the viscous fingering (i.e. instability in the displacement front) and the chance of developing premature breakthrough can be reduced and the microscopic displacement efficiency would also be improved. Among the techniques used to improve the mobility ratio of a gas flood, a direct thickening of the AG mixture by using additive polymers may be the best method to increase sweep efficiency in Field A as the field has a high salinity formation water and low water saturation in the reservoir. The AG in Field A contains 25 mol% of CO₂. The presence of CO₂ is considered as a positive factor as it may make the identification of suitable soluble polymers in the AG mixture easier because a number of studies have focused on polymer and small molecule solubility in CO₂. [158, 227, 228] Despite this, there are significant challenges in identifying soluble polymers because most polymers are insoluble in compressed fluids which have limited their widespread application.

To date, most of the research works regarding gas thickening agents have almost exclusively focused on polymers for CO₂ gas because it is widely used as the displacing fluid in EOR projects in the United States, Canada and elsewhere.[167] In addition, CO₂ is a slightly more powerful solvent than alkane components (CH₄ and C₂H₆) to dissolve polymers due to the quadrupole interactions relative to polymer-CO₂ segment.[158, 261] It is important to note that CO₂ is still considered a poor solvent when compared to more conventional organic solvents. However, some materials (hydroxyaluminum disoaps, trisurea) show greater solubility in liquid propane and butane than do in pure CO₂. [65, 227] There have been few attempts at identifying polymers which could thicken pure light hydrocarbon gases. In the late 1960s, initial attempts were made to thicken light alkanes as evident from several registered patents.[68, 69, 155] Henderson et al.[155] proposed some thickener polymers for buffer hydrocarbon. The identified polymers included poly methyl laurylate,

polybutadiene and poly alkyl styrene. These polymers at a concentration of 0.25 vol% are capable of increasing the viscosity of light hydrocarbon gases by about 0.1%. Additional patents were filed later by Dauben et al.[69] who also achieved a 2-3 fold viscosity enhancement for condensate mixtures contains 75% propane and 25% heptane-rich at 0.25 wt% of polyisobutylene. However, none of the patented work indicated the method(s) used to measure the viscosity enhancements of the solutions examined.[71] Heller et al.[64] successfully synthesised various α -olefin polymers (n-decene, n-pentene and n-hexene) which could be dissolved in CO₂ and LPG (n-butane and n-propane). Concentrations of 1-2.2 wt% of these polymers in liquid n-butane resulted in a 5 fold viscosity enhancement. Although, these polymers were found to be slightly soluble in CO₂, none could effectively increase the CO₂ viscosity.

In an attempt to identify polymers with small molecular chains as thickener candidates for light hydrocarbon gases and CO₂, Enick et al.[65] examined a series of hydroxylaluminum disoaps that could increase the viscosity of propane, pentane and hexane at diluted concentrations of 1 wt% without a co-solvent being required. Such findings proved that such small molecular chain polymers also may be capable of serving as thickener agents for miscible gas flooding. Dhuwe et. al and Lee et al.[71, 231] also reported that the solubility of silicone polymers in compressed liquid propane and butane is quite high for high molecular weight of poly(dimethylsiloxane) (PDMS) at low temperature. However once the temperature increases, it needs a higher pressure to get the polymer dissolved in the solution due to large difference of free volume between the solvent and polymer at high temperature, leading to separation. PDMS in ethane required a higher pressure to dissolve because the difference between the solubility parameters value (14.9-15.5 MPa^{0.5}) of PDMS and ethane (11.7 MPa^{0.5}) is more than 2.05 MPa^{0.5}. [231] Therefore, PDMS was an ineffective thickener in ethane and more effective in thickening propane and butane at 2 wt% and 62.05 MPa at 25 °C. Doherty et al.[227] also found that branched benzene trisurea solubility increases the propane viscosity between 1.2 to 1.5 fold at temperatures from 25 to 80 °C and the concentration of 1.5 wt%.

Recently, Dhuwe et al.[70] reported to have found small associative molecular thickeners for ethane, propane, and butane at the temperature range of 298-373 K and pressures of up to 62 MPa. They found tributyltin fluoride (TBTF) to dissolve in all above three gases without any heating/cooling cycle requirement. At 298 K the TBTF

was found to enhance the viscosity of all three light components by 70-100 fold at 1 wt% concentration. However, as the temperature increased, the thickening ability of the polymer substantially decreased due to degradation. Dhuwe et al.[70] found hydroxyaluminum di-2ethylhexanoate (HAD2EH) to be soluble in liquid propane and butane, but insoluble in liquid ethane. Furthermore, this small molecule was shown to be a good viscosifier for butane, but not as effective for propane. Also, addition of phosphate ester and a cross-linker mixture to natural gas liquid,[259] improved the viscosity just slightly compared to those caused by TBTF and HAD2EH.[70]

In the Dhuwe et al. study, the viscosity was measured using a falling ball viscometer. Another study evaluated the solubility and viscosity enhancing property of ultrahigh molecular weight drag reducing agent (DRA) poly- α -olefin, and high molecular weight PDMS (Mw 980,000) in NGL. At a concentration of 0.5 wt%, DRA polymer was found to be soluble in butane and propane above the vapour pressure for the temperature range of 298-333 K, and soluble in ethane above 20 MPa.[231] Above 3.5 MPa, DRA polymer proved to be a better thickener for butane and propane, and an ineffective thickener for ethane for pressures of up to 62 MPa due to its low solubility. This means that an NGL with high concentration of ethane requires higher pressure to dissolve the DRA polymer. A high molecular weight PDMS was found to be an ineffective thickener in NGL application for EOR.[231]

None of the above materials tested by other researchers have been used as a direct thickener specifically for an AG mixture containing primarily CH₄, NGL components and CO₂. In fact, the available data about the direct thickening of an AG mixture are very scarce in the literature. Therefore, in the case of Field A, none of the materials tested to date can be used as a thickener for the field's AG mixture which is being used for miscible gas flooding. There are similar fields around the globe containing a significant fraction of CO₂ (15-80%)[262-264] which makes this research more relevant to other field scenarios.

This study is to assess the solubility of a library of low/high molecular weight polymers in an AG mixture enriched with CO₂ and then examine their effectiveness to control the gas mobility in miscible gas EOR. In order to achieve this objective, first, a library of polymers was chosen to be tested for their solubility. The polymers were chosen based on the existing available data in the literature covering the solubility of

commercially available polymers in CO₂ and light hydrocarbons. Considering the composition of Field A AG, the solubility of a total of 32 polymers in a gas mixture containing 60% methane, 6% ethane, 9% propane, and 25% CO₂ was determined using a parallel gravimetric extraction method proposed by Bray et al.[265] The parallel gravimetric extraction is considered as a high throughput and effective technique for preliminary screening of polymers with regards to their solubility in a gas mixture. After selecting the polymers with the highest weight extracted during the high throughput solubility experiments, a series of cloud point pressure measurements were performed at different temperatures. The cloud point pressures were measured using different enriched gas mixtures using a high pressure windowed cell. These experiments were to check the compatibility of the polymers with the range of pressures applicable to Field A. In the next stage of the work, the polymer that has a lower cloud point pressure in the AG mixture at Field A reservoir conditions was examined for possible viscosity enhancement in the AG mixture, this was accomplished by using a manufactured capillary viscometer at different temperatures and different concentrations. Lastly, the potential of the polymer thickener as an EOR agent was evaluated using reservoir condition core flooding experiments. The core-flood experiments would reveal if a thickener can improve the sweep efficiency of the gas flood for Field A at lab scale. For these experiments representative carbonate core plugs and crude oil from the Field A were used.

4.2 Experimental Methodology

4.2.1 Materials

A complete list of the polymers/oligomers chosen initially to be investigated in this study is provided in Table 4.1. The polymers/oligomers were sourced from a number of international commercial suppliers (i.e. Jiangsu Yinyang Gumbase Material, Fluka AG, BASF- ICIS, DOW Corning, and Sigma-Aldrich). The gas mixture chosen to represent the average of major components of injected gas in Field A included three hydrocarbon gas mixtures (CH₄ 60 mol%, C₂H₆ 9 mol%, C₃H₈ 6 mol%, and CO₂ 25 mol%; CH₄ 75 mol%, C₂H₆ 9 mol%, C₃H₈ 6 mol%, and CO₂ 10 mol%; and CH₄ 40 mol%, C₂H₆ 7 mol%, C₃H₈ 3 mol%, and CO₂ 50 mol%) purchase from BOC Gas, Australia. The CMG WinProp Module (Version 2011) was used to estimate the density

of the HC gas mixtures as needed at different pressure and temperature values using Robinson equation of state (EOS).

The light crude oil was collected at the wellhead from the Field A, Oman. The density and viscosity of the dead crude oil were 0.81 g.cm^{-3} and 2.7 cP (377 K and 55 MPa), respectively. Since this was a dead oil sample, most of the light fractions had been flashed out of the oil and, therefore, there was no light hydrocarbon under C_5 in its composition (Table 4.2). The oil composition was obtained using gas chromatography with a flame ionization detector (GC-FID). Considering the available Field A brine composition, a synthetic brine was prepared in the laboratory using analytical grade salts and with a total dissolved solids of 275 g.L^{-1} ($\text{NaCl } 220 \text{ g.L}^{-1}$ and $\text{KCl } 55 \text{ g.L}^{-1}$). For the core flooding experiments, a number of relatively tight carbonate core plugs drilled from the Field A wells at reservoir depths of 4995 to 5000 meters were used.

Table 4.1 Library of polymers/oligomers used in parallel gravimetric extraction experiments.

Sample number	Polymer/oligomer/small molecule material name	Molecular weight	Degree of polymerization	Supplier
1	poly(vinyl acetate)	250,000	2,903.9	Jiangsu Yinyang Gumbase Material
2	poly(vinyl acetate)	150,000	1,742.3	Jiangsu Yinyang Gumbase Material
3	poly(vinyl acetate)	80,000	929.2	Jiangsu Yinyang Gumbase Material
4	poly(vinyl acetate)	55,000	639.8	Jiangsu Yinyang Gumbase Material
5	poly(vinyl acetate)	16,000	185.8	Jiangsu Yinyang Gumbase Material
6	poly (vinyl acetate co-vinyl alcohol)-40%	72,000	1,636.3	Fluka AG
7	poly (vinyl acetate co-vinyl alcohol)-80%	9,000	204.5	Fluka AG
8	poly (vinyl acetate co-vinyl alcohol)-88%	96,000	2,181.8	Fluka AG
9	poly(ethylene glycol)	8,000	21	BASF- ICIS
10	poly(dimethylsiloxane)	170,000	-	DOW Corning
11	poly(vinyl pyrrolidine)	10,000	4,000	BASF- ICIS
12	poly(4-vinyl pyridine)	60,000	570.6	BASF- ICIS
13	poly(4-vinyl pyridine)	50,000	475.5	BASF- ICIS
14	poly(methyl methacrylate)	15,000	148.3	Sigma Aldrich
15	hydroxyethyl-cellulose	140,000	-	Sigma Aldrich
16	poly (ethylene vinyl acetate)	55,000	481.8	Sigma Aldrich

17	cellulose acetate autyrate	70,000	-	Sigma Aldrich
18	poly(vinyl methyl ether)	60,500	1,041.6	Sigma Aldrich
19	poly (vinyl ethyl ether)	4,337	52.7	Sigma Aldrich
20	poly(dimethylsiloxane)	97,300	-	Sigma Aldrich
21	poly(butyl methacrylate)	337,000	2,369.9	Sigma Aldrich
22	poly (ethylene succinate)	10,000	69.3	Sigma Aldrich
23	poly(isobutylene)	200,000	3,564.6	Sigma Aldrich
24	poly(butadiene)	3,000	55.4	Sigma Aldrich
25	poly(propylene glycol) mono butyl ether	1,000	11.1	Sigma Aldrich
26	poly (propylene carbonate)	50,000	489.7	Sigma Aldrich
27	methyl- β -cyclodextrin	1,310	1	Sigma Aldrich
28	poly(methyl hydro siloxane)	3,200	-	Sigma Aldrich
29	poly(propylene glycol)	2,700	35.4	Sigma Aldrich
30	1,4-di-tert-butylbenzene	190	1	Sigma Aldrich
31	poly(vinyl methyl ketone)	500,000	7,133.6	Sigma Aldrich
32	poly(1-decene)	544	6.4	Sigma Aldrich

Table 4.2 Compositional analysis results of Field A dead oil in mole percentage

Component	Mole %	Component-cnt	Mole %
H ₂	0	C ₁₆	4.15
H ₂ S	0	C ₁₇	3.85
CO ₂	0	C ₁₈	3.77
N ₂	0	C ₁₉	3.97
C ₁	0	C ₂₀	3.27
C ₂	0	C ₂₁	2.99
C ₃	0	C ₂₂	2.87
iC ₄	0	C ₂₃	2.67
nC ₄	0	C ₂₄	2.47
C ₅	0	C ₂₅	2.19
iC ₅	0.01	C ₂₆	2.1
nC ₅	0.02	C ₂₇	1.99
C ₆	0.33	C ₂₈	1.85
C ₇	1.54	C ₂₉	1.85
C ₈	3.71	C ₃₀	1.77
C ₉	4.84	C ₃₁	1.64
C ₁₀	5.54	C ₃₂	1.43
C ₁₁	5.15	C ₃₃	1.35
C ₁₂	4.72	C ₃₄	1.26
C ₁₃	5.08	C ₃₅	1.2
C ₁₄	4.63	C ₃₆₊	10.93
C ₁₅	4.86	Total	100

4.2.2 Experimental Setup and Procedure

4.2.2.1 Polymer Solubility Measurements

4.2.2.1.1 High Throughput Gravimetric Extraction (HTGE)

In the literature, the HTGE screening method has been described as a rapid method to use when testing a large library of polymers for their solubility in gases and supercritical solvents (SCF). Figure 4.1 shows the schematic diagram of the gravimetric extraction experiment used in this research. The polymer extraction vessel is designed and built to hold 40 polymer samples at a time. To test every batch of polymers, first, an accurate weight balance was used to weigh the polymer samples. The polymer samples were weighed into open-ended Borosilicate glass tubes with a length of 60 mm and an ID of 6.6 mm. A piece of quartz frit was placed into the bottom opening of every tube to retain the sample. The quartz frit would let the gas mixture into the tube from bottom during the extraction experiment but would prevent the polymer sample from being drained from the tube. The top opening of every tube was then secured with a piece of tissue paper (KIMTECH science). The tissue would prevent any possible overflow of the polymer sample but would not prevent the gas mixture from freely flowing through the glass tube while extracting the polymer sample (if soluble). The tubes were secured in between specially designed slotted stainless steel disks before being placed inside the extractor shell (Figure 4.1). An AG mixture was introduced into the extraction vessel and pressurised to 55 MPa at constant flow rate (200 cc/min) using a gas compressor (Haskel, AGT-30/75). The gas was then flowed through the vessel under in-situ pressure and temperature for two hours at constant flow rate 80 cc/min. A dome-loaded back pressure regulator (BPR) connected to a syringe pump was used to control the gas pressure inside the vessel during the experiment. While the effluent gas from the extractor was vented into a fume cupboard, a water trap was used to catch the polymer material dropping out as the gas flashed to atmospheric pressure. After a predetermined period of the time, the gas injection was stopped and gas inside the extractor was slowly vented at 0.6 MPa/min, controlled by regulating pilot pressure applied to the BPR. Upon reaching atmospheric pressure, the glass tubes were carefully removed and individually reweighed to determine any weight loss that they may have endured. Every batch of polymers were tested twice at the same conditions. By comparing the results of every

two replicate experiments, the weight loss results were found to be reproducible within $\pm 2 - 4\%$ of the extracted weight. The gas mixture used in the extraction experiments contained 60 mol% methane, 9 mol% ethane, 6 mol% propane, and 25 mol% CO₂.

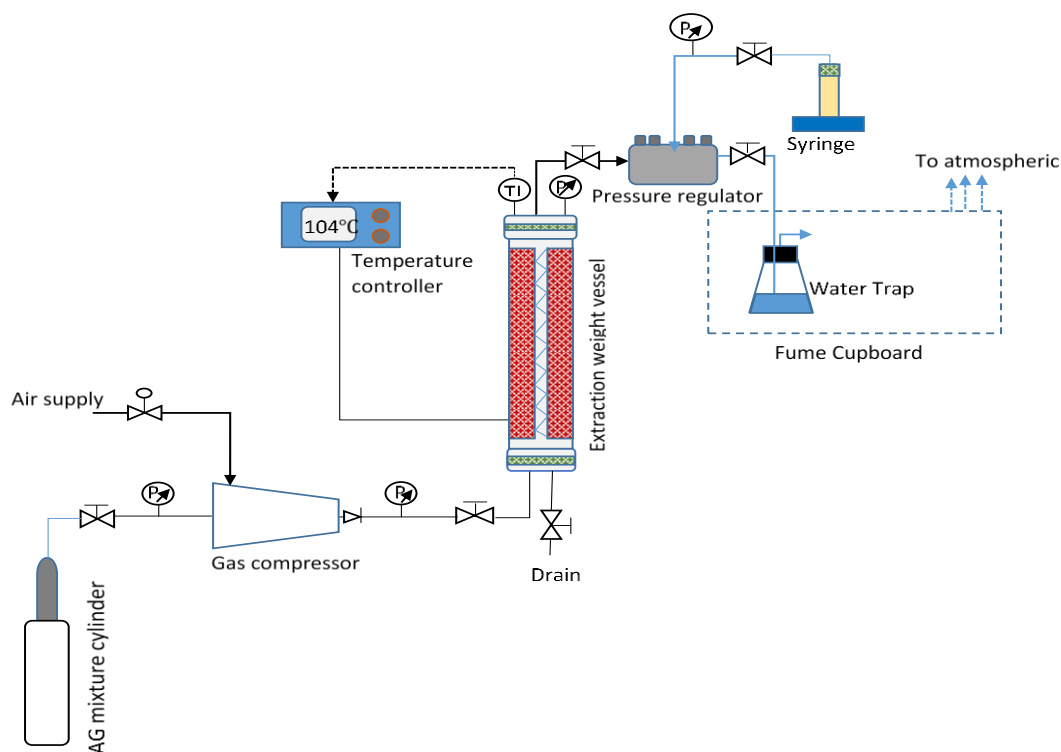


Figure 4.1 Schematic diagram of gravimetric extraction equipment used for rapid measurement of polymers solubility in AG mixture.

4.2.2.1.2 Cloud Point Curve Measurements

The cloud point pressure curves were determined using a standard technique set out in the literature involving isothermal compression and then slow decompression of binary mixtures of known compositions.[266] Cloud point pressure measurements were carried out for the three polymers/ oligomers that indicate a high level of extraction in the HTGE experiment to confirm its solubility in the AG mixture. Cloud point pressures were determined at a temperature range of 298 K-377 K for PDMS and poly(methyl hydro siloxane) (PMHS) (both at 1.5 wt%) in AG mixture. For poly(1-decene) (P-1-D), the cloud point pressures were measured at the temperature range of 358-377 K and at different P-1-D concentrations (1.5-9 wt%).

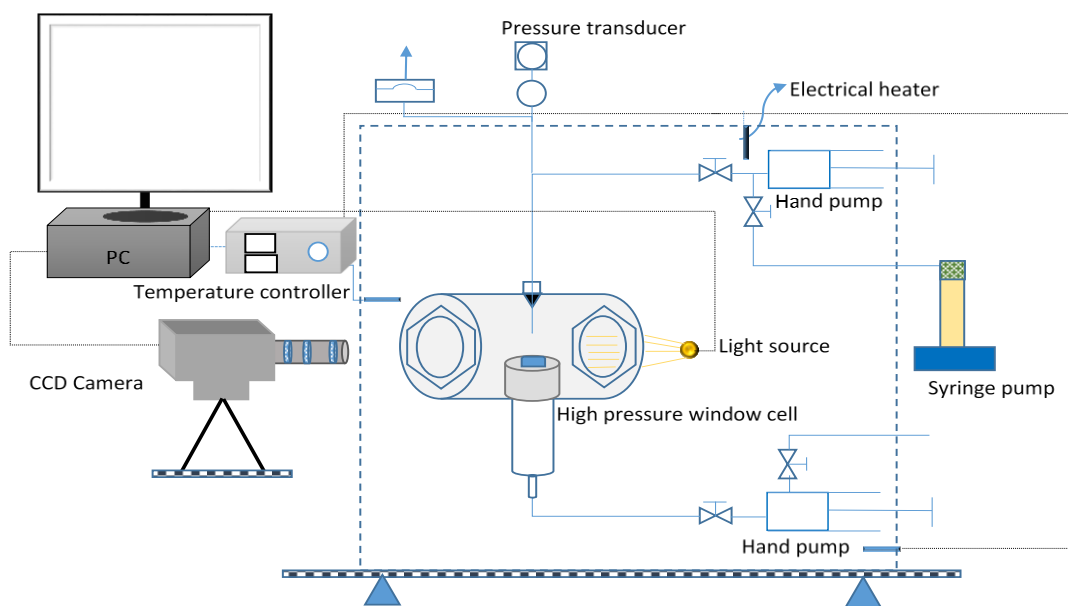


Figure 4.2 Schematic diagram of experimental setup used for cloud point pressure measurements.

Prior to each cloud point pressure measurement for a polymer/oligomer with known solubility (determined by HTGE method), the windowed cell (Figure 4.2) was cleaned with acetone and toluene sequentially. In each test run, the entire high pressure cell was thoroughly cleaned with acetone and then with toluene. The combination of solvents would remove the polymers residues from the cell. The cell is cleaned at a temperature less than 323 K. Then, it was placed under vacuum for a few hours to dry. For every polymer/oligomer, depending on its solubility in the AG mixture, a small amount of it was accurately weighed and placed on a clean thin glass plate. The weight of the polymer or oligomer was needed to place the required amount of it on the glass plate and also be able to calculate the exact composition of the polymer/AG mixture (in wt%) during the experiment knowing the volume of the high pressure windowed cell (i.e. 20 cm³). Then the glass plate was transferred to the view cell and placed horizontally on a small stand in the cell. The cell was closed, sealed, and displaced slowly with low pressure AG mixture to purge any air from the system. Then the temperature was raised to the reservoir in-situ value. The cell pressure was increased by introducing the AG mixture slowly using a syringe pump with increments of each 0.4 MPa until a single transparent phase of polymer/AG solution was achieved. This process was done under no stirring for the solution and monitored through the see through windows of the cell and using the instrument's camera. At this stage, the polymer had completely dissolved in the AG solution. Then the cloud point pressure

of the mixture at the set temperature was determined by slowly lowering the pressure by increments of each 0.4 MPa until the AG solution became cloudy. The pressure at which it was no longer possible to see the back of the cell through the polymer/gas solution (90% reduction in transmitted light intensity) was recorded as the cloud point pressure. For any given weight percent of every polymer/oligomer, this process was repeated three times. The results were found to be reproducible within ∓ 0.5 MPa.

4.2.2.2 Viscosity Measurements

The viscosity of the AG mixture and oligomer-thickened AG were measured in a capillary viscometer (CVL-1000, Core Laboratories Inc.) (Figure 4.3). It is specifically designed to measure the viscosity of single phase fluids at high pressure and high temperature within the range of 0.01 to 10,000 cP. It operates based on the Hagen-Poiseuille law, measuring the exerted pressure drop across a capillary tube while flowing a fluid through the tube at a predetermined flowrate (0.01 to 1.5 ml.min⁻¹). A principle of the Poiseuille equation is employed in this viscometer to measure the viscosity of the single-phase AG mixture μ_{AG} or thickened AG solution μ_{sol} (cP):

$$\mu_{sol} = \frac{\pi (r_{eff})^4 \Delta P}{8 Q L} \quad \text{Eq 4. 1}$$

$$\mu_{sol} = K \frac{\Delta P}{Q} \quad \text{Eq 4. 2}$$

Where, Q m³.s⁻¹ is the injection rate of thickened AG solution through the capillary tube, ΔP (bar) is the measured pressure drop across the capillary tube, r_{eff} (mm) and L (mm) are the effective radius and the length of capillary tubing. K is a factor that depends only on the parameters of the tubing:

$$K = \frac{\pi (r_{eff})^4}{8 L} \quad \text{Eq 4. 3}$$

The K factor values for the capillary tubing mounted in the viscometer (5 m length and 0.18 mm internal diameter) was calculated from determined linear slopes ($\Delta P/Q$) at two temperatures 298 K and 377 K and four different injection rates of (0.05, 0.08 , 0.1 and 0.2) $\text{cm}^3 \cdot \text{min}^{-1}$ using a known viscosity of water at temperature and pressure . The K values found from the calibration are equal 0.036 at 298K and 0.033 at 377 K. Then, Falcon software estimates the K values for measuring the fluid viscosity over temperatures ranges of 358 to 377 K to be equal 0.033.

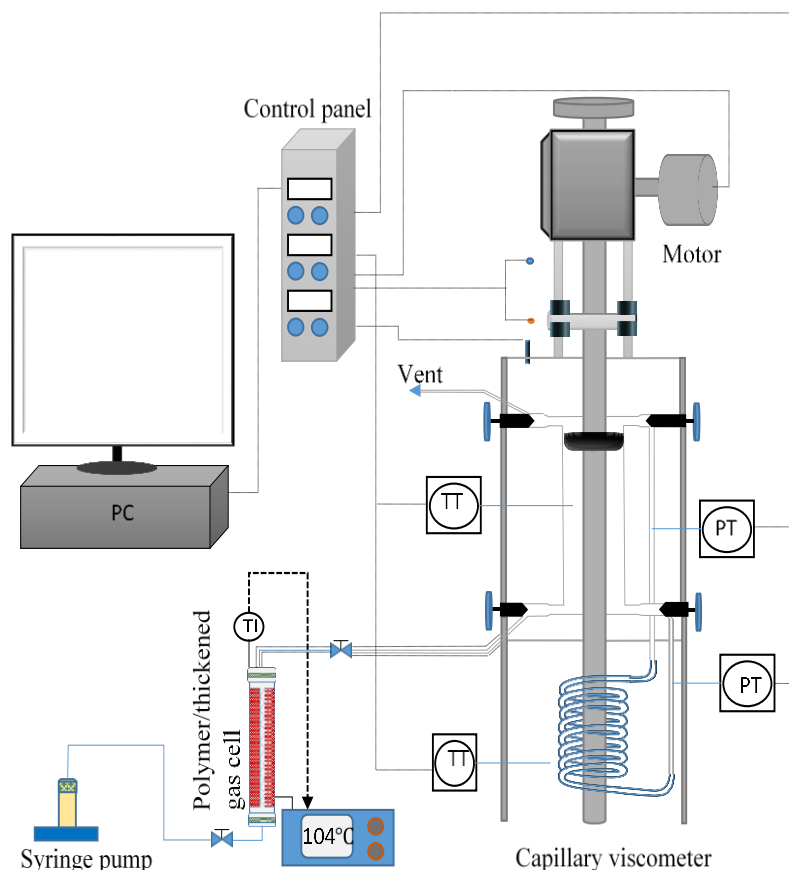


Figure 4.3 Schematic of Capillary Viscometer used for viscosity measurements (55 MPa and 377 K).

Due to the small ID of the coiled capillary tube (0.18 mm) in the viscometer, there was a concern that at the conclusion of every measurement, any leftover oligomer inside the tube could not be completely cleaned impacting the next measurement with the next AG/oligomer solution. Therefore, prior to re-measuring the viscosity of every solution, the coiled capillary tubing was replaced with a new one and the instrument was recalibrated. For every experiment, the instrument was heated to the desired temperature and then vacuumed before being filled and pressurised with the oligomer

thickened AG or the AG mixture on its own. After attaining stability in the viscometer, the solution was passed through the capillary tube at different injection rates. The flow rates were kept low enough to have laminar flow (Reynolds number less than 2000) in every viscosity measurement. Using the viscometer's software, a range of suitable flow rates could be predicted. Such a range was found to be 0.1 to 0.3 cm³.min⁻¹ for the oligomer/AG solutions and 0.05 to 0.1 cm³.min⁻¹ for the AG mixture. The viscosity of every solution was measured at least three times to ensure the reproducibility of the results.

4.2.2.3 Core Flooding Experiments

A schematic diagram of the core flooding setup used for the oligomer-thickened AG and AG mixture flooding is shown in Figure 4.4. The apparatus consisted of four modules: a core holder, injection system, heating system and production system. The core holder was of Core Laboratories' HCH Series, Biaxial type. As can be seen from Figure 4.4, the injection system consisted of four one-liter fluid accumulators, one for each of the injection fluids. The syringe pumps were all of pulsation free, positive displacement type (Vinci Technology) providing constant pressure or constant injection flow rate with high precision. The fluid accumulators and the core-holder were heated to the desired temperature using heating jackets (SRH Etched foil, Watlow, USA) and the flow-lines and other fittings/connections carrying the injection/production fluids were heated using suitable heating tapes (Stretch-To-Length, Watlow, USA). The temperature was also regulated during the experiments using a digital temperature controller (Standard-89000-00, Digi-Sense, USA). On the production side, the pore pressure was regulated using a dome-loaded back pressure regulator whose pilot pressure was provided by a syringe pump. Tall-form accurately graduated cylinders were also used to collect and measure the produced fluid at atmospheric conditions. In addition to analog pressure gauges installed at various spots to monitor the pressure within various components of the core-flood system, two digital pressure transducers (KELLER, K-107) were installed at the inlet and outlet of the core-holder to monitor and record the differential pressure across the core plug with an accuracy of ± 1 psi.

For every experiment a composite rock sample was constructed using two reservoir core plugs from Field A. Each composite core was about 14 cm long and 3.8 cm in

diameter. The core-plugs were initially cut in synthetic formation brine and then cleaned using toluene and methanol in a temperature controlled Dean- Stark extractor. Subsequently, they were dried in an oven at 358 K for about 24 h. Prior to being flooded, the porosity and gas permeability of each plug was measured using an automatic porosi-permeameter (AP-608 instrument, Coretest Systems Inc.). The composite sample was then wrapped in a combination sleeve made up of FEP heat shrink and Viton rubber and placed inside a horizontal core-holder. After applying the next effective pressure of 6.82 MPa as the overburden pressure, the sample was vacuumed for 24 hours. Then, the overburden pressure, temperature and pore pressure were raised gradually to their respective in-situ values. At all stages, the overburden pressure was maintained 6.82 MPa higher than pore pressure reaching a final value of 62 MPa, eventually.

After reaching the full in-situ pore pressure, to ensure that the sample was completely saturated with the formation brine, the sample was subjected to brine injection at a constant flow rate of $0.2 \text{ cm}^3 \cdot \text{min}^{-1}$ for two days. At the conclusion of the saturation process, the absolute permeability for the composite core was determined at three different flow rates (0.2, 0.4 and $0.8 \text{ cm}^3 \cdot \text{min}^{-1}$). The brine saturated core plugs were then exposed to the reservoir dead oil which was injected at a rate of $0.3 \text{ cm}^3 \cdot \text{min}^{-1}$ for three to four days until reaching steady state conditions corresponding to irreducible water saturation. During this time, the volumes of the produced oil and brine were recorded. This preparation process was repeated at every test after the composite core plugs were cleaned from the previous test. After the irreducible water saturation was achieved in each test, the AG mixture and/or thickened AG solution were injected at a constant injection rate of $0.4 \text{ cm}^3 \cdot \text{min}^{-1}$ in all three flooding tests.

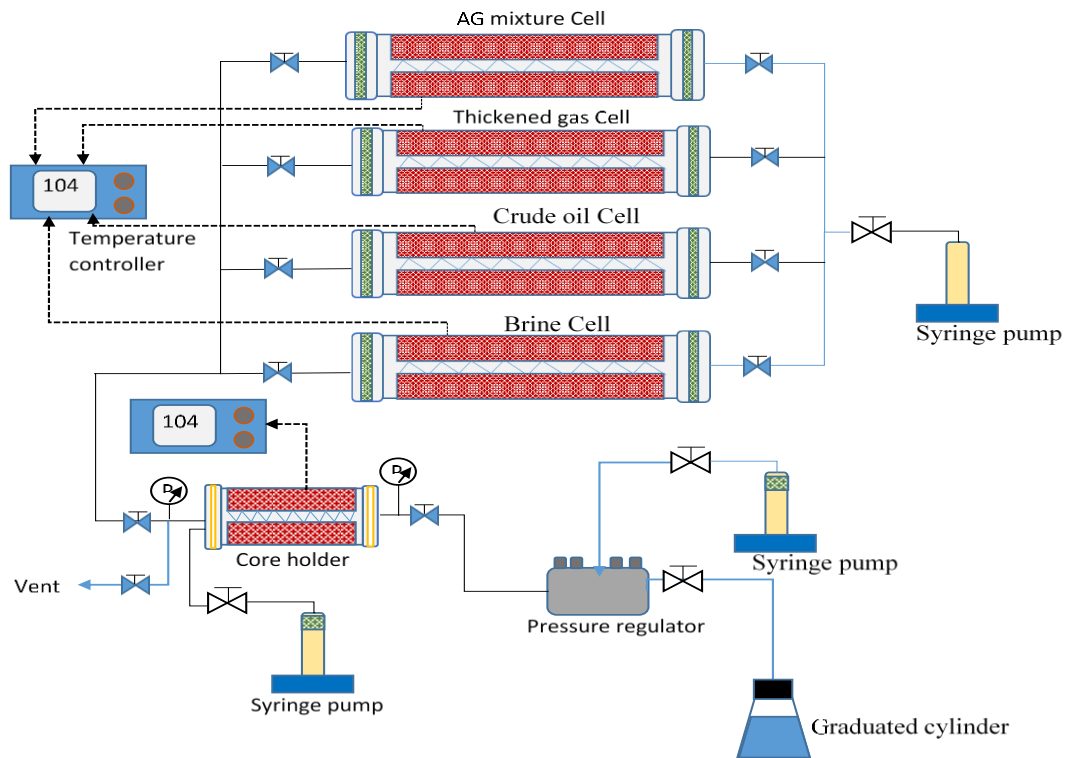


Figure 4.4 Schematic diagram of the core-flood setup.

For the first test, only the P-1-D-thickened AG solution was employed as a secondary oil recovery. This P-1-D-thickened AG solution was injected at a constant injection rate until a total of 9 PV (pore volume) of thickened AG solution was injected and no more oil was produced. After successfully completing the first test, the core was thoroughly cleaned and prepared for the second test. In this test both the AG mixture and the P-1-D -thickened AG solution (P 1-D, 5 wt%) were introduced into the core. At first the AG mixture was injected at a rate of $0.4 \text{ cm}^3 \cdot \text{min}^{-1}$ until there was no more oil produced from the composite core plugs which was roughly 3.6 PV. The subsequent P-1-D-thickened AG solution was then introduced into the core to aid in the production of the remaining oil in the core plugs.

The third test was mainly focused around the breakthrough of the AG mixture, in this particular test the core plugs were flooded with the AG mixture at the same injection rate until breakthrough is detected. As soon as breakthrough was observed, the P-1-D thickened AG solution was commenced to produce the residual oil and the solution injection was continued until a total of 9 PV was injected.

In each test, the cumulative produced oil volume inside the graduated cylinder was recorded and the gas was released into the atmosphere through the fume cupboard

(Johndec, M 1.5). At the end of each test, an oil recovery factor versus injected gas/oligomer pore volume plot was generated from the production and injection data. It should also be mentioned that, there was no brine production during all three tests.

4.3 Results and Discussions

4.3.1 Polymers/Oligomers Solubility in the AG Mixture

In general, solubility of polymers/oligomers in gas mixtures containing mainly CH₄ is very low as the light alkanes are very weak supercritical solvents (SCF) unless the system pressure and temperature are and/or the density of the components are considerably high.[158] In addition, it is difficult to perform molecular dynamic simulation studies for gas mixtures containing more than one component to determine the solubility of polymers in them at any given pressure and temperature. Therefore, as the only viable option, the previously described high- throughput extraction method was used to screen the solubility of the selected 32 polymers/oligomers in supercritical hydrocarbon gas mixture (CH₄ 60 mol%, C₂H₆ 9 mol%, C₃H₈ 6 mol% and CO₂ 25 mol%). Figure 4.5 shows the percentage of the original weight of every polymer or oligomer extracted by the AG mixture. As pointed out before, the 32 polymers/oligomers examined were commercially available materials which had been tested by other researchers to be soluble in pure CO₂ at high and/or low pressures. Based on the solubility data presented in this graph, the polymers/oligomers may be divided into four categories. The first category are those with high level of extraction (> 96%) under the conditions explored in this work. This category contains three oligomers and one polymer namely P-1-D (Mw 544), 1,4-di-tert-butylbenzene (Mw 190), PMHS (Mw 3,200) and PDMS (Mw 97,300). The second category contains the polymers/oligomers with a moderate level of extraction (45-85%). This category covers another three polymers and one oligomer namely PDMS (Mw 170,000), poly(vinyl methyl ether) (Mw 60,500), poly(vinyl ethyl ether) (Mw 4,337), and poly(propylene glycol) (Mw 2,700). These materials would need more pressure and/or more volume of gas passing through the extraction vessel so they may dissolve completely in the AG mixture. The third category includes those with a low level of extraction (5-20%). The materials in this category include poly(ethylene glycol) (Mw 8,000), poly(ethylene succinate) (Mw 10,000), polybutadiene (Mw, 3000) and poly(propylene glycol) mono butyl ether (Mw 1,000). From the second and third

category, it can be seen that the polymer backbone and molecular weight architectures affect the polymer solubility in the AG mixture. For instance, the weight extraction of poly(vinyl alkyl ether) increases with increase in the length of the alkyl tail from methyl to ethyl (45-85%). As the length of alkyl tail on this polymer increases, the free volume of this polymer is expected to increase, which makes this polymer easier to dissolve in the AG mixture if the alkyl tail increases to propyl or butyl. For the molecular weight effects, the PDMS (Mw 170,000) in category two was much less soluble in the AG mixture than PDMS (Mw 97,000) in category one due to the entropic effects associated with the higher molecular weight of PDMS. The final category includes those polymers with negligible, < 5% extraction. These polymers belong to the carbonated and hydroxyl end groups such as poly vinyl acetate (PVAc) and poly (vinyl acetate co-vinyl alcohol) (PVA-coVA). These end groups enhanced the solubility of low/high molecular weight polymers in pure CO₂ under high pressure,[267] but unfortunately, that did not occur in the case of the AG mixture even when enriched with CO₂.

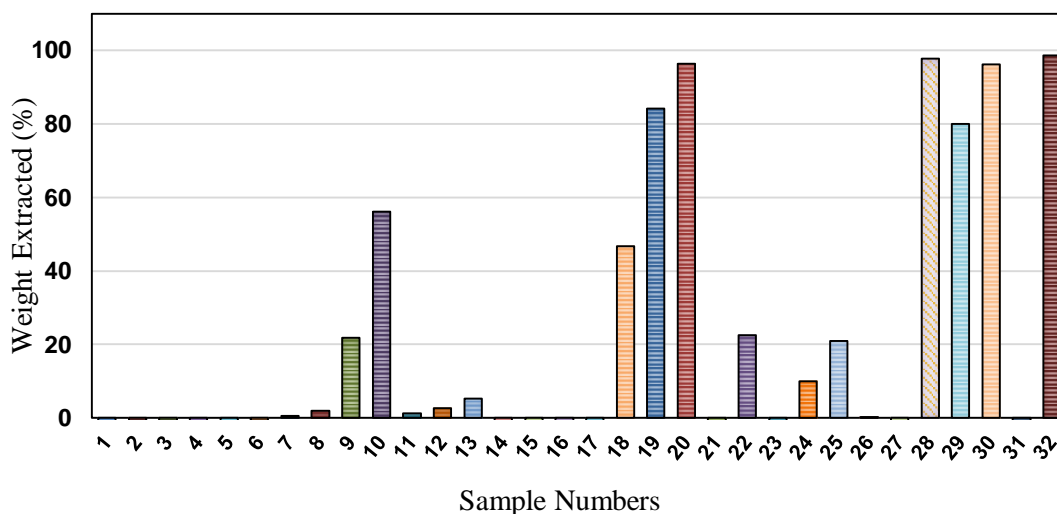


Figure 4.5 Extracted weight % in the AG mixture for a library the 32 polymers/oligomers at 55 MPa and 337 K. The name of the polymers/oligomers whose numbers are presented on the horizontal axis can be found in Table 4.1.

The polymer/oligomer concentration in the AG mixture is determined using the following equation:

$$\chi_{\text{sol}} = \frac{m_p}{m_p + \rho_{\text{AG}} \cdot (V_{\text{cell}} - \frac{m_p}{\rho_p})} \quad \text{Eq 4. 4}$$

Where ρ_p (g.cm^{-3}) and m_p (g) are the density and mass of the polymer that is dissolved into the AG mixture. V_{cell} is the volume of the windowed cell which is equal to 20 cm^3 . ρ_{AG} (g.cm^{-3}) is the density of the AG mixture at reservoir pressure and temperature which is estimated using the CMG WinProp model.

The solubility of those polymers/oligomers with high extraction percentages (Category 1 from above) was further verified using conventional cloud point pressure measurements conducted over a range of temperatures (concentration was 1.5 wt%). A 1,3-di-tert-butylbenzene substance has been excluded from the cloud point pressures measurements because it has a low molecular weight (190 g.mol^{-1}) and is expected to have an insignificant effect on the results. However, it is included in the previous test to validate the high soluble polymers results from the HTGE experiment, as this is also proved by Miller, M.B., et al.(2012) that 2,4-di-tert-butylbenzene was soluble in CO_2 and CO_2/H_2 mixture.[268] Figure 4.6 shows the measured cloud point pressures for PDMS, PMHS and P-1-D at different temperatures. As can be seen, PDMS and PMHS were found to be completely soluble in the AG mixture over the whole range of temperatures investigated (298-383 K) while for P-1-D, that was found to be the case only at temperatures above 358 K. These measurements indicate that P-1-D and PMHS can be adequately dissolved into the AG mixture under Field A reservoir conditions. Under the Field A temperature, PDMS has a much higher cloud point pressure than other two oligomers due to the energetic and entropic effects.[269] In general, most of the polymers and oligomers exhibit LCST (Lower critical solution temperature) trends in the volatile hydrocarbon components and CO_2 .[158] As the temperature increases, a higher pressure is required to dissolve the polymer or oligomer in a mixture. As apparent from Figure 4.6 PMHS exhibits similar trend to the PDMS in the light hydrocarbon gases and CO_2 mixture. The solubility of both additives have a strong dependency on temperature as their molecular weights are less than $100,000 \text{ g.mol}^{-1}$. In a previous study, Zeman et al.[270] found that PDMS has a high solubility in light hydrocarbon gases ($\text{C}_2\text{H}_6 - \text{C}_4\text{H}_{10}$) because of the large thermal expansion coefficient for the PDMS and low reduced temperature values for the solvents. However, this

solubility reduces with reducing the molecule size of alkane, similar to earlier described work that Dhuwe et al. found PDMS to be less soluble in ethane than propane and butane.[231] Therefore, in this study, PDMS becomes less soluble in the AG mixture as CH₄ is the main constituent of the gas mixture. In addition, due to the entropic effects, the density of PDMS decreases and its free volume increases at high temperature, making PDMS to be less soluble in the AG mixture as the temperature is increased. Therefore, it needs a higher pressure to dissolve completely in the gas mixture at high temperatures.

The observed solubility for silicone polymer/oligomer (PMDS and PHMS) and poly alfa-olefin (PAO) oligomer (P-1-D) in the gas mixture is probably due to partial presence of CO₂ in the mixture and the influence of high temperature and pressure. Generally, the solubility of polymers in a mixture consisting of low molecular weight components increases at elevated temperature due to the dominance of dispersion interactions.[158] In the experiments conducted here, P-1-D behaves as a single phase liquid in the AG mixture only at temperature above 358 K, unlike PDMS and PMHS, which start behaving as single-phase liquids in the gas mixture at 298 K as can be seen in Figure 4.6. Thermodynamically, the heat of mixing depends on the difference between the cohesive energy of a solution, as the temperature rises, the cohesive energy of the mixture becomes greater than the total cohesive energies of the component liquids.[271] The temperature and pressure needed to obtain the solubility of the polymers in SCF depend on the intermolecular interaction between solvent-polymers segment and polymer-polymer and solvent-solvent in solution.[272] A P-1-D has flexible alkyl branching groups on each other carbon of their backbone chain. These flexible alkyl groups can shape themselves in numerous conformations, forming random oligomer coil. These conformations impact on the accessibility of light gas to the oligomer coil. As the temperature increases, the solvent becomes more effective and the oligomer coil expands which causes a lower contact surface area between molecules and decreases the intermolecular interactions.[273] If the temperature is high enough as is in Field A, the energetic interaction between the oligomers and solvents outweigh the oligomers segment-segment and solvent-solvent interaction. In Figure 4.6, above 358 K the P-1-D becomes completely soluble in the mixture which can obtain a single phase solution at suitable pressure. Therefore, given these solubility conditions, P-1-D is expected to dissolve in the AG mixture at Field A conditions.

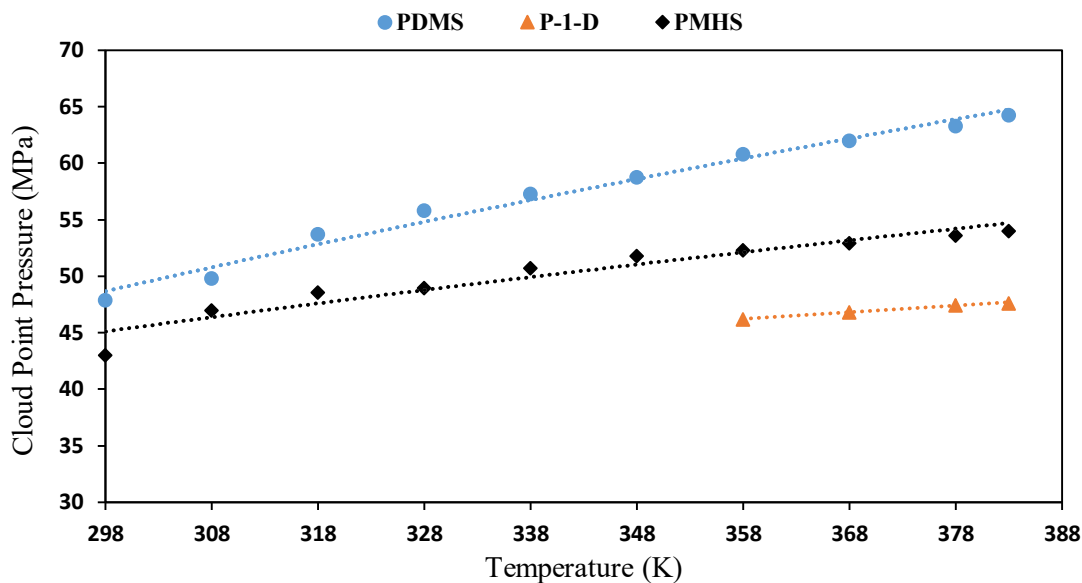


Figure 4.6 Measured cloud point pressures for three polymers at 1.5wt% in the AG mixture at different temperatures.

CO₂ is a weak solvent for many polymers. Several studies have reported that silicone polymer and PAO oligomer are soluble in CO₂ under supercritical conditions.[64, 66, 274-277] Partial presence of CO₂ in a hydrocarbon gas mixture can have a large influence on the cloud point pressure of the polymer/oligomer- gas mixture as evident from Figures 4.7 and 4.8. The cloud point pressures were measured for PMHS and P-1-D at a concentration of 1.5 wt% in three AG mixtures containing different CO₂ weight fractions (CH₄ 75 mol%, C₂H₆ 9 mol%, C₃H₈ 6 mol%, and CO₂ 10 mol%; CH₄ 60 mol%, C₂H₆ 9 mol%, C₃H₈ 6 mol%, and CO₂ 25 mol%; and CH₄ 40 mol%, C₂H₆ 7 mol%, C₃H₈ 3 mol%, and CO₂ 50 mol%). It is found that as the CO₂ content in the AG mixture increases, the cloud point pressure decreases across all temperatures. As can be seen from the two figures, a 15% increase in the CO₂ content (from 10 to 25 mol%) in the gas mixture causes a reduction in cloud point pressure of around 3 MPa for both oligomers. These results may indicate that the presence of CO₂ in the AG mixture can possibly facilitate the dissolution of silicone and POA oligomers in the gas mixture. In comparison to the silicone oligomer in pure CO₂, Lee et al.[278] found the cloud point pressures of low molecular weight (Mw 3,780) PDMS (10 MPa, 14 MPa) at the concentration 2 wt% and different temperatures (296 K and 313 K) to be 4.7-3.4 times less than that of the AG enriched by CO₂. That is because PDMS molecules are more CO₂-philic than light hydrocarbon.

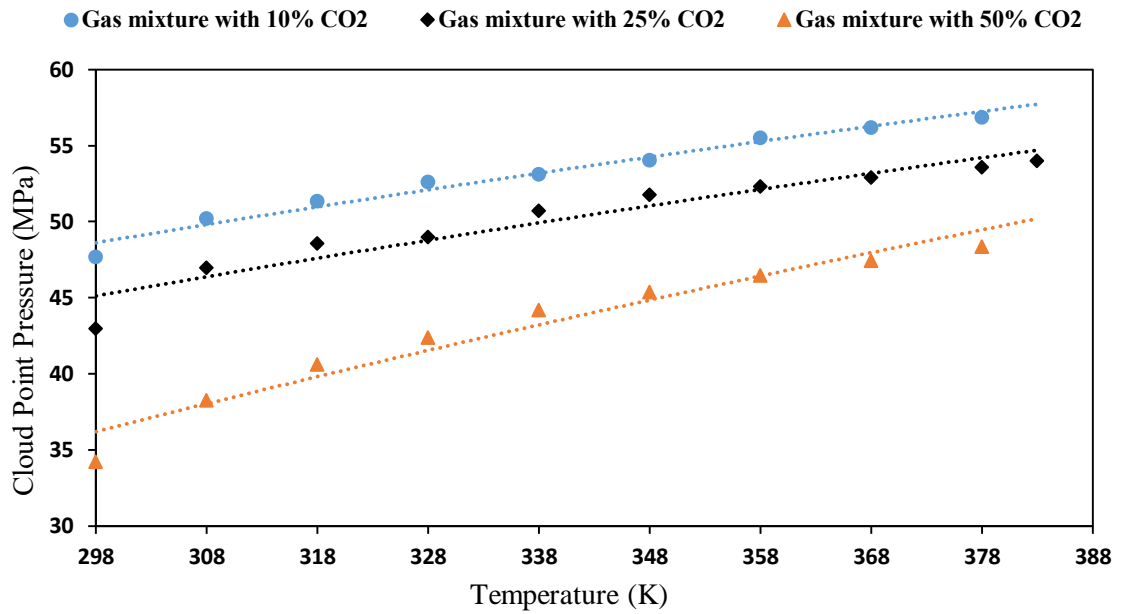


Figure 4.7 Measured cloud point pressures for PMHS at 1.5 wt% in the AG mixture containing different percentages of CO₂ at different temperatures.

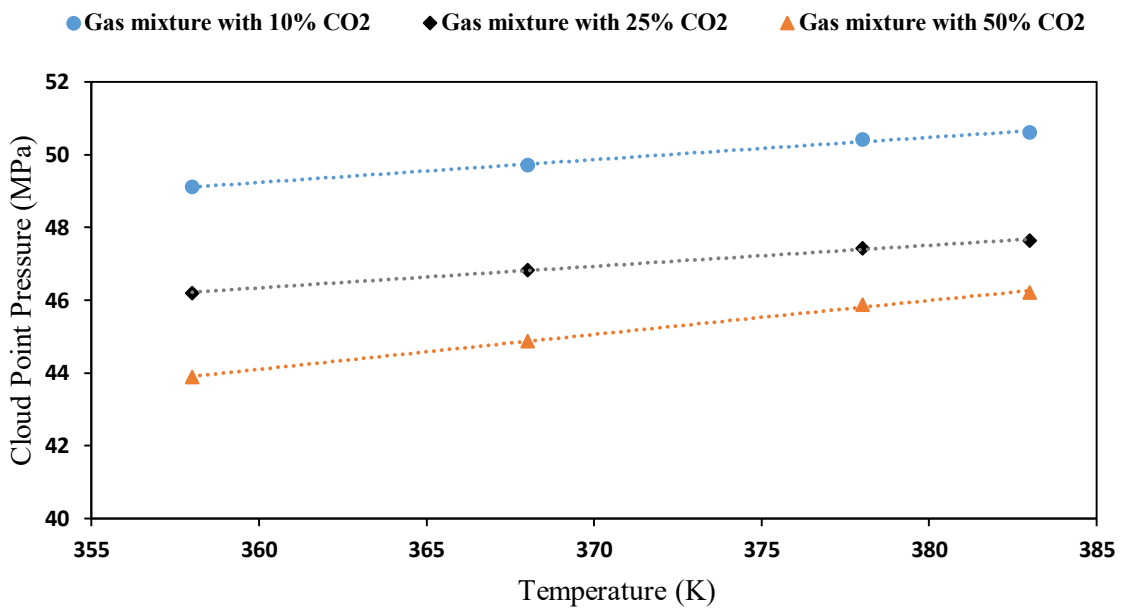


Figure 4.8 Measured cloud point pressures for P-1-D at 1.5 wt% in the AG mixture containing different percentages of CO₂ at different temperatures.

Based on the earlier presented solubility results (Figure 4.6), among the three materials examined, P-1-D has a lower cloud point pressure in the AG mixture at Field A reservoir conditions. Lower cloud point pressure may also make it possible to increase its concentration in the gas mixture to values higher than 1.5 wt% to further increase the AG mixture viscosity. In comparison, the cloud point pressures of both

PDMS and PMHS are considerably higher even exceeding the reservoir pressure limit (55 MPa). Therefore, the concentrations for both additives cannot be increased to more than 1.5 wt%. Furthermore, according to the data reported in the literature, at 298 K, the miscibility pressures of PDMS (2 wt%) with pure CO₂, ethane, propane and butane (23 MPa, 12 MPa, 1.07 MPa and 0.31 MPa, respectively) are much less than the miscibility pressure of PDMS and PMHS in the AG mixture (47 MPa and 43 MPa, respectively).[231, 278] This is because CH₄ is the main component in the mixture making PDMS less soluble. A 1- 2 wt% solution of PDMS in CO₂ or NGL enhanced the viscosity to only 1.5 to 2 fold only at 298 K. [231] Hence, PDMS and PMHS may not be expected to be suitable thickeners at higher temperature. Therefore, the focus of any further assessments has been placed solely on P-1-D.

The cloud point pressure for P-1-D was measured in the AG mixture containing CH₄ 60 mol%, C₂H₆ 9 mol%, C₃H₈ 6 mol%, and CO₂ 25 mol%, at three temperatures of 358 K, 368 K and 377 K and for a range of concentrations. The results of the measurements are plotted in Figure 4.9. As can be seen from the figure, at all three temperatures, the measured cloud point pressure increases linearly with P-1-D concentration. As expected, with increasing temperature, a higher pressure is needed to dissolve the P-1-D /AG mixture in a single phase. At 9 wt% of P-1-D in the mixture, the required pressure has to be 51.4 MPa at 377 K which is still below the reservoir pressure of 55 MPa. Hence, P-1-D oligomer can be adequately dissolved into this mixture at reservoir conditions even for concentrations higher than 9 wt%. This behaviour is because of the solvent entropy effect on the oligomer solubility as described earlier. At high temperature, changes in the cloud point pressure are very subtle, as can be seen in Figure 4.8. The reason behind such a behaviour can be explained as follows. Generally, as the temperature increases the free volume difference between the solvent and the polymer would increase leading to the system phase separation which then requires elevated pressures for the solution to remain a single phase.[158] However, at high pressure, the molar volume of the solvents reduces and the difference in free volume decreases between the polymer and the solvent which leads to the enthalpy of mixing dominating over the entropic of mixing.[158] That can be attributed to the cloud point pressure curve being relatively constant with increasing temperature. Figure 4.9 shows the results of cloud point pressure measured for P-1-D at different known solubilities and temperatures. At all

three temperatures, the measured cloud point pressures increase linearly with P-1-D solubility weight.

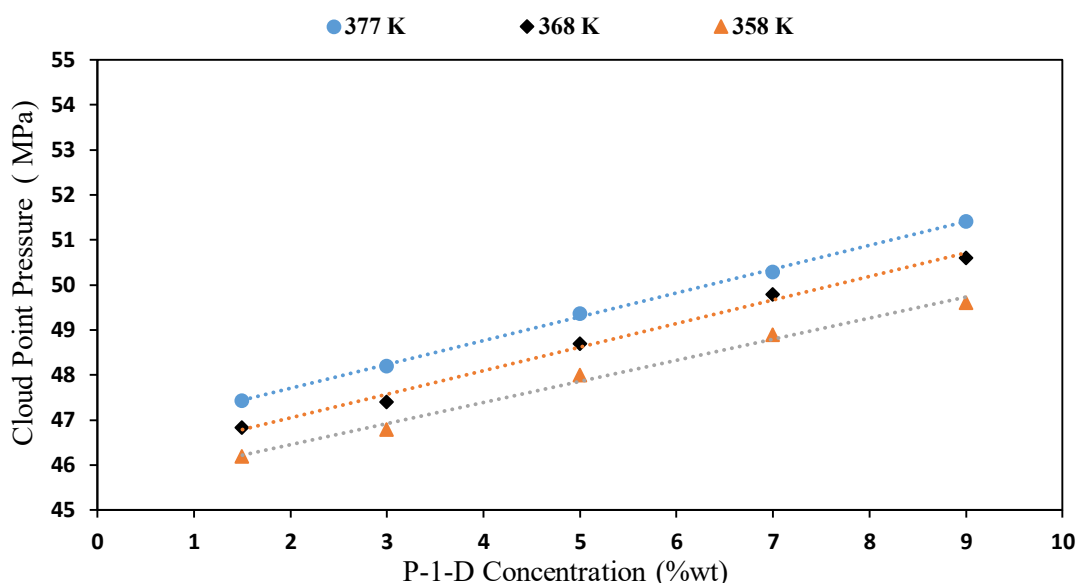


Figure 4.9 Measured cloud point pressures for P-1-D at different concentrations and temperatures.

4.3.2 P-1-D-Thickened AG Viscosity

The viscosity of the P-1-D- thickened AG mixture was measured at two pressures of 52 and 55 MPa (both are above its cloud point), three temperatures of 358 K, 368 and 377 K and varying the oligomer concentration between 0 and 9 wt%. The results of the measurements are presented in Figures 4.10 and 4.11 in the form of the actual measured viscosities and relative viscosities ($\frac{\mu_{sol}}{\mu_{AG}}$), respectively. As can be seen from these two figures, there is a significant increase in P-1-D-thickened AG mixture viscosity (2-7.4 fold) with increase in the P-1-D concentration. Overall, the relationship between viscosity and P-1-D concentration seems to be linear. The temperature also tends to have a moderate effect on the measured data with viscosity of the solution decreasing almost linearly with increase in temperature. In general, the thermal degradation of any polymeric additives at 373 K is very unlikely to occur much less affect their rheological properties. Such a loss can cause a significant reduction of viscosity in most polymers due to the weakness of intermolecular association of polymer-polymer segments. However, in this study, P-1-D has been found to be an effective thickener for the AG mixture tested even above 373 K at high pressure. It seems that this oligomer is thermally stable at high temperatures as demonstrated by

other studies too where it was dissolved in 1- hexane and 1-octane mixture at high temperature and high pressure.[279, 280] In general, poly- α olefins, such as P-1-D, have excellent thermal and oxidative stability, high viscosity index (VI) and low pour point due to the lower branching ratio (0.19).[281] A high VI means the rate of viscosity drop is low as the fluid temperature increases due to expansion of the oligomer coil with increasing temperature.[282] As previously shown in the P-1-D-AG mixture, the AG mixture solvents become more effective as the temperature increases which leads to the P-1-D dissolving through the expansions of the P-1-D molecules. Conversely, as the temperature decreases, AG solvents become less effective as the macromolecules contract leading to the precipitation of the P-1-D. In addition, this oligomer is stable at high temperature due to the flexible alkyl branching group on the C-C backbone chain and that its synthesis process takes place at high temperature (398 K) in the isomerization reaction resulting in a better thermal stability.[283, 284] Hence, P-1-D does not tend to affect its rheological properties at high temperature and maintains its ability to enhance the AG mixture tested here.

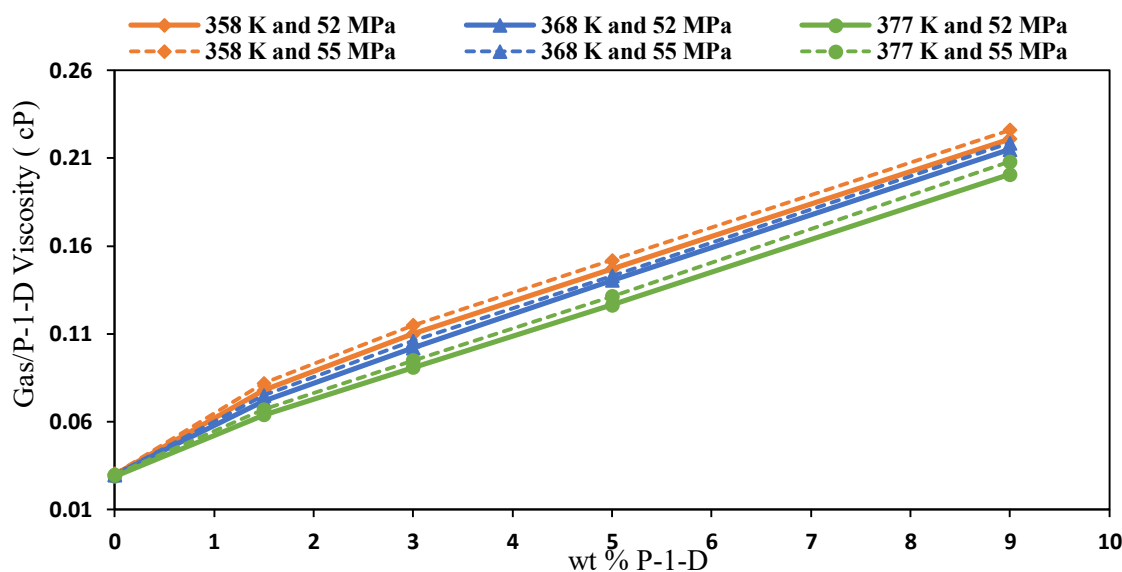


Figure 4.10 Measured P-1-D-thickened AG gas viscosity at different P-1-D concentrations, temperatures, and pressures.

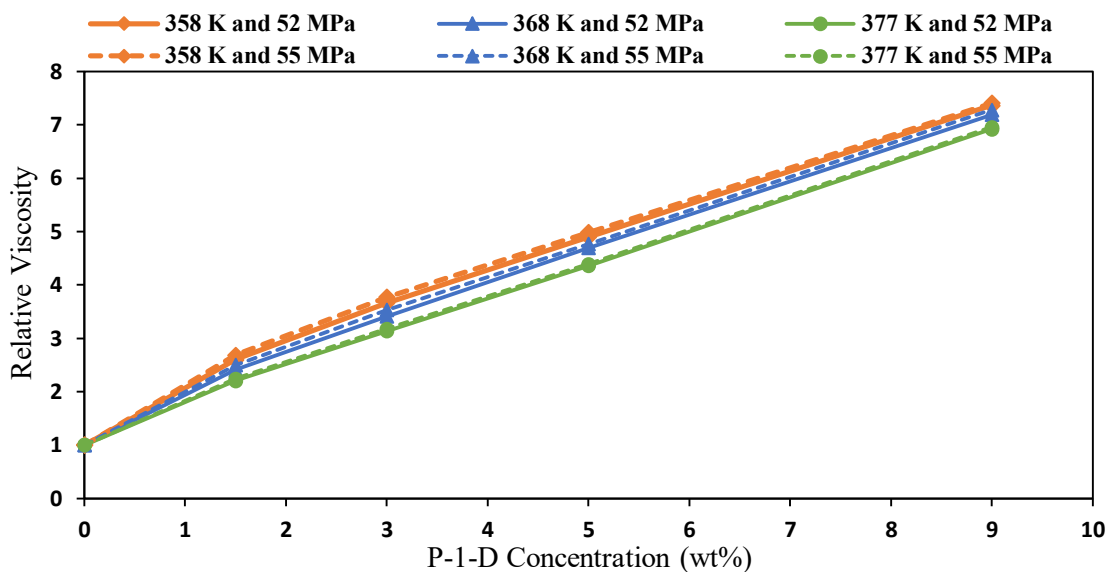


Figure 4.11 Relative viscosity $\left(\frac{\mu_{sol}}{\mu_{AG}}\right)$ at different P-1-D concentrations, temperatures, and pressures.

As reported by Heller et al.,[64] dissolution of poly-1-hexenes at concentration 1-2.2 wt% resulted in significant increases in the viscosity of n-butane and n-hexane (5 fold). In a recent publication, Zhang et al.[178] also found the viscosity of CO₂ to increase significantly by 13 fold using less than 1 wt% of P-1-D at 329 K. However, Zhang et al. findings do not correlate and are inconsistent with the results of other previous research work[52] as well as the present study. In most studies reported in the literature, low/high molecular weight polymers and small molecules that have been reported to thicken CO₂ used concentrations 1.5-7 wt%.[52] This experimental result demonstrates that the HC gas mixture can be thickened using P-1-D which is consistent with previous research reported with gas thickener.

As can be seen from Figures 4.10 and 4.11, with increase in pressure, there is a slight increase in the viscosity of the oligomer/AG solution at all the temperatures and oligomer concentrations explored. Dhuwe et al have reported a similar effect where they thickened the light alkanes using an ultrahigh molecular weight poly α -olefin drag reducing agent.[70, 231] The above-described behaviour is because the strength of alkanes increases with density and pressure, which can be reflected on the swelling and overlapping between the polymer or oligomer chains. With temperature increase, there is also a slight viscosity reduction of the oligomers/AG solution at all the oligomer concentrations tested. For instance, at 5 wt% oligomer concentration, a 0.38

fold reduction can be seen between temperatures of 368 and 377 K. Overall, there is a linear relationship between the temperature and viscosity reduction of the oligomer/AG solution.

The P-1-D viscosity enhancement results achieved are indeed very promising. Such data open up the potential of thickened AG injection in Field A and other similar fields toward enhancing the oil recovery beyond original estimates. The results of this study can be extended to reservoirs other than Field A, but in doing so two important factors that may require attention are the availability of sour gases (H_2S and CO_2) in a field's AG mixture and possibility of having ultra high in-situ temperature. As the results of this study indicate, the presence of sour gases (H_2S and CO_2) in the AG mixture can possibly facilitate the dissolution of POA oligomers in the gas mixture. If a low amount of CO_2 is present in the mixture, it may be difficult to obtain polymer solubility in it. In the case of ultra high temperatures (e.g 423 K), the ability of a polymer to increase the gas viscosity would be a concern as such an ultra high temperature would suppress any viscosity enhancement achievable at lower temperatures.

4.3.3 Core-Flood Experiments

Three core-flood experiments were conducted under secondary and tertiary modes to investigate the effectiveness of the thickened AG mixture (5 wt% P-1-D) in enhancing the recovery from the Field A, and related fields. All three experiments were performed under the reservoir conditions of 377 K and 55 MPa. At this P-1-D concentration, the injected AG viscosity is enhanced from 0.0299 to 0.131 cP (4.38 fold) under reservoir conditions. The pore pressure applied during the core flooding was higher than the minimum miscibility pressure (MMP) for the AG mixture used. The MMP for the AG mixture in the Field A dead oil was estimated from the CMG WinProp module to be 40 MPa. Table 4.3 presents the petrophysical properties of the carbonate composite core plugs, the experimental conditions and the ultimate oil recovery factor for the flooding tests using the AG mixture as well as the thickened mixture. In all three flooding experiments, the residual water saturation was found to be very low because the oil and water viscosities (2.7 and 0.4 cP, respectively) are close enough at reservoir conditions and also the high pore pressure applied in the system. The irreducible water saturation in a laboratory scale depends on the capillary properties of the rock or the viscous forces between the oil and water.[285] In addition,

the results that we have obtained in the experiment are in line with those obtained by Larsen et al. as he has stated that water saturation can be reduced to zero if a high capillary pressure is applied and if the water in the core has a continuous phase which leads to an escape route for the water.[286]

Table 4.3 Summary of the Core-Flooding Experiment Data (377 K and 55MPa).
 K: permeability; ϕ : porosity; S_{wirr} : irreducible water saturation; S_{oi} : oil saturation; RF_{AG} : AG recovery factor; $RF_{thick'd AG}$: thickened AG recovery factor; and RF_{total} : total recovery factor.

Test No.	EOR mode	K mD	ϕ %	S_{wirr} %	S_{oi} %	RF_{AG} %	$RF_{thick'd AG}$ %	RF_{total} %
1	secondary	8.2	14.20	2.5	97.5	-----	96.75	96.75
2	tertiary	5.2	14.59	2	98	84.2	10.2	94.5
3	tertiary	2.9	15.15	1.8	98.2	20	77.5	96.66

The oil recovery profiles for all three tests are plotted in Figure 4.12 until 3.6 PV and in Figure 4.13 until 9 PV of thickened gas injected. In the first test, the thickened AG injection was conducted under secondary recovery mode. As such the thickened gas injection commenced at injection rate $0.4 \text{ cm}^3 \cdot \text{min}^{-1}$ when water saturation was at residual corresponding to maximum possible oil saturation in the core sample. In this test, the gas breakthrough occurred after 0.29 PV of thickened gas injection corresponding to an oil recovery of 30%. After the breakthrough, the oil recovery factor continued to increase steadily up until 64% or 0.85 PV of thickened gas injection. After that, the oil recovery continued at lower rates until the end of the experiment corresponding to 9 PV of gas injection and a final recovery of 96.75% of the OOIP. In the second test the thickened AG gas was injected to recover oil under tertiary mode after injecting the unthickened gas on its own under secondary mode. Initially, the AG mixture was injected at $0.4 \text{ cm}^3 \cdot \text{min}^{-1}$ and the breakthrough occurred at just 0.163 PV of gas injection which is much earlier than the first test. This early breakthrough time is due to the large viscosity contrast between the oil and unthickened AG mixture. As can be seen from Figure 4.12, in test 2, the oil recovery at breakthrough is about 20%, which is lower than that of test 1 by about 33%. In summary, addition of the oligomer (P-1-D) to the injected AG mixture helped to

improve the displacement efficiency by reducing the viscosity contrast and delaying the breakthrough. The viscosity contrast can be further reduced resulting in better displacement performance by dissolving more than 5% of P-1-D in the AG mixture. In the second test, at 3 PV gas injection, the oil almost stopped from being produced but the injection continued until 3.6 PV of gas injection at which point the oil recovered had reached 84.2% corresponding to a residual oil saturation of 13.8%. Subsequently, the injection of the P-1-D-thickened AG solution was commenced. After the injection of 5.4 PV of the thickened gas, owing to 4.38 fold increase in the viscosity of the injected gas, the oil recovery factor increased by 10% to a final value of 94.2% but still less than the final value achieved in test 1 by more than 2.5%.

The third core-flooding test was conducted with P-1-D-thickened AG solution injected immediately after the breakthrough of the unthickened AG mixture. As can be seen in Figure 4.12, the AG mixture breakthrough occurred after 0.168 PV were injected which corresponds to an oil recovery of 21%. As may be expected, the breakthrough properties (injected volume and recovery factor) of these test are much closer to those of the second test. In test 3, during the early times of the post-breakthrough thickened gas injection, the oil recovery profile shows values slightly less than those achieved in test 1 for the same values of recovery (Figure 4.12). However, with further injection the two curves seem to overlap resulting in almost identical final recovery factors for the two floods. Given the current condition of Field A where gas breakthrough has already been experienced in some production wells, the results of the third test may be the most relevant if the thickened gas injection is to be implemented in this field.

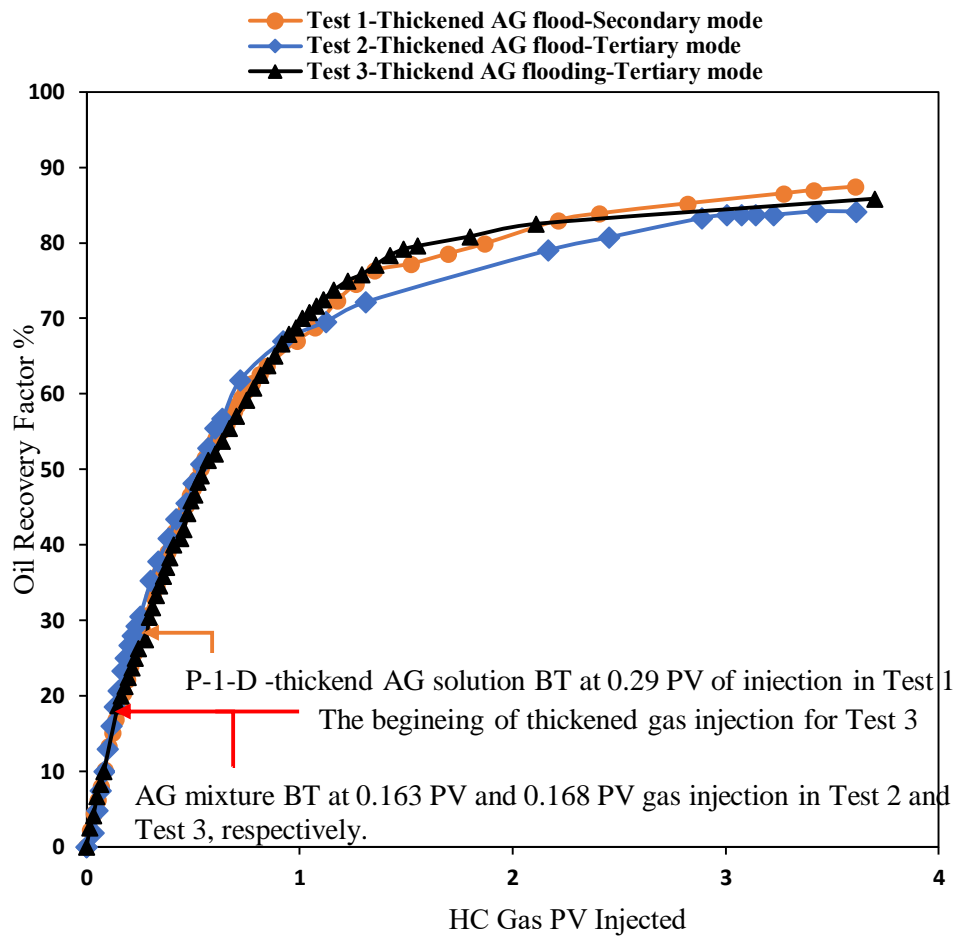


Figure 4.12 Measured oil recovery factor versus 3.6 of total injected pore volume of AG mixture or P-1-D-thickend AG solution at flow rate 0.4 cm³.min⁻¹, reservoir temperature 377 K, and pressure 55 MPa.

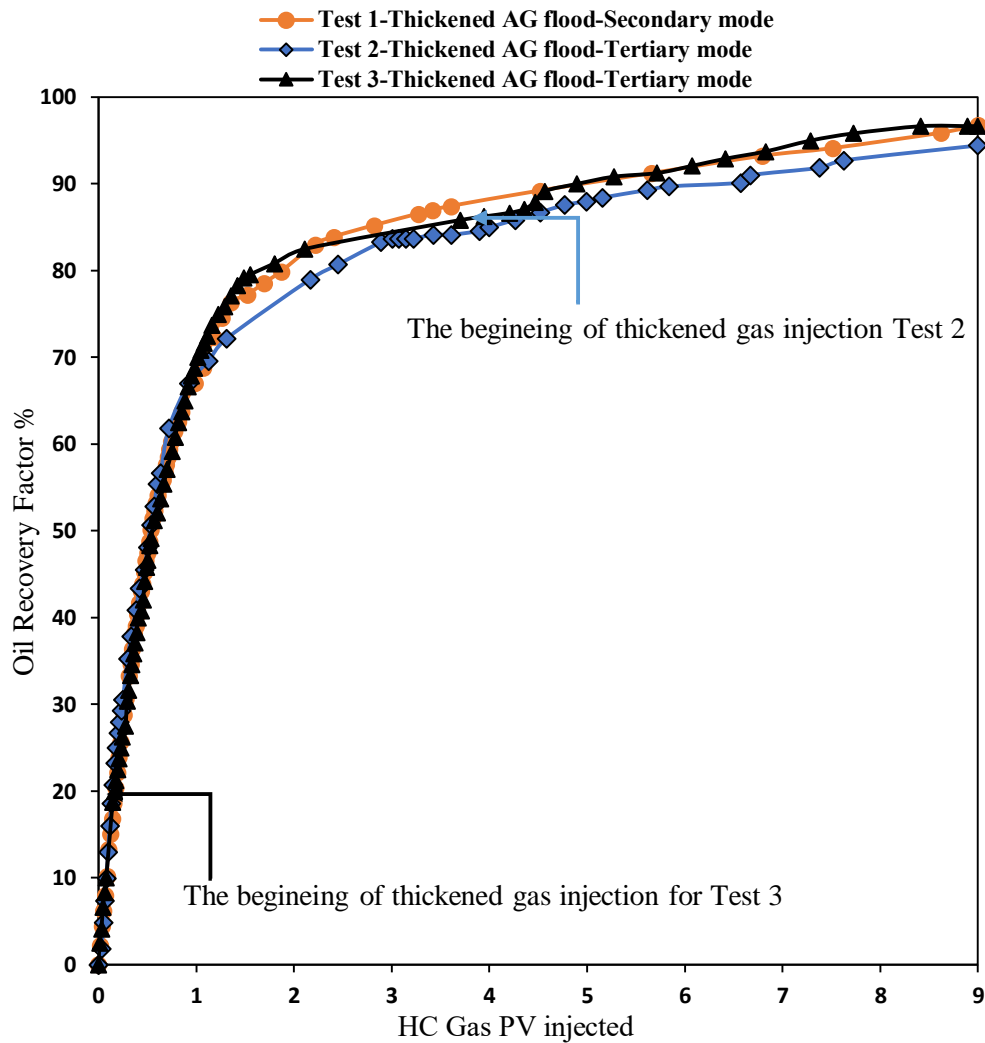


Figure 4.13 Measured total oil recovery factor versus 9 of total injected pore volume of AG mixture or P-1-D-thickend AG solution at flow rate $0.4 \text{ cm}^3 \cdot \text{min}^{-1}$, reservoir temperature 377 K , and pressure 55 MPa .

4.4 Summary and Conclusions

The solubility of 32 commercial polymers/oligomers was assessed in an AG mixture using a rapid screening method (gravimetric extraction method) and was reinforced using conventional cloud point testing. These methods examined a number of commercial polymers/oligomers that were found to be soluble in a hydrocarbon gas mixture as the solvent. In particular, a polymer and two oligomers were discovered to be soluble in the AG mixture. The solubility profiles of these three additives were further studied by measuring the cloud point pressures using a high-pressure cell equipped with a see through window. P-1-D and PMHS oligomers were found to be soluble in AG mixture under actual reservoir conditions. The oligomer-thickened AG

solution viscosity was measured using a standard capillary viscometer. The measured thickened AG solution viscosities show that only P-1-D has the ability to enhance the AG mixture viscosity between 2 to 7.4 fold at high pressure and high temperature, while PMHS cannot increase the AG mixture viscosity at low concentrations. It is found that a 5 wt% concentration of P-1-D in AG mixture can effectively increase AG mixture viscosity by 4.38 fold at 377 K and 55 MPa. Three composite core flooding tests were conducted for AG mixture and thickened AG solution flooding to assess the effect of 4.38 fold viscosity increase on oil recovery and gas breakthrough in secondary and tertiary mode recoveries. In secondary mode recovery, the P-1-D- thickened AG solution achieved a higher oil recovery factor than AG mixture injection and delayed the breakthrough to 0.29 PV. In tertiary mode recovery, the subsequent injection of the P-1-D-thickened AG solution showed the ability to mobilise and produce some of the residual oil left after AG mixture flooding completed. In summary, a direct thickening of AG mixture by P-1-D at high pressure and high temperature can improve gas mobility and sweep efficiency resulting in enhanced ultimate oil recovery

Chapter 5. Experimental Evaluations of Polymeric Solubility and Thickeners for Supercritical CO₂ at High Temperature for Enhanced Oil Recovery*

5.1 Introduction

Miscible gas injection (MGI) is one of the most-effective tertiary recovery methods used in the petroleum industry for improving oil recovery.[10] The MGI is an effective method in which the injected gas (i.e. CO₂, associated gas (AG), or natural gas liquids) alters the in-situ oil properties such as viscosity and density, allowing the otherwise trapped oil to become mobile and easily displaced.[11, 12] Although, this technique has the potential to improve the microscopic sweep efficiency, it suffers from numerous challenges at the macroscopic level.[35] An unfavourable mobility ratio in which the less-viscous gas displaces the more-viscous oil in the subsurface is one of the major causes leading to a reduced overall sweep efficiency. In addition, pronounced reservoir heterogeneity makes the situation worse by further promoting gas channelling through high permeability streaks, leading to a low overall oil recovery factor.[49, 260]

Field A is located in the Harweel cluster in southern Oman and is recognised as a viable candidate for miscible gas injection. It is believed that with the implementation of MGI, an estimated 47% of the original oil in place (OOIP) could be recovered.[32] In fact, the MGI process is already being implemented in which the field's AG mixture is the main gas source.[30] The injection process has been carried out by reinjecting the AG mixture into the reservoir at high pressures (up to 55 MPa) and due to the high reservoir temperatures (up to 377 K) the gas becomes miscible with the oil. However, even though the oil in Field A is light (42° API), the significant viscosity contrast between the injected gas (0.1-0.03 cP) and oil (0.23 cP) leads to viscous fingering, early breakthrough, and high gas-to-oil ratio, which would compromise the macroscopic sweep efficiency of the field. Therefore, MGI presents significant technical challenges in terms of implementation. For example, early gas breakthrough

(BT) has resulted in poor volumetric sweep reducing the overall efficiency of the MGI process.

To overcome the above mentioned challenges associated with the MGI flooding, several solutions have been proposed in the literature include water alternating gas flooding (WAG),[53, 54, 89] foam flooding,[57, 58, 61, 62] and the use of thickening agents to increase the injection gas viscosity.[66] In field applications, CO₂-WAG flooding can result in an incremental oil recovery of 5-10% of OOIP.[75] However, operational difficulties and challenges (e.g. excessive water production, corrosion, gravity segregation, and water blocking) prevent WAG technique from reaching its full potential to improve oil recovery. In addition, the WAG approach would not be applicable to Field A. As a closed system with very low initial water saturation, the surface facilities available in this area have not been designed to handling large quantities of water.

An alternate approach to decreasing the injection gas mobility is the use of foaming agents. However, this technique suffers from various conceptual, operational, and economical challenges that limit its use in the oil fields in the Middle East.[56, 60] In general, the major challenges associated with the foam flooding process are controlling the propagation of the foam over long distances in the reservoir and the need for large volumes of the foam.[52] In addition, surfactant micelle stability (required for foam effectiveness) is difficult to achieve in the harsh reservoir conditions (i.e. high formation brine salinity and high temperatures).[56] As such, the effectiveness of foam flooding in Field A is significantly impaired because the formation brine salinity is 275,000 ppm and the reservoir temperature is 377 K.

A conformance and mobility control technique that does not suffer from the limitations associated with WAG and foam flooding processes is the use of gas thickening agents in the injection gas. Numerical approximations for mixtures generally predict that the overall viscosity will increase with the component viscosity and mole fraction of the more viscous component.[287] Over the past few decades, many researchers have tested polymer, oligomer, and small molecule additives that can dissolve into CO₂, NGL, and AG and increase the injection gas viscosity, which would lead to improved performance for the MGI process.[52, 70, 71, 157, 167, 227, 231, 288] The major limitation is the limited solubility of the polymer/oligomer in the

injected gas mixtures thus limiting its ability to increase viscosity and ultimately improve oil recovery. In this context, compared to CO₂, it is more challenging to identify soluble polymers for hydrocarbon compressed fluids (e.g. AG and NGL). In our previous work, three additives (PDMS, PMHS and P-1-D) were identified to be soluble in AG of Field A at 55 MPa and 377 K. P-1-D was found to be an effective AG thickener at high concentrations (5-9 wt%), which may make the AG thickening process uneconomical.[288] Therefore, to improve this approach this study is focused on CO₂ whose viscosity enhancement would be easier to achieve for two primary reasons. First, compared to AG, many more low and high molecular weight polymers are soluble in CO₂. Second, in general a lower polymer/oligomer concentration is required to enhance the CO₂ viscosity to the required level as the initial viscosity of pure CO₂ is higher than the AG at the reservoir conditions of interest.[288] For example, less than 3 wt% of oligomer (e.g. P-1-D) in scCO₂ is required to reach a target viscosity of 0.13 cP, as opposed to 5 wt% needed to achieve the same viscosity for the AG.[288] A simulation study performed for Field A in chapter 3 indicates that if the viscosity of CO₂ was increased by 0.1 to 0.16 cP, a high ultimate oil recovery (68 to 72% OOIP) would be achieved with the thickened CO₂ flooding compared to the 63% recovery achieved from pure CO₂ flooding.[34] A dilute concentration (1.5-3 wt%) of polymer in CO₂ is expected to be enough to increase the CO₂ viscosity to this level.

Enick et al. have provided a comprehensive review of the studies that have attempted to thicken CO₂ using various chemical additives over the past 40 years.[52] This review states that a high molecular weight fluoroacrylate–styrene copolymer (polyFAST) identified as the best CO₂ thickener. A 1.5 wt% of poly FAST in CO₂ increased the viscosity by a factor of 19 at 298 K and 34.48 MPa. The fluorinated acrylate polymer poly(1,1-dihydroperfluorooctyl acrylate) or PFOA has been shown to slightly increase the viscosity of CO₂ by 2.5 fold at 323 K and 31 MPa. Polyperfluoroacrylates have been considered to be among the most CO₂-philic material; however, this class of polymers are expensive and are coming under increasing environmental scrutiny. A group of researchers at Chevron and The New Mexico Petroleum Recovery Research Centre attempted to thicken CO₂ using a high-molecular-weight polydimethylsiloxane (PDMS) at a diluted concentration of 0.03 wt%. However, with the limited solubility of PDMS in CO₂, there was no significant

viscosity change reported at 298 K and 18.96 MPa.[66] It was also shown that the addition of 20 wt% toluene co-solvent enables up to 4 wt% of PDMS polymer material to dissolve in CO₂ resulting in fluid viscosity increase of 30 fold.[63] However, the high concentration of co-solvent makes the field application of this solution mixture impractical.[52, 157] In a recent work, aromatic amide based groups were incorporated into the PDMS polymer backbone to promote the formation of supramolecular structures in solution ultimately enhancing the viscosity of scCO₂. [167] They observed that amide-terminated-PDMS oligomers with simple aromatic groups and attachments of electron-deficient aromatic groups onto these amides (4-nitrobenzamide and biphenyl-4-carboxamide anthraquinone-2-carboxamide) were not effective thickeners for pure CO₂. However, other compounds (4-nitrophenyl, biphenyl, anthraquinone, and branched anthraquinone amides) were found to be effective thickeners of hexane. In addition, these compounds were found to be useful thickeners in the presence of substantial amount of hexane as co-solvent into a CO₂ solution. For example, at the temperature and pressure of 348 K and 34.5 MPa, respectively, a transparent solution composed of 13.3% branched anthraquinone amides, 26.7% hexane and 60% CO₂, was found to have a viscosity 3 times greater than that of a CO₂/hexane mixture without a thickener. Furthermore, in another recent study, Doherty et al. examined a series of cyclic amide and urea compounds as small molecule thickeners for light hydrocarbon solvents and scCO₂. [227] They found that propyltris(trimethylsiloxy)silane-functionalised benzene trisurea and trisurea compounds functionalised with varying proportions of propyltris(trimethylsiloxy)silane and propyl-poly(dimethylsiloxane)-butyl groups were capable of thickening scCO₂ (3-300 fold) at remarkably low concentrations (0.5-2 wt%) in the presence of hexane as a co-solvent at high concentrations (18-48 wt%). [227] However, due to the high concentration of the required co-solvent, the associated relatively high cost and environmental concerns severely limit the applicability of this approach. [52, 157, 289]

To avoid the aforementioned concerns of either high cost or environment issues associated with silicone or fluororous materials, many researchers have focused on the synthesis and design of alternative CO₂ soluble oligomers and polymers. To date, these include polymers/oligomers such as poly(vinyl acetate) (PVAc), poly(propylene glycol), poly(vinyl ethyl ether) (PVEE) and poly(1-decene) (P-1-D) have been studied

as CO₂-philic materials.[66, 165, 178, 196, 290] PVAc is known as the second most CO₂ soluble polymer among the non-fluorous polymers with PDMS being the most soluble.[162] Tapriyal et al. observed no viscosity increase with 1-2 wt% of PVAc (MW 11000) in CO₂ at 298 K and 64 MPa.[162] The dissolution of a high molecular weight PVAc in CO₂ required very high pressure to achieve a transparent solution which indicated solubilisation of the polymer.[197] In many instances, there is a strong correlation between solubility and scCO₂ density. A higher density (corresponding to a higher pressure or lower temperature) generally improves solubility. Heller et al.[64, 66] found that certain poly α -olefins (PAO) (i.e. P-1-D, poly (1-hexane) and PVEE) to be slightly soluble in CO₂ at 298-331 K and 17.1-20 MPa. However, none of these materials increased the viscosity of CO₂.

A recent study[178] examined the solubility of low molecular weight polymers PVEE (MW 3,800) and P-1-D (MW 910) in scCO₂. These compounds had been studied previously;[66] however, in this later study an in-house constructed capillary viscometer was also used to measure the viscosity of polymer-thickened CO₂ across 14.6-20 MPa pressure at a temperature of 329 K. They reported that at concentrations of less than 1 wt%, these two oligomers increased the viscosity of scCO₂ by 13-14 fold. However, many researchers have disputed these results[52, 157, 172] arguing that to thicken CO₂ significantly to the reported levels concentrations in the range of 1.5-7 wt% would be required for high molecular weight polymers (which are more viscous) and that at 1 wt% concentration low molecular weight polymers are not capable of thickening CO₂ to the reported levels. In addition, the CO₂ thickening ability of low molecular weight P-1-D and PVEE have been studied using the high-pressure falling cylinder or the rolling ball viscometry tests.[172] They reported that neither of these oligomers was capable of increasing scCO₂ viscosity by more than 5% at concentrations of 0.5 wt%.[172] It is worth noting that these results have not been validated yet using a commercially constructed capillary viscometer.

As revealed by the literature review presented so far, many studies have attempted to evaluate the suitability of a number of polymer/oligomer additives to viscosify CO₂. However, none of these were conducted at high temperatures (>373 K). High temperatures are particularly challenging because the scCO₂ density decreases with temperature leading to a lower solvation potential.[291] At high temperatures, the lower potential to dissolved polymers necessary to increase viscosity is further

complicated by the tendency for the viscosity of fluid mixtures to decrease with increasing temperature.[292] In fact, to our knowledge, all the relevant available data in the literature have been obtained at moderate temperatures of less than 331 K. There are many oil fields around the globe with high in-situ temperatures (e.g. Field A in the southern Oman) and none of the material tested to date may be of use for possible CO₂ flooding in those fields.[293]

To cover the above identified gap in the knowledge and help with further recovery from Field A, this work has assessed the properties of a library of low- and high-molecular weight non-fluorous polymers in scCO₂ at high temperatures for their ability to control the gas mobility in miscible CO₂-EOR processes. To achieve this objective, first, a number of polymers and oligomers were selected for solubility tests. These particular polymers and oligomers were selected on the basis of the existing available data in the literature related to solubility and viscosity in scCO₂. In total, the solubility of 26 polymers/oligomers in scCO₂ was determined using a high-throughput parallel gravimetric extraction method.[265] This method is very effective and efficient in that it allows for rapid preliminary screening of polymers/oligomers as solubility in CO₂ is an absolute requirement for an effective viscosifier. After the polymers/oligomers with the highest solubility during the high-throughput experiments were selected, a series of cloud point pressure measurements were performed on them at different temperatures. The purpose of these experiments was to determine the compatibility of the polymers or oligomers with the range of pressures applicable to Field A. In the last stage of the work, additives displaying low enough cloud point pressures at Field A's reservoir temperature of 377 K were examined for their viscosity enhancement potential in scCO₂ using a commercially manufactured capillary viscometer at different pressure, temperature and oligomer concentration conditions.

5.2 Experimental Methodology

5.2.1 Materials

A complete list of the polymers and oligomers chosen initially to be investigated in this study is provided in Table 5.1. The polymers and oligomers were sourced from a number of international commercial suppliers (i.e. Jiangsu Yinyang Gumbase Material, Fluka AG, BASF- ICIS, DOW Corning, China Skyrun Industrial Co., and

Sigma-Aldrich). The CO₂ density was calculated using the National Institute of Standards and Technology (NIST) webbook correlation.[294] The density was needed at different pressure and temperature values for mixture concentration calculations.

5.2.2 Experimental Setup and Procedure

5.2.2.1 Polymer Solubility Measurements

5.2.2.1.1 High-Throughput Gravimetric Extraction (HTGE)

The high-throughput gravimetric extraction (HTGE) screening method has been described in the literature, as a rapid method to use when testing a large library of polymers for their solubility in supercritical solvents (SCF).[265, 267] Figure 5.1 shows the schematic diagram of the gravimetric extraction setup used in this study. The detailed procedure that was followed for conducting the experiments is explained in chapter 4 but is covered here again in brief. The polymer/oligomer samples were accurately weighed (100 mg) into open-ended borosilicate glass tubes with a length of 60 mm and an ID of 6.6 mm. Each tube was prepared with a piece of quartz frit in its bottom opening and wrapped with a piece of tissue paper over its top opening. This configuration would allow the CO₂ to freely flow through the glass tubes while extracting the polymer samples. Also, any insoluble polymer sample or the unextracted residues would be retained inside the tube for further evaluation. The tubes were loaded into a specially designed holder in parallel and then placed inside the extractor vessel (Figure 5.1). The CO₂ was then passed through the vessel under in-situ pressure (55 MPa) and temperature (377 K) for two hours at the constant flow rate of 80 cc/min. The cell pressure was controlled using a dome-loaded back pressure regulator whose pilot pressure was regulated using a syringe pump. Subsequently, the CO₂ injection was stopped and the CO₂ inside the extractor was slowly vented at the rate of 0.6 MPa.min⁻¹. Upon reaching atmospheric pressure, the sample holder removed from the vessel and the glass tubes were carefully removed and individually reweighed to determine any weight loss under the extraction conditions applied. The procedures was repeated twice at the same conditions for every batch of polymers tested. By comparing the results of every two replicate experiments, the weight loss results were found to be reproducible within ± 2 -4% of the extracted weight.

Table 5.1 The library of polymers and oligomers used in parallel gravimetric extraction experiments.

Sample No	Polymer, oligomer and small molecules Name	Molecular weight (g.mol ⁻¹)	Glass transition temperature T _g (K)	Melting temperature T _m (K)	Crystallinity exhibits	Supplier
1	poly(vinyl acetate)	250,000	301-318	333-338	No; refs [295, 296]	Jiangsu Yinyang Gumbase Material
2	poly(vinyl acetate)	150,000	301-318	333-338	No; refs [295, 296]	Jiangsu Yinyang Gumbase Material
3	poly(vinyl acetate)	116,000	301-318	333-338	No; refs [295, 296]	Jiangsu Yinyang Gumbase Material
4	poly(vinyl acetate)	80,000	301-318	333-338	No; refs [295, 296]	Jiangsu Yinyang Gumbase Material
5	poly (vinyl acetate co-vinyl alcohol)-40%	72,000	350-358	433	Yes; refs [295, 297]	Fluka AG
6	poly (vinyl acetate co-vinyl alcohol)-80%	9,000	350-358	445	Yes; refs [295, 297]	Fluka AG
7	poly (vinyl acetate co-vinyl alcohol)-88%	96,000	350-358	453	Yes; refs [295, 297]	Fluka AG
8	poly(ethylene glycol)	8,000	213	339	Yes; refs [298]	BASF- ICIS
9	poly(vinyl pyrrolidine)	10,000	403	423	Yes; refs [299]	BASF- ICIS
10	poly(4-vinyl pyridine)	60,000	415	533	Yes; refs [300]	BASF- ICIS
11	poly(4-vinyl pyridine)	50,000	415	533	Yes; refs [300]	BASF- ICIS
12	poly(methyl methacrylate)	15,000	378	433	Yes; refs [301, 302]	Sigma-Aldrich

13	hydroxyethyl-cellulose	14,0000	393	413	Yes; refs [303]	Sigma-Aldrich
14	poly(ethylene vinyl acetate)	55,000	233	333	Yes; refs [304]	Sigma-Aldrich
15	cellulose acetate Butyrate	70,000	369-434	444-473	Yes; refs [305]	Sigma-Aldrich
16	poly(vinyl methyl ether)	60,500	242	-	No; refs [306, 307]	Sigma-Aldrich
17	poly(vinyl ethyl ether)	4,337	213	-	No; refs [307]	Sigma-Aldrich
18	poly(isobutyl vinyl ether)	4,000	250	438	Yes; refs [308, 309]	China Skyrun Industrial Co
19	poly(dimethylsiloxane)	5,180	183	233-243	Yes; refs [310-312]	Sigma-Aldrich
20	poly(butyl methacrylate)	33,7000	295-308	-	Yes; refs [302]	Sigma-Aldrich
21	poly(ethylene succinate)	10,000	272	376-379	Yes; refs [313-315]	Sigma-Aldrich
22	poly(isobutylene)	500,000	209	460	Yes; refs [316-318]	Sigma-Aldrich
23	poly(propylene carbonate)	50,000	295-318	423	Yes; refs [319]	Sigma-Aldrich
24	methyl- β -cyclodextrin	1,310	317	453-455	-	Sigma-Aldrich
25	poly(vinyl methyl ketone)	500,000	301	433	Yes; refs [302]	Sigma-Aldrich
26	poly(1-decene)	544	208	257	No, refs [320]	Sigma-Aldrich

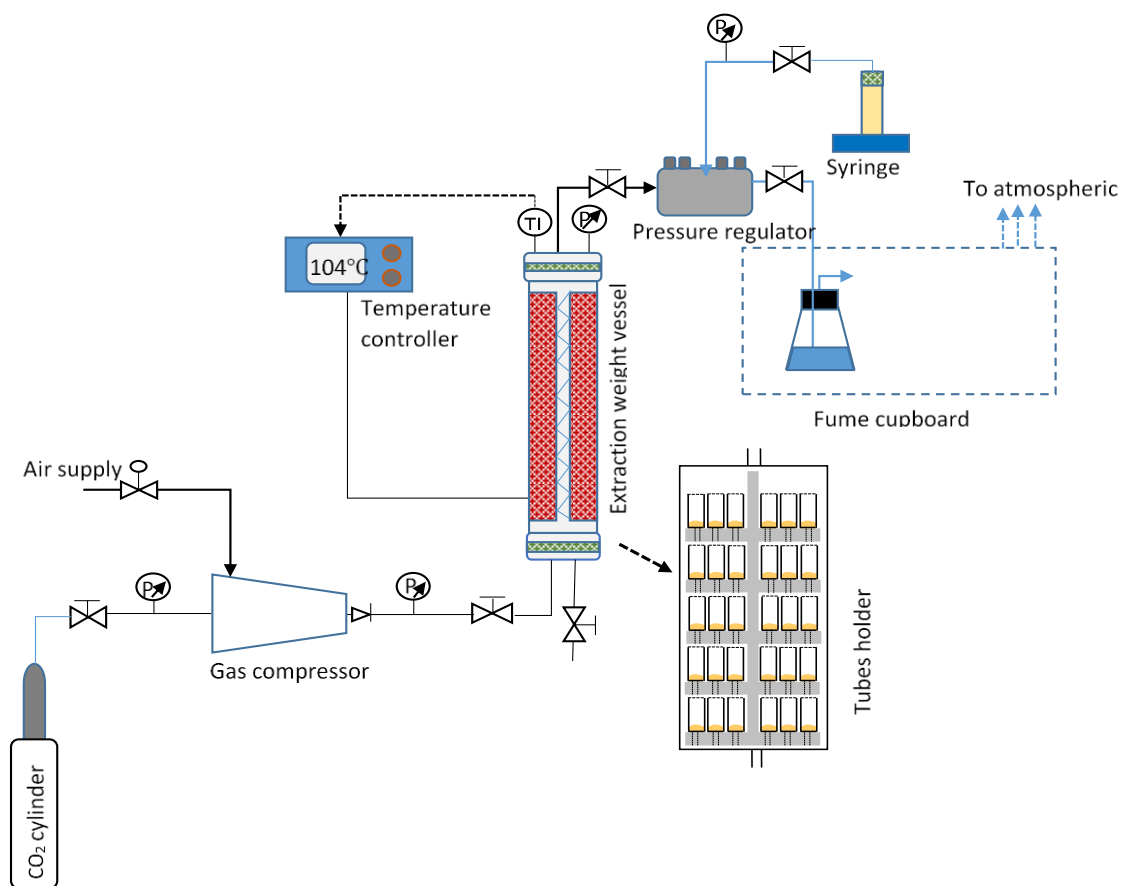


Figure 5.1 Schematic diagram of gravimetric extraction equipment used for rapid measurement of polymers/oligomers solubility in AG mixture.

5.2.2.1.2 Cloud Point Measurements

The cloud point pressure versus temperature curves were determined in a high pressure-high temperature windowed cell (Figure 5.2, IFT700, Vinci Technologies) using a standard technique set out in the literature involving isothermal compression and then slow decompression of binary mixtures of known compositions.[266] These measurements were carried out for three polymers/oligomers with high level of extraction in the HTGE experiments (i.e. PVEE, Piso-BVE, and P-1-D) to confirm their solubility in scCO₂. Cloud point pressures were determined for range of concentrations for PVEE (0.81 to 2 wt%) and Piso-BVE (0.81 to 3 wt%) in the temperature range of 329-377 K. For P-1-D, the cloud point pressures were measured for the concentration and temperature ranges of 1 to 5 wt% and 358-377 K, respectively.

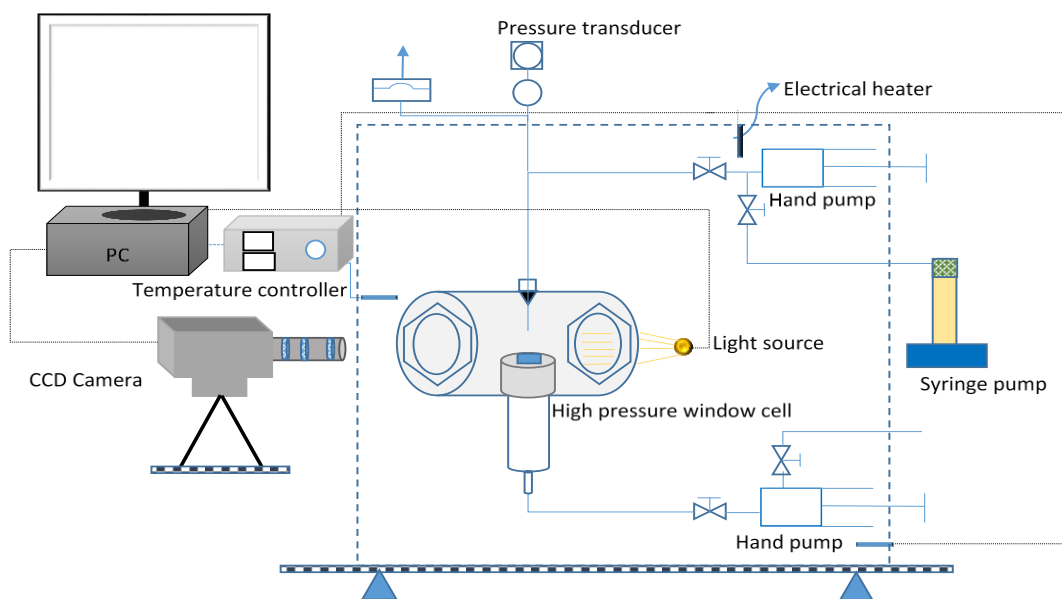


Figure 5.2 Schematic diagram of experimental setup used for cloud point pressure measurements.

To ensure the integrity of our experimental results, the high pressure windowed cell and all of its components were thoroughly cleaned with acetone followed by toluene at 323 K before each measurement to remove any trace of contaminants including residual polymers that may compromise our results. The high pressure cell was then vacuumed for few hours to dry. Knowing the solubility of our polymers and oligomers in CO₂ from the HTGE experiments, for each measurement, a precise amount of a polymer or oligomer was weighed and placed on a clean glass plate. Doing so allowed us to determine the polymer/oligomers concentration (wt%) in CO₂ in the pressure cell whose internal volume was known (20 cm³). The glass plate was then placed on the turntable inside the pressure cell before it was tightly sealed. The system was then purged with low-pressure CO₂ to remove any trapped air. Subsequently, we increased the temperature of the system to the desired value and allowed sufficient time for the temperature to stabilise. Then CO₂ was slowly injected into the cell using a syringe pump to increase the cell pressure at 0.4 MPa increments until a single transparent phase of the polymer/CO₂ solution was formed. It is worth noting that no stirring was required during the experiment, and a high-definition camera provided a visual confirmation as whether the polymer/oligomer was completely dissolved in CO₂. Then, to determine the cloud point pressure³ of the polymer/oligomer thickened CO₂ solution at a given temperature, the pressure of the system was decreased at 0.4 MPa increments until the solution began to appear cloudy in the cell. This process continued

until it was no longer possible to see the other side of the cell through the polymer/oligomer gas solution (90% reduction in transmitted light intensity), at which point the cell pressure was recorded as the cloud point pressure for the test temperature.

For any combination of polymer/oligomer concentration and temperature, the process of cloud point pressure measurement was repeated three times to ensure the reproducibility of our result. We found the cloud point pressures to be reproducible within ± 0.2 - 0.5 MPa.

5.2.2.2 Viscosity Measurements

A high-pressure high-temperature capillary viscometer (Figure 5.3, CVL-1000, Core Laboratories Inc.) was used to measure the viscosity of pure CO₂ (μ_{CO_2}) as well as the polymer/oligomer thickened solution (μ_{sol}). Operating on the basis of Hagen-Poiseuille Law, the viscometer measures the pressure drop created across a long capillary tube when a fluid is flowed through the tube at a known flow rate.

Prior to each experiment, a polymer/oligomer thickened CO₂ solution was prepared inside a fluid accumulator at a predetermined polymer/oligomer concentration using the following procedure. First, the accumulator was cleaned with acetone and toluene to remove any residual polymer from the previous test and then dried with compressed air under a fume cupboard. Then a precise amount of a polymer or oligomer was weighed (to give a predetermined concentration value) and placed inside the accumulator whose storage volume had already been adjusted to 30 cm³ using its floating piston. The accumulator was then vacuumed to remove any trapped air. The accumulator as well as the flow-lines and fittings/connections carrying the solution into the viscometer were heated to a predetermined temperature using suitable heating tapes and heating jackets (SRH etched foil jacket and stretch-to-length heating tape, Watlow). Subsequently, pure CO₂ was injected into the accumulator and pressurised to the desired pressure (above the cloud point pressure). After that, the setup was left for 3 to 4 hours to ensure the polymer or oligomer would completely dissolved into CO₂. Then, the viscometer was also heated to the desired temperature and vacuumed before being filled and pressurised with the polymer/oligomer thickened CO₂ so its viscosity could be measured. In order to ensure the reproducibility of our results, for every pressure- temperature-concentration combination, the viscosity measurement

was repeated three times. In doing so, we found our measurements to be reproducible within $\pm 0.1\%$.

It is worth noting that cleaning the viscometer after each experimental run was an area of concern, as there was a possibility that flushing the extremely narrow capillary tubes (ID = 0.18 mm) with solvent (toluene) might not clean residual polymer from the system, which would impact on the viscosity result of the next measurement. To address this concern, we used a new capillary tube and the instrument was recalibrated each time.

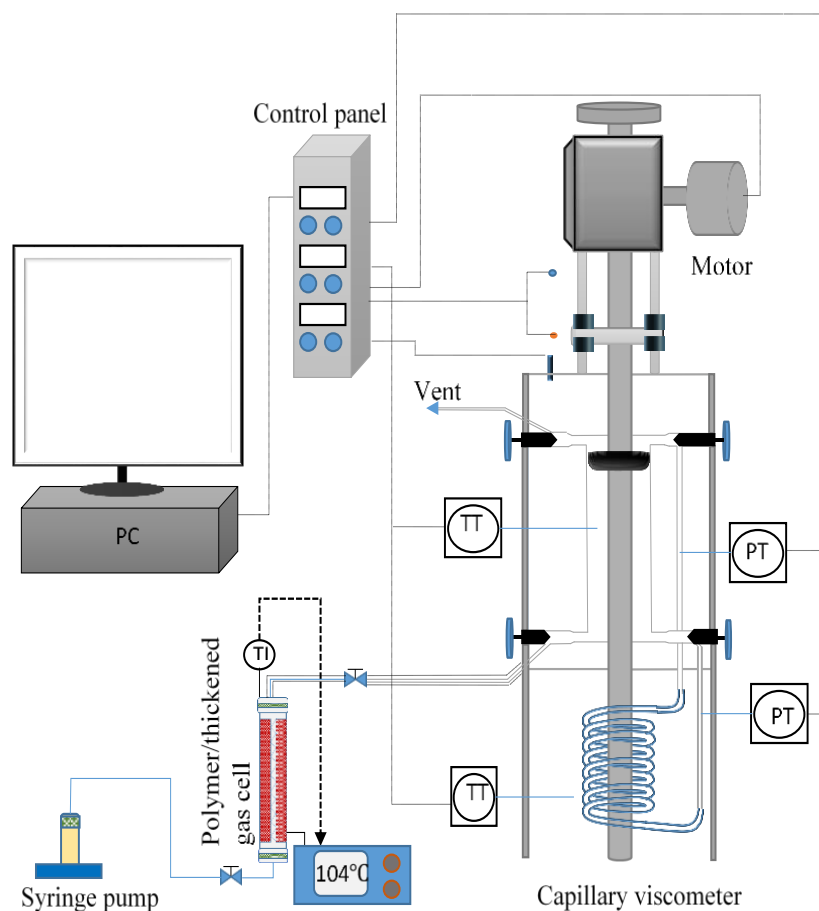


Figure 5.3 Schematic of the capillary viscometer used for viscosity measurements (50-55 MPa and 329-377 K).

5.3 Results and Discussions

5.3.1 Polymers/Oligomers Solubility in the CO₂

5.3.1.1 High-Throughput Gravimetric Extraction (HTGE) Screening Method

Figure 5.4 shows the percentage of the original weight extracted by CO₂ for each of the 26 different polymers/oligomers during the HTGE experiments measured at 377 K for three different pressures (i.e. 41, 48, and 55 MPa). Larger extraction indicates a higher solubility in scCO₂. As pointed out before, all 26 polymers/oligomers examined were commercially available and their solubility in pure CO₂ at lower temperature conditions had already been confirmed by other researchers. Based on the solubility data presented in Figure 5.2, the polymers and oligomers are divided into four categories in Table 5.2.

Table 5.2 Classification of polymers/oligomers based on extraction ability in scCO₂.

category 1	high level of extraction (> 96%)	P-1-D (Mw 544, PVEE (Mw 4,337), PISO-BVE (Mw 4,000)W and PDMS (Mw 5,180)
category 2	moderate level of extraction (45-85%)	PVAc (Mw 80,000), PVAc (Mw 116,000), PVME and Poly (ethylene succinate)*
category 3	low level of extraction (5 – 20%)	poly(vinyl pyrrolidone), P4V pyrdine, methyl-β-cyclodextrin and hydroxyethyl-cellulose
category 4	negligible (< 5%) extraction	high molecular weight polymers and copolymers containing carboxyl or hydroxyl functional groups such as poly vinyl acetate (PVAc) and poly(vinyl acetate-co-vinyl alcohol) (PVAc co-VA)

*These polymers require more pressure or more volume of the gas passed through the extraction vessel so they may completely dissolve in scCO₂.

Figure 5.4 also reveals the effect of pressure on CO₂ solubility of the polymers and oligomers with appreciable amount of weight extraction. For category 1 polymers, including PVEE and PDMS, the pressure change has a minor effect on the solubility, which is consistent with previous studies at lower temperatures.[64, 66, 178] For polymers, the solubility decreases slightly at 48 MPa and sharply at 41 MPa. This is consistent with a lower solvation ability at lower scCO₂ densities.[291] Notably, at 41 MPa, the carboxyl functionalised polymer (i.e. PVAc) did not indicate any weight

extraction because this polymer requires very high pressures (43–69 MPa) to become soluble in scCO₂.^[188] Furthermore, it can be seen from Table 5.1 that the non-crystalline polymers/oligomers or polymers/oligomers with a low melting points are soluble in scCO₂, whereas the crystalline polymers with high melting points are more difficult to dissolve in scCO₂. This is in line with previous reports in which the dissolution of crystalline polymer with weak polymer-solvent interactions was found to be impossible below the melting temperature.^[321] For the dissolution of the crystalline compounds, the melting temperature must be surpassed. In this work, only the polymers and oligomers with melting points below 377 K were soluble in scCO₂ and above that were non-soluble. As a major conclusion drawn from Figure 5.4, based on their solubility, the four additives of PVEE, P-isoBVE, PDMS and P-1-D can be considered as viable candidates for application in Field A. The rest of the polymers are rejected on the basis of insufficient solubility under the pressure/temperature conditions used in this study.

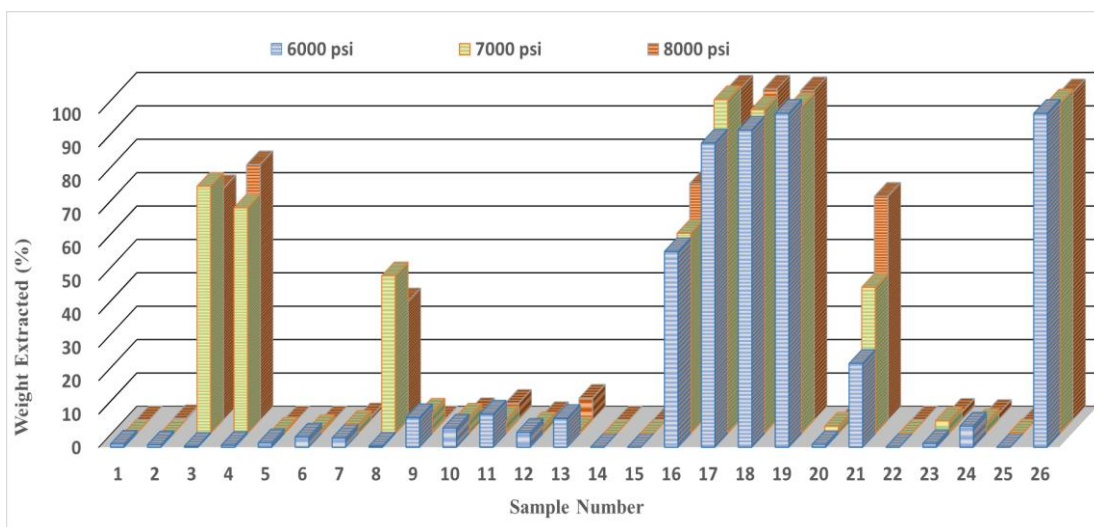


Figure 5.4 Extracted weight % in scCO₂ for the library of the 26 polymers/oligomers at 41, 48 and 55 MPa and 337 K. The name of the polymers/oligomers whose numbers are presented on the horizontal axis are defined provided in Table 5.1.

5.3.1.2 Cloud Point Pressure Determinations

The solubility of those polymers/oligomers with high extraction percentages (i.e. category 1 and 2 from Table 5.2) were further verified using the conventional cloud point pressure measurements conducted over a range of temperatures and polymer concentrations. Cloud point pressure experiments confirmed that the PVAc and PVME

included in category 2 only partially dissolved in scCO₂ at pressures of 41 to 55 MPa and temperature of 377 K. This observation is consistent with the results obtained from the HTGE measurements. Due to their only partial dissolution in scCO₂ under the study conditions, these were not considered for viscosity measurement studies. PDMS was excluded from the cloud point pressure measurements because the phase behaviour in scCO₂ at high temperatures has already been well studied.[63, 66, 167, 189, 278, 322-324] Furthermore, PDMS was shown to be an ineffective CO₂ thickener at high temperatures. PDMS has also been tested for its solubility in NGL and shown to be an ineffective NGL thickener.[231] However, in this work, PDMS was used in the extraction tests to validate our methods as PDMS has proved to be more CO₂-philic than other hydrocarbon-based polymers.[52]

The phase behaviour of polymers in scCO₂ containing functional groups with oxygen within the polymer backbone has been assessed by Kilic et al.[165] These researchers found that the presence of ether oxygen in a polymer exhibits induces a lower miscibility pressure in scCO₂ due to the strong interaction forces between CO₂ and the ether group (Lewis acid and Lewis base interactions) as well as their high chain flexibility (low glass transition temperature and low surface tension).[165] Figure 5.5 shows the measured cloud point pressures for ether containing polymers, which include PVEE and Piso-BVE, over the temperature range of 329-377 K and concentrations of 0.81-3 wt%. These results show that both polymers exhibit LCST (lower critical solution temperature) behaviour in CO₂ in which cloud point pressure increases with temperature. This is caused by the reduction in the solubility power of CO₂ toward PVEE and Piso-BVE due to a decrease in fluid density with increasing temperature leading to an entropic effect (i.e. a reduction in the free volume difference between CO₂ and polymers). Compared to Piso-BVE, the cloud point curves for PVEE are more sensitive to changes in temperature at all polymer weight loadings. In general, the LCST curve behaviour is controlled by the free volume difference between the solvent and polymer in addition to the polymer expansion coefficient.[158, 325] Therefore, Piso-BVE gains more free volume than PVEE due to the steric bulkiness of the iso-butyl functional group and the increase in the side chain length of Piso-BVE. It becomes easier to dissolve the polymers in CO₂ if the free volume of a polymer is increased.[326] Previous studies have found that at a low temperature (295 K), PVEE has better miscibility than PVME because the increase in the side chain length

enhances the free volume, which results in CO₂ becoming more accessible to the polymer with the longer side-chain branches for better solute–solvent interactions.[165] In this work, we observed similar effects for Piso-BVE and PVEE solubility in CO₂ at high temperatures. Piso-BVE has a lower cloud point pressure curve compared to PVEE and appears to be more CO₂-philic than PVEE. However, at moderate temperatures (< 346 K), PVEE has a lower miscibility pressure than Piso-BVE. It is likely that the thermal expansion of free volume in the PVEE structure is higher than Piso-BVE below this temperature. With increasing temperature, the polymer chain mobility is greatly increased, providing the motional space corresponding to an increase in polymer free volume.[290] Hence, as the temperature increases, the cloud point pressure difference between both polymers in CO₂ becomes larger.

The temperature dependency of the solubility of P-1-D in CO₂ was also studied and the results are presented in Figure 5.6. In contrast to PVEE and Piso-BVE, the cloud point pressure decreases with temperature increase implying that the P-1-D solubility in CO₂ increases with temperature. It is evident then that P-1-D exhibits UCST (upper critical solution temperature) phase behaviour in scCO₂. However, its solubility is relatively insensitive to temperature change compared to PVEE and Piso-BVE. This is due to the fact that the enthalpic interaction between CO₂ and P-1-D in the solution increases slightly with increasing temperature. Previous work showed that P-1-D exhibited solubility value of 10.3 g/L at 19.9 MPa and 298 K.[64, 66] Terry et al. also found P-1-D to be partially soluble in CO₂ at 11.7 MPa and 344 K.[67] In a recent study, P-1-D had a solubility 0.081 wt% in CO₂ at 20.1 MPa and 329 K.[178] However, in our work we found this oligomer completely dissolves up to 5 wt% in CO₂ only at temperatures above 358 K. Below this temperature, P-1-D was only partially soluble even at the pressure of 55 MPa. Although, the solubility increased significantly with temperature. This characteristic enables P-1-D to be used at concentrations higher than 1 wt% to increase CO₂ viscosity at high temperatures, indicating that P-1-D could be an effective thickener for deep reservoirs such as Field A.

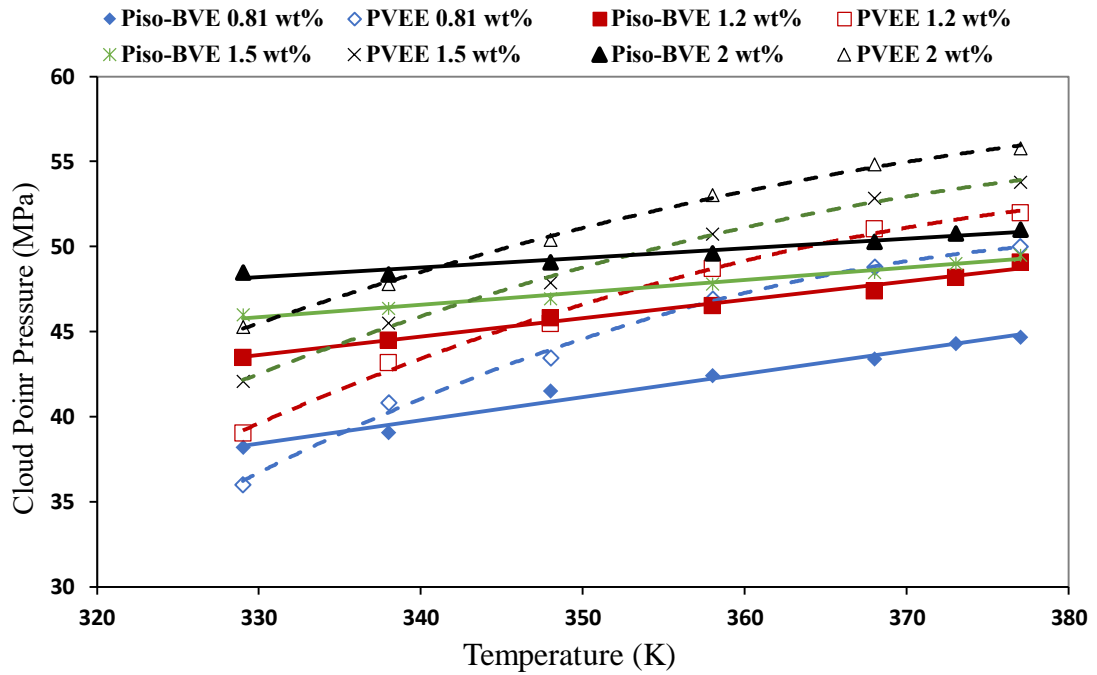


Figure 5.5 Compare cloud point pressures between PVEE and PISO-BVE at different concentrations and temperatures.

Based on the cloud point pressure measurement results presented above, the three polymers/oligomers (PVEE, PISO-BVE, and P-1-D) have high or adequate level of solubility in scCO₂ under the in-situ conditions encountered in Field A. P-1-D has a lower cloud point than PVEE and PISO-BVE at comparable concentrations. This could be due to the difference in molecular weight between the polymers and oligomer or different solubility phase behaviours (LCST versus UCST). The lower cloud point pressure of P-1-D in scCO₂ makes it possible to increase its concentration in CO₂ to values higher than 5 wt% to further increase the CO₂ viscosity. At 5 wt% of P-1-D in CO₂, the minimum required pressure to have it fully soluble is 45.3 MPa at 377 K, which is still below the reservoir pressure of 55 MPa. In comparison, the cloud point pressures for both PVEE and PISO-BVE are considerably higher at high temperatures. As a result, at 377 K, the concentration of PVEE and PISO-BVE cannot increase to more than 2 and 3 wt%, respectively, because above these concentrations the cloud point pressure would exceed the reservoir pressure of 55 MPa. However, at the above concentrations, both polymers can be considered adequately soluble in CO₂ at the Field A's reservoir conditions.

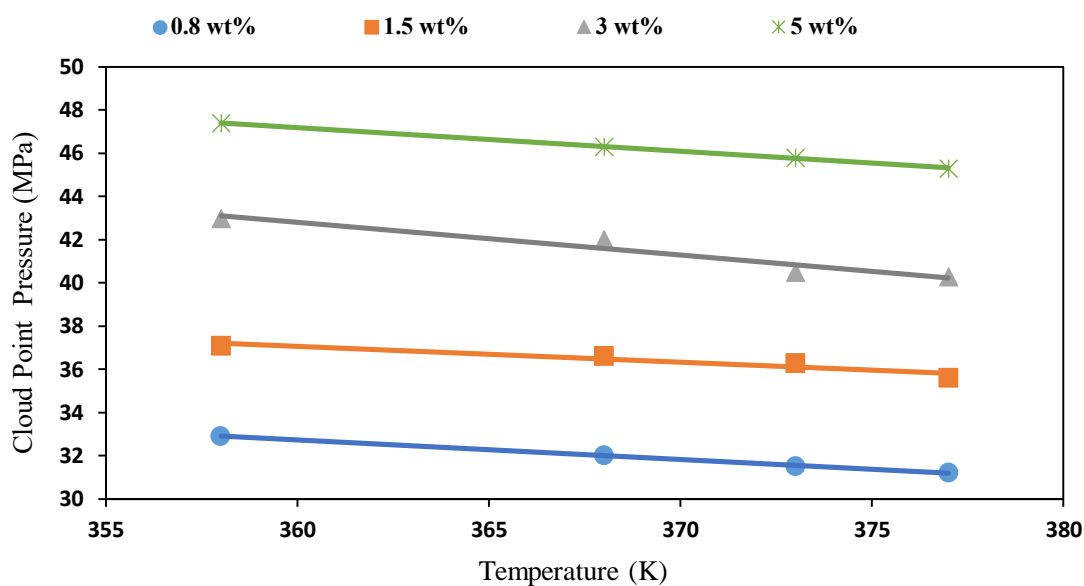


Figure 5.6 Measured cloud point pressures for P-1-D at different concentrations and temperatures.

5.3.2 CO₂ Viscosity Enhancement Measurements

The viscosity of solutions prepared by dissolving the three different polymers/oligomers (either P-1-D, PVEE, or Piso-BVE) separately into scCO₂ at different pressures (50, 53, and 55 MPa) and temperatures (329-377 K). For the measurements, the polymer and oligomer concentrations varied between 0.81 to 5 wt% for P-1-D, 1.2 to 2 wt% for PVEE and 1.5 to 3 wt% for Piso-BVE. The measured results are presented in Figure 5.7-5.9 in the form of relative viscosity (i.e. μ_{sol}/μ_{CO_2}), and in Table 5.3 in the form of actual measured viscosity values for all three additives at 377 K. As evident from the figures and the table, for all three polymers/oligomers, there were a considerable increase in the viscosity of CO₂ can be achieved at a range of temperatures and pressures. Although, as expected, the viscosity of the polymer or oligomer-thickened CO₂ exhibits a decreasing trend as the temperature increases.[292] There is also a slight increase in relative viscosity with increasing pressure at all temperatures and concentrations due to the polymer/oligomer coil expansion caused by an increase in solvent strength with increasing density. The same effect has also been observed with PDMS and DRA polymer in NGL.[231]

5.3.2.1 PVEE and Piso-BVE Results

Figure 5.7 shows the thickening ability of PVEE in CO₂ for the concentrations of 1.2 to 2 wt% over a range of temperatures (329-377 K) and two pressures of 53 and 55 MPa. As can be seen, for all temperatures, the viscosity of the thickened CO₂ increases significantly with increase in the PVEE concentration. Also, the data follow a similar trend across all temperatures examined as the pressure and polymer concentration change. The relative viscosity decreases almost linearly with increase in temperature. However, the reduction rate is slightly higher above 348 K because the intramolecular associations between the polymer and CO₂ molecules are reduced as the temperature increases. For example, at 53 MPa, the relative viscosity of 1.5 wt% PVEE in CO₂ decreases by 1-5% over 329-348 K, whereas at the same concentration, the relative viscosity decrease by 6.8-10% over 348-377 K. Not surprising, the enhancement in CO₂ viscosity by PVEE is the lowest at Field A's high in situ temperature of 377 K. For example, as revealed by Figure 5.7, at 2 wt% concentration, 55 MPa and 377 K, the relative viscosity is close to 1.7 while it is about 2.1 at 329 K for the same concentration and pressure. Furthermore, as revealed by the cloud point pressure measurements, 2 wt% is the highest achievable concentration of this polymer under the in-situ conditions of Field A.

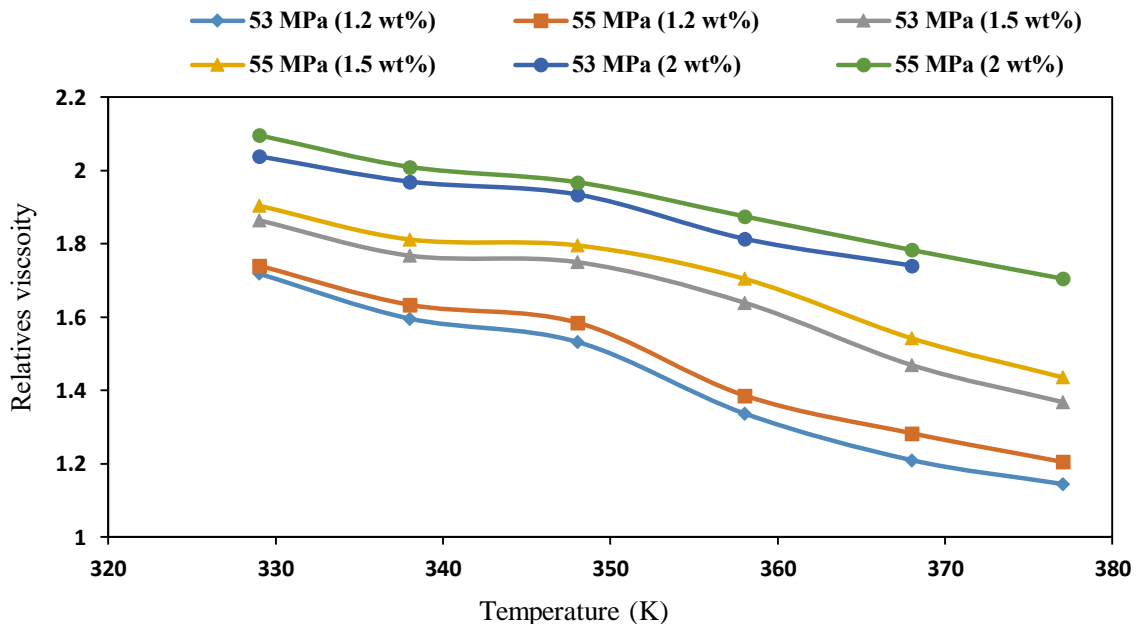


Figure 5.7 Relative viscosity (μ_{sol}/μ_{CO_2}) at different PVEE concentrations, temperatures and pressures.

The level of viscosity enhancement attained by dissolution of PISO-BVE in scCO₂ at the two concentrations of 1.5 and 3 wt% and pressures of 50, 53, and 55 MPa over temperatures ranging 329 to 377 K is given in Figure 5.8. As can be seen, compared to PVEE, the relative viscosities for PISO-BVE are substantially less under the same or similar conditions. For example, over the temperature range of 329-377 K, 1.5 wt% of PISO-BVE, resulted in 1 to 1.23 fold increase in the CO₂ viscosity, while the same concentration of PVEE improved the viscosity by 1.36 to 1.9 fold over the same temperature range. This indicates that the CO₂ viscosity enhancement capacity of alkyl vinyl ether polymers decreases with increase in their backbone length. At the lower PISO-BVE concentration of 1.5 wt%, the CO₂ viscosity enhancement is negligible relative to just supercritical CO₂ at temperatures above 368 K and over the pressure range 50 to 55 MPa. The viscosity increases modestly with an increase in the polymer concentration to 3 wt%. For example, at 377 K, 3 wt% of PISO-BVE produces a relative viscosity of 1.2. Overall, the poly alkyl vinyl ether may result in subtle viscosity enhancement when dissolved in CO₂ at elevated temperatures. Also, the steric effect and increase in the alkyl arm length have a negative effect on their ability to increase viscosity.

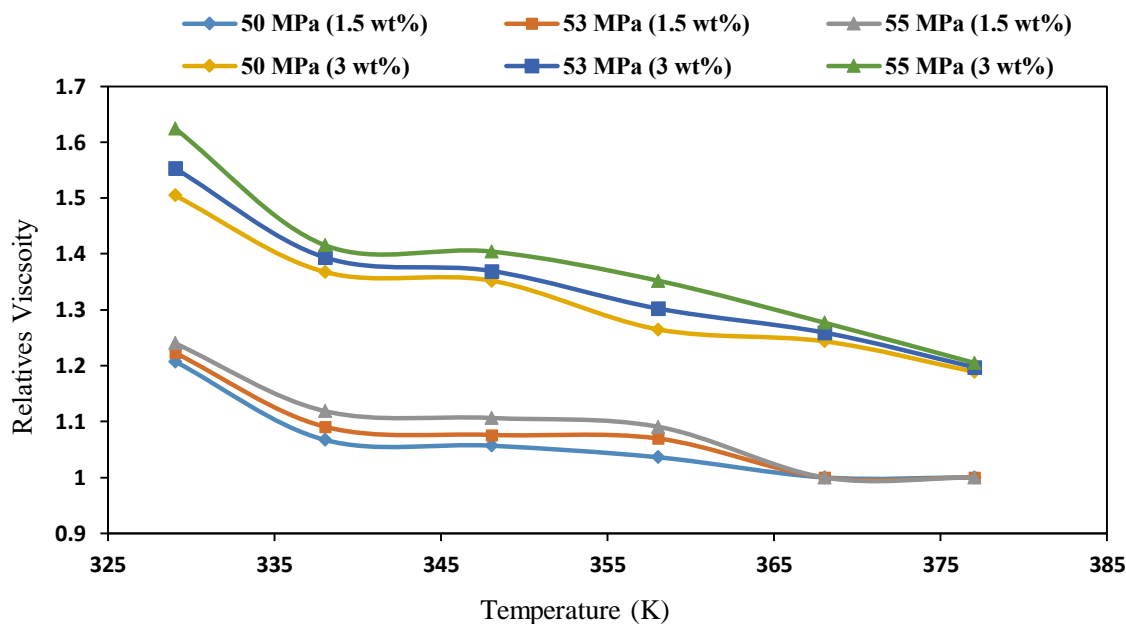


Figure 5.8 Relative viscosity ($\mu_{\text{sol}}/\mu_{\text{CO}_2}$) at different PISO-BVE concentrations, temperatures and pressures.

5.3.2.2 P-1-D Result

The CO₂ viscosity enhancement capacity of P-1-D over the concentration, pressure and temperature ranges of 0.81 to 5 wt%, 50 to 55 MPa and 358 to 377 K, respectively, is illustrated in Figure 5.9. As can be seen, despite P-1-D having a low molecular weight, a considerable increase in the CO₂ viscosity (1.2-2.77 fold) could be achieved at concentrations of 1.5 wt% and above. In comparison, Zheng et al.[178] found that the same polymer, initially tested by Heller et al.[66], could thicken CO₂ by 15 fold at the concentration of 0.81 wt%. Our results significantly differ from those reported by Zheng et al. In our first measurements, we found the oligomer or polymers to precipitate inside the capillary tube of our viscometer upon depressurisation. Therefore, to avoid any undesirable effects, as mentioned in our experimental procedure section, we decided to replace the capillary tube from one measurement to the next. We found hot toluene to be insufficient at completely dissolving and removing the residual polymer/oligomer deposited in such a small diameter tube.

After all three polymers/oligomers were tested, despite the significant difference in their molecular weights, P-1-D was found to be a promising CO₂ thickening agent under the high temperature conditions of Field A (i.e. 377 K). Other research work have also demonstrated the thermal stability of P-1-D at high temperatures.[288] For example, at 377 K, 55 MPa and 1.5 wt% concentration, P-1-D improved the CO₂ viscosity by 1.7 fold while under the same conditions, PVEE and Piso-BVE yielded 1.39 and 1 fold increases in the viscosity, respectively.

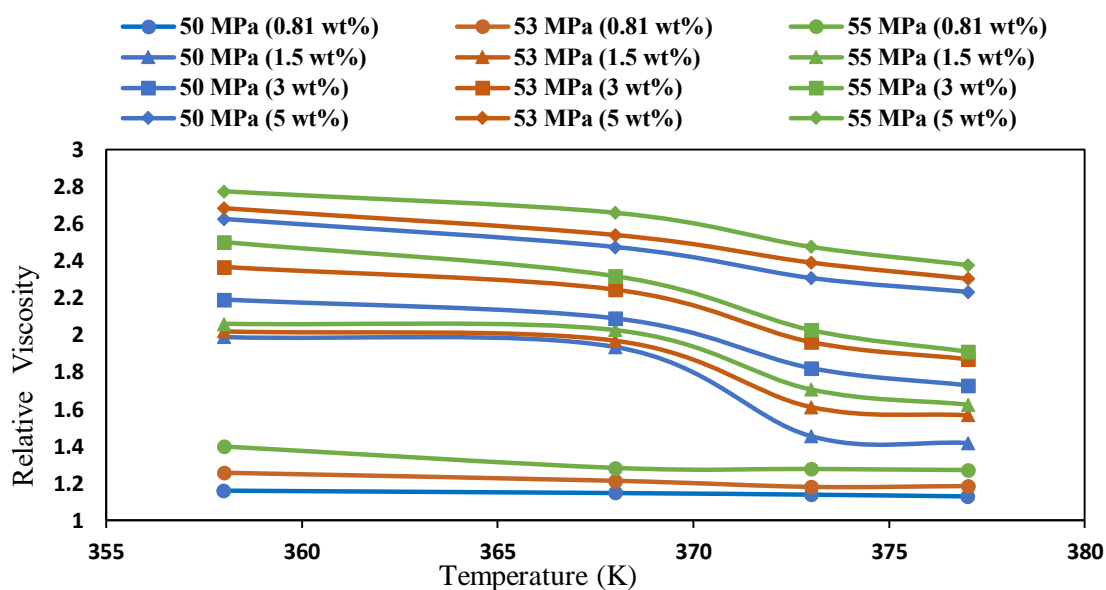


Figure 5.9 Relative viscosity (μ_{sol}/μ_{CO_2}) at different P-1-D concentrations, temperatures and pressures.

Table 5.3 The measured viscosities for pure CO₂ and CO₂ thickened using different concentrations of PVEE, Piso-BVE and P-1-D at different pressures and temperature (377 K).

Polymer	Concn	Pure CO ₂ viscosity, cP			Polymer/thickened CO ₂ viscosity, cP		
		55 MPa	53 MPa	50 MPa	55 MPa	53 MPa	50 MPa
P-1-D	0.81	0.077	0.076	0.074	0.094	0.09	0.088
	1.5	0.077	0.076	0.074	0.125	0.119	0.102
	3	0.077	0.076	0.074	0.147	0.142	0.133
	5	0.077	0.076	0.074	0.183	0.175	0.16
Piso-VBE	1.5	0.077	0.076	0.074	0.078	0.076	0.074
	3	0.077	0.076	0.074	0.094	0.09	0.088
PVEE	1.2	0.077	0.076	0.074	0.094	0.087	-
	1.5	0.077	0.076	0.074	0.112	0.104	-
	2	0.077	0.076	0.074	0.133	-	-

5.4 Summary and Conclusions

The solubility of 26 commercial polymers/oligomers in scCO₂ at reservoir conditions was examined using a fast and efficient gravimetric extraction method. Then, a series of cloud point pressure measurements at 377 K was used to validate the solubility of polymer/oligomer candidates with high extraction weights. A total of three polymers/oligomers (PVEE, Piso-BVE, and P-1-D) were found to be adequately soluble in scCO₂ under the Field A's in-situ reservoir conditions. Subsequently, these polymers/oligomers were assessed at diluted concentrations (0.81-5 wt%) for their CO₂ viscosification capacity at different pressures and high temperatures. In general, it is known that increasing the temperature results in a decrease in the viscosification capacity of polymers while increasing pressure causes a slight improvement at all temperatures and concentrations.

Our results show that P-1-D and PVEE could be considered as effective CO₂ thickeners at Field A's conditions. P-1-D increases the CO₂ viscosity by 1.2-2.77 fold

over the concentration and temperature ranges of 0.81-5 wt% and 358 -377 K, respectively, while 1.2-2 wt% of PVEE improves CO₂ viscosity by 1.2-2.1 fold over the temperature range of 329-377 K. The enhancements in CO₂ viscosities reported above are significantly less than those (13-14 fold) reported by Zhang et al. at comparable compositions and temperatures.

Our results indicate that change in the alkyl arm and steric effect on the alkyl vinyl ether have great influence on the solubility of polymers in CO₂ but are ineffective in changing the CO₂ viscosity. Piso-BVE exhibits a higher solubility in CO₂ than PVEE at high temperatures, but its viscosity enhancement capacity is lower than PVEE at comparable concentrations and molecular weights. For example, PVEE increases the viscosity of scCO₂ by 43% at the concentration of 1.5 wt% and temperature of 377 K, while the same concentration of Piso-BVE cannot increase CO₂ viscosity noticeably at 377 K. Piso-BVE is required at high concentrations to change the CO₂ viscosity at high temperatures. This research concludes that P-1-D has a better CO₂ viscosity enhancement ability than PVEE and Piso-BVE, making it a suitable candidate for improving gas mobility in Field A and, under high temperatures in general, during CO₂ flooding.

Chapter 6. A New Approach of Alternating Thickened-Unthickened Gas Flooding for Enhanced oil Recovery*

6.1 Introduction

Miscible gas injection (MGI) is an effective enhanced oil recovery method used worldwide in the petroleum industry especially for the recovery of light oil[10, 257, 327] as the miscible conditions are more easily achieved for lighter oils.[328] Many MGI processes involve the injection of the associated gas (AG) or CO₂, which have both been recognised as excellent candidates for miscible gas flooding.[7, 22, 329] However, under reservoir conditions, injected gas typically has a significantly lower viscosity than the in-situ oil leading to an unfavourable mobility ratio that results in viscous fingering and gas channelling that eventually leads to premature breakthrough and low volumetric sweep efficiency.[330] To overcome this, one approach is the direct thickening of the injected gas with additives that increase the viscosity and help to effectively control gas mobility and improve sweep efficiency.[52, 66, 69, 155, 208, 331] In our previous studies, we identified poly (1-decene) (P-1-D) as a viable gas thickener for both AG mixture and CO₂ over a range of concentrations (1.5 to 5 wt% and 1.5 to 9 wt% for CO₂ and AG, respectively).[288, 332]

For many years, direct gas thickening has been recognised as a game changing technology to increase oil recovery in MGI processes.[52] This technique owes its progress to thermal stability and chemical inertness (with no or minimal interaction with reservoir sediment) of the chemical additives making them ideal for application in harsh reservoir conditions (i.e. high formation salinity and temperature).[52] Unlike foam injection and water alternating gas (WAG) flooding, the application of gas thickeners is not dependent on the reservoir rock petrophysical properties and fluid saturations.[52] Field A in southern Oman has suffered from early gas breakthrough due to the high mobility of the AG mixture injected as part of an MGI process.[32, 288] The field has a harsh reservoir environment with a formation brine salinity of 275,000 ppm TDS (total dissolved solids) and a reservoir temperature of 377 K with low in-situ water saturation.[30, 31] It has been shown that both foam and WAG flooding are not applicable in this field as means of mobility control.[288] Hence, with

Field A, it is believed that AG mixture thickening may be the only viable approach to counteract unfavourable mobility conditions and improve sweep efficiency.

Over the past 40 years, several polymer and oligomer additives that are soluble in CO₂ and hydrocarbon gas mixture have been tested to examine their potential to raise injected gas viscosity (ideally to the reservoir oil viscosity).[52, 64, 66, 69-72, 164, 231, 333] To date, high molecular weight (M_w 540,000) fluoroacrylate–styrene copolymer (polyFAST) has been identified as the most effective CO₂ thickener in terms of improving CO₂ viscosity.[170, 191] However, the cost (\$132/kg) associated with this copolymer has prevented its application outside the laboratory.[167] In addition, polymers of this type containing large amounts of fluorine, are environmentally and biologically persistent.[188] Polydimethylsiloxane (PDMS) is also a polymer that is soluble in CO₂ at high molecular weight and has been shown to thicken CO₂ and hydrocarbon gas thickeners.[52, 63, 71, 157, 164, 227] In particular, it has been found that extremely high molecular weight PDMS (M_w 197,000) with the addition of a large amount of a co-solvent (20 wt% toluene) is an effective thickener for CO₂ enhanced oil recovery (CO₂-EOR).[63] Furthermore, application of high molecular weight PDMS results in a modest increase in natural gas liquid (NGL) viscosity at 298 K and 7 MPa.[231] However, with elevated temperatures, PDMS requires higher pressures for dissolution into CO₂, NGL, or AG.[71, 172, 231, 288] Further, the high cost of high M_w PDMS polymer ((\$9/g) and high concentration of co-solvent required make the field application for this polymer impractical.[52, 72, 157] In addition, it has been found that PVAc (M_w 11,000) is also soluble and is considered a non-fluorous polymers with PDMS (MW 13,000) that is most soluble in CO₂; PDMS is more soluble than PVAc.[189, 197] Therefore, the dissolution of the high M_w of PVAc in CO₂ requires a very high pressure to obtain a single phase fluid. It was also determined that the viscosity did not increase with 1-2 wt% of PVAc (M_w 11000) in CO₂ at 298 K and 64 MPa.[162] For non-fluorous oligomer additives, Heller et al.[66] showed that due to low solubility in CO₂, PVEE (M_w 3800) and P-1-D that only a very slight increase in viscosity (7-25%) at 298 and 306 K is observed. Further, they found that low molecular weight poly α -olefins (P-1-D, poly(1-pentene) and poly(1-hexane) can induce the butane viscosity by 5 fold at a concentration of 2.2 wt%.[64] In our previous studies,[288] P-1-D (M_w 544) was found to have sufficient solubility in both CO₂ and AG mixtures (at temperatures above 358 K and pressures

of 50-55 MPa) to significantly increase gas viscosity. The viscosity enhancement of P-1-D in AG mixture (25 mol% CO₂) and CO₂ was measured in a capillary viscometer at different pressures (50-55 MPa), a temperature of 377 K, and varying P-1-D concentrations (1.5-9 wt%). [288, 332] Figure 6.1 shows the viscosity measured for P-1-D-thickened CO₂ (1.5-5 wt%) and P-1-D thickened AG mixture (1.5-9 wt%) at 377 K for over 50-55 MPa pressure range. As can be seen from this figure, in both solutions, there is a significant and almost linear increase in the viscosity of both thickened solutions with increases in the P-1-D concentration. However, P-1-D-thickened CO₂ has much higher viscosity than the P-1-D-thickened AG mixture at all measured concentrations. For example, at 5 wt% P-1-D, the CO₂ viscosity falls in the range of 0.14-0.18 cP over the pressure range of 50-55 MPa, while over the same pressure range, the AG mixture viscosity is in the range of 0.126-0.131 cP. This is due to the difference in viscosity of the pure AG mixture and CO₂ at these pressures (i.e. 0.074-0.077 cP for CO₂ and 0.029-0.03 cP for the AG mixture). Therefore, for the two solutions to have comparable viscosities, the AG mixture requires higher concentrations of oligomer. For example, in order to enhance the viscosity to 0.13 cP, 5 wt% of P-1-D is needed for the AG mixture while CO₂ would only require a concentration of 3 wt% only.

In a reservoir simulation study (chapter 3), it was determined that in Field A, due to its low in-situ oil viscosity, an increase of 0.1 to 0.16 cP (3.3 to 5.3 fold) in the viscosity of the injected gas (AG mixture or CO₂) would be adequate to improve the gas mobility favourably and enhance the sweep efficiency. [34] To achieve this, thickener concentrations in the range of 3-5 wt% would be required rendering application in the field infeasible due to the large quantity of polymers/oligomers that would be required. This has precluded the use of thickeners in any oil field around the world. Overall, given the results of the viscosity measurements, P-1-D may be regarded as a suitable thickener for both CO₂ and AG mixtures at high temperatures and high pressure such as those found in Field A. However, the amounts of P-1-D needed to reach the target injection gas viscosity for Field A (0.13-0.16 cP) is quite high if the injection is to be performed using a continuous thickened gas injection scheme.

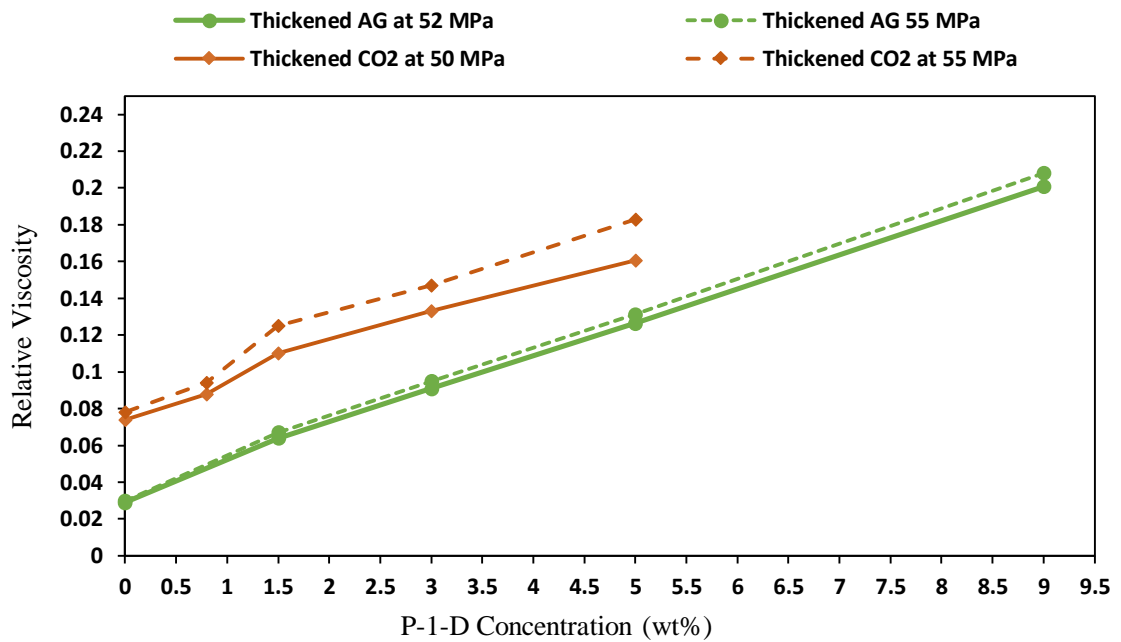


Figure 6.1 Measured P-1-D-thickend AG and CO₂ solution viscosities at different P-1-D concentrations, temperatures (377 K), and pressures (50-55MPa) from a capillary viscometer (0.01-15,000 cP).[288, 332]

To address this issue, this study investigates a new approach that can lower the volume of thickeners utilised during field-scale applications. WAG flooding has been studied and applied in the field for enhanced oil recovery (EOR) applications for many years. Herein, we proposed an injection scheme similar to WAG in which thickened gas (CO₂ or AG) would be injected in alternation with an unthickened AG mixture. Compared with the case of continuous thickened gas injection, the alternating injection scheme would be technically and economically beneficial for application in the MGI process as it would require lower amounts of the thickening agents. For this study, P-1-D was used to evaluate the potential of the above mentioned alternating injection scheme, and a total of 12 core-flooding tests were conducted on fractured and non-fractured composite rock samples. The tests followed four different injection schemes: (1) continuous unthickened AG flooding, (2) continuous thickened AG flooding, (3) thickened AG alternating AG flooding (TAG-A-AG), and (4) thickened CO₂ alternating AG flooding (TCO₂-A-AG)). The core-flooding experiments were all conducted at constant pressure (53 MPa) and temperature (377 K) using carbonate core plugs and crude oil sourced from Field A.

6.2 Experimental Methodology

6.2.1 Materials

For this study, low molecular weight P-1-D was purchased from Sigma-Aldrich. The molecular weight of P-1-D was determined in GPC to be equal 544 g.mol⁻¹ (Mn is 473 g.mol⁻¹, and poly dispersity is 1.15). CO₂ gas (99.999 mol%) and AG mixture (CH₄ 60 mol%, C₂H₆ 9 mol%, C₃H₈ 6 mol%, and CO₂ 25 mol%) were purchased from BOC Gas, Australia. Both gas cylinders are provided in G-size cylinders for each at pressure 5.5 and 4.14 MPa, respectively. CMG WinProp Module (version 2016) was used to estimate the density of the AG mixture and CO₂ for solution concentration calculations.

The original light oil sample was collected at the wellhead from Field A, Oman. For this study, the light gas components under C₅ were flushed out at ambient pressure and temperature to achieve a dead oil. The density and viscosity of the dead oil were measured to be 0.81 g.cm⁻³ and 2.7 cP (377 K and 53 MPa), respectively. The composition of the dead oil sample is given in Table 6.1 as obtained using gas chromatography with a flame ionization detector (GC-FID). For the core-flooding experiments, synthetic brine was prepared by dissolving analytical grade NaCl and KCl into deionised water. The solution was prepared according to Field A's formation brine composition (total dissolved solid concentration of 275 g.L⁻¹ consisting of 220 g.L⁻¹ NaCl and 55 g.L⁻¹ KCl). A number of relatively tight carbonate core plugs were collected from Field A wells at reservoir depths of 4995-5000 m. The permeability and porosity of non-fractured plugs were in the range of 2-30 mD and 13-14.26%, respectively. The fractured plugs had substantially higher permeability but almost the same porosity as the non-fractured plugs falling in the range of 156-265 mD and 13.8-15.8%, respectively.

Table 6.1 Compositional analysis results of Field A dead oil in mole percentage

Component	Mole %	Component-cnt	Mole %
H ₂	0	C ₁₆	4.15
H ₂ S	0	C ₁₇	3.85
CO ₂	0	C ₁₈	3.77
N ₂	0	C ₁₉	3.97
C ₁	0	C ₂₀	3.27
C ₂	0	C ₂₁	2.99

C ₃	0	C ₂₂	2.87
iC ₄	0	C ₂₃	2.67
nC ₄	0	C ₂₄	2.47
C ₅	0	C ₂₅	2.19
iC ₅	0.01	C ₂₆	2.1
nC ₅	0.02	C ₂₇	1.99
C ₆	0.33	C ₂₈	1.85
C ₇	1.54	C ₂₉	1.85
C ₈	3.71	C ₃₀	1.77
C ₉	4.84	C ₃₁	1.64
C ₁₀	5.54	C ₃₂	1.43
C ₁₁	5.15	C ₃₃	1.35
C ₁₂	4.72	C ₃₄	1.26
C ₁₃	5.08	C ₃₅	1.2
C ₁₄	4.63	C ₃₆₊	10.93
C ₁₅	4.86	Total	100

6.2.2 Core Flooding Experimental Setup and Procedure

In this study, a total of twelve reservoir condition core-flooding tests were conducted using the experimental setup shown in Figure 6.2. Extensive details about the setup is mentioned in chapter 4. The flooding tests were performed on two non-fractured and two fractured core plugs which were stacked together to form two longer ($L \sim 14\text{cm}$) composite cores. Each core plug was about 7 cm long and 3.85 cm in diameter. Figure 6.3 is a photo and X-ray image of the composite core that included two plugs with a microfracture along their length. The presence of the microfracture is clearly visible in the X-ray image. Each composite core underwent all four injection schemes of miscible gas flooding outlined earlier (i.e. continuous unthickened AG flooding, continuous thickened AG flooding (TAG) (5 wt% of P-1-D), thickened AG alternating AG flooding (TAG-A-AG) (ratio, 1:2; 5 wt% of P-1-D)) and, thickened CO₂ alternating AG flooding (TCO₂-A-AG) (ratio, 1:2; 3 wt% of P-1-D). In addition, two more thickened AG alternating AG flooding (TAG-A-AG) ratios of 1:3 and 1:5 were also evaluated on each composite core. Table 6.2 provides further details about the core-flooding tests performed on each of the two composite cores. To achieve miscibility, all experiments were conducted using a back pressure of 53 MPa which is higher than the MMP of either the crude oil or dead oil from Field A (38 and 33 MPa,

respectively[32]). A brief description of the procedure followed for each flooding test is presented below.

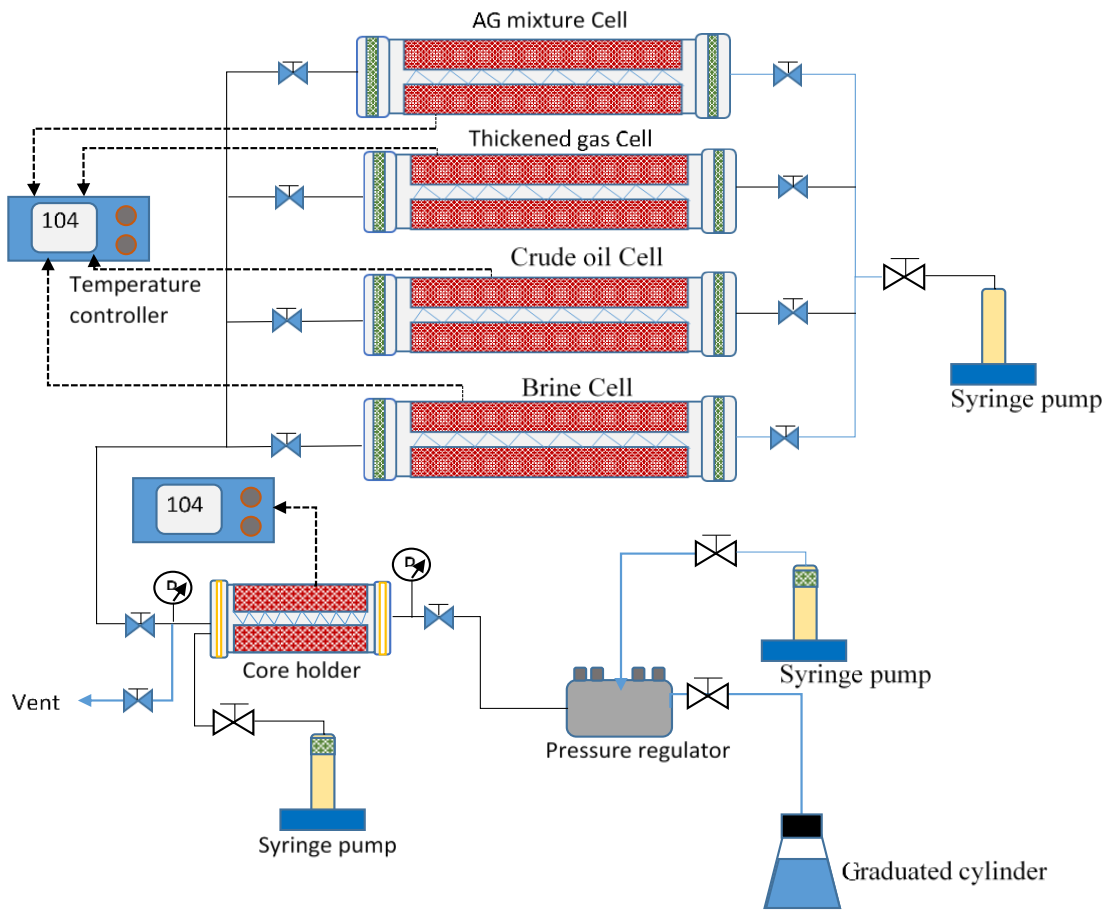


Figure 6.2 Schematic diagram of the core-flood setup.

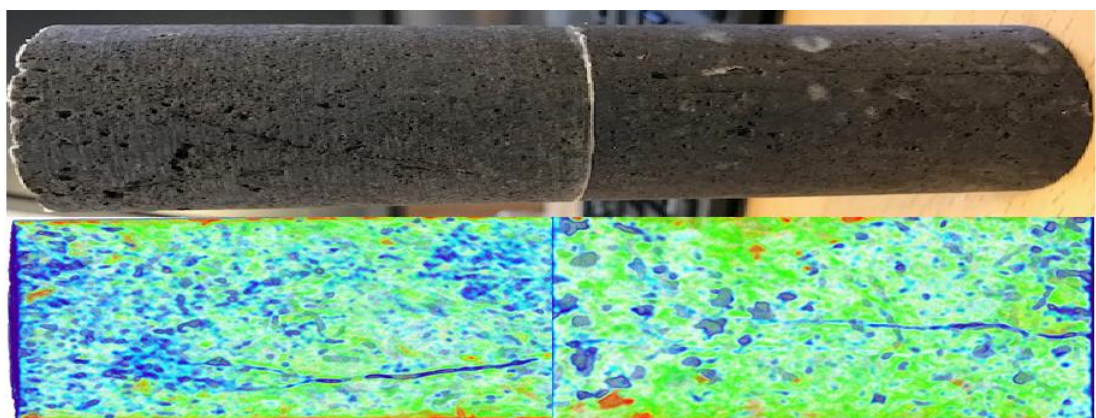


Figure 6.3 Fracture visualisation in composite core plugs sample and CT scan.

Table 6.2 Details of the 6 core-flooding test performed in each composite core plugs setups.

Test number	Injection schemes	TAGR	Thickened gas injected time in each cycle	Unthickened gas injected time in each cycle
test #1	continuous unthickened AG	-	-	-
test #2	continuous TAG	-	-	-
test #3	TAG-A-AG	1:2	30 minutes	1 hour
test #4	TAG-A-AG	1:3	20 minutes	1 hour
test #5	TAG-A-AG	1:5	12 minutes	1 hour
test #6	TCO ₂ -A-AG	1:2	30 minutes	1 hour

Each core plugs was placed in a temperature controlled Dean-Stark extractor and cleaned with toluene and methanol in turn to remove any hydrocarbon and salt residues. Subsequently, they were dried in an oven at 358 K for 24 h or until their weights stabilised indicating no more loss of solvent. Subsequently, the porosity and permeability of each plug was measured using an automatic porosi-permeameter (AP-608 instrument, Coretest Systems Inc.). The composite sample was then assembled and wrapped in a combination sleeve made up of aluminium foil, FEP heat shrink and Viton rubber[334] and placed inside a horizontal core-holder and vacuumed for 24 h while applying an effective overburden pressure of 2.75 MPa. Synthetic formation brine was then injected to raise the pore pressure gradually while simultaneously increasing the overburden pressure and temperature to their respective in-situ values. During this process, the overburden pressure was always maintained 6.89 MPa higher than the pore pressure until reaching the final in-situ value of 62 MPa. After achieving pressure and temperature stability in the system, synthetic brine was injected continuously at the flow rate of 0.15-0.3 cm³.min⁻¹ for 48 h to ensure that the plugs was completely saturated with the brine. Full saturation was verified by a constant and stable differential pressure across the sample. Afterwards, the brine was injected at several flow rates (0.08, 0.16, and 0.32 cm³.min⁻¹ for non-fractured plugs and 0.5, 1

and $2 \text{ cm}^3 \cdot \text{min}^{-1}$ for the fractured plugs) to measure the absolute permeability. Next, the brine saturated sample was displaced by reservoir dead oil which was injected at $0.3 \text{ cm}^3 \cdot \text{min}^{-1}$ for three to four days until there no more brine was produced, indicating that irreducible water saturation was achieved. During this time, the produced brine and oil volumes were recorded. The preceding steps (i.e. sample preparation, brine saturation, and displacement with dead oil flooding) were repeated before the commencement of every new test. Once the connate water saturation was achieved in each of the twelve tests, unthickened AG mixture, TAG (5 wt% of P-1-D), TAG-A-AG (5 wt% of P-1-D), and/or TCO₂-A-AG (3 wt% of P-1-D), were injected at the constant injection rate of $0.4 \text{ cm}^3 \cdot \text{min}^{-1}$. For this step, the volume of any produced oil during the gas injection stage was recorded against time. For all the flooding tests, injection was terminated at 8.3 total pore volume (PV) of either unthickened AG, thickened AG, or thickened CO₂ injected.

6.3 Results and Discussions

6.3.1 Core-Flood Experiments

The absolute permeability of the composite sample determined by varying the brine injection rate as previously described above is given in Tables 6.3 and 6.4. For this study, 12 core-flooding experiments were conducted using four different flooding schemes to study the effect of thickened/unthickened AG mixture in two composite samples. For all the flooding experiments, a very low irreducible water saturation was attained at the end of the initial oil injection stage. This is believed to be due to the low viscosity difference between the oil (2.7 cP) and water (0.4 cP) at reservoir conditions and the high pore pressure used for the test.[288]

6.3.1.1 Oil Recovery in Non-Fractured Core Plugs

6.3.1.1.1 Effect of Injection Scheme

For the non-fractured core plugs, the measured oil recovery profiles for tests #1-4 (which were continued until reaching 8.3 PV of total gas injection) are plotted in Figure 6.4. In test#1, the unthickened AG mixture flood was conducted under secondary recovery mode and the gas breakthrough (BT) occurred after 0.092 PV of AG mixture injection corresponding to an oil recovery of 14.5%. After BT, the oil

production rate was reduced gradually reaching an almost zero value at the end of the injection resulting in the ultimate oil recovery of 90.3%. In test#2, a continuous thickened AG mixture (5 wt% of P-1-D) was injected at $0.4 \text{ cm}^3 \cdot \text{min}^{-1}$; as expected, the gas BT was delayed compared to that in test#1. BT occurred at 0.142 PV of TAG injection corresponding to an oil recovery of 40.4%. This delayed BT is due to the lower viscosity contrast between the oil (2.7 cP) and the TAG mixture (0.13 cP). After BT, the oil recovery gradually increased until the end of the experiment corresponding to 8.3 PV of TAG injection resulting in the final oil recovery of 97.14%, which is almost 7% higher compared to that of test#1. In general, the increased oil recovery factor may be mainly attributed to the improved viscosity contrast of the thickened gas flood, reducing the injection gas mobility and subsequently delaying gas BT. However, the delay in BT allows the injected gas to come in contact with more oil in the sample's pore volume further enhancing other miscible injection recovery mechanisms such as oil viscosity reduction, oil swelling, and extraction of hydrocarbon fractions by CO_2 available in the AG mixture. In summary, the addition of oligomer to the injected AG mixture enhances the overall injection gas utilisation and the conformance of the flood which improves the volumetric sweep efficiency and the oil recovery factor.

Table 6.3 Summary of the core-flooding experiments conducted on non-fractured core plugs (377 K and 53 MPa). K, Permeability; ϕ , Porosity; $S_{\text{oil,max}}$, oil saturation upon the achievement of irreducible water; Injected TAGR, injected thickened ratio; BT, breakthrough in pore volume; and RF_{total} , ultimate oil recovery factor.

Test No.	Injection scheme	ϕ %	K mD	$S_{\text{oil,max}}$ %	Injected TAGR	BT P.V	RF_{total} (%)
1	unthicken AG	14.26	19.08	94.5	---	0.092	90.33
2	continuous thickened AG	13.73	11.1	93.4	---	0.142	97.14
3	thickened CO_2 alter AG	13.73	12.58	97.5	1:2	0.108	96.96
4	thickened AG alter AG	14.26	30.53	96.3	1:2	0.108	96.52
5	thickened AG alter AG	14.85	27.26	95.8	1:3	0.091	95.06
6	thickened AG alter AG	14.26	35.24	94.18	1:5	0.096	91.7

As observed from the above results, a moderate viscosity enhancement (4.38 fold) can result in reasonable improvement in the displacement efficiency and oil recovery factor. However, as mentioned earlier, the large quantity (5 wt%) of polymer or

oligomer required to reach this level of viscosity enhancement for the AG mixture makes continuous TAG injection uneconomical for Field A. In this study, the potential of the alternating injection scheme has been tested (tests #3 and #4) using the two thickened gases of TCO₂ (3 wt% of P-1-D) and TAG (5 wt% of P-1-D) using the same TAGR of 1:2 for both gases. As can be seen in Figures 6.4 and 6.5, the oil recoveries for both floods are higher than that of the continuous unthickened AG flood and close to the ultimate oil recovery of the continuous TAG flood. During the early injection times (until 2.2 PV of gas injection), TCO₂-A-AG flooding results in higher recovery than TAG-A-AG flooding. However, with further injection the two recovery profiles coalesce, resulting in almost identical final recovery factors (96.9% and 96.5%, respectively). As may be expected since the unthickened AG mixture is injected first, the BT times of these tests are similar to that of the unthickened AG mixture flooding test.

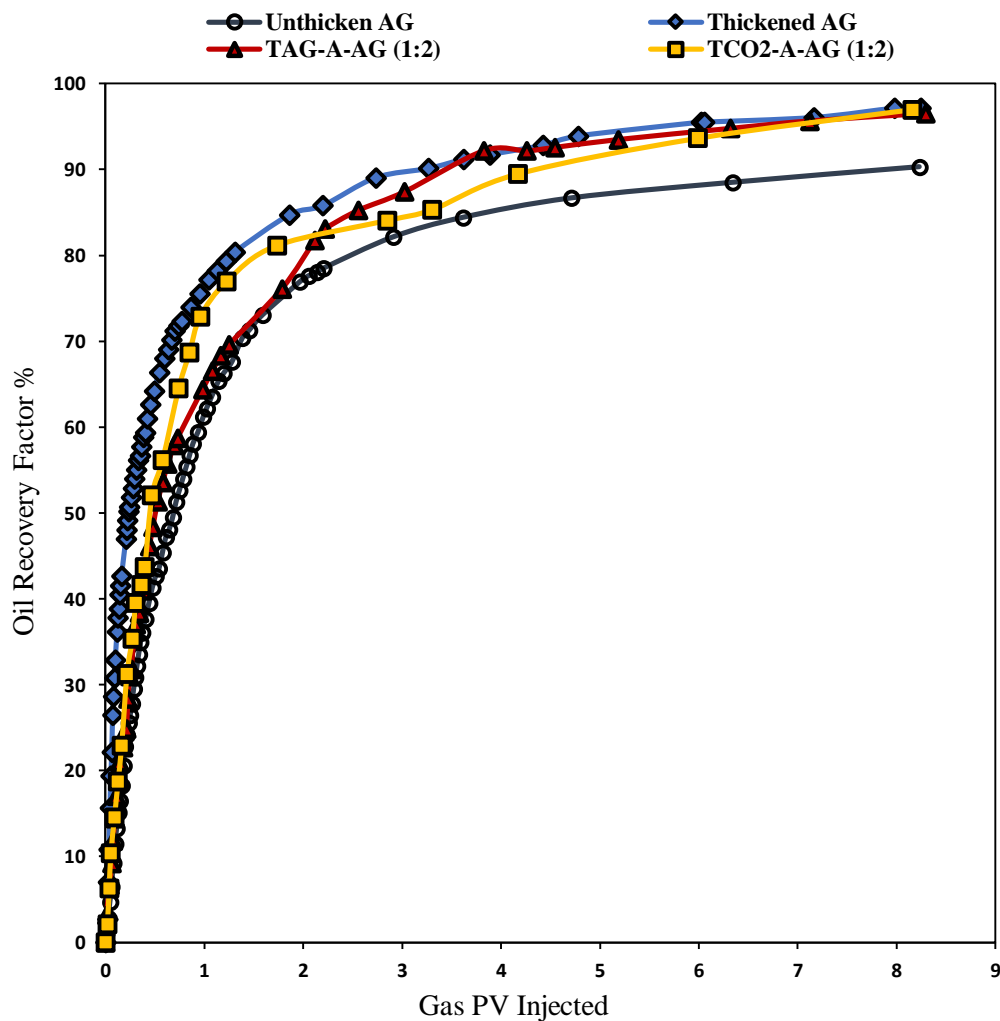


Figure 6.4 Measured oil recovery profiles for the four injection schemes of continuous unthickened AG flooding, continuous thickened AG flooding, thickened AG alternating AG flooding (TAG-A-AG) (ratio: 1:2), and thickened CO₂ alternating AG flooding (TCO₂-A-AG) (ratio: 1:2) in non-fractured composite sample, all conducted at 377 K and 53 MPa.

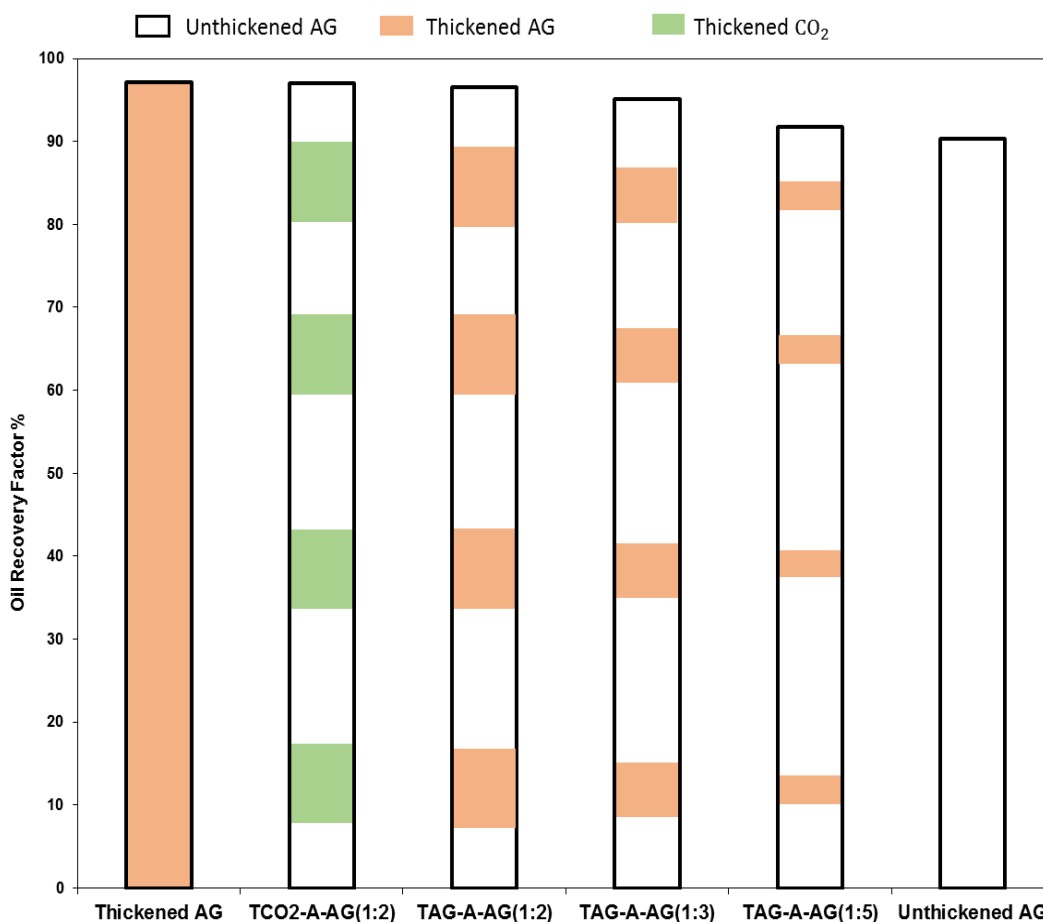


Figure 6.5 Graphical representation of the injection patterns and measured ultimate oil recovery factors for different injection schemes and different TAGR in non-fractured core plugs.

6.3.1.1.2 TAGR Effect on the Performance of TAG-A-AG Injection

In addition to the four core-flooding experiments discussed earlier, two additional TAG-A-AG flooding experiments were carried out on the non-fractured plugs to investigate the effect of variation in the TAGR on the performance of the alternating injection scheme. The new tests were performed with two different alternating TAGRs of 1:3 and 1:5 (tests #5 and #6). For comparison purposes, the measured oil recovery profiles of three TAG-A-AG tests (ratios of 1:2, 1:3 and 1:5) along with those

belonging to the continuous TAG and unthickened AG flooding experiments are plotted in Figures 6.5 and 6.6. As can be seen from both figures, the TAGRs of 1:2 and 1:3 resulted in distinctly higher oil recoveries (96.52% and 95.06%, respectively) compared to those in the unthickened AG flooding and only slightly less than that obtained for continuous TAG flooding whereas the recovery factor of the ratio 1:5 (91.7%) is noticeably lower and is almost identical to that of the unthickened AG flooding. During the alternating TAG process, when the thickened AG reaches the core plugs, the conformance control and gas retention inside the plugs improve, providing the AG mixture with better opportunity to further penetrate more of the pore volume of the cores and mobilise further oil from the core plugs. However, such an effect seems to diminish when TAGR reaches 1:5 as the positive effects of the TAG on recovery are diluted by large amounts of unthickened AG injected. Overall, given the negligible difference between the recoveries obtained from TAGRs of 1:2 and 1:3 and the downside from using more thickened gas than necessary, the optimum TAGR for flooding the non-fractured cores would be 1:3 as it requires significantly less oligomer compared with a TAGR of 1:2.

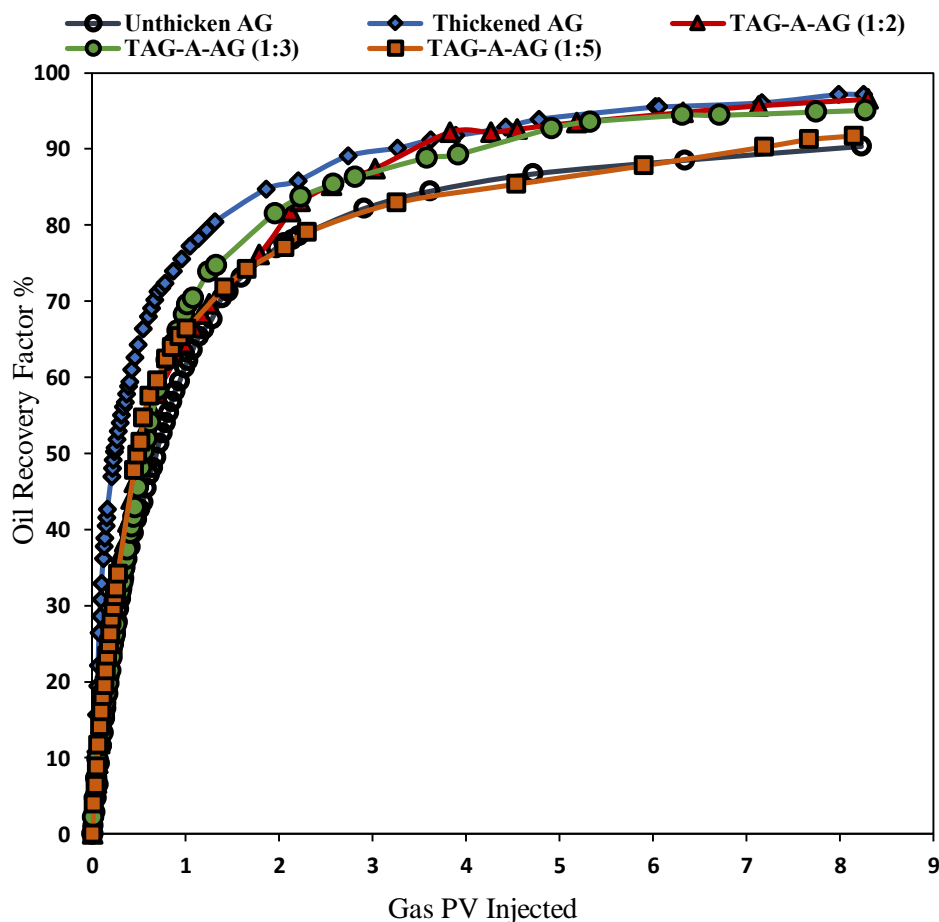


Figure 6.6 Measured oil recovery profiles for the four injection schemes of continuous unthickened AG flooding, continuous thickened AG flooding and thickened AG alternating AG flooding (TAG-A-AG) (ratios: 1:2, 1:3 and 1:5) in non-fractured composite sample, all conducted at 377 K and 53 MPa.

6.3.1.2 Oil Recovery in Fractured Core Plugs

As indicated earlier, the second composite sample included two fractured core plugs (Figure 6.3). An identical set of core-flooding experiments as that conducted on the non-fractured composite sample (tests #1-6) were also conducted on the fractured sample (tests #7-12). A short summary of all six experiments (tests 7-12) along with some of their main outcomes are presented in Table 6.4.

6.3.1.2.1 Effect of Injection Scheme

The primary objective of tests #7-10 conducted on the fractured plugs was to investigate the effect of injection scheme on the performance of miscible gas flood. The measured oil recovery profiles for the above experiments are plotted in Figure 6.7. Similar to the results obtained for the non-fractured plugs, the oil recovery factor of the continuous TAG flood (test #8) is similar to that obtained by the alternating TCO₂-A-AG (TAGR 1:2) flood (test #9) (95.3% and 95.2%, respectively) and significantly higher than those of the unthickened AG (80.3%) (test #7) and alternating TAG (93.2%) (test #10). The mechanism for the high recovery of the TAG flood is similar to that of the non-fractured sample and is attributed to the lower viscosity contrast between the injected gas and the displaced oil. As can be seen in Figures 6.7 and 6.8, unthickened AG flood (test #7) shows the lowest ultimate recovery (even lower than test #1 which is identical except that a non-fractured core is used) due to both the unfavourable mobility ratio of the flood and the channeling of the AG mixture through the microfracture resulting in a low volumetric sweep efficiency.

Compared with the continuous unthickened AG flood, the two alternating injection schemes result in significant additional oil (13-15%) being produced. Unlike the results obtained for the non-fractured plugs (by comparing with Figure 6.4), during early to intermediate flood times, Figure 6.7 indicates that TAG-A-AG injection seems to have a higher microscopic displacement efficiency than TCO₂-A-AG injection. Notably, around 5.3 PV of TCO₂-A-AG injected, the oil production rate increases significantly leading to a higher ultimate oil recovery factor for this flood. This

phenomenon may be explained using the expected interactions between the in-situ oil and either AG or CO₂. After BT, the injected gas would increasingly lose contact with any residual oil left inside the plugs resulting in less mass transfer (or mutual interactions) to occur between the injected gas and the residual oil. However, as the thickened gas is injected alternatingly into the core plugs, the mobility of the flood would improve enabling the gas to reach the residual oil left behind in the unswept regions of the plugs. Eventually, either CO₂ or the AG mixture undergo progressive multiple contact with the residual oil and the oil becomes diluted and mobilised. Nonetheless, in the case of the alternating TCO₂ injection, the expected mutual interactions between the oil and TCO₂ take a longer time to occur delaying the dilution and mobilisation of the oil.[80] Visual indications of the above process was observed in the last stage of the oil production in the related core flooding experiments. As can be seen in Figure 6.9, the produced oil by TAG-A-AG flooding seems more diluted early on (indicated by a yellow-shift in the fluorescence color) compared to the oil produced by alternating TCO₂-A-AG which looks less diluted further along in the recovery process. According to Bourdet et al.[335], while the light alkane fractions from the AG (i.e. methane and ethane) dissolve into the light crude oil used here, molecular transfer from the oil to the AG phase also occurs, resulting in a change in the fluorescence color of the oil from blueish to yellowish. As can be seen from Figure 6.9, a more pronounced change in the fluorescence color was observed with alternating TAG flood. In this case, the loss of low molecular weight aromatic molecules into the vapour phase is more pronounced with the injection of the AG mixture. The dilution of oil by gas solvents causes a further reduction of the residual oil viscosity[336] and subsequently the viscosity contrast. Hence, the oil dilution effect in combination with improved mobility control impacts on the oil recovery process.

Overall, it may be concluded that the addition of the oligomer or polymer into the gas (either AG mixture or CO₂) and injecting it continuously or alternatingly can improve the oil recovery in the fractured core plugs as was the case for non-fractured plugs. The thickened gas injection leads to better mobility control and an increase in the contact time between the oil and injected gas contributing to a higher oil recovery. However, the presence of the fracture gives rise to gas channeling counteracting the positive effect of improved mobility to some extent.

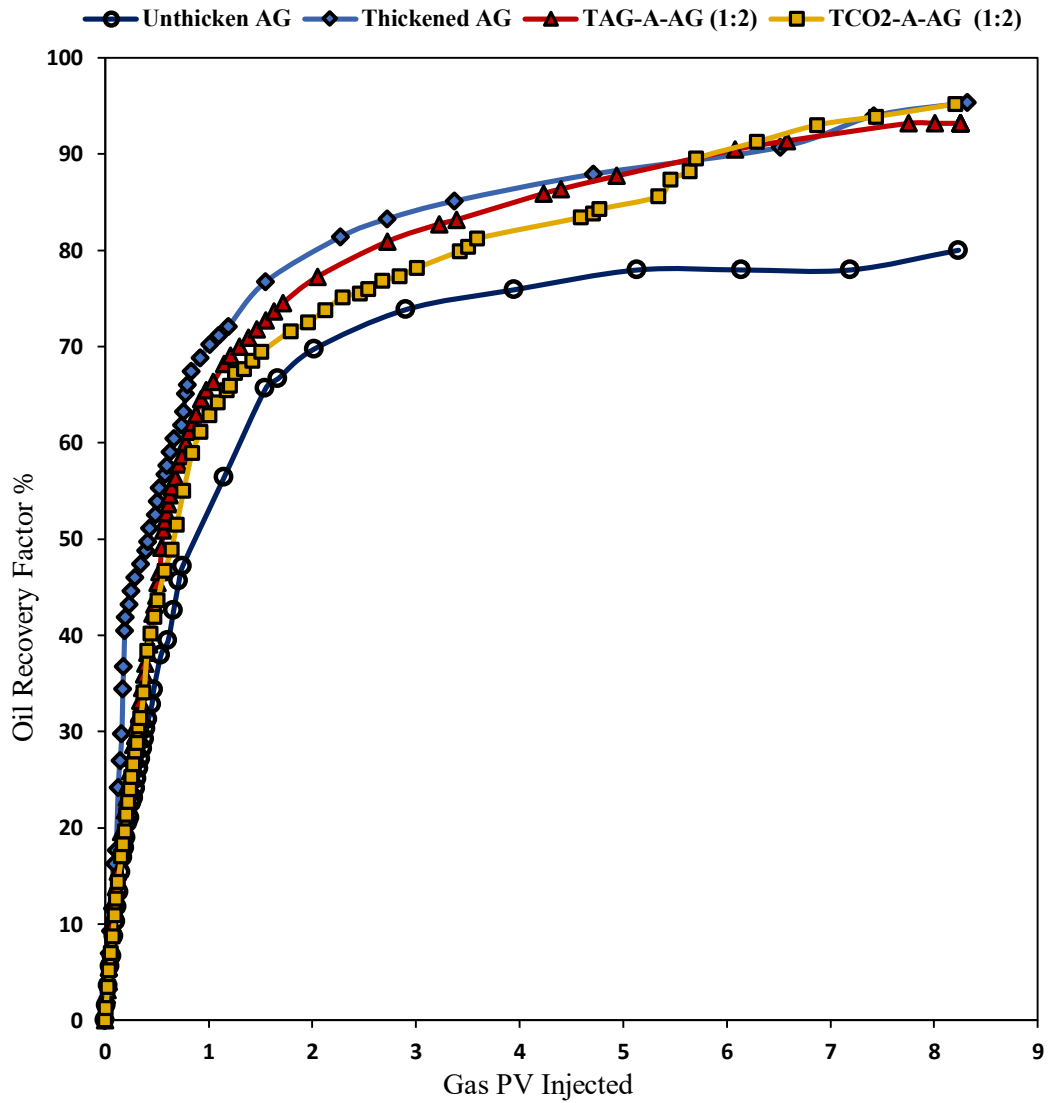


Figure 6.7 Measured oil recovery profiles for the four injection schemes of continuous unthickened AG flooding, continuous thickened AG flooding, thickened AG alternating AG flooding (TAG-A-AG) (ratio: 1:2), and thickened CO₂ alternating AG flooding (TCO₂-A-AG) (ratio: 1:2) in a fractured composite sample, all conducted at 377 K and 53 MPa.

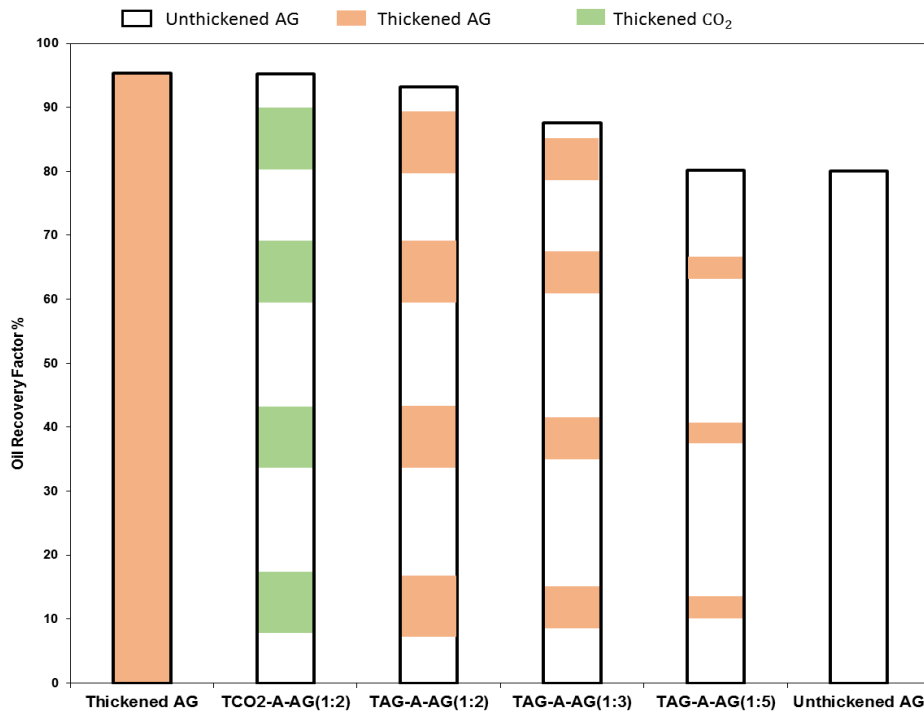


Figure 6.8 Comparison of measured ultimate oil recovery factors at different injection schemes and different TAGR in fractured core plugs.

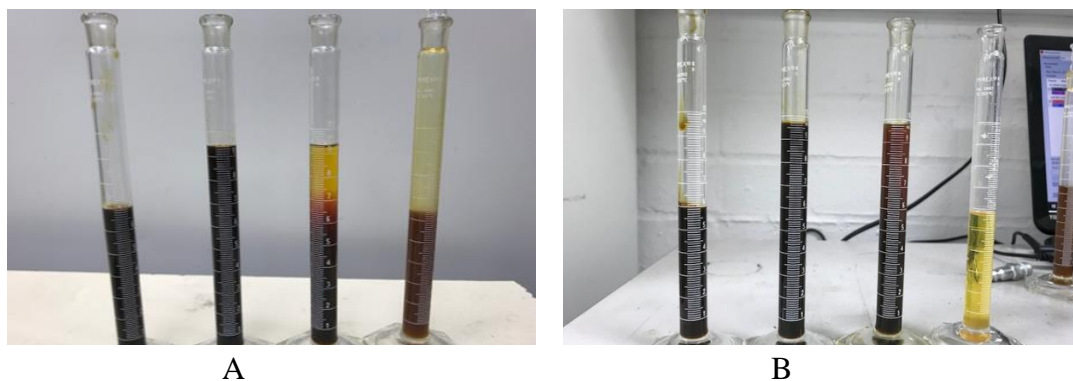


Figure 6.9 Collected oil produced in graduated cylinders from core-flooding tests in fractured core plugs: A, TCO₂-A-AG (1:2); and B, TAG-A-AG (1:2). The fluorescence color changes of residual oil in the last cylinder is dark brown in alternating TCO₂ flooding and yellow color in TAG alternating flooding.

6.3.1.2.2 TAGR Effect on the Performance of TAG-A-AG Injection

Similar to the study for non-fractured cores, test #11 and #12 (TAG-A-AG floods with TAGR values of 1:3 and 1:5, respectively) were conducted in the fractured core plugs to investigate the effect of TAGR on the oil recovery process. Various details of these two experiments are provided in Table 6.4. Figure 6.10 provides a comparison between the measured oil recovery profiles of experiments with different TAGRs (1:2,

1:3 and 1:5) and those of the continuous TAG and unthickened AG floods. As can be seen in Figure 6.8 and table 6.4, the three experiments with different TAGRs resulted in distinctly different ultimate oil recoveries. The TAGR values of 1:2 and 1:5 have recoveries very close to those of the continuous TAG and continuous unthickened AG floods, respectively. Figure 6.10 reveals that initially, the recovery profiles for TAGRs 1:2 and 1:3 are almost identical; however, with further injection, TAGR 1:2 deviates toward higher recovery. Such an effect may be attributed to the positive effects of larger TAGR resulting in better recovery. For the TAGR of 1:5, initially reasonable increases in the oil production rate are achieved; however, with further injection the presence of oligomer in the small thickened AG slugs fails to remain effective. At the end, unthicken AG and thickened AG alter AG (TAGR 1:5) exhibit the similar flooding performance. A similar behaviour can be observed for TAGR of 1:3; however, larger slugs of the thickened AG results in higher recovery compared with TAGR of 1:5. Therefore, the optimum TAGR for the alternating flooding in the fractured composite sample is 1:2, which unlike the non-fractured core has a significantly higher recovery factor than that with the 1:3 ratio.

Overall, the alternating flooding scheme utilising slugs of either TAG or TCO₂ was found to be capable of improving the oil sweep efficiency resulting in further enhancement in the oil recovery. With the TAGR of 1:2, the alternating scheme was even found to be as effective as the continuous TAG flood while consuming considerably less amounts of the oligomer making it economically more attractive.

Table 6.4 Summary of the core-flooding experiment conducted on fractured core plugs (377 K and 53 MPa) for fractured core plugs. K, Permeability; ϕ , Porosity; $S_{oil,max}$, Oil saturation upon the achievement of irreducible water; injected TAGR, injected thickened ratio; BT, breakthrough in pore volume; and RF_{total} , ultimate oil recovery Factor.

Test No	Injection scheme	ϕ %	k mD	$S_{oil,max}$ %	Injected TAGR	BT P.V	RF_{total} (%)
7	unthicken AG	14.0	187	85.0	-	0.069	80.0
8	continuous thickened AG	13.8	156	92.2	-	0.108	95.3
9	thickened CO2 alter AG	15.3	230	91.2	1:2	0.092	95.2
10	thickened AG alter AG	14.5	155	92.2	1:2	0.092	93.2
11	thickened AG alter AG	15.8	265	86.3	1:3	0.076	87.6

12	thickened AG alter AG	15.3	203	87.2	1:5	0.076	80.2
----	--------------------------	------	-----	------	-----	-------	------

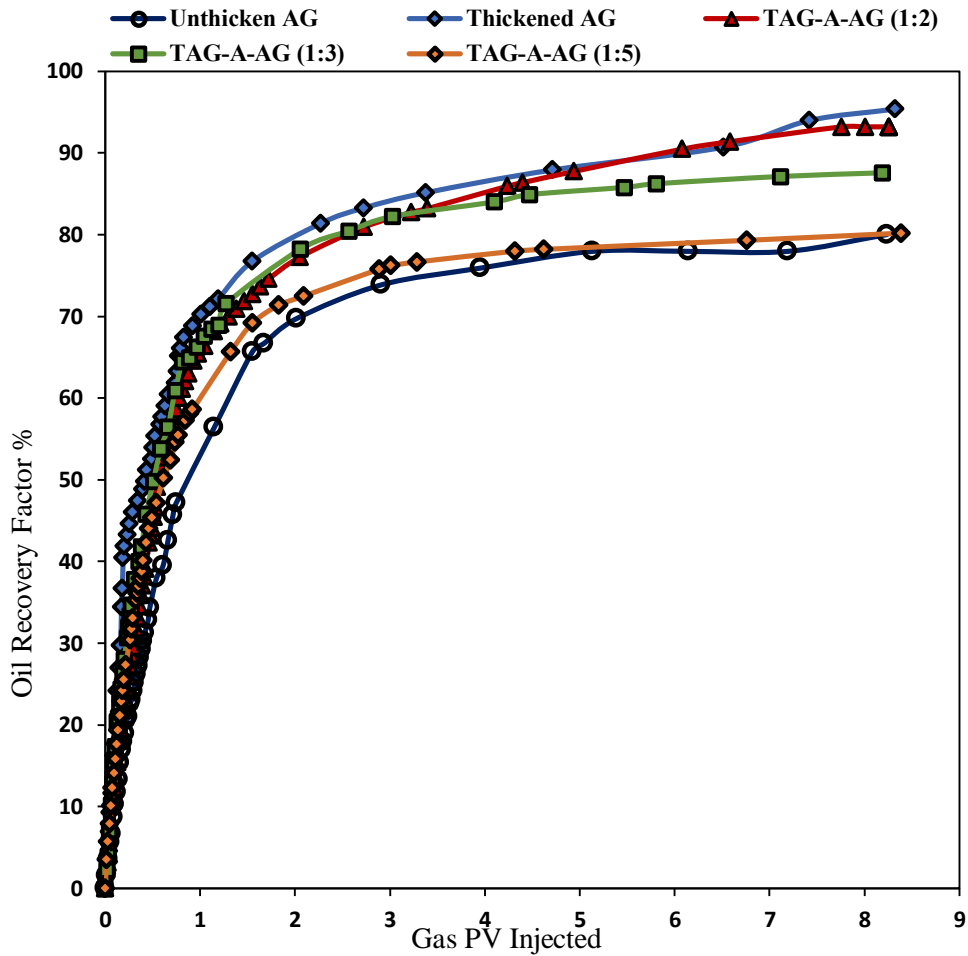


Figure 6.10 Measured oil recovery profiles for the four injection schemes of continuous unthickened AG flooding, continuous thickened AG flooding, and thickened AG alternating AG flooding (TAG-A-AG) (ratios: 1:2, 1:3 and 1:5) in a fractured composite sample, all conducted at 377 K and 53 MPa.

6.3.1.3 Comparison of the Oil Recovery Factor in Fractured and Non-fractured Core Plugs

The oil recovery profiles for continuous TAG and continuous unthickened AG flooding in both non-fractured and fractured core plugs are plotted and compared in Figure 6.11. As expected, the recovery factors for both floods are higher in the non-fractured plugs. This is because the displacement efficiency in the fractured core plugs is lowered by gas channeling through the microfractures. Naturally, continuous TAG flooding achieved a higher recovery factor than unthickened AG injection in both sample types. However, the difference between the two recovery factors is

substantially higher for the fractured plugs: a difference of 15.3% for the fractured plugs compared with a more subtle 6.81% difference for the non-fractured plugs. This comparison demonstrates the outstanding capability of the thickened gas injection in improving the flood conformance in the presence of the microfracture thus counteracting its negative effects on recovery. Therefore, it may be concluded that thickened gas injection relative to unthickened gas injection is more effective in improving the oil recovery process in heterogeneous reservoirs such as Field A.

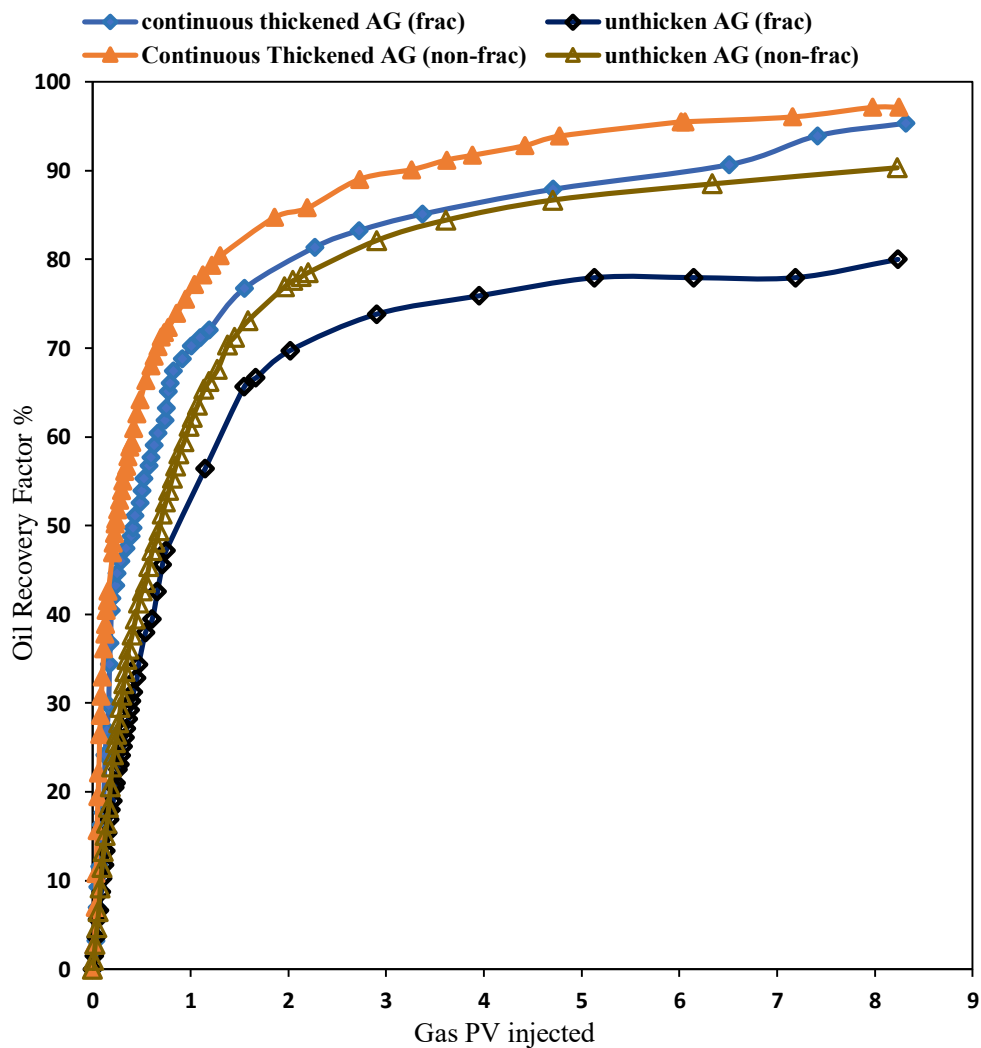


Figure 6.11 Measured oil recovery profiles for continuous TAG and continuous unthickened AG floods in non-fractured and fractured core plugs, all conducted at 377 K and 53 MPa.

The measured oil recovery profiles for TAG-A-AG and TCO₂-A-AG (ratio of 1:2 for both) in both non-fractured and fractured cores are in Figure 6.12. For early injection times with the non-fractured plugs, TCO₂-A-AG flood gives a higher

recovery factor than that of the TAG-A-AG flood. However, with further injection, the two recovery curves seem to overlap, resulting in almost identical ultimate recovery factors for both floods. Whereas in the fractured plugs, the TCO₂-A-AG flood gives lower oil recovery than the TAG-A-AG flood until about 5.3 PV of gas injection beyond which the TCO₂-A-AG flood seems to achieve a better displacement sweep efficiency, attaining a higher oil recovery at the later stages of the recovery process. The reason behind this behaviour has been discussed in previous sections of this chapter. Unlike the previous comparison between continuous TAG and unthickened TAG, the difference in performance between fractured and non-fractured cores is less significant.

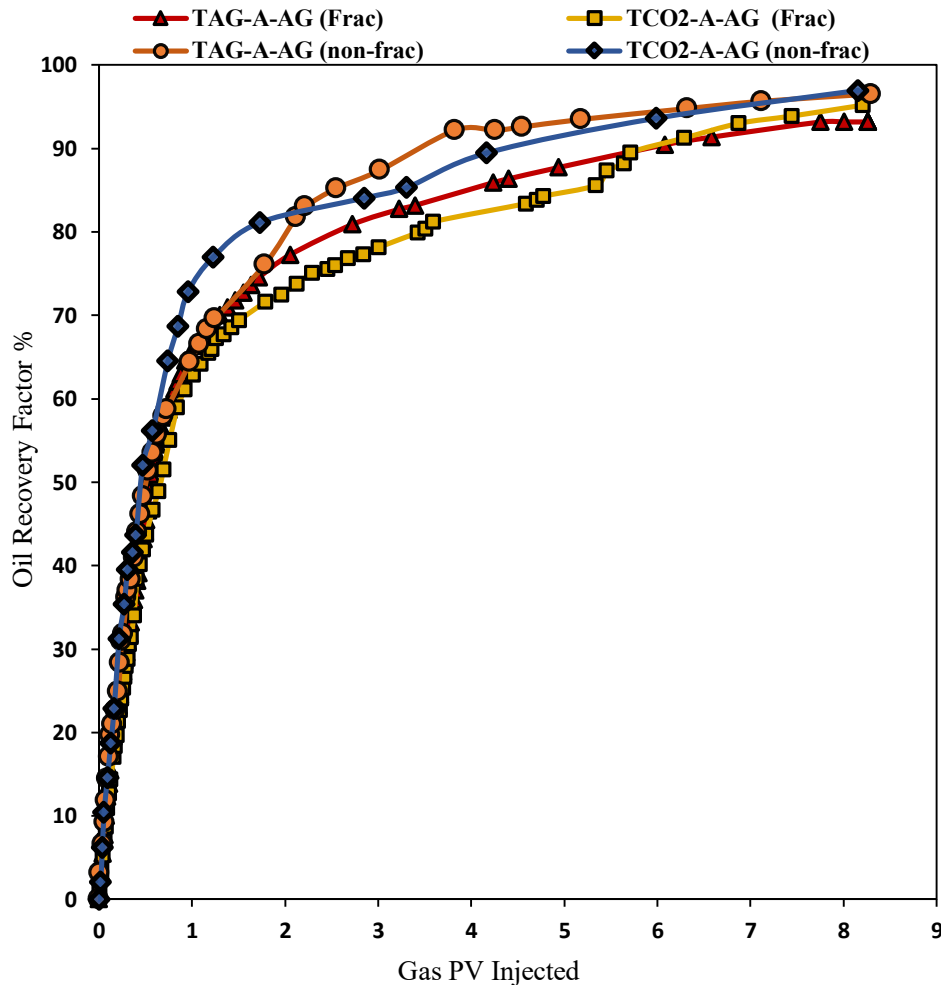


Figure 6.12 Measured total oil recovery factor versus 8.3 of total injected pore volume of TAG-A-AG and TCO₂-A-AG in non-fractured and fractured core plugs at a flow rate of 0.4 cm³.min⁻¹, reservoir temperature of 377 K, and pressure of 53 MPa.

6.3.2 Additives Cost Analysis

This section is devoted to a rough cost analysis for using P-1-D in CO₂ or AG mixture injection. According to PAO supplier, the price of the P-1-D is about USD \$3/kg. The concentrations used in the core flooding experiments were 5 wt% of P-1-D in AG mixture and 3 wt% in CO₂. A 5 wt% of P-1-D in the AG mixture would result in around \$70/m³ of AG mixture, which needs to be added to the initial cost of AG mixture which is approximately \$0.23/m³. 3 wt% of P-1-D in CO₂ would cost \$74/m³ of CO₂, which is in addition to the initial cost of CO₂ (\$0.026/m³). Although the concentration of P-1-D in CO₂ is lower than that in the AG mixture, a higher cost resulted from adding P-1-D to CO₂, because the density of CO₂ is higher than that of the AG mixture, which impacts directly the amount of oligomer required. Continuous thickened gas at these concentrations would be expensive and result in a negative cash flow. An alternating injection of the thickened gas might be economically possible if it works at the reservoir scale. According to the core flooding experiments conducted here, the optimum ratio is 1:2. With this ratio, the P-1-D amount required would be reduced to 1/3. This is equivalent to 1.7 wt% of oligomer/AG continuous injection and 1 wt% of P-1-D/CO₂ injection. Therefore, the amount of oligomer in both solvents is substantially reduced, thus potentially influencing project economics.

6.4 Summary and Conclusion

In this study, a total of twelve core flood tests were conducted using four different injection schemes (continuous unthickened AG, continuous TAG, TAG-A-AG, and TCO₂-A-AG) on non-fractured and fractured composite samples from Field A located in the south of Oman. It is found that the continuous TAG injection and alternating injection of TAG or TCO₂ with unthickened AG are all capable of mobilising high proportions of the in-situ oil and achieving higher oil recovery factors. In TAG-A-AG flooding, different TAGRs were also utilised to optimise the injection ratio during alternating TAG injection. According to the results, the optimum TAGR is approximately 1:3 in non-fractured plugs and 1:2 in fractured plugs. These optimum TAGRs achieved considerably higher oil recovery factors than that of the unthickened AG flooding but marginally less than that of the continuous TAG flooding. However, during alternating injections less polymer/oligomer is required. Hence, the alternating

injection of TAG or TCO₂ with unthickened AG seems to create a balance between improving the sweep efficiency and the use of costly polymer or oligomer additives.

Overall, the core-flooding experiments verified the performance of alternating thickened gas (CO₂ or AG) injection at the laboratory-scale to be close to that of the continuous thickened AG but with considerable reduction of polymer amounts used. However, further work is required to investigate the feasibility of this injection scheme for field application. One approach to adequately address this uncertainty is to conduct a field-scale numerical simulation incorporating the laboratory results using appropriate upscaling techniques.

Chapter 7. Effects of Oligomers Dissolved in CO₂ or Associated Gas on IFT and Miscibility Pressure with a Gas-light Crude Oil System*

7.1 Introduction

Miscible gas injection (MGI) is widely considered as an effective enhanced oil recovery (EOR) process that can increase recovery by achieving miscibility between the injected gas (CO₂, associated gas (AG), etc.) and reservoir oil. The MGI process proceeds via a number of well-known mechanisms such as oil viscosity reduction, decrease in the interfacial tension (IFT) and oil swelling.[15, 16, 20, 337] These mechanisms play important roles of varying degrees depending primarily on in-situ reservoir conditions, type of the gas injected and composition of the in-situ oil.[338] During MGI, the injected gas starts to become miscible with the reservoir oil at and above the minimum miscibility pressure (MMP). In other words, at and above the MMP, the gas (typically existing in a supercritical state) acts as a solvent when comes in contact with the reservoir oil and can effectively reduce the remaining volume of oil to near zero under ideal conditions.[4] The injected gas can either gradually develop dynamic miscibility with the reservoir oil through multiple-contact miscibility or can become miscible with oil immediately when the two fluids are brought contact through first contact miscibility.[260] As the two fluids become completely miscible and form a single phase in the reservoir, the displacement efficiency improves, while maintaining the reservoir pressure, resulting in higher oil recovery. As an essential MGI mechanisms, with miscibility, the interfacial tension between the fluids is decreased to essentially zero giving rise to elimination or a significant reduction in the capillary pressure between the fluids and improvement in the displacement efficiency and oil recovery.[49]

Field A is located in the Harweel cluster in southern Oman and is recognised as a viable candidate for an MGI campaign.[31, 339] It is found that with the implementation of MGI, an estimated 47% of the original oil in place (OOIP) could be recovered.[32] As part of the gas injection development, produced AG is re-injected at high pressure (up to 55MPa) into this high temperature reservoir (up to 377 K). This

creates conditions where the gas becomes miscible with the oil.[31] The MMP for the live oil-AG system in Field A was measured by slim tube technique to be 38.3 MPa.[32] However, the implementation of an MGI process in Field A faces technical challenges including viscous fingering, early gas breakthrough and a high gas-to-oil ratio (GOR). These difficulties are caused by a number of factors including a high viscosity contrast between the injected AG (0.01- 0.03 cP) and the in-situ oil (0.24 cP) as well as reservoir heterogeneity which compromise macroscopic sweep efficiency.[32, 288] In fact, early breakthrough has already been observed in some of the production wells in Field A, resulting in a high production GOR. Furthermore, the in-situ environment in Field A is very harsh with a high salinity of 275,000 ppm and a high temperature of 377 K.[30] Based on our previous studies,[288, 332] a direct thickening agent could be a viable technique to reduce the viscosity contrast which would mitigate some of the technical challenges allowing the advantages of both the chemical and miscible gas EOR methods to come to fruition.

For over 40 years, direct gas thickening has been recognised as a potential game-changing technology with the potential to increase the oil recovery associated with an MGI program.[52] This technique is considered to be one of the most promising approaches where the chemical and thermal stability of many viable additives is ideal for harsh reservoir environments such as that of Field A.[52] Several polymer/oligomer additives into CO₂ and hydrocarbon mixtures have been tested and shown to increase the injected gas viscosity to levels close to that of the reservoir oil viscosity.[52, 64, 66, 69-72, 164, 231, 333] To date, a high molecular weight fluoroacrylate-styrene copolymer (polyFAST) (M_w 540,000) has been identified in other research work as the best CO₂ thickener in terms of viscosity enhancement.[170, 191] However, the cost and environmental issues with this polymer has prevented its use in the field.[167] Non-fluorinated polymers and oligomers (i.e. poly dimethylsiloxane (PDMS, M_w 197,000), poly vinyl ethyl ether (PVEE, M_w 3800-4,337) and poly (1-decene) (P-1-D, M_w 544-900)) have also been identified as CO₂ and hydrocarbon solvents thickeners.[52, 66, 71, 157, 162, 164, 178, 227] All of these polymers are known as being among the most CO₂ soluble polymers among the non-fluorous polymers with poly(vinyl acetate) (PVAc) being the second most soluble (which is not used due to its tendency to hydrolyse).[162] High molecular weight PDMS (M_w 197,000) with the addition of a 20 wt% toluene as a co-solvent was also

found to be an effective thickener for improved the oil recovery in CO₂-EOR.[63] Furthermore, at 298 K and 7 MPa, high Mw PDMS increases the viscosity of natural gas liquid (NGL) modestly.[231] Generally, with increase in temperature, a higher pressure is required for polymer dissolution in CO₂, NGL, and AG because increased temperature causes a significant difference in the free volume between the polymer and solvent at high temperature, leading to phase separation.[71, 172, 231, 288] Heller et al.[66] determined that both PVEE and P-1-D only slightly increase CO₂ viscosity at 298 K and 306 K and this is attributed primarily to its low solubility. In our previous studies,[288, 332] P-1-D exhibited adequate solubility in CO₂ and AG mixture to enhance viscosity significantly at temperatures above 358 K over the 50-55 MPa pressure range. Below this temperature, P-1-D oligomer was only partially soluble in both solvents. It was found that P-1-D can change the viscosity of CO₂ by 2-2.7 fold at concentrations of 1.5-5 wt% [332] and enhance AG mixture viscosity by 2-7.4 fold at concentrations of 1.5-9 wt%.[288] In addition, 1.2-2 wt% of PVEE improves CO₂ viscosity by 1.2-1.8 fold at 377 K.[332] Although, P-1-D has a low molecular weight, the viscosity increase can be explained as follows. The flexible alkyl branching groups on the C-C backbone available in the P-1-D may have effect on the viscosity increase because these side chain groups can shape themselves in numerous conformations forming a random coil in solution. In addition, the branch chains close to each other in this oligomer contribute to increasing the attractive intermolecular forces between the oligomers chains which could in principle increase the effective molecular weight.[235, 340, 341] In recent publications, Sun et al.[342] and Xue et al.[343] have also found in molecular dynamic simulation studies that low molecular weight poly(vinyl acetate-co-vinyl ether) (PVAEE, Mw ~ 4300) can increase the viscosity of CO₂ by 2-4 fold at concentration of 1.19 wt% and 2.35 wt% at 308 K[343] and copolymer of Heptadecafluorodecyl acrylate (HFDA) and CO₂-phobic monomer vinyl n-Octanoate (VOc), vinyl acetate (VAc), vinyl pivalate (VPi) (Mw ~3000-3500) increase the viscosity of CO₂ by 62 times at 5 wt%.[342] This is attributed to stronger intermolecular aggregation, binding effect and decreasing diffusion coefficient which means the polymer chains have the ability to reduce the movement of CO₂ molecules, which demonstrate thickening ability of a low molecular weight polymer.[342, 343] Numerical simulations show that a viscosity increase of 1.5-5 fold of the injected gas (AG or CO₂) in Field A is adequate to improve gas mobility and sweep efficiency to an acceptable level.[34]

The main parameters required to design a polymer/oligomer-thickened gas flooding process is the cloud point pressure and MMP between the crude oil and polymer/oligomer-thickened gas. To the best of our knowledge, there has been no study conducted to date to evaluate the effects of a dissolved thickener on the equilibrium IFT and miscibility pressures (MMP and P_{\max}) for an oligomer-thickened AG-crude oil system where P_{\max} is referred to as the first contact miscibility pressure (FCM). Gu et al.[178, 344] found at 329 K that the equilibrium IFT of either PVEE or P-1-D thickened CO_2 with crude oil are much lower than that of the pure CO_2 /crude oil system. These results indicate, for the case investigated by these researchers, that the thickening of CO_2 lowers the miscibility pressures. However, at high temperature (e.g. 377 K in Field A) the effects of these oligomers on IFT might be different, especially because P-1-D is more soluble in CO_2 and AG at high temperature. Therefore, in this study, we investigate the effect of dissolved P-1-D in CO_2 and AG mixture and dissolved PVEE in CO_2 on the equilibrium IFTs and miscibility pressures (MMP and P_{\max}) at the temperature of 377 K using the vanishing interfacial tension (VIT) technique. The MMP and P_{\max} are obtained through the reduction of the equilibrium IFT achieved by increasing the pressure and then extrapolating to an equilibrium IFT of zero.[345] In this work, we compare the solubility of P-1-D in Field A's AG mixture and CO_2 as well as the solubility of PVEE in CO_2 at 377 K and 50-55 MPa (i.e. Field A's in-situ conditions) to provide guidance on the design of the thickened gas flooding.[288, 332] The equilibrium IFTs for the light oil/unthickened gas (AG and CO_2) systems and light oil/oligomer thickened gas (i.e. oligomer-thickened AG and oligomer-thickened CO_2) systems are measured at equilibrium conditions using the axisymmetric drop shape analysis (ADSA) technique for the pendant drop.[346] Finally, the effect of the dissolved oligomers in the thickened gas/light oil system on miscibility pressures (MMP and P_{\max}) was determined under partial oligomer dissolution in the gas phase at reservoir conditions.

7.2 Experimental Methodology

7.2.1 Materials

In this study, low molecular weight oligomers (P-1-D, 544 g.mol^{-1} and PVEE, $4,337 \text{ g.mol}^{-1}$) were purchased from Sigma-Aldrich Corporation. The molecular weight of both oligomers was measured using gel permeation chromatography (GPC). Carbon

dioxide (99.999 mol%) and AG mixture (CH₄ 60 mol%, C₂H₆ 9 mol%, C₃H₈ 6 mol% and CO₂ 25 mol %) purchased from BOC Gas, Australia. The CMG WinProp Module (version 2016) and the National Institute of Standards and Technology's (NIST)[294] online correlations were used to estimate the density of the AG mixture and CO₂, respectively. The light oil sample used here was collected at the wellhead from Field A, southern Oman. The light gas components under C₅ were flushed out at ambient pressure and temperature to achieve a dead oil. The density and viscosity of the light oil were measured in a high pressure densitometer and capillary viscometer to be 0.81 g.cm³ and 2.7 cP (377K and 55 MPa), respectively. The composition of the light oil is given in Table 7.1 as determined by gas chromatography with a flame ionization detector (GC-FID). The density of the light oil used for IFTs measurements is plotted in Figure 7.1.

Table 7.1 Compositional analysis results of Field A dead oil in mole percentage

Component	Mole %	Component-cnt	Mole %
H ₂	0	C ₁₆	4.15
H ₂ S	0	C ₁₇	3.85
CO ₂	0	C ₁₈	3.77
N ₂	0	C ₁₉	3.97
C ₁	0	C ₂₀	3.27
C ₂	0	C ₂₁	2.99
C ₃	0	C ₂₂	2.87
iC ₄	0	C ₂₃	2.67
nC ₄	0	C ₂₄	2.47
C ₅	0	C ₂₅	2.19
iC ₅	0.01	C ₂₆	2.1
nC ₅	0.02	C ₂₇	1.99
C ₆	0.33	C ₂₈	1.85
C ₇	1.54	C ₂₉	1.85
C ₈	3.71	C ₃₀	1.77
C ₉	4.84	C ₃₁	1.64
C ₁₀	5.54	C ₃₂	1.43
C ₁₁	5.15	C ₃₃	1.35
C ₁₂	4.72	C ₃₄	1.26
C ₁₃	5.08	C ₃₅	1.2
C ₁₄	4.63	C ₃₆₊	10.93
C ₁₅	4.86	Total	100

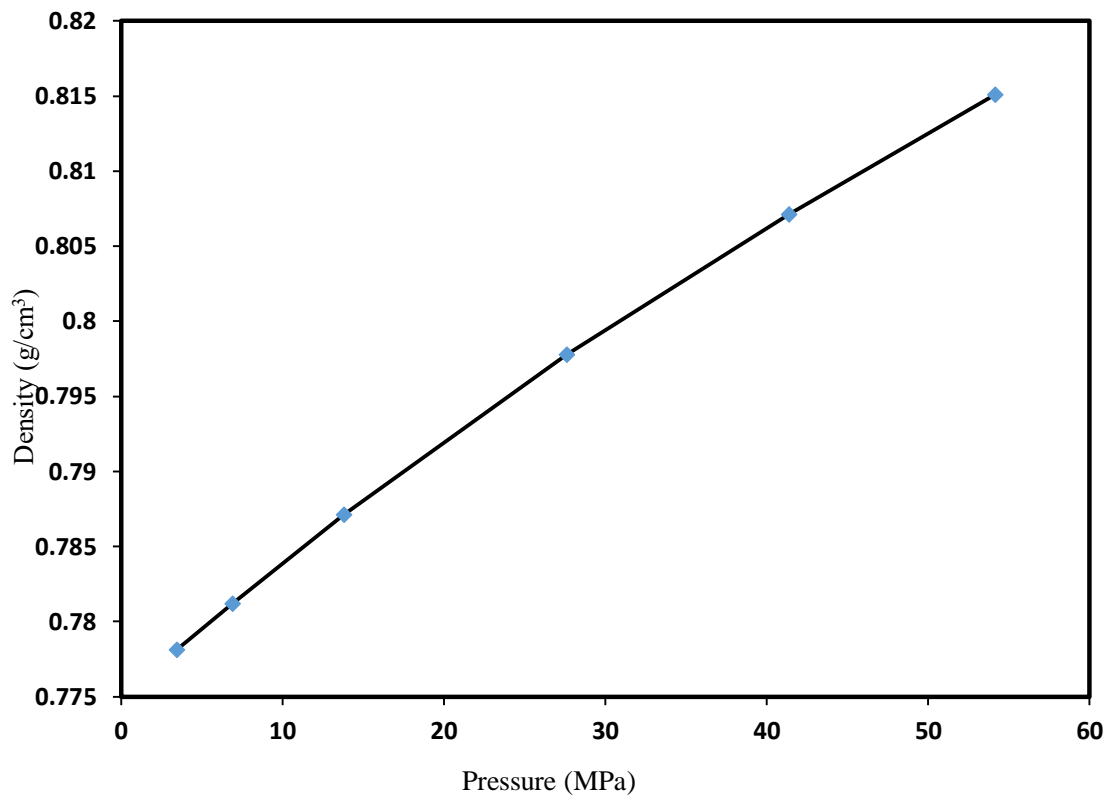


Figure 7.1 Light oil measured density at 377K and different pressures.

7.2.2 Experimental Setup and Procedure

7.2.2.1 Equilibrium IFTs and Miscibility Pressures Measurements

The minimum miscibility pressure (MMP) and first contact pressure (P_{\max}) were determined using the VIT technique involving the measurements of equilibrium IFTs between the crude oil and gas samples (CO_2 or AG mixture) with increase in pressure.[347] The IFT 700 (Vinci-Technologies, France) was used to measure the equilibrium IFT of the light oil-(unthickened or thickened) gas systems at 377 K. The schematic diagram of the experimental apparatus for measuring the equilibrium IFT is given in Figure 7.2. This instrument is designed to conduct IFT measurements by applying the axisymmetric drop shape analysis (ADSA) technique[346] for the pendant drop formed inside a high-pressure view cell of 20 cm^3 inner volume at elevated pressures and temperatures.

Prior to each IFT measurement, the windowed cell (Figure 7.2) was cleaned at a temperature of approximately 323 K with acetone and toluene sequentially. This protocol and the combination of solvents removes any tracers of oil and oligomer. After cleaning, the cell was placed under vacuum for a few hours to dry. Then, it was preheated to reservoir temperature (377 K) using an internal heater within the setup. After reaching a stable temperature value, the gas samples were introduced slowly into the IFT cell. The cell pressure was increased slowly using a syringe pump until reaching the desired value. At this stage, the required experimental parameters (such as fluid density and needle diameter) were entered into the software to be used later in calculating the IFT. An initial pressure of 4.28 MPa was used to determine the equilibrium IFT for both the light oil/gas system and light oil/oligomer thickened gas system. After achieving pressure and temperature stability, light oil was injected through a needle from the crude oil storage cylinder to form a pendent drop. Once a pendent drop was well-shaped inside the cell, the dynamic equilibrium IFT measurement was started by the ADSA software. Sequential digital images of the dynamic pendent oil drop were acquired and stored automatically. The IFTs were determined after a sufficient time (approximately 30 minutes) to reach an equilibrium state, where the IFT did not change with the time. The IFT measurements were repeated with two to three different pendent oil drops to assess experimental repeatability at every pressure. The average value of the three IFTs measurements is reported in this study. We found our measurements to be reproducible within ± 0.3 - 0.5 mN.m⁻¹.

For the light oil/oligomer-thickened gas (CO₂ or AG mixture) systems, equilibrium IFT measurements at lower pressures were determined under partial oligomer dissolution conditions due to the high cloud point pressure for both gas samples. The above described experimental procedures were repeated at each pressure (with the additional steps required to add the oligomer into the gas solution). For instances where oligomer-thickened gas was used, a known weight of the oligomer was placed in a metal plate inside the cell after cleaning. Then, it was placed under vacuum for a few hours to dry. The cell was then preheated to 377 K and pressurised to the desired pressure using a syringe pump. Below the cloud point pressure, the oligomer was only partially soluble in the gas phase. A sufficient time (3-4 hours) was given before introducing a pendent oil drop at each pre-specified pressure to ensure the system

reached an equilibrium state. It should be noted that with the low concentrations used in this study, the effect of oligomer dissolution in the gas on its density was assumed to be negligible.

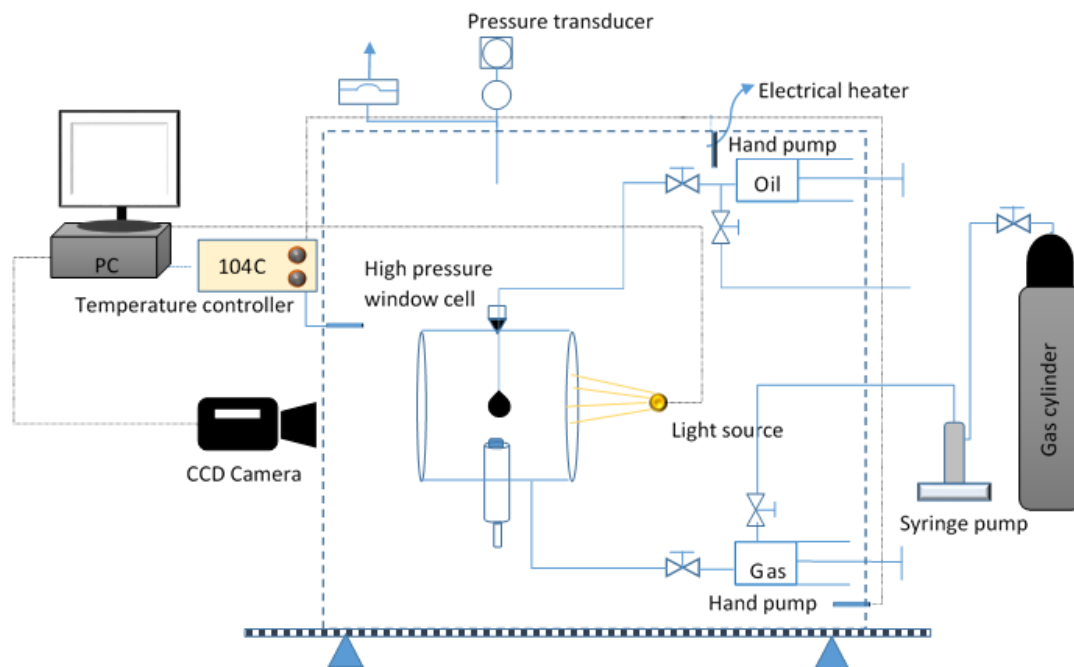


Figure 7.2 Schematic diagram of the experimental setup used for IFT measurements.

7.3 Results and Discussions

7.3.1 P-1-D Behaviour in CO₂ and AG mixture

The solubility testing for 26 polymers/oligomers in CO₂ and 32 polymers/oligomers in AG mixture at high temperature and high pressure have been discussed in our previous studies.[288, 332] In those studies, P-1-D was found to be highly soluble in both CO₂ and AG mixture at temperatures of 358 to 377 K as two supercritical solvents. As can be seen in Figures 7.3 and 7.4, the solubility of P-1-D in pure CO₂ follows an UCST (upper critical solution temperature) type behaviour while it lies close to the LCST (lower critical solution temperature) trend for AG mixture (which contains 25 mol% CO₂). It is worth noting typical UCST and LCST curves exhibit much, much steeper slopes on a P-T diagram which is not apparent here but the observations support these assumptions. This difference in behaviour indicates that at high temperature the mechanism responsible for the solubility of P-1-D in the AG mixture is different than that for pure CO₂. At high temperature, the interchange energy

in the CO₂-oilgomer system is dominated by CO₂-oilgomer segment dispersion interactions. For the AG mixture-oligomer system, the induction cross interactions for the mixture containing alkanes do not have solvent-solvent quadrupole self-interactions (as they do not contain double bonds) and the solvent-solvent quadrupole interactions derived from CO₂ are diminished.[326] In general, the oligomer would dissolve if the oligomer-solvent interaction outweighs the solvent-solvent and oligomer-oligomer interactions. The characteristics of P-1-D-CO₂ phase behaviour are attributed to enthalpic interactions between the P-1-D and CO₂ since the cloud point pressure curve exhibits similar USCT characteristics as can be seen in Figure 7.3. As the system temperature increases, the P-1-D-CO₂ cloud point pressure decreases and the quadrupole CO₂-CO₂ interactions diminish. CO₂ density is not a major driver for this system of behaviour since CO₂ and P-1-D have similar densities at high pressure and temperature. Therefore the enthalpic interactions are dominant in this system. For the AG mixture, it is likely that the free volume between the P-1-D and AG mixture solvents are the main driving factor for solubility of the oligomer in the AG mixture. With increasing temperature, the density of the AG mixture decreases causing an increase in the free volume between the P-1-D segments and the AG mixture solvent molecules which is consistent with the cloud point pressure curve for P-1-D-AG mixture system exhibiting LSCT characteristics as can be seen in Figure 7.4. However, the cloud point pressure curves are not as steep as often observed with LCST curves due to the low molecular weight of P-1-D. In addition, at high pressure the solvent is highly compressed and the change of molar volume is smaller with increasing temperature. As a result, the changes of cloud point pressure at high temperature are subtle, leading to the cloud point pressure curve being less steep with increasing temperature. In comparison to the literature, the phase behaviour of polyolefin exhibits an LCST trend in hydrocarbon solvents[348] and UCST trend in CO₂[349] due to the presence of quadrupole interaction for the CO₂ molecule (which contain double bonds).

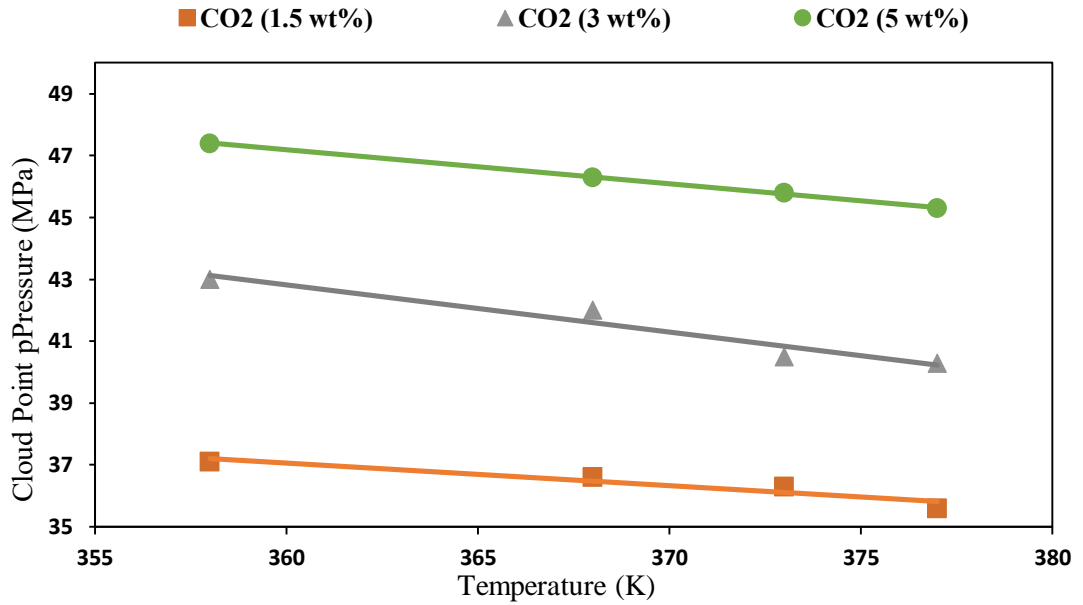


Figure 7.3 Measured cloud point pressures for P-1-D at different concentrations and temperatures in CO₂. [332]

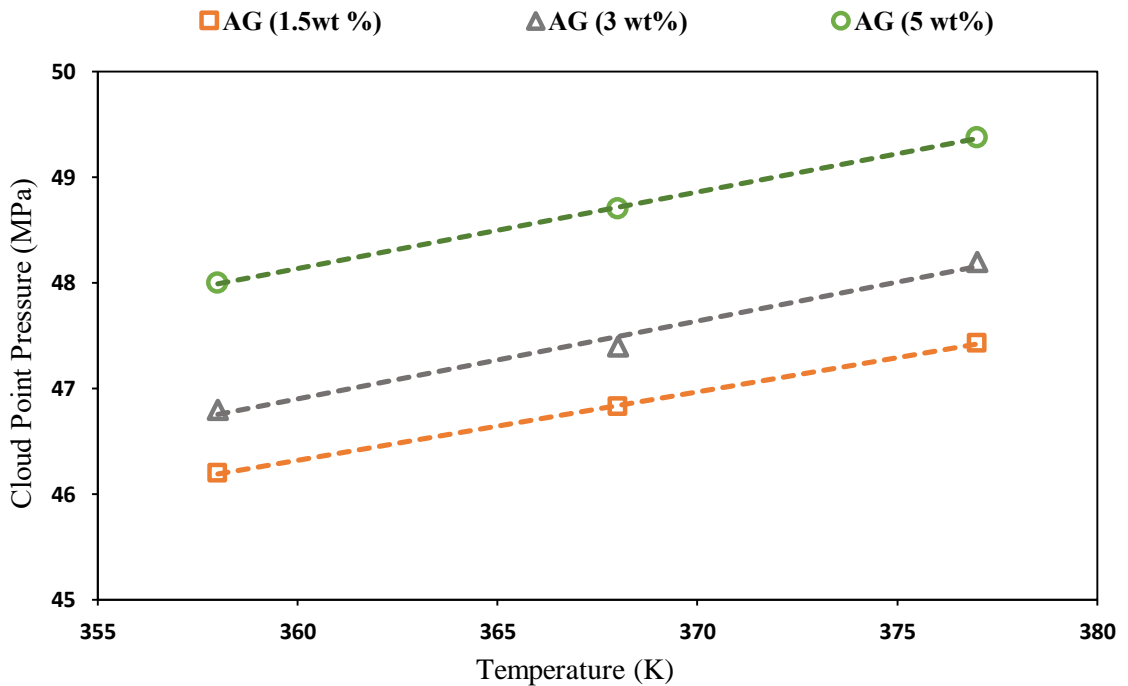


Figure 7.4 Measured cloud point pressures for P-1-D at different concentrations and temperatures in AG mixture. [288]

Figure 7.5 shows the cloud point pressure trends of 1.5 wt% P-1-D in pure CO₂ and AG mixtures with differing mol % of CO₂ contents (10 mol%, 25 mol%, 50 mol% and 100 mol%). As the CO₂ content in the AG mixture increases, there is a monotonic

decrease (continuing to the case of pure CO₂) in the pressure required to obtain a single phase. In AG mixture, the density drives the solvation power of the supercritical fluid. When the temperature increases, the density of the AG mixture decreases, resulting in a higher molar volume and a larger free volume. This results in reduced entropic interactions between the oligomer and AG mixture and a low degree of solvation. As the amount of CO₂ increases, CO₂-CO₂ quadrupole interactions become more important and are overcome through enthalpic interactions. Under these conditions, a temperature increase results in improved solvation of the oligomer. By varying the concentration of CO₂ in the AG mixture, the balance of these opposing effects is varied. In summary, the solubility of P-1-D in CO₂ is a function of enthalpy and in AG mixture is a function of entropy (molar volume) at high temperature and pressure. Hence, solubility of P-1-D in both solvents is governed primarily by oligomer-solvent interactions.

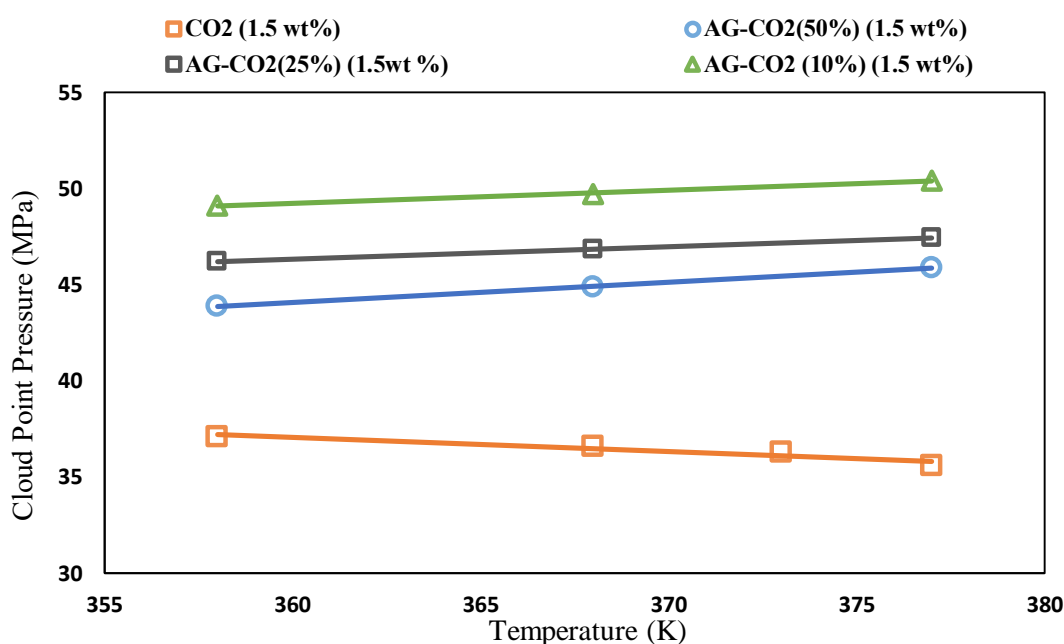


Figure 7.5 Measured cloud point pressures for P-1-D at 1.5wt% concentration in the AG mixture containing different percentages of CO₂ at different temperatures.[288, 332]

7.3.2 PVEE Behaviour in CO₂

According to the screening method used in our previous studies,[288, 332] PVEE has a high solubility in CO₂ but exhibits partial dissolution in AG mixture at 377 K and 55 MPa. These results are consistent with results obtained through in our

conventional cloud point pressure measurements over a range of temperatures and polymer concentrations. Cloud point pressure experiments confirmed PVEE to be fully soluble in CO₂ at the pressure range of 48.3 -54.4 MPa and temperature of 377 K and only partially soluble in AG mixture at the pressure of 55 MPa and temperature of 377 K.[288, 332] For the dissolution of PVEE (which contains alkene functional groups) in CO₂, the intermolecular quadrupolar interactions between CO₂ and PVEE are important. According to Kilic et al.[165], the presence of ether oxygens in the chain of the polymer is responsible for the lower miscibility pressure as a result of potential interactions between CO₂ and the ether groups (i.e. a Lewis acid/base interaction). However, the accessible position of ether group in the side chain of PVEE, make the CO₂ less accessible to ether oxygen.[196] The primary reason for the limited solubility of PVEE in the AG mixture can be attributed to the diminished levels of CO₂ and more limited intermolecular interactions between the alkanes in the AG mixture and PVEE. Furthermore, the solubility of PVEE is relatively sensitive to the temperature and concentration as they change. This is due to the fact the entropic interactions between PVEE and CO₂ in the solution are the main drive for miscibility of PVEE in CO₂ and these interactions decrease significantly with increase in temperature. To overcome this limitation, a high pressure is required to dissolve PVEE in CO₂. In comparison to P-1-D solubility in CO₂, PVEE has relatively higher cloud point pressure under the in situ conditions encountered for Field A at the same concentration. Therefore, the higher cloud point pressure for PVEE in CO₂ makes it difficult to increase its concentration above 2 wt%. The lower cloud point pressure of P-1-D allows its use at concentrations up to and beyond 5 wt%. Both PVEE and P-1-D were considered adequately soluble in CO₂ at a dilute concentration at Field A's reservoir conditions while only P-1-D is adequately soluble in the Field's AG mixture.

7.3.3 Equilibrium IFT and MMP Measurements

7.3.3.1 Gas Compositions Effects

For both of the light oil/CO₂ and light oil/AG mixture systems, IFT was measured at a constant temperature of 377 K with increasing pressure starting at 4.8 MPa until miscibility was achieved. This serves as a baseline for comparison when the oligomer would be introduced into the system at a later stage. The measured equilibrium IFT data for both systems (Figure 7.6) indicate that there are two distinct pressure ranges

where the equilibrium IFTs are reduced linearly with pressure. Based on the VIT technique, the measured equilibrium IFT is extrapolated to zero using linear regression in the first and second ranges to determine MMP and P_{max} , respectively.[347] For CO₂, it is common that a higher pressure is required to achieve MCM and FCM as the temperature increases.[18] Over the whole pressure range studied, the measured equilibrium IFTs for the light oil/AG mixture system were higher than those for the light oil/CO₂ system. Consequently, MMP and P_{max} were significantly higher with the light oil/AG mixture system. The higher miscibility pressures for the AG mixture are caused by the fact that for this gas the lightest hydrocarbon gases (particularly CH₄) dissolve into the crude oil from the gas phase but the extraction of light to intermediate hydrocarbon components from the crude oil into the gas is much lower compared to that into pure CO₂. The reduction in the equilibrium IFT with increasing pressure is mainly caused by two physical and one chemical processes that occur simultaneously when the gas comes in contact with crude oil.[17, 337] The two physical processes are gas dissolution into crude oil and light hydrocarbon components extraction from the crude oil into the gas.[17, 350] It is well known that CO₂ is very soluble into light oil and has a strong ability to extract light to intermediate components from the crude oil.[17] These two processes significantly contribute to the light oil/CO₂ system having a lower IFT and miscibility pressure. Yang et al.[351] found that the reduction in IFT between the gas phase and the crude oil is affected by the intermolecular forces (i.e. attractive forces) and distances operating within the gas/crude oil system. At constant temperature, as pressure increases, the intermolecular distance between the gas phase (CO₂ or light HC) molecules or crude oil molecules decreases resulting in an increase in the intermolecular force operating within the gas and crude oil molecules.[351] Meanwhile, the intermolecular forces between crude oil molecules is much larger than those between the gas molecules.[352] However, the intermolecular forces between the gas molecules increase much faster with pressure than those between the crude oil molecules as the gas phase is considerably more compressible. Therefore, at a higher pressure, the strength of the intermolecular forces associated with the gas molecules approach that of the forces between the crude oil molecules resulting in a reduced IFT between the two phases. In summary, a smaller difference in the intermolecular forces acting within the two phases results in lower interfacial tensions and eventually with increasing pressure the interfacial tension reaches zero and miscibility between two phases is observed.[351]

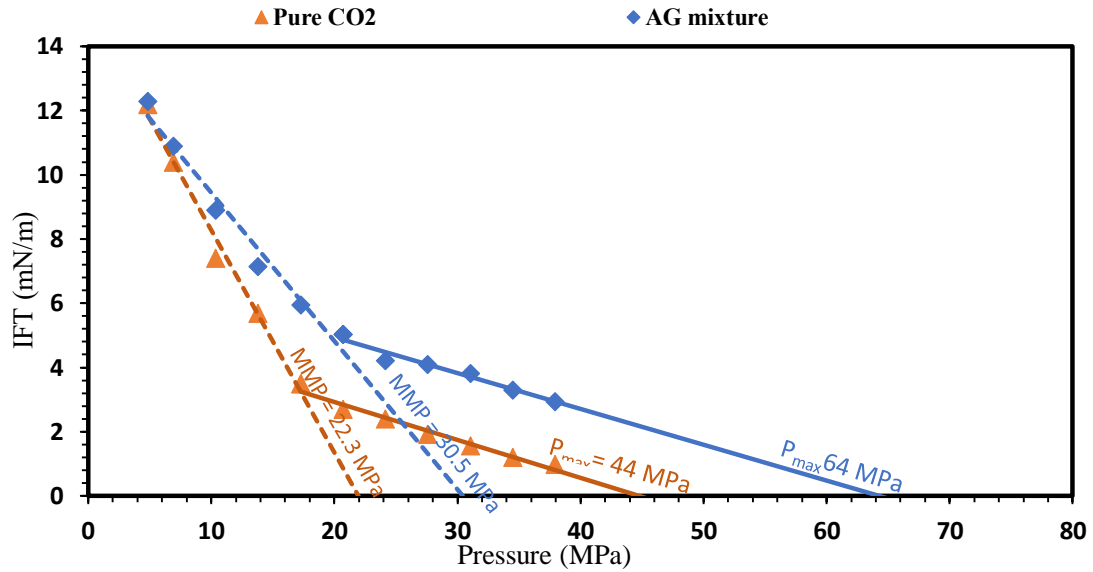


Figure 7.6 Measured IFTs and miscibility pressures (MMP and P_{max}) for light oil/AG mixture system and light oil/ CO_2 system at different equilibrium pressures at constant temperature (377 K).

With regards to the interactions of the AG mixture (containing both CO_2 and light hydrocarbons) with the light oil, the main intermolecular forces operating within the AG mixture are dispersion forces (while the CO_2 also exhibits quadrupole-quadrupole interactions with itself). While the intermolecular forces operating within the crude oil is a combination of dispersion and dipole-dipole forces.[351] In comparison with crude oil, the intermolecular force operating within gas molecules is much weaker than that operating within crude oil molecules.[351] Comparatively, for the AG mixture, a higher pressure is required to achieve comparable intermolecular forces relative to those within the crude oil components. The intermolecular attraction forces between the molecules of a gas are directly related to its critical temperature.[353] CO_2 has a higher critical temperature (304 K) than methane (190 K) and slightly lower than ethane (305 K).[354] In addition, the distance between the CO_2 molecules is shorter compared with methane and ethane.[354] The shorter intermolecular distance and higher critical temperature results in an increase in the intermolecular force. As the AG mixture mainly contains methane (60 mol%), the intermolecular interaction difference between the AG mixture and the light oil is higher compared to the difference between CO_2 and light oil. Therefore, the larger difference in intermolecular force strength within the individual phases (i.e. AG mixture and light oil) leads to an increase in the IFT. Consequently, the miscibility pressures of light crude oil and AG

mixture system is larger than the CO₂ and light crude oil system as can be seen in Figure 7.6. In fact, the MMP and P_{max} increase linearly with CH₄ content in the AG gas mixture.[17] Therefore, the increase in the MMP and P_{max} for AG mixture containing a 60 mol% CH₄ content is consistent with prior studies whose results are reported in the literature. However, as the pressure conditions are high in Field A, the AG mixture can still be miscible with the light crude oil. Meanwhile, the CO₂ content in the produced gas may to some extent have a considerable effect on the miscibility development due to its ability to extract intermediate hydrocarbons.

7.3.3.2 Oligomer-Thickened Gas Effects

7.3.3.2.1 Light Crude Oil and Oligomer-Thickened CO₂ System

Unfortunately, the cloud point pressures of both P-1-D and PVEE in both solvents (i.e. CO₂ and AG mixture) are high making it difficult to measure the equilibrium IFTs; all the measurements completed here start from low pressure and increase to the miscibility pressure. However, the cloud point pressure of both of these oligomers is marginally located above the MCM pressure and just below the FCM pressure. Therefore, the measured equilibrium IFTs were performed below the cloud point pressures where both oligomers are partially soluble in CO₂ and AG mixture. The equilibrium IFTs for the light oil/P-1-D thickened CO₂ and light oil/PVEE thickened CO₂ systems were measured at 377 K and pressure ranges from 4.8 MPa up to the miscible conditions. Therefore, the oligomer concentrations in the solution are qualitative, and the effects on IFTs and miscibility pressures were measured with this assumption. As shown in Figures 7.7 and 7.8, the measured equilibrium IFTs between the light oil and each oligomer-thickened CO₂ system is slightly lower than that for the light oil/pure CO₂ system. A slight decrease of IFT values in the first linear is attributed to the small amount of oligomer dissolution into the CO₂ phase. This results in only a slight reduction of MMP with the oligomer-thickened CO₂ system. Using the VIT technique, the MMPs for light oil/pure CO₂, light oil/P-1-D-thickened CO₂ and light oil/PVEE-thickened CO₂ systems are determined to be 22.1, 21.5 MPa and 21.6 MPa, respectively.

Moreover, with increasing pressure (i.e. in the second linear regime), more oligomer dissolves into the CO₂ phase and the effect of each oligomer on the equilibrium IFT is

more obvious as it can be seen in Figures 7.7 and 7.8. The measured equilibrium IFT values for both light oil/oligomer-thickened CO₂ systems are much lower than the equilibrium IFT values with the light oil/pure CO₂ system. Accordingly, the first contact miscibility pressure (P_{max}) of both light oil/oligomers-thickened CO₂ systems (39 MPa for P-1-D-thickened and 38.7 MPa for PVVEE-thickened) are lower than that for the pure CO₂/light oil system (at 44 MPa). These differences are substantially larger than the differences in the MMP values of these systems. Nevertheless, we can conclude in general that more dissolution of oligomers (P-1-D and PVVEE) into the CO₂ result in a lower IFT and consequently a lower MMP and P_{max} .

The mechanism for the above observed reduction is attributed to the intermolecular forces between the oligomer molecules and CO₂ molecules due to intermolecular distance between their molecules is reduced and in particular the effect of the ether group (PVVEE) on further enhancing the intermolecular interactions between CO₂ and PVVEE. Therefore, the differences between the intermolecular forces within the oligomer-thickened CO₂ and crude oil phases diminish with increasing pressure and the thickened CO₂ becomes more soluble in light crude oil. Consequently, the IFTs between light crude oil and oligomer-thickened CO₂ are lower. Hence, a slightly lower operating/injection pressure is required to achieve MMP and P_{max} with oligomers-thickened CO₂ flooding. The cloud point pressure at 377 K for P-1-D (1.5-5 wt%)-thickened CO₂ is below the FCM pressure (P_{max}); whereas, the cloud point pressure for PVVEE (1.2-2 wt%) is higher than P_{max} . Gu et al.[344] found for both oligomers at the lower temperature of 329 K that a low concentration (0.15 wt%) of dissolved oligomer in CO₂ leads to a lower equilibrium IFT and miscibility pressure. Therefore, we can conclude that at both low[344] (at 329 K) and high temperatures (this study at 377 K) the dissolution of PVVEE and P-1-D in CO₂ can lower the miscibility pressure. These effects could positively contribute to achieving miscibility development at lower pressure and enhance recovery efficiency from depleted oil reservoirs.

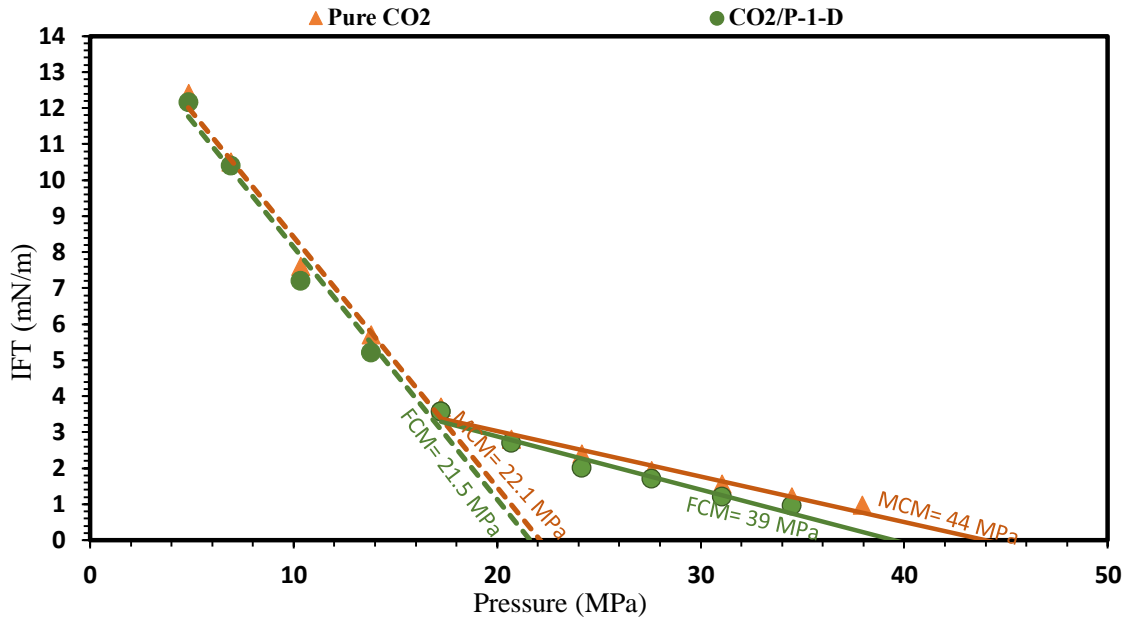


Figure 7.7 Measured IFTs for the light oil/P-1-D-thickened CO₂ system and light oil/CO₂ system at different equilibrium pressures and constant temperature (377 K).

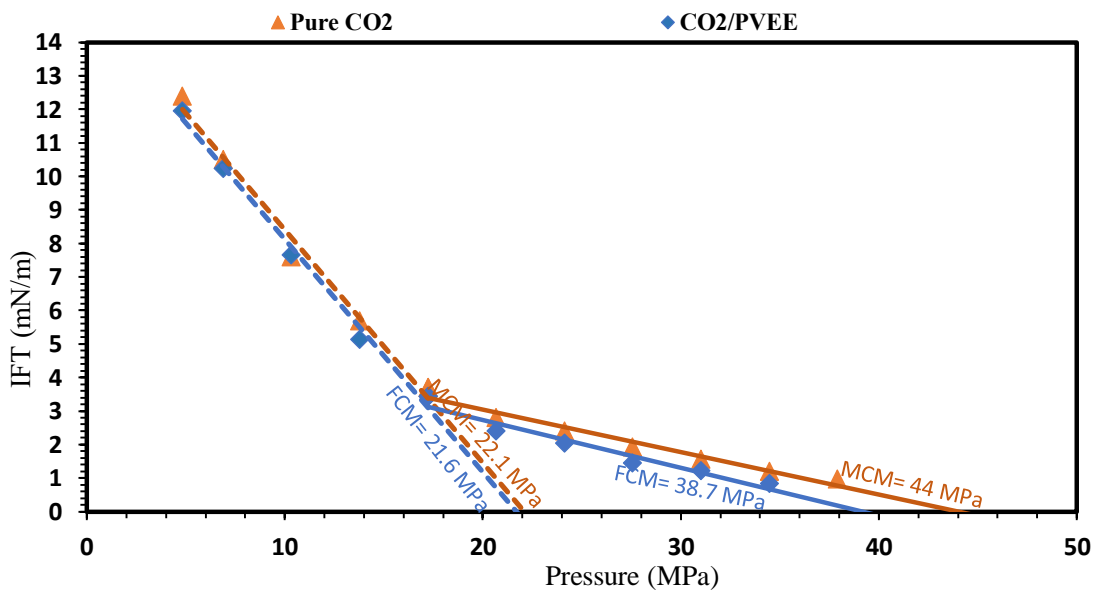


Figure 7.8 Measured IFTs for the light oil/PVEE-CO₂ system and light oil-CO₂ system at different equilibrium pressures and constant temperature (377 K).

7.3.3.2.2 Light Crude Oil and P-1-D-Thickened AG Mixture System

Equilibrium IFTs for the light crude oil/P-1-D-thickened AG mixture system were also measured at 377 K under partial dissolution conditions to determine the effects on IFT and miscibility pressures (MMP and P_{max}) of this system. As can be seen from

Figure 7.9, these measurements resulted in 34 MPa and 68 MPa as the MMP and P_{\max} for the above system, respectively, which are considerably higher (by approximately 3.5-4 MPa) than those for the light oil/AG mixture system (30.5 MPa and 64 MPa, respectively). Similar to the results observed for the pure CO₂ system, it can be seen in Figure 7.9 that the measured equilibrium IFTs with light oil/P-1-D-thickened AG mixture system exhibit two distinct linear regimes. However, unlike the CO₂ system where oligomer dissolution causes a decrease in the IFT and miscibility pressure, the IFT and miscibility pressures are increased with the AG mixture.

In the first regime, the AG mixture solubility in light crude oil and P-1-D presumably causes a reduction in the equilibrium IFT as pressure increases. Even though only a small amount of P-1-D dissolves into the AG mixture at low pressure, the intermediate components (ethane and propane) and CO₂ would dissolve in P-1-D making the AG mixture more lean causing a noticeable increase in the equilibrium IFTs and miscibility pressure values. While in the second linear regime, the dissolution of P-1-D in AG mixture increases substantially as the pressure approaches the cloud point pressure. This has slight effects on the measured equilibrium IFT. For this regime, the equilibrium IFTs with oligomer-thickened AG are still higher than those for AG mixture without oligomer, but the IFT increase is less than that in the first regime due to the further oligomer dissolution. Obviously, the rate of the equilibrium IFT reduction with light oil/P-1-D-thickened AG mixture system is much slower compared to the equilibrium IFT reduction with light oil/AG mixture system, especially at high pressure (above 28 MPa), where the solubility of the P-1-D in the AG mixture increases with pressure. Overall, the AG mixture composition change (where components of the AG dissolve into P-1-D as a plasticizer) increase the equilibrium IFT values with the P-1-D- AG and light crude oil system.

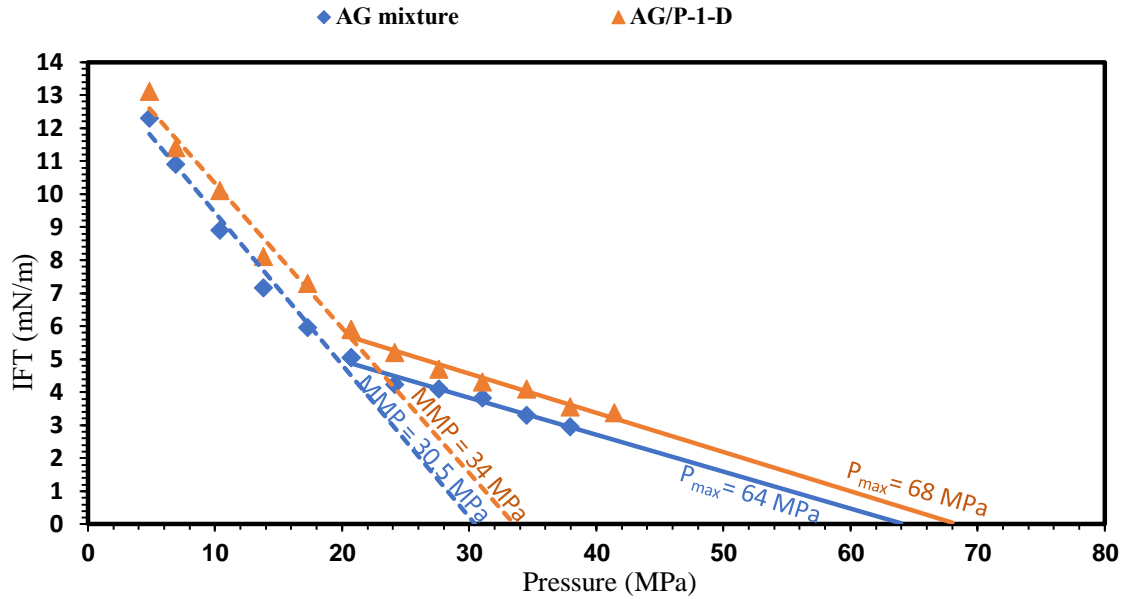


Figure 7.9 Measured IFTs for light crude oil/P-1-D-AG system and light crude oil-AG mixture system at different equilibrium pressures, different P-1-D concentrations (and constant temperature (377 K)).

In general, equilibrium IFT is determined through the dynamic interactions between the two fluid phases through mass transfer of components (due to mutual solubility of components in both phases) and changes in the thermodynamic equilibrium state (i.e. enthalpic and entropic interactions).[355, 356] The molecules in each phase are attracted to each other through dispersion and dipole (for polar molecules), quadrupole (for CO₂) intermolecular forces.[351, 355, 356] When it comes to the P-1-D-thickened AG impact on the IFT at high pressure, the dominant factors are the entropy change and AG solubility. At high pressure and high temperature, dispersion forces between AG and P-1-D are nearly identical as suggested by the observation that the cloud point pressure does not change significantly with P-1-D concentration in the AG mixture. Therefore, the dispersion force does not play a major role in increasing the IFT with light oil/P-1-D-thickened AG system.

Based on the discussion presented in Appendix A, the difference in the solubility parameters for light crude oil, AG, CO₂ and P-1-D can be used as a criterion for the solubility and hence the interfacial tension between oil and other mixtures. Figure 7.10 shows the solubility parameters for light oil, P-1-D, CO₂, AG (ranging from lean to rich), methane, ethane and propane and methane at 377 K. The solubility parameters for CO₂ are calculated as a function of temperature and pressure.[357] For methane,

the pressure and temperature dependency of the solubility parameters are calculated too.[358] The solubility parameters for P-1-D in the range 16.1 to 16.9 MPa are obtained from the literature.[359] For the AG mixtures and crude oil the solubility parameter are calculated based on the Peng-Robinson equation of state.[360] Lean AG is formed by reducing the C_2H_6 and C_3H_8 composition in the AG mixture while rich AG is formed by a relative increase in C_2H_6 and C_3H_8 composition.

At 377 K, the difference in the solubility parameters for CO_2 and crude oil over the whole pressure range is less than the difference between those for the AG and crude oil. This implies that CO_2 and crude oil tend to have a lower IFT at these pressures and temperatures compared to the AG and oil (Figure 7.6). Dissolving P-1-D in CO_2 at pressures above the cloud point pressure of the mixture (36 MPa at 377K) results in an increase in the solubility parameter and therefore the solubility parameter difference between oil and the CO_2 /P-1-D system would decrease. This results in a decrease in the IFT between oil and CO_2 when P-1-D is dissolved in it as confirmed experimentally (see Figure 7.7).

To explain the increase in IFT when P-1-D is added to the AG/crude oil system, we can consider the selective partitioning of certain components in the AG mixture into the liquid P-1-D phase. The measured cloud point pressure of P-1-D in the AG is approximately 47 MPa at 377 K. Dissolving the oligomer in the AG at pressures lower than the cloud point pressure results in a two phase system where one phase is rich in AG and the other rich in the oligomer. The increase in IFT can be explained with the intermediate components transferring into the oligomer phase from the AG phase during the dissolution process; in other words, the oligomer would extract C_2H_6 and C_3H_8 components from the AG mixture. This results in a leaner AG mixture that has a lower solubility parameter compared with the original AG. Solubility parameter reduction due to the dissolution of the oligomer would lead to increase in the difference between the solubility parameters of the oil and AG (lean AG) resulting in an increase in the IFT between the two phases. Experimentally, we have observed the evolution of the dissolved gas from P-1-D in the high pressure view cell at three pressures (3.44 MPa, 6.89 MPa and 20.68 MPa) using the rapid expansion technique.[361-365] Our experimental observations confirm that plasticization phenomenon of the dissolved gas would occur in the P-1-D/AG system below the cloud point pressure. Photos from the actual visual cell showing the evolution of the dissolved AG mixture and resulting

expansion in the P-1-D are included in Figure 7.11. The released dissolved gas from P-1-D creates large individual bubbles at 3.44 MPa but exhibits a foaming effect at 6.89 and 20.68 MPa. Such a change in the behaviour is because the solubility of the gas in the oligomer is a function of pressure and temperature (i.e. higher solubility at higher pressures). Although these experiments do not necessarily confirm which gas components (i.e. light or intermediate) have dissolved in the oligomer, the intermediate hydrocarbon gas components and CO₂ are more soluble in the oligomer than methane. [269, 366-368] Shah et al.[368] found that propane and CO₂ were more soluble in all silicone polymers compared with methane at any given temperature and pressure. Hence, the dissolved gas in P-1-D, as detected in our experiments, most probably is ethane, propane and CO₂. Therefore, we conclude that for P-1-D/AG system, below cloud point pressure, the plasticization effects results in AG mixture becoming lean noticeably affecting the IFT values of the system.

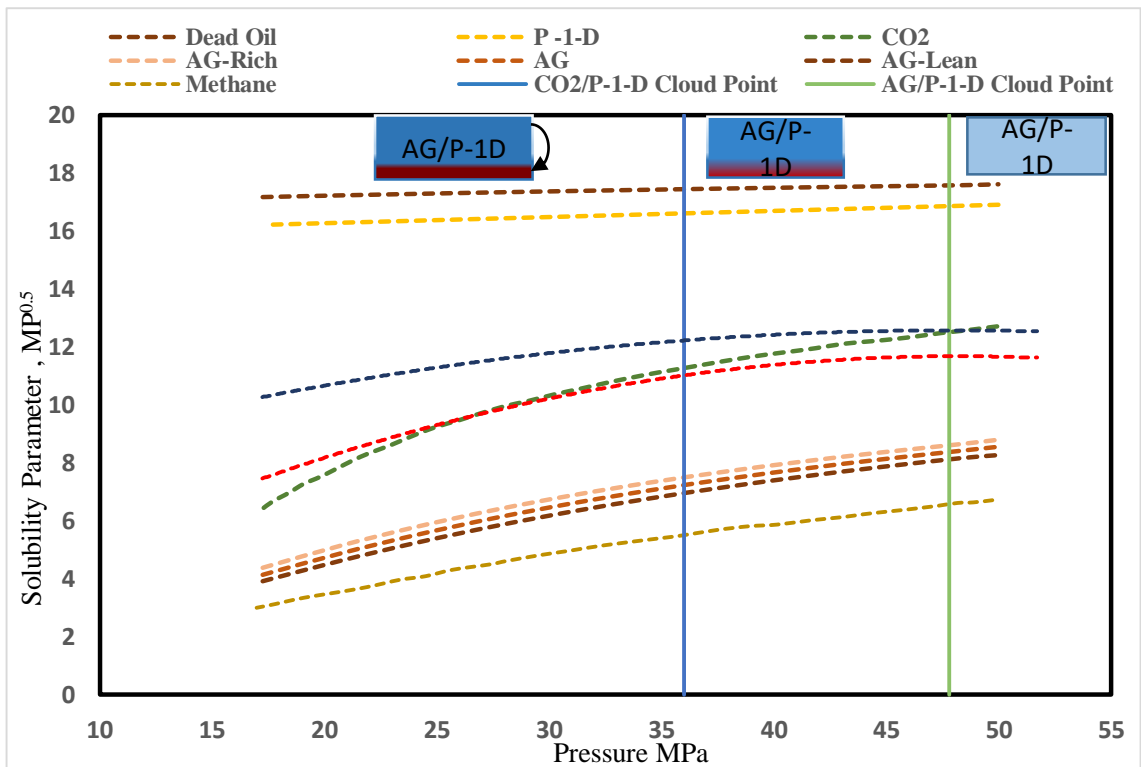


Figure 7.10 Solubility parameters of light oil, P-1-D, CO₂, AG rich, AG, AG lean, methane, ethane and Propane at different pressures and temperature of 377 K.

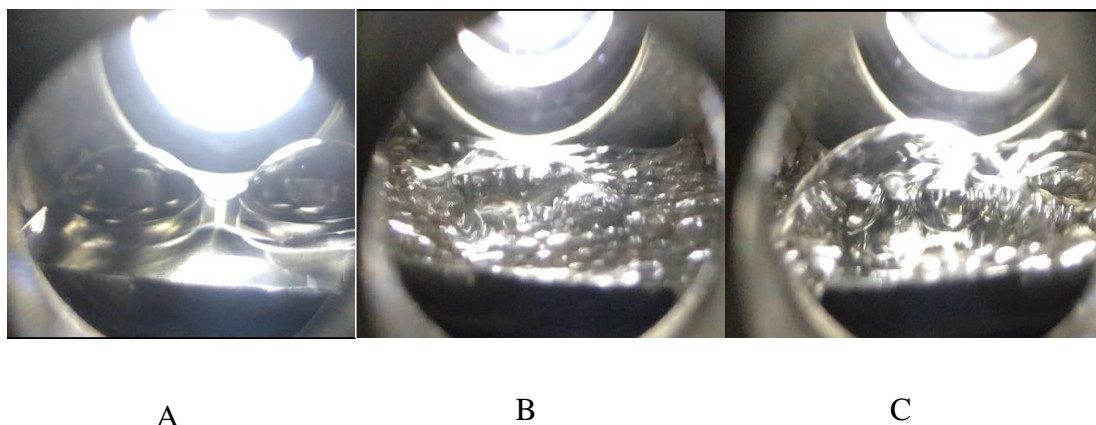


Figure 7.11 Photographs showing the evolution of the dissolved gas from P-1-D during pressure release after its exposure to the AG mixture at temperature of 377 K and three pressures of 3.44 MPa (A), 6.89 MPa (B) and 20.68 MPa (C).

7.4 Summary and Conclusion

In this study, firstly, a comparison between the phase behaviours of poly (1-decene) (P-1-D) and poly vinyl ethyl ether (PVEE) solubilities in different solvents (CO_2 and AG mixtures) is made using cloud point pressure measurements. Then, a qualitative assessment of the effect of dissolved oligomers (P-1-D and PVEE) in AG mixture and CO_2 on the equilibrium IFTs and miscibility pressures (MMP and P_{max}) when these two gases are in contact with a light oil are determined using the VIT technique. A comparison between the measured cloud point pressures shows that the phase behaviour of P-1-D-thickened AG mixture system differs from that of the P-1-D-thickened CO_2 system. The P-1-D- thickened AG mixture system exhibits an LCST (Lower Critical Solution Temperature) trend, while a UCST (Upper Critical Solution Temperature) trends is observed for the P-1-D-thickened CO_2 and PVEE-thickened CO_2 systems. In addition, the solubility of P-1-D in CO_2 is a function of enthalpy and in AG mixture is a function of entropy (molar volume) at high temperature and pressure. Meanwhile, the solubility of PVEE is entropically driven through the molecular interactions between ether oxygen in the side chain of PVEE and electron-acceptor in the carbon atom of CO_2 . At the same conditions and concentrations, P-1-D has a much higher solubility in pure CO_2 than PVEE.

The measured equilibrium IFTs for the light oil/AG mixture system at all pressures were found to be higher than those for the light oil/ CO_2 system. Consequently, the

miscibility pressures (MMP and P_{\max}) of the light oil/AG mixture system (30.5 MPa and 64 MPa) were found to be higher than those of the light oil/CO₂ system (22.3MPa and 44 MPa). Thus, the light hydrocarbon gases (CH₄ and C₂H₆) have weak effects on miscibility development compared to pure CO₂ with the CO₂ content in the AG mixture having a considerable effect in lowering the miscibility pressure. Furthermore, the measured equilibrium IFTs of the light oil/P-1-D-thickened CO₂ and the light oil/PVEE-thickened CO₂ systems were found to be slightly lower than those of the light oil/CO₂ system. Consequently, both additives of P-1-D and PVEE can slightly reduce MMP and considerably reduce the P_{\max} . In contrast, the plasticization effects of dissolved gas in P-1-D and dissolved P-1-D in AG mixture cause an increase in the IFTs and miscibility pressures of the light oil/AG mixture system at reservoir conditions. Overall, the cloud point pressure of P-1-D-thickened CO₂ and P-1-D-thickened AG mixture systems are located within multi-contact miscibility threshold, while that of the PVEE-thickened CO₂ is located above first contact miscibility pressure.

Chapter 8. Conclusions and Recommendations

8.1 Conclusions

Direct thickening using chemical additives is one of the techniques proposed to reduce the mobility of the injected gas in the reservoir during an MGI process. The reduced gas mobility then would effectively increase the sweep efficiency and enhance oil recovery. This thesis presents for the first time, the details and outcomes of numerical simulation and experimental evaluations of the effectiveness of thickened AG mixture and thickened CO₂ injections at high temperature for MGI process with the specific focus on Field A located in the southern Oman. In the numerical work, different thickened and unthickened gas injections were simulated using a box model under Field A's in-situ conditions to evaluate the potential of thickened gas injection in this field. In addition, the simulation study evaluated the direct effect of different gas compositions on the oil properties and incremental impact on oil recovery during the floods. In the laboratory measurements, the solubility of a large library of polymers/oligomers (26 commercial products for CO₂ and 32 for the AG mixture) in the AG mixture and supercritical CO₂ were determined using a rapid screening method (gravimetric extraction method) whose results were then validated using conventional cloud point pressure testing. Subsequently, based on the measured solubility of each polymer/oligomer in either the AG mixture or CO₂, any additive that had a lower cloud point pressure in these gas solvents at Field A reservoir conditions was examined for possible viscosity enhancement in both gases at different pressures and temperatures. The effectiveness of the attained viscosity improvements to enhance oil recovery during the MGI process were then examined using core flooding experiments. In addition, during this study, a new approach was invented for gas mobility control that can considerably lower the volume of thickeners utilised during a field-scale application. The advantage of this approach was demonstrated under laboratory conditions where it effectively reduced the consumption of thickening agents during the core flooding experiments. The final stage of the experimental work was conducted to evaluate the effect of the dissolution of the final selected oligomers (P-1-D and PVEE) in CO₂ and Field A's AG mixture on the equilibrium IFTs and miscibility pressures using the VIT technique and also to examine the phase behaviour of the solutions obtained by dissolving these oligomers in both gases.

In general, the results of the study reveal that the final selected additives have different phase behaviours in different gases used and also were capable of increasing the gas viscosity at high temperatures (377 K) when used at high concentrations (1.5-9 wt%). Furthermore, the alternating thickened-unthickened gas injection could improve the sweep efficiency of the gas flood for Field A at the laboratory scale to levels similar to that obtainable by continuous thickened gas injection while reducing the amount of additives needed. The most significant findings of this work are summarised below as sorted according to the way various chapters are presented in this thesis:

8.1.1 Numerical Study of Using Polymer to Improve the Gas Flooding in the Harweel Cluster

- This part of the study revealed a progressive oil viscosity reduction with incremental increase in the dissolution of an injection gas into the oil. It was found that the presence of CO₂ in the AG mixture lowers the ability of the gas mixture to reduce the oil viscosity. In other words, the oil viscosity reduction by the dissolution of hydrocarbon gases was found to be much more pronounced than that of pure CO₂.
- The dissolution of light hydrocarbon gases into the oil leads to a decrease in the oil density, while the opposite takes place with pure CO₂ dissolution. Therefore, the presence of CO₂ in the AG mixture not only leads to an increase in the density of the AG mixture but also makes the AG mixture to be less effective in decreasing the oil density. This results in a minimal difference between the densities of the injected gas and the light oil of Field A.
- Injection of NGL (C₂-C₄) has a higher swelling factor after dissolution in Field A's oil than pure CO₂ and AG mixture.
- Adding a thickener to the AG, NGL and CO₂ for miscible gas injection in Field A results in a significant increase in the ultimate oil recovery factor (7-20%) as caused by improved sweep efficiency, delayed gas breakthrough and reduced production GOR.
- The simulation work demonstrated the potentials of thickening AG and NGL over CO₂ for improving the gas mobility and sweep efficiency in a light oil reservoir such as Field A.

8.1.2 Experimental Study of Miscible Thickened Natural Gas Injection for Enhanced Oil Recovery

- This part of the study found three additives (oligomer/polymer) that were completely or partially soluble in Field A's AG mixture at the pressure of 55MPa and temperature of 377K, including P-1-D, PMHS, and PDMS. The P-1-D oligomer was found to be adequately soluble in the AG mixture under actual reservoir conditions while PMHS and PDMS needed a higher pressure to dissolve completely at high temperature due to the entropic effects and mainly the presence of methane in the AG mixture. In addition, it was found that the presence of CO₂ and propane in the gas mixture could possibly facilitate the dissolution of these additives in the AG mixture.
- The measured viscosity of the oligomer-thickened AG mixture showed that only P-1-D was capable of increasing the viscosity of the AG mixture while PMHS could not improve the viscosity at low concentration (1.5 wt%). The viscosity of the P-1-D-thickened AG mixture could be increased between 2 to 7.4 fold at the concentration range of 1.5-9 wt%. Hence, the P-1-D can be considered as an effective thickener for AG mixture at high pressure and temperature.
- The core-flooding experiments examined the effect of increasing the viscosity of the AG mixture by 4.38 fold (0.13 cP) using P-1-D on oil recovery and gas breakthrough under the secondary and tertiary recovery modes. The thickened AG mixture injection resulted in delayed gas breakthrough leading to additional oil recoveries between 10 and 12%.
- In summary, the injection of a directly thickened AG mixture has the potential to improve the gas mobility and sweep efficiencies, resulting in increased ultimate oil recovery.

8.1.3 Experimental Evaluations of Polymeric Solubility and Thickeners for Supercritical CO₂ at High Temperature for Enhanced Oil Recovery

- A total of three additives (polymer/oligomer) were found to be adequately soluble in CO₂ under the Field A's in-situ reservoir conditions, including PVEE, PISO-BVE, and P-1-D.
- The viscosity measurements for oligomer-thickened CO₂ solution showed P-1-D and PVEE to be able to improve the viscosity of CO₂ at Field A's condition. The concentration range of 0.81-5 wt% of P-1-D in CO₂ could considerably increase the CO₂ viscosity by 1.2-2.77 fold over the temperature range of 358 -377 K, while 1.2-2 wt% of PVEE could enhance the CO₂ viscosity by 1.2-2.1 fold over the temperature range of 329-377 K.

Therefore, P-1-D and PVEE could be considered as effective CO₂ thickeners at Field A's conditions.

- Piso-BVE exhibited a higher solubility in CO₂ than PVEE at high temperatures. This is attributed to the change of the alkyl arm and steric effect on the alkyl vinyl ether. However, the viscosity enhancement capacity of Piso-BVE was found to be lower than PVEE at comparable concentrations and molecular weights.
- In summary, P-1-D has a much better CO₂ viscosity enhancement ability than PVEE and Piso-BVE, making it a suitable candidate for improving gas mobility in Field A, and under high temperatures in general, during CO₂ flooding.

8.1.4 New Approach of Alternating Thickened-Unthickened Gas Flooding for Enhanced oil Recovery

- This part of the study included twelve core floods conducted using different injection schemes and different thickened AG injection ratios (TAGR). The experiments demonstrated that the both injection schemes of continuous thickened AG (TAG) flooding and alternating injection of TAG or thickened CO₂ (TCO₂) with unthickened AG (TAG-A-AG or TCO₂-A-AG) are capable of mobilising high proportions of the in-situ oil and achieving higher oil recovery factors.
- The optimum TAGR was found to be approximately 1:3 in non-fractured plugs and 1:2 in fractured plugs. These optimum TAGRs achieved considerably higher oil recovery factors than that of the continuous unthickened AG flooding but marginally less than that of the continuous TAG flooding.
- Although the optimum TAGRs achieved slightly less oil recovery than that of the continuous TAG flooding, the alternating injection scheme creates a balance between improving the sweep efficiency and the amount of additives required, which can bring the economic viability of the direct gas thickening approach within reach.
- Overall, the core-flooding experiments verified the performance of alternating thickened gas (CO₂ or AG) injection at the laboratory-scale to be close to that of the continuous thickened AG but with considerable reduction of polymer amounts used.

8.1.5 Effects of Oligomers Dissolved in CO₂ or Associated Gas on IFT and Miscibility Pressure with a Gas-light Crude Oil System

- The cloud point pressure measurements indicated that the phase behaviour of P-1-D-thickened AG mixture system differs from that of the P-1-D-thickened CO₂ system. The latter system follows a UCST trend while the behaviour of the former lies close to the LCST trend. Such an outcome indicates that the solubility of P-1-D in CO₂ is a function of enthalpy and in AG mixture is a function of entropy.
- P-1-D has a much higher solubility in pure CO₂ than PVEE at the same conditions and concentrations. The solubility of PVEE in CO₂ is entropically driven through the molecular interactions between ether oxygen atom in the PVEE and the carbon atom in CO₂.
- The dissolution of P-1-D and/or PVEE in CO₂ results in a slight reduction in the IFTs and miscibility pressures of the light oil/CO₂ system.
- The plasticization effects of the dissolved hydrocarbon gases in P-1-D and the dissolution of P-1-D in the AG mixture causes an increase in the IFT and miscibility pressure of the light oil/AG mixture.
- Overall, the cloud point pressure of P-1-D-thickened CO₂ and P-1-D-thickened AG mixture systems are located within multi-contact miscibility threshold, while that of the PVEE-thickened CO₂ is located above the first contact miscibility pressure.

8.2 Recommendations for future work

This study has succeeded in achieving a number of important outcomes related to the direct gas thickening and alternating thickened-unthickened gas flooding under high pressure-temperature conditions. It has also managed to uncover several other aspects of this process that may require further in depth investigation but due to time constraints could not be addressed in this study. What follows is an outline of recommended further work that could complement this study and potentially improve the industry's confidence in employing the direct gas thickening approach at the field-scale.

- In this study, the required concentrations of the final selected thickener (i.e. P-1-D) for both the AG mixture and CO₂ are too high (3-9 wt%) which would make the use of this additive for continuous thickened gas injection impractical at the field-scale. However, as seen in Chapter 6, the new suggested approach of alternating injection of TAG or TCO₂

with unthickened AG demonstrated that this injection scheme is capable of mobilising considerable incremental oil and achieve high oil recoveries while lowering the volume of thickeners utilised at the laboratory-scale to 1/3. Given the above encouraging laboratory-scale outcome, further work at the larger field-scale using numerical simulation followed by economic analysis are required to investigate and verify the feasibility of this technique for field applications.

- Despite many efforts made to date to identify a viable thickener for the CO₂ or hydrocarbon gases, a non-fluorous additive material that could lead to adequate increase in the viscosity of CO₂ or hydrocarbon gases at concentrations of less than 1 wt% without the requirement of a co-solvent is yet to be identified. As revealed by the literature review presented in Chapter 2, only two non-fluorous high Mw polymers (PDMS, DRA) are capable of increasing the viscosity of CO₂ or NGL components at concentrations of less than 1 wt%, but, unfortunately, they required a co-solvent to attain solubility. In addition, these high Mw additives do not have the ability to enhance the viscosity of these gases at high temperatures (e.g. 373 K) when used at the concentrations of less than 1 wt%. In general, the current study indicates that P-1-D has a better viscosity enhancement ability when dissolved in CO₂ and AG mixture at high temperatures but only at high concentrations. Considering the results reported in the literature and those obtained in this work, another possible way may exist to adequately and viably increase the viscosity of CO₂ or AG mixture at high temperatures. The new proposed approach is based on taking advantage of the high temperature conditions to create a macro/micro-emulsion solution as a way of improving the viscosity of an injected gas that may need lower concentration of the additive with the presence of water.
- Another promising route would be to control the gas mobility using nanoparticles which can stabilise an emulsion or a foaming agent in CO₂ flooding. There have been several studies evaluating low cost, commercially available nanoparticles for stabilising CO₂ foams such as bare-silica and fly ash nanoparticles.[369, 370] However, as reported in the literature, the negative effect of particles retention on the core permeability and porosity is the main problem in applying such a technique.
- The only type of heterogeneity whose effect on the recovery process was experimentally investigated in this work was the presence of a fracture. Therefore, another aspect that is worth investigating is the effect of other heterogeneity types on the results obtained from core-flooding experiments. This may be achieved by creating different controlled core-

scale heterogeneity arrangements (i.e. permeability sequence in vertical and horizontal direction) and employing X-ray CT scanning to visualise their effect on multiphase flow at the core-scale.

- There are a number of ongoing immiscible gas flooding projects around the world. These fields normally contain oils that have high molecular weight and therefore the miscibility pressure is much higher than the injection/reservoir pressure. This study demonstrated that the minimum miscibility pressure can be lowered by the dissolution of chemical additive in the injection gas. As indicated in Chapter 2, there are several polymer and small molecules additives that can be dissolved in CO₂ or hydrocarbon gases. The effect of these additives on the equilibrium IFT and MMP of such crude oils may be worth investigating.

APPENDICES

Appendix A

A.1 Gas/liquid IFT and miscibility-Background

Interfacial tension (IFT) is a property of the interface between two fluid phases and is strongly dependent on mass transfer interactions occurring between the two phases. The two thermodynamic properties, solubility and miscibility, are strongly correlated to interfacial tension in that solubility is typically linearly correlated to the reciprocal of interfacial tension and the condition of zero interfacial tension between the fluid phases implies miscibility.[371]

Attempts to calculate surface tension or surface energy from the knowledge of intermolecular potentials have been made since Laplace in the early 19th century. Surface tensions or energies of many simple liquids have been calculated in terms of intermolecular forces from theories which are based on simplified assumptions such as the cell model of liquid structure. Nevertheless, the results are in good agreement with experimental results.[372]

Since the heat of vaporisation arises from intermolecular forces, it can be shown that there is a close relation between surface energy and heat of vaporisation.[372] It has been shown that the work necessary to bring a molecule from the interior of the liquid to the surface is half the work necessary to take the molecule out of the liquid.[372] If q and v are the heat of vaporisation and the volume per molecule, respectively, the following relation holds:

$$\lambda \equiv \frac{q}{Uv^{\frac{2}{3}}} = 2$$

Where the λ is Stephan's constant and U is surface energy. The cohesive energy density and the solubility parameter (δ) are derived from the heat of vaporisation (ΔE^v) and liquid molar volume (v)[373, 374]:

$$\delta = (\text{Cohesive Energy Density})^{1/2} = \sqrt{\frac{\Delta E^v}{v}}$$

The solubility parameter (δ) is an important quantity in predicting solubility relations[373, 374] Thermodynamics requires that the free energy of mixing must be zero or negative for the solution process to occur spontaneously. The free energy change for the dissolution process is given by the relation:

$$\Delta G^M = \Delta H^M - T\Delta S^M$$

Where ΔG^M is the free energy of mixing, ΔH^M is the heat of mixing, T is the absolute temperature and ΔS^M is the entropy change in the mixing process. The heat of mixing (ΔH^M) is given by Hildebrand and Scott as [357]:

$$\Delta H^M \approx \Delta E^M = \phi_1\phi_2v_m(\delta_1 - \delta_2)^2$$

Where the ϕ_1 and ϕ_2 are volume fractions of solvent and solute (Polymer Science) and v_m is the average molar volume of the solvent.

It is important to note that the solubility parameter, or rather the difference in solubility parameters ($\delta_1 - \delta_2$) for the solvent-solute combination, is important in determining the solubility in a system.[357, 373] It has been definitively shown that solubility parameters can be used to predict both positive and negative heats of mixing.[357] Interfacial tension between two phases can be correlated by the mutual solubility such that a higher solubility implies a lower interfacial tension between the phases. In other words, complete solubility or total miscibility is equivalent to a scenario with no interfacial tension.[371, 375]

Appendix B Official Permissions and Copyrights

Sultanate of Oman
Ministry of Oil & Gas
Muscat

بِسْمِ اللَّهِ الرَّحْمَنِ الرَّحِيمِ



سُلْطَنَةُ عُومَانِ
وَزَارَةُ النِّفْطِ وَالعِجَازِ
مَسَقَط

MOG Ref: 7119/1/6901 /2018

Date: 4th December 2018

Dr. Ali Al Gheithy
Petroleum Engineering Functional Director
PDO

After Compliments,

Subject: REQUEST FOR RELEASE OF TECHNICAL MATERIAL

Title:

Enhanced Oil Recovery, Chapter1: Introduction and Background.

Reference to your letter dated 27th of November 2018, on the above subject, please be advised that **MOG** has no objection for PDO to release the data of this chapter to support a PhD student at Curtin University.

Best regards,



Saif Hamed Al-Salmi
Director General of Exploration
and Production of Oil & Gas.



Sultanate of Oman
Ministry of Oil & Gas
Muscat

بِسْمِ اللَّهِ الرَّحْمَنِ الرَّحِيمِ



سُلْطَنَةُ عُومَانِ
وَزَارَةُ النِّفْطِ وَالْغَازِ
مَسَقَط

MOG Ref:7119/1/1890

Date: 20th March 2017.

Dr. Ali Al-Gheithy.
Petroleum Engineering Functional Director
PDO

Fax:

After Compliments,

Subject: Request for Release of Technical Material

Title:

A Numerical Study of Using Polymer to Improve the Gas Flooding in The Harweel Cluster

Reference to your letter dated **2nd March 2017**, please be advised that **MOG** in principle has no objection for PDO to present the above titled subject that is proposed to be presented during **SPE reservoir characterization and Simulation Conference** to be held on 8th -10th May 2017 in Abu Dhabi. However, PDO is requested to provide final paper/presentation for MOG's final review and approval.

Best regards,


20.3.17

Dr. Mohammed Al-Balushi
A/Director General of Exploration
and Production of Oil & Gas .



c.c: Nasser Mohammed Saba Al Hinai (n.alhinai@postgrad.curtin.edu.au)

**Society of Petroleum Engineers LICENSE
TERMS AND CONDITIONS**

Jan 06, 2019

This is a License Agreement between Nasser Mohammed Al Hinai ("You") and Society of Petroleum Engineers ("Society of Petroleum Engineers") provided by Copyright Clearance Center ("CCC"). The license consists of your order details, the terms and conditions provided by Society of Petroleum Engineers, and the payment terms and conditions.

All payments must be made in full to CCC. For payment instructions, please see information listed at the bottom of this form.

License Number	4482271081221
License date	Dec 03, 2018
Licensed content publisher	Society of Petroleum Engineers
Licensed content title	SPE Reservoir Characterisation and Simulation Conference and Exhibition
Licensed content date	Jan 1, 2017
Type of Use	Thesis/Dissertation
Requestor type	Academic institution
Format	Electronic
Portion	chapter/article
Number of pages in chapter/article	17
The requesting person/organization is:	Nasser Al Hinai / Curtin University
Title or numeric reference of the portion(s)	Chapter 3
Title of the article or chapter the portion is from	A Numerical Study of Using Polymers to Improve the Gas Flooding in the Harweel Cluster
Editor of portion(s)	N/A
Author of portion(s)	Nasser M Al Hinai
Volume of serial or monograph.	N/A
Page range of the portion	1-17
Publication date of portion	2017
Rights for	Main product
Duration of use	Life of current edition
Creation of copies for the disabled	no
With minor editing privileges	yes
For distribution to	Worldwide
In the following language(s)	Original language of publication
With incidental promotional use	no
The lifetime unit quantity of new product	Up to 999
Title	A Numerical Study of Using Polymers to Improve the Gas Flooding in the Harweel Cluster

1/8/2019

RightsLink Printable License

Institution name	Curtin University
Expected presentation date	Dec 2018
Order reference number	CAO2794
Billing Type	Invoice
Billing Address	Chef Sense - Du B KVC5001B 19 B McManus street Perth, Australia 6107 Attn: Nasser Mohammed Al Hinai
Total (may include CCC user fee)	0.00 USD

Sultanate of Oman
Ministry of Oil & Gas
Muscat

سلطنة عمان



سلطنة عمان
وزارة النفط والغاز
مسقط

MOG Ref: 7119/11227

Date: 9th January 2017.

Dr. Ali Al-Gheithy
Petroleum Engineering Functional Director
PDO

Fax: 24607061

After Compliments,

Subject: REQUEST FOR RELEASE OF TECHNICAL MATERIAL


Title:

**Experimental Study of Miscible Thickened Natural Gas Injection for
Enhanced Oil Recovery**

Reference to your letter dated 28th December 2016, on the above titled subject, please be advised that MOG has no objection for PDO to publish the paper as illustrated in your letter PDO/UPD/Dec.16/03. However, the approval is subjected on implementing below considerations;

1. Field names should be removed
2. Unnecessary detailed information should be minimized (e.g. reservoir rock and fluid properties)
3. Any confidential contractor information or product name should be bound by the confidential agreement in place.

Best regards,


Salf Hamed Al-Salmani
Director General of Exploration
and Production of Oil & Gas



CIC: NASSER AL-HINAI (HLD055) L

P.O. Box : 551 Muscat Postal Code : 100

ص.ب. 551، مسقط، الرمز البريدي 100



Title: Experimental Study of Miscible Thickened Natural Gas Injection for Enhanced Oil Recovery

Author: Nasser M. Al Hinai, A. Saeedi, Colin D. Wood, et al

Publication: Energy & Fuels

Publisher: American Chemical Society

Date: May 1, 2017

Copyright © 2017, American Chemical Society

Logged in as:

Nasser Mohammed Al Hinai

Account #:

3001369917

LOGOUT

PERMISSION/LICENSE IS GRANTED FOR YOUR ORDER AT NO CHARGE

This type of permission/license, instead of the standard Terms & Conditions, is sent to you because no fee is being charged for your order. Please note the following:

- Permission is granted for your request in both print and electronic formats, and translations.
- If figures and/or tables were requested, they may be adapted or used in part.
- Please print this page for your records and send a copy of it to your publisher/graduate school.
- Appropriate credit for the requested material should be given as follows: "Reprinted (adapted) with permission from (COMPLETE REFERENCE CITATION). Copyright (YEAR) American Chemical Society." Insert appropriate information in place of the capitalized words.
- One-time permission is granted only for the use specified in your request. No additional uses are granted (such as derivative works or other editions). For any other uses, please submit a new request.

BACK

CLOSE WINDOW

Sultanate of Oman
Ministry of Oil & Gas
Muscat

بِسْمِ اللَّهِ الرَّحْمَنِ الرَّحِيمِ



سُلْطَنَة عُومَان
وَزَارَة النِّفْطِ وَالْغَازِ
مَسْقَط

MOG Ref: 7119/1/6970
2017.

Date: 14th November

Dr. Ali Al-Gheithy
Petroleum Engineering Functional Director
PDO

After Compliments,

Subject: REQUEST FOR RELEASE OF TECHNICAL MATERIAL

Title:

Experimental evaluations of polymeric solubility and thickener in CO₂ at high temperature for enhanced oil recovery

Reference to your letter dated 2nd of November 2017, on the above subject, please be advised that MOG has no objection for PDO to release the paper attached with your letter PDO/UPD/Oct.17/04.

Best regards,

Saif Hamed Al-Salmi
Director General of Exploration
and Production of Oil & Gas .



**Title:**Experimental Evaluations of
Polymeric Solubility and
Thickeners for Supercritical CO₂
at High Temperatures for
Enhanced Oil Recovery**Author:**Nasser M. Al Hinai, Ali Saeedi,
Colin D. Wood, et al**Publication:** Energy & Fuels**Publisher:** American Chemical Society**Date:** Feb 1, 2018

Copyright © 2018, American Chemical Society

Logged in as:

Nasser Mohammed Al Hinai

Account #:

3001369917

[LOGOUT](#)**PERMISSION/LICENSE IS GRANTED FOR YOUR ORDER AT NO CHARGE**

This type of permission/license, instead of the standard Terms & Conditions, is sent to you because no fee is being charged for your order. Please note the following:

- Permission is granted for your request in both print and electronic formats, and translations.
- If figures and/or tables were requested, they may be adapted or used in part.
- Please print this page for your records and send a copy of it to your publisher/graduate school.
- Appropriate credit for the requested material should be given as follows: "Reprinted (adapted) with permission from (COMPLETE REFERENCE CITATION). Copyright (YEAR) American Chemical Society." Insert appropriate information in place of the capitalized words.
- One-time permission is granted only for the use specified in your request. No additional uses are granted (such as derivative works or other editions). For any other uses, please submit a new request.

[BACK](#)[CLOSE WINDOW](#)

Sultanate of Oman
Ministry of Oil & Gas
Muscat

بِسْمِ اللَّهِ الرَّحْمَنِ الرَّحِيمِ



سُلْطَنَةُ عُومَانِ
وَزَارَةُ النِّفْطِ وَالْغَازِ
مَسَقَط

MOG Ref: 7219/1/ 4059 /2018.

Date: 3rd July 2018

Dr. Ali Al-Gheithy.
Petroleum Engineering Functional Director
PDO

After Compliments,

Subject: Request for Release of Technical Material

Titled:

A New Approach to Alternating Thickened-Unthickened Gas Flooding for Enhanced Oil Recovery.

Reference to your letter dated 24th June 2018, please be advised that MOG has no objection for PDO to present the above titled technical paper to the selected journal.

Best regards,

Saif Bin Hamad Al-Salmi
Director General of Exploration
and Production of Oil & Gas.





Title: New Approach to Alternating Thickened–Unthickened Gas Flooding for Enhanced Oil Recovery

Author: Nasser M. Al Hinaï, A. Saeedi, Colin D. Wood, et al

Publication: Industrial & Engineering Chemistry Research

Publisher: American Chemical Society

Date: Oct 1, 2018

Copyright © 2018, American Chemical Society

Logged in as:

Nasser Mohammed Al Hinaï

Account #:
3001369917

[LOGOUT](#)

PERMISSION/LICENSE IS GRANTED FOR YOUR ORDER AT NO CHARGE

This type of permission/license, instead of the standard Terms & Conditions, is sent to you because no fee is being charged for your order. Please note the following:

- Permission is granted for your request in both print and electronic formats, and translations.
- If figures and/or tables were requested, they may be adapted or used in part.
- Please print this page for your records and send a copy of it to your publisher/graduate school.
- Appropriate credit for the requested material should be given as follows: "Reprinted (adapted) with permission from (COMPLETE REFERENCE CITATION). Copyright (YEAR) American Chemical Society." Insert appropriate information in place of the capitalized words.
- One-time permission is granted only for the use specified in your request. No additional uses are granted (such as derivative works or other editions). For any other uses, please submit a new request.

[BACK](#)

[CLOSE WINDOW](#)

From: Journal of the Taiwan Institute of Chemical Engineers

Subject: A manuscript number has been assigned: JTICE-D-19-00154

To: <nasser.alhinai5@gmail.com>

Ms. Ref. No.: JTICE-D-19-00154

Title: Effects of oligomers dissolved in CO₂ or associated gas on IFT and miscibility pressure with a gas-light crude oil system

Journal of the Taiwan Institute of Chemical Engineers

Dear Mr. nasser alhinai,

Your submission "Effects of oligomers dissolved in CO₂ or associated gas on IFT and miscibility pressure with a gas-light crude oil system" has been assigned manuscript number JTICE-D-19-00154.

To track the status of your paper, please do the following:

1. Go to this URL: <https://ees.elsevier.com/jtice/>
2. Enter your login details
3. Click [Author Login]

This takes you to the Author Main Menu.

4. Click [Submissions Being Processed]

Thank you for submitting your work to Journal of the Taiwan Institute of Chemical Engineers.

Kind regards,

Editorial Office

Editorial Office

Journal of the Taiwan Institute of Chemical Engineers

For further assistance, please visit our customer support site at <http://help.elsevier.com/app/answers/list/p/7923>. Here you can search for solutions on a range of topics, find answers to frequently asked questions and learn more about EES via interactive tutorials. You will also find our 24/7 support contact details should you need any further assistance from one of our customer support representatives.

From: Sara Bacvarova <sara.b@intechopen.com>

Date: Thu, 24 Jan 2019 at 21:16

Subject: IntechOpen - Acceptance - "Enhanced Oil Recovery Processes - New Technologies"

To: Nasser Al Hinai <nasser.alhinai5@gmail.com>

Dear Ph.D. Al Hinai,

Following up on my previous email, I would like to confirm that the editor, Dr. Laura Romero-Zerón has approved your proposal "Direct Gas Thickeners" and has no further suggestions for you at this time. Please continue with the writing process.

After the full chapter review, you will receive the notification regarding the definitive acceptance of your work in the book.

NEXT STEP:

Submit your full chapter (10 to 20 pages) by: March 31st, 2019

For the preparation of your chapter please use the Template Guidelines that can be found by signing in to your Author Panel under the Quick Links section.

To sign in to your Author Panel please use the following link:

<https://mts.intechopen.com/booksprocess/action/chapter/191727>

All chapters are published under the CC Attribution 3.0 Unported License. By submitting your manuscript you accept the terms and conditions set forth in our Copyright Agreement and acknowledge and accept the Open Access Publishing Fee policy. You can find more information in the Quick Links section on your Author Panel.

If you have any additional questions or concerns, do not hesitate to contact me.

Cordially,

Sara Bacvarova

Author Service Manager

IntechOpen

The Shard, 32 London Bridge Street, London SE1 9SG, United Kingdom

+442080895700

www.intechopen.com

INTECHOPEN LIMITED, Registered in England and Wales No. 11086078

We are IntechOpen, the world's leading publisher of Open Access books

Built by scientists, for scientists

Appendix C Attributions of Co-authors




Paper title: “Numerical Study of Using Polymer to Improve the Gas Flooding in the Harweel Cluster”, SPE Reservoir Characterization and Simulation Conference and Exhibition, SPE-185999-MS

Nasser. M. Al Hinai^{,†,‡}, A. Saeedi[†], Colin D. Wood[‡] and R. Valdez[‡]*

[†] Department of Petroleum Engineering, Curtin University, 6151 Kensington, Western Australia.

[‡] Department of Exploration Geophysics, Curtin University, 6151 Kensington, Western Australia.

[‡] Petroleum Development Oman L.L.C.

Author Name	conception and design	Acquisition of data & method	Data conditioning & manipulation	Analysis & statistical method	Interpretation & discussion	Final approval
A. Saeedi (Co-author-1)	✓	✓			✓	✓
I acknowledge that these represent my contributions to the above research output. Signature : 						
Colin D. Wood (Co-author-2)	✓	✓			✓	✓
I acknowledge that these represent my contributions to the above research output. Signature : 						
R. Valdez (Co-author-3)		✓				✓
I acknowledge that these represent my contributions to the above research output. Signature : 						

Paper title: “**Experimental Study of Miscible Thickened Natural Gas Injection for Enhanced Oil Recovery**”, Energy Fuels, 2017, 31 (5), pp 4951–496

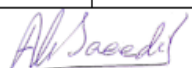
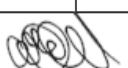
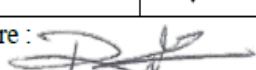

Nasser. M. Al Hinai^{†,‡,¶}, A. Saeedi[†], Colin D. Wood[‡], R. Valdez[§] and Lionel Esteban[‡]*

[†] Department of Petroleum Engineering, Curtin University, GPO Box U1987, Perth, W.A. 6151, Australia

[‡] Commonwealth Scientific and Industrial Research Organization, Perth, W.A. 6151, Australia

[§] Kinder Morgan CO2, 1001 Louisiana St, Suite 1000, Houston, Texas 77002, United States

[¶] Petroleum Development Oman L.L.C., P.O. Box 81, Code 100, Muscat, Sultanate of Oman

Author Name	conception and design	Acquisition of data & method	Data conditioning & manipulation	Analysis & statistical method	Interpretation & discussion	Final approval
A. Saeedi (Co-author-1)	✓	✓			✓	✓
I acknowledge that these represent my contributions to the above research output. Signature : 						
Colin D. Wood (Co-author-2)	✓	✓			✓	✓
I acknowledge that these represent my contributions to the above research output. Signature : 						
R. Valdez (Co-author-3)						✓
I acknowledge that these represent my contributions to the above research output. Signature : 						
Lionel Esteban (Co-author-4)						✓
I acknowledge that these represent my contributions to the above research output. Signature : 						

Paper title: “Experimental Evaluations of Polymeric Solubility and Thickeners for Supercritical CO₂ at High Temperatures for Enhanced Oil Recovery” Energy Fuels, 2018, 32 (2), pp 1600–1611

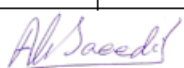

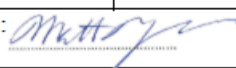
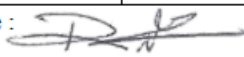
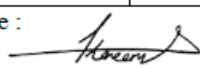

Nasser. M. Al Hinai^{*,†,‡,¶}, A. Saeedi[†], Colin D. Wood[‡], Matthew Myers[‡], Raul Valdez[§], Abdul Kareem Sooud[†], and Ahmed Sari[†]

[†] Department of Petroleum Engineering, Curtin University, GPO Box U1987, Perth, W.A. 6151, Australia

[‡] Commonwealth Scientific and Industrial Research Organization, Perth, W.A. 6151, Australia

[§] Kinder Morgan CO₂, 1001 Louisiana St, Suite 1000, Houston, Texas 77002, United States

[¶] Petroleum Development Oman L.L.C., P.O. Box 81, Code 100, Muscat, Sultanate of Oman

Author Name	conception and design	Acquisition of data & method	Data conditioning & manipulation	Analysis & statistical method	Interpretation & discussion	Final approval
A. Saeedi (Co-author-1)	✓	✓			✓	✓
I acknowledge that these represent my contributions to the above research output. Signature : 						
Colin D. Wood (Co-author-2)	✓	✓			✓	✓
I acknowledge that these represent my contributions to the above research output. Signature : 						
Matthew Myers (Co-author-3)	✓	✓			✓	✓
I acknowledge that these represent my contributions to the above research output. Signature : 						
R. Valdez (Co-author-4)						✓
I acknowledge that these represent my contributions to the above research output. Signature : 						
Abdul Kareem Sooud (Co-author-5)						✓
I acknowledge that these represent my contributions to the above research output. Signature : 						
Ahmed Sari (Co-author-6)						✓
I acknowledge that these represent my contributions to the above research output. Signature : 						

Paper title: “New Approach to Alternating Thickened–Unthickened Gas Flooding for Enhanced Oil Recovery” *Ind. Eng. Chem. Res.*, 2018, 57 (43), pp 14637–14647

Nasser. M. Al Hinai^{*,†,‡,¶}, *A. Saeedi*[†], *Colin D. Wood*[‡], *Matthew Myers*[‡], *R. Valdez*[§], *Quan Xie*[†], and *Fayang Jin*[‡]

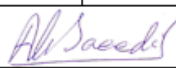
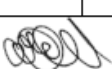

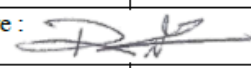

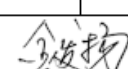
[†] Department of Petroleum Engineering, Curtin University, GPO Box U1987, Kensington, Western Australia 6151

[‡] State Key Laboratory of Oil and Gas Reservoir Geology and Exploitation, Southwest Petroleum University, Chengdu, Sichuan 610500, China

[¶] Petroleum Development Oman L.L.C., P.O. Box 81, Code 100, Muscat, Sultanate of Oman

[‡] Commonwealth Scientific and Industrial Research Organization, Kensington, Western Australia 6151

[§] Kinder Morgan CO₂, 1001 Louisiana Street, Suite 1000, Houston, Texas 77002, United States

Author Name	conception and design	Acquisition of data & method	Data conditioning & manipulation	Analysis & statistical method	Interpretation & discussion	Final approval
A. Saeedi (Co-author-1)	✓	✓			✓	✓
I acknowledge that these represent my contributions to the above research output. Signature : 						
Colin D. Wood (Co-author-2)	✓	✓			✓	✓
I acknowledge that these represent my contributions to the above research output. Signature : 						
Matthew Myers (Co-author-3)	✓	✓			✓	✓
I acknowledge that these represent my contributions to the above research output. Signature : 						
R. Valdez (Co-author-4)						✓
I acknowledge that these represent my contributions to the above research output. Signature : 						
Quan Xie (Co-author-5)						✓
I acknowledge that these represent my contributions to the above research output. Signature : 						
Fayang Jin (Co-author-6)						✓
I acknowledge that these represent my contributions to the above research output. Signature : 						

Paper title: "Effects of Oligomers Dissolved in CO₂ or Associated Gas on IFT and Miscibility Pressure with a Gas-Light Crude Oil System", Energy & Fuels (submitted).

Nasser. M. Al Hinai^{*†,‡,||}, Matthew Myers[‡], Seyed. Ali[€], Colin D. Wood[‡], R. Valdez[§],
Fayang Jin[‡], Quan Xie[†] and A. Saeedi[†]

[†] Department of Petroleum Engineering, Curtin University, GPO Box
U1987, Kensington, Western Australia 6151

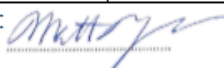



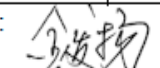
[‡] State Key Laboratory of Oil and Gas Reservoir Geology and Exploitation, Southwest
Petroleum University, Chengdu, Sichuan 610500, China


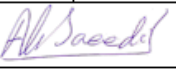
^{||} Petroleum Development Oman L.L.C., P.O. Box 81, Code 100, Muscat, Sultanate of Oman

[‡] Commonwealth Scientific and Industrial Research Organization, Kensington, Western
Australia 6151

[§] Kinder Morgan CO₂, 1001 Louisiana Street, Suite 1000, Houston, Texas 77002, United
States

[€] Research Institute of Petroleum Industry (RIPI), Tehran, Iran, PO. Box: 18745-4163

Author Name	conception and design	Acquisition of data & method	Data conditioning & manipulation	Analysis & statistical method	Interpretation & discussion	Final approval
Matthew Myers (Co-author-1)	✓	✓			✓	✓
I acknowledge that these represent my contributions to the above research output. Signature: 						
Ali Mousavi Dehghani (Co-author-2)					✓	✓
I acknowledge that these represent my contributions to the above research output. Signature: 						
Colin D. Wood (Co-author-3)	✓	✓			✓	✓
I acknowledge that these represent my contributions to the above research output. Signature: 						
R. Valdez (Co-author-4)						✓
I acknowledge that these represent my contributions to the above research output. Signature: 						
Fayang Jin (Co-author-5)						✓
I acknowledge that these represent my contributions to the above research output. Signature: 						
Quan Xie (Co-author-6)						✓

I acknowledge that these represent my contributions to the above research output. Signature :						
<i>A. Saeedi</i> (Co-author-7)	✓	✓			✓	✓
I acknowledge that these represent my contributions to the above research output. Signature :						

References

1. Alvarado, V. and E. Manrique, *Enhanced Oil Recovery: an Update Review*. Energies, 2010. **3**(9): p. 1529-1575.
2. Muggeridge, A., et al., *Recovery Rates, Enhanced Oil Recovery and Technological Limits*. Philosophical Transactions of the Royal Society of London A: Mathematical, Physical and Engineering Sciences, 2014. **372**(2006): p. 20120320.
3. Ahmed, T., *Reservoir Engineering Handbook*. 2006: Elsevier.
4. Lake, L.W., *Enhanced Oil Recovery*. 1989, Upper Saddle River, New Jersey: Prentice-Hall.
5. RESEARCH, G.V., *Enhanced Oil Recovery Market Size, Share & Trend Analysis Report By Technology, By Application And Segment Forecasts, 2018 - 2025*. 2018, CISION PR Newswire: Grand View Research. p. 129 pages.
6. Escobar, E. *EOR Evolution*. 2014 June 2014 [cited 2018 16/07/2018]; Available from: <http://www.oedigital.com/subsea/item/6068-eor-evolution>.
7. Al-Mutairi, S.M. and S.L. Kokal. *EOR Potential in the Middle East: Current and Future Trends*. in *SPE EUROPEC/EAGE Annual Conference and Exhibition*. 2011. Vienna, Austria: Society of Petroleum Engineers.
8. Al-Adawy, M. and M. Nandyal. *Status and Scope for EOR Development in Oman*. in *Middle East Oil Show*. 1991. Bahrain: Society of Petroleum Engineers.
9. Henni, A., *Oman Champions EOR in the Middle East*. Journal of Petroleum Technology, 2014. **66**(11): p. 86-89.
10. Terry, R.E., *Enhanced Oil Recovery*. Encyclopedia of physical science and technology, 2003. **18**: p. 503-518.
11. Zick, A. *A Combined Condensing/Vaporizing Mechanism in the Displacement of Oil by Enriched Gases*. in *SPE annual technical conference and exhibition*. 1986. New Orleans, Louisiana Society of Petroleum Engineers.
12. Asgarpour, S., *An Overview of Miscible Flooding*. Journal of Canadian petroleum technology, 1994. **33**(02).
13. Dong, M., et al., *A Comparison of CO₂ Minimum Miscibility Pressure Determinations for Weyburn Crude Oil*. Journal of petroleum science and engineering, 2001. **31**(1): p. 13-22.
14. Stalkup, F.I. *Displacement Behavior of the Condensing/Vaporizing Gas Drive Process*. in *SPE annual technical conference and exhibition*. 1987. Dallas, Texas: Society of Petroleum Engineers.
15. Holm, L. and V. Josendal, *Mechanisms of Oil Displacement by Carbon Dioxide*. Journal of petroleum Technology, 1974. **26**(12): p. 1,427-1,438.
16. Simon, R. and D. Graue, *Generalized Correlations for Predicting Solubility, Swelling and Viscosity Behavior of CO₂-Crude Oil Systems*. Journal of Petroleum Technology, 1965. **17**(01): p. 102-106.
17. Gu, Y., P. Hou, and W. Luo, *Effects of Four Important Factors on the Measured Minimum Miscibility Pressure and First-Contact Miscibility Pressure*. Journal of Chemical & Engineering Data, 2013. **58**(5): p. 1361-1370.
18. Hemmati-Sarapardeh, A., et al., *Experimental Determination of Interfacial Tension and Miscibility of the CO₂-Crude Oil System; Temperature, Pressure, and Composition Effects*. Journal of Chemical & Engineering Data, 2013. **59**(1): p. 61-69.
19. Solutions, M.T. *Miscible Gas Injection: Facts about Miscible Displacements*. [cited 2015 11 August]; Available from: <http://www.mktechsolutions.com/Miscible%20Gas%20Displacements.html>.
20. Holm, L., *Miscible Displacement*. Petroleum Engineering Hand Book, Society of Petroleum Engineers, Richardson, TX, 1987: p. 1-45.
21. Stalkup Jr, F.I., *Status of Miscible Displacement*. Journal of Petroleum Technology, 1983. **35**(04): p. 815-826.
22. Belhaj, H., H. Abukhalifeh, and K. Javid, *Miscible Oil Recovery Utilizing N₂ and/or HC Gases in CO₂ Injection*. Journal of Petroleum Science and Engineering, 2013. **111**: p. 144-152.
23. Whittaker, S. and E. Perkins, *Technical Aspects of CO₂ Enhanced Oil Recovery and Associated Carbon Storage*, in *Global CCS institute*. 2013.
24. Algharaib, M.K., *Potential Applications of CO₂-EOR In the Middle East*, in *SPE Middle East Oil and Gas Show and Conference*. 2009, Society of Petroleum Engineers: Manama, Bahrain.

25. Al-Hajeri, S.K., et al., *Design and Implementation of the First CO₂-EOR Pilot in Abu Dhabi, UAE*, in *SPE EOR Conference at Oil & Gas West Asia*. 2010, Society of Petroleum Engineers: Muscat, Oman.
26. Al-Hajeri, S.K., et al., *Integrated History Matching Simulation Study of the First Miscible CO₂-EOR Pilot in Abu Dhabi Heterogeneous Carbonate Oil Reservoir*, in *SPE Middle East Oil and Gas Show and Conference*. 2011, Society of Petroleum Engineers: Manama, Bahrain.
27. Saadawi, H.N. *Surface Facilities for a CO₂-EOR Project in Abu Dhabi*. in *SPE EOR Conference at Oil & Gas West Asia*. 2010. Muscat, Oman: Society of Petroleum Engineers.
28. Al-basry, A.H., et al. *Lessons Learned from the First Miscible CO₂-EOR Pilot Project in Heterogeneous Carbonate Oil Reservoir in Abu Dhabi, UAE*. in *SPE Middle East Oil and Gas Show and Conference*. 2011. Manama, Bahrain: Society of Petroleum Engineers.
29. Alajmi, A.F., et al., *Experimental Investigation of CO₂ Miscible Flood in West Kuwait*. *Journal of Engineering Research*, 2015. **3**(3).
30. Al Hadhrami, A., et al. *Challenges and Learning from Developing Deep High Pressure Sour Reservoirs in Southern Oman by EOR MGI*. in *Abu Dhabi International Petroleum Exhibition and Conference*. 2014. Society of Petroleum Engineers.
31. Al-Hadhrami, A.K., et al. *The Design of the First Miscible Sour Gasflood Project in Oman*. in *International Petroleum Technology Conference*. 2007. Dubai, UAE: International Petroleum Technology Conference.
32. Al-Riyami, Q.M., et al. *Precambrian field Oman from Greenfield to EOR*. in *SPE Middle East Oil and Gas Show and Conference*. 2005. Kingdom of Bahrain Society of Petroleum Engineers.
33. Laws, M., et al. *Optimization of Stimulation Techniques for HP, Deep Wells in the Harweel Cluster, Oman* in *Paper SPE 93494 presented in the SPE Middle East Oil and Gas Show and Conference, Mar.* 2005. Kingdom of Bahrain
34. Hinaï, N.M.A., et al., *A Numerical Study of Using Polymers to Improve the Gas Flooding in the Harweel Cluster*, in *SPE Reservoir Characterisation and Simulation Conference and Exhibition*. 2017, Society of Petroleum Engineers: Abu Dhabi, UAE
35. Kokal, S. and A. Al-Kaabi, *Enhanced Oil Recovery: Challenges & Opportunities*. World Petroleum Council: Official Publication, 2010: p. 64-68.
36. Chierici, G.L., *Principles of Petroleum Reservoir Engineering*. Vol. 2. 2012: Springer Science & Business Media.
37. Nicolaides, C., et al., *Impact of Viscous Fingering and Permeability Heterogeneity on Fluid Mixing in Porous Media*. *Water Resources Research*, 2015. **51**(4): p. 2634-2647.
38. Chang, Y.-B., et al., *CO₂ Flow Patterns Under Multiphase Flow: Heterogeneous Field-Scale Conditions*. *SPE Reservoir Engineering*, 1994. **9**(03): p. 208-216.
39. Homsy, G.M., *Viscous Fingering in Porous-Media*. *Annual Review of Fluid Mechanics*, 1987. **19**(1): p. 271-311.
40. Habermann, B., *The Efficiency of Miscible Displacement as a Function of Mobility Ratio*, in *35th Annual Fall Meeting of SPE*. 1960: Denver, California. p. 264-272.
41. Araktingi, U.G. and F.M. Orr Jr, *Viscous Fingering in Heterogeneous Porous Media*. *SPE Reservoir Engineering*, 1993. **1**(01): p. 71-80.
42. Fu, X., L. Cueto-Felgueroso, and R. Juanes, *Viscous Fingering with Partially Miscible Fluids*. *Physical Review Fluids*, 2017. **2**(10): p. 104001.
43. Moortgat, J., *Viscous and Gravitational Fingering in Multiphase Compositional and Compressible Flow*. *Advances in Water Resources*, 2016. **89**: p. 53-66.
44. Suekane, T., et al., *Three-Dimensional Viscous Fingering of Miscible Fluids in Porous Media*. *Physical Review Fluids*, 2017. **2**(10): p. 103902.
45. Brock, D.C. and F.M. Orr, Jr., *Flow Visualization of Viscous Fingering in Heterogeneous Porous Media*, in *SPE Annual Technical Conference and Exhibition*. 1991, Society of Petroleum Engineers: Dallas, Texas.
46. Blunt, M. and M. Christie, *Theory of Viscous Fingering in two Phase, three Component Flow*. *SPE Advanced Technology Series*, 1994. **2**(02): p. 52-60.
47. Cheek, R.E. and D.E. Menzie, *Fluid Mapper Model Studies of Mobility Ratio*. *Society of Petroleum Engineers Journal*, 1955. **204**: p. 278-281.
48. Sahimi, M., M.R. Rasaei, and M. Haghghi, *Gas Injection and Fingering in Porous Media*, in *Gas Transport in Porous Media*. 2006, Springer. p. 133-168.
49. Pande, K. *Effects of Gravity and Viscous Crossflow on Hydrocarbon Miscible Flood Performance in Heterogeneous Reservoirs*. in *SPE Annual Technical Conference and Exhibition*. 1992. Society of Petroleum Engineers.

50. Scott, J., *Control of Gravity Segregation by High Density Fluid Injection*, C.S.O. Co, Editor. 1972, U.S. Patent 3661208.
51. Moissis, D., M. Wheeler, and C. Miller, *Simulation of Miscible Viscous Fingering using a Modified Method of Characteristics: Effects of Gravity and Heterogeneity*. SPE Advanced Technology Series, 1993. **1**(01): p. 62-70.
52. Enick, R.M., et al. *Mobility and Conformance Control for CO₂ EOR via Thickeners, Foams, and Gels--A Literature Review of 40 Years of Research and Pilot Tests*. in *SPE Improved Oil Recovery Symposium*. 2012. Society of Petroleum Engineers.
53. Bhatia, J., et al., *Production Performance of Water Alternate Gas Injection Techniques for Enhanced Oil Recovery: Effect of WAG Ratio, Number of WAG Cycles and the Type of Injection Gas*. International Journal of Oil, Gas and Coal Technology, 2014. **7**(2): p. 132-151.
54. Bhatia, J.C., et al. *Investigations on Gas Trapping Phenomena for Different EOR-Water Alternate Gas Injection Methodologies*. in *International Petroleum Technology Conference*. 2011. International Petroleum Technology Conference.
55. Caudle, B.H. and A.B. Dyes, *Improving Miscible Displacement by Gas-Water Injection*, in *32nd Annual Fall Meeting of Society of Petroleum Engineers*. 1958, Society of Petroleum Engineers: Dallas, Tex. p. 281-283.
56. Al Sumaiti, A., et al., *Tuning Foam Parameters for Mobility Control Using CO₂ Foam: Field Application to Maximize Oil Recovery from a High Temperature High Salinity Layered Carbonate Reservoir*. Energy & Fuels, 2017. **31**(5): p. 4637-4654.
57. Karin, M.a.J., J.N., *Adsorption of Foam-Forming Surfactants for Hydrocarbon-Miscible Flooding at High Salinities*. In *Foams: Fundamentals and Applications in the Petroleum Industry*. Advances in Chemistry, American Chemical Society, 1994: p. 242, 7, 259-316.
58. Schramm, L.L., K. Mannhardt, and J.J. Novosad. *Selection of Oil-Tolerant Foams for Hydrocarbon Miscible Gas Flooding*. in *Proceedings 14th International Workshop and Symposium, Int. Energy Agency Collab. Proj. on EOR, Salzburg*. 1993.
59. Talebian, S.H., et al. *Foam Assisted CO₂-EOR: Concepts, Challenges and Applications*. in *SPE Enhanced Oil Recovery Conference*. 2013. Kuala Lumpur, Malaysia: Society of Petroleum Engineers.
60. Talebian, S.H., et al., *Foam Assisted CO₂-EOR: A Review of Concept, Challenges, and Future Prospects*. Journal of Petroleum Science and Engineering, 2014. **120**: p. 202-215.
61. Xu, X., A. Saeedi, and K. Liu, *Laboratory Studies on CO₂ Foam Flooding Enhanced by a Novel Amphiphilic ter-Polymer*. Journal of Petroleum Science and Engineering, 2016. **138**: p. 153-159.
62. Xu, X., et al. *Laboratory Investigation on CO₂ Foam Flooding for Mature Fields in Western Australia*. in *Offshore Technology Conference Asia*. 2016. Kuala Lumpur, Malaysia: Offshore Technology Conference.
63. Bae, J. and C. Irani, *A Laboratory Investigation of Viscosified CO₂ Process*. SPE Advanced Technology Series, 1993. **1**(01): p. 166-171.
64. Dandge, D. and J. Heller. *Polymers for Mobility Control in CO₂ Floods*. in *SPE International Symposium on Oilfield Chemistry*. 1987. San Antonio, Texas Society of Petroleum Engineers.
65. Enick, R. *The Effect of Hydroxy Aluminum Disoaps on the Viscosity of Light Alkanes and Carbon Dioxide*. in *SPE International Symposium on Oilfield Chemistry*. 1991. Anaheim, California Society of Petroleum Engineers.
66. Heller, J., et al., *Direct thickeners for mobility control of CO₂ floods*. Society of Petroleum Engineers Journal, 1985. **25**(05): p. 679-686.
67. Terry, R.E., et al., *Polymerization in Supercritical CO₂ To Improve CO₂/Oil Mobility Ratios*, in *SPE International Symposium on Oilfield Chemistry*. 1987, Society of Petroleum Engineers: San Antonio, Texas
68. C Jr, A.R., *Oil Recovery Process by Miscible Displacement*. 1969, U.S. Patent 3444930
69. Dauben, D.L., Reed, J., Shelton, J., Lyman, Y., *Recovery of Oil with Viscous Propane*. 1971, U.S. Patent 3570601.
70. Dhuwe, A., et al., *Small Associative Molecule Thickeners for Ethane, Propane and Butane*. The Journal of Supercritical Fluids, 2016. **114**: p. 9-17.
71. Lee, J., et al., *Polymeric and Small Molecule Thickeners for CO₂, Ethane, Propane and Butane for Improved Mobility Control*, in *SPE Improved Oil Recovery Conference*. 2016, Society of Petroleum Engineers: Tulsa, Oklahoma, USA
72. Enick, R. and D. Olsen, *Mobility and Conformance Control for Carbon Dioxide Enhanced Oil Recovery (CO₂-EOR) via Thickeners, Foams, and Gels--A Detailed Literature Review of 40*

- Years of Research*. 2012, U.S. Dept. of Energy, National Energy Technology Laboratory(NETL).
73. Kulkarni, M.M. and D.N. Rao, *Experimental Investigation of Miscible and Immiscible Water-Alternating-Gas (WAG) Process Performance*. Journal of Petroleum Science and Engineering, 2005. **48**(1-2): p. 1-20.
 74. Skauge, A. and J. Stensen. *Review of WAG Field Experience*. in *Oil Recovery–2003, 1st International Conference and Exhibition, Modern Challenges in Oil Recovery*. 2003.
 75. Christensen, J.R., E.H. Stenby, and A. Skauge, *Review of WAG Field Experience*. SPE Reservoir Evaluation & Engineering, 2001. **4**(02).
 76. Masoud, M., *Comparing Carbon Dioxide Injection in Enhanced Oil Recovery with other Methods*. Austin Chemical Engineering, 2015. **2**(2): p. 1019.
 77. Surguchev, L.M., et al., *Screening of WAG Injection Strategies for Heterogeneous Reservoirs*, in *European Petroleum Conference*. 1992, Society of Petroleum Engineers: Cannes, France.
 78. Chen, S.-M., D.R. Allard, and J. Anli, *Factors Affecting Solvent Slug Size Requirements in Hydrocarbon Miscible Flooding*, in *SPE Enhanced Oil Recovery Symposium*. 1984, Society of Petroleum Engineers: Tulsa, Oklahoma.
 79. Sanchez, N.L., *Management of Water Alternating Gas (WAG) Injection Projects*, in *Latin American and Caribbean Petroleum Engineering Conference*. 1999, Society of Petroleum Engineers: Caracas, Venezuela.
 80. Han, L. and Y. Gu, *Optimization of Miscible CO₂ Water-Alternating-Gas Injection in the Bakken Formation*. Energy & Fuels, 2014. **28**(11): p. 6811-6819.
 81. Bennion, D.B. and S. Bachu. *Permeability and Relative Permeability Measurements at Reservoir Conditions for CO₂-Water Systems in Ultra Low Permeability Confining Caprocks*. in *EUROPEC/EAGE Conference and Exhibition*. 2007. London, U.K.: Society of Petroleum Engineers.
 82. Bennion, B. and S. Bachu. *Relative Permeability Characteristics for Supercritical CO₂ Displacing Water in a Variety of Potential Sequestration Zones*. in *SPE Annual Technical Conference and Exhibition*. 2005. Society of Petroleum Engineers.
 83. Ramachandran, K.P., O.N. Gyani, and S. Sur, *Immiscible Hydrocarbon WAG: Laboratory to Field*, in *SPE Oil and Gas India Conference and Exhibition*. 2010, Society of Petroleum Engineers: Mumbai, India.
 84. Skauge, A., and Aarra, M. *Effect of Wettability on the Oil Recovery by WAG*. in *Proceedings 7th European Symposium on Improved Oil Recovery*. 1993. Moscow.
 85. Skauge, A. *Summary of Core Flood Results in Connection with WAG Evaluation*. in *the Tenth Wyoming Enhanced Oil Recovery Symposium*. 1994. University of Wyoming, Laramie, Wyoming.
 86. Olsen, G., A. Skauge, and J. Stensen. *Evaluation of the Potential Application on the WAG Process in a North Sea Reservoir*. in *IOR 1991-6th European Symposium on Improved Oil Recovery*. 1991.
 87. Skauge, A. and J.A. Larsen. *Three-Phase Relative Permeabilities and Trapped Gas Measurements Related to WAG Processes*. in *SCA 9421, proceedings of the International Symposium of the Society of Core Analysts*. 1994. Stavanger, Norway.
 88. Al-Shuraiqi, H., A. Muggeridge, and C. Grattoni. *Laboratory Investigations of First Contact Miscible WAG Displacement: the Effects of WAG Ratio and Flow Rate*. in *SPE International Improved Oil Recovery Conference in Asia Pacific*. 2003. Kuala Lumpur, Malaysia Society of Petroleum Engineers.
 89. Srivastava, J. and L. Mahli. *Water Alternating Gas (WAG) Injection a Novel EOR Technique for Mature Light Oil Fields a Laboratory Investigation for GS-5C Sand of Gandhar Field*. in *A paper presented in biennial international conference and exposition in petroleum geophysics, Hyderabad*. 2012.
 90. Christensen, J.R., E.H. Stenby, and A. Skauge, *Review of WAG Field Experience*, in *International Petroleum Conference and Exhibition of Mexico*. 1998, Society of Petroleum Engineers: Villahermosa, Mexico.
 91. Faisal, A., et al., *Injectivity and Gravity Segregation in WAG and SWAG Enhanced Oil Recovery*, in *SPE Annual Technical Conference and Exhibition*. 2009, Society of Petroleum Engineers: New Orleans, Louisiana.
 92. Jenkins, M.K., *An Analytical Model for Water/Gas Miscible Displacements*, in *SPE Enhanced Oil Recovery Symposium*. 1984, Society of Petroleum Engineers: Tulsa, Oklahoma.
 93. Holloway, H.D. and R.A. Fitch, *Performance of a Miscible Flood with Alternate Gas-Water Displacement*. Journal of Petroleum Technology, 1964. **16**(04).

94. Holm, L.W., *Propane-Gas-Water Miscible Floods In Watered-Out Areas of the Adena Field, Colorado*. Journal of Petroleum Technology, 1972. **24**(10).
95. Cuesta, J. and G. MERRITT. *Caroline WAG Project, Injectivity and Interference Test-A Field Example*. in *Journal OF Candian Petroleum Technology*. 1982. Calgary, Canada: Candian INST Mining Metallurgy Petroleum
96. Moffitt, P.D. and D.R. Zornes, *Postmortem Analysis: Lick Creek Meakin Sand Unit Immiscible CO₂ Waterflood Project*, in *SPE Annual Technical Conference and Exhibition*. 1992, Society of Petroleum Engineers: Washington, D.C.
97. Slotte, P., H. Stenmark, and T. Aurdal, *Snorre WAG Pilot*. RUTH, 1992. **1995**: p. 85-91.
98. Surguchev, L., *WAG Injection*, in *Report*. 1990, RF-Rogaland Research: Stavanger. p. 90.
99. Huang, E.T.S. and L.W. Holm, *Effect of WAG Injection and Rock Wettability on Oil Recovery During CO₂ Flooding*. SPE Reservoir Engineering, 1988. **3**(01): p. 119-129.
100. Stalkup, F.I., *Displacement of Oil by Solvent at High Water Saturation*. Society of Petroleum Engineers Journal, 1970. **10**(04): p. 337-348.
101. Raimondi, P. and M.A. Torcaso, *Distribution of the Oil Phase Obtained upon Imbibition of Water*. Society of Petroleum Engineers Journal, 1964. **4**(01): p. 49-55.
102. Bedrikovetsky, P., *WAG Displacements of Oil-Condensates Accounting for Hydrocarbon Ganglia*. Transport in Porous Media, 2003. **52**(2): p. 229-266.
103. Zahoor, M., M. Derahman, and M. Yunan, *WAG Process Design—an Updated Review*. Brazilian Journal of Petroleum and Gas, 2011. **5**(2).
104. Dorostkar, M., et al., *A Laboratory Study of Hot WAG Injection into Fractured and Conventional Sand Packs*. Petroleum Science, 2009. **6**(4): p. 400-404.
105. Selamat, S.B., et al., *Evaluation and Optimization of Enhanced Oil Recovery by WAG Injection at Tapis and Guntong Fields, Malaysia*, in *SPE Enhanced Oil Recovery Conference*. 2011, Society of Petroleum Engineers: Kuala Lumpur, Malaysia.
106. Bond, D., I. Holbrook, and C. LACK, *Gas Drive Oil Recovery Process*. 1958, U.S. Patent 2866507.
107. Li, R.F., et al., *Foam Mobility Control for Surfactant EOR*, in *SPE Symposium on Improved Oil Recovery*. 2008, Society of Petroleum Engineers: Tulsa, Oklahoma, USA.
108. Xu, X., *A Novel CO₂ Flooding Based EOR for Sandstone Reservoirs*, in *Department of Petroleum Engineering*. 2016, Curtin University.
109. McLendon, W.J., et al., *Assessment of CO₂-Soluble Non-Ionic Surfactants for Mobility Reduction using Mobility Measurements and CT Imaging*. Journal of Petroleum Science and Engineering, 2014. **119**: p. 196-209.
110. Schievelbein, V.H., *Method for Decreasing Mobility of Dense Carbon Dioxide in Subterranean Formations*. 1991, U.S. Patent 5033547.
111. AlSumaiti, A.M., et al., *Laboratory Study of CO₂ Foam Flooding in High Temperature, High Salinity Carbonate Reservoirs Using Co-injection Technique*. Energy & Fuels, 2018. **32**(2): p. 1416-1422.
112. Haruki, M., et al., *Study on Phase Behaviors of Supercritical CO₂ Including Surfactant and Water*. Fluid Phase Equilibria, 2007. **261**(1): p. 92-98.
113. Ryoo, W., S.E. Webber, and K.P. Johnston, *Water-in-Carbon Dioxide Microemulsions with Methylated Branched Hydrocarbon Surfactants*. Industrial & Engineering Chemistry Research, 2003. **42**(25): p. 6348-6358.
114. Fan, X., et al., *Oxygenated Hydrocarbon Ionic Surfactants Exhibit CO₂ Solubility*. Journal of the American Chemical Society, 2005. **127**(33): p. 11754-11762.
115. Chen, Y., et al. *Ethoxylated Cationic Surfactants for CO₂ EOR in High Temperature, High Salinity Reservoirs*. in *SPE Improved Oil Recovery Symposium*. 2012. Tulsa, Oklahoma, USA Society of Petroleum Engineers.
116. Kuehne, D., et al. *Evaluation of Surfactants for CO₂ Mobility Control in Dolomite Reservoirs*. in *SPE/DOE Enhanced Oil Recovery Symposium*. 1992. Tulsa, Oklahoma: Society of Petroleum Engineers.
117. Radke, C.J. and J.V. Gillis, *A Dual Gas Tracer Technique for Determining Trapped Gas Saturation During Steady Foam Flow in Porous Media*, in *SPE Annual Technical Conference and Exhibition*. 1990, Society of Petroleum Engineers: New Orleans, Louisiana.
118. A. Gauglitz, P., et al., *Foam Generation in Homogeneous Porous Media*. Chemical Engineering Science, 2002. **57**(19): p. 4037-4052.
119. Blackwell, R., J. Rayne, and W. Terry, *Factors Influencing the Efficiency of Miscible Displacement*. Society of Petroleum Engineers Journal, 1959.

120. Xu, Q., *Theoretical and Experimental Study of Foam for Enhanced Oil Recovery and Acid Diversion*, in *Petroleum and Geosystems Engineering 2003*, University of Texas.
121. Schramm, L.L., *Surfactants: Fundamentals and Applications in the Petroleum Industry*. 2000: Cambridge University Press.
122. Schramm, L.L., *Foam Sensitivity to Crude Oil in Porous Media*. ACS Advances in Chemistry Series, 1994. **242**: p. 165-200.
123. Gillis, J. and C. Radke, *A Dual-Gas Tracer Technique for determining Trapped Gas Saturation during Steady Foam Flow in Porous Media*. 1990, University of California: Lawrence Berkeley National Laboratory.
124. Llana, O., *Mobility Control of Chemical EOR Fluids Using Foam in Highly Fractured Reservoirs in Faculty of the Graduate School*. 2011, The University of Texas at Austin.
125. Friedmann, F. and J. Jensen. *Some Parameters Influencing the Formation and Propagation of Foams in Porous Media*. in *SPE California Regional Meeting*. 1986. Oakland, California: Society of Petroleum Engineers.
126. Nguyen, Q.P., et al. *Experimental and Modeling Studies on Foam in Porous Media: a Review*. in *SPE International Symposium on Formation Damage Control*. 2000. Lafayette, Louisiana Society of Petroleum Engineers.
127. Wellington, S. and H. Vinegar. *CT Studies of Surfactant-Induced CO₂ Mobility Control*. in *SPE Annual Technical Conference and Exhibition*. 1985. Society of Petroleum Engineers.
128. Zhang, Y., P. Luo, and S.-S.S. Huang. *Improved Heavy Oil Recovery by CO₂ Injection Augmented with Chemicals*. in *International Oil and Gas Conference and Exhibition in China*. 2010. Beijing, China Society of Petroleum Engineers.
129. Farajzadeh, R., *Enhanced Transport Phenomena in CO₂ Sequestration and CO₂ EOR*, in *Faculty of Civil Engineering and Geosciences*. 2009, Delft University of Technology.
130. Rao, D., *Gas Injection EOR-A New Meaning in the New Millennium*. Journal of Canadian Petroleum Technology, 2001. **40**(02).
131. Charanjit, R. and G.G. Bernard, *Method of Secondary Recovery Employing Successive Foam Drives of Different ionic Characteristics*, U.O.C.o. California, Editor. 1967, U.S. Patent 3323588.
132. Marsden, S., *Foams in Porous Media*. 1986, Stanford Univ., CA (USA). Petroleum Research Inst.
133. Ayirala, S.C., *Surfactant-Induced Relative Permeability Modifications for Oil Recovery Enhancement*, in *Department of Petroleum Engineering*. 2002, Louisiana State University.
134. Zanganeh, M.N., *Simulation and Optimization of Foam EOR Processes*. 2011: Delft University of Technology.
135. Khatib, Z., G. Hirasaki, and A. Falls, *Effects of Capillary Pressure on Coalescence and Phase mobilities in Foams Flowing Through Porous Media*. SPE reservoir engineering, 1988. **3**(03): p. 919-926.
136. Zanganeh, M.N., et al., *The Method of Characteristics Applied to Oil Displacement by Foam*. SPE journal, 2011. **16**(01): p. 8-23.
137. Adkins, S.S., et al., *Morphology and Stability of CO₂-in-Water Foams with Nonionic Hydrocarbon Surfactants*. Langmuir, 2010. **26**(8): p. 5335-5348.
138. Liu, Y., R.B. Grigg, and B. Bai, *Salinity, pH, and Surfactant Concentration Effects on CO₂-Foam*, in *SPE International Symposium on Oilfield Chemistry*. 2005, Society of Petroleum Engineers: The Woodlands, Texas.
139. Handy, L.L., et al., *Thermal Stability of Surfactants for Reservoir Application (includes associated papers 11323 and 11597)*. Society of Petroleum Engineers Journal, 1982. **22**(05).
140. Mayberry, D.J. and S.I. Kam, *The use of Fractional-Flow Theory for Foam Displacement in Presence of Oil*. SPE Reservoir Evaluation & Engineering, 2008. **11**(04): p. 707-718.
141. Nikolov, A., et al. *The Effect of Oil on Foam Stability: Mechanisms and Implications for Oil Displacement by Foam in Porous Media*. in *SPE Annual Technical Conference and Exhibition*. 1986. New Orleans, Louisiana Society of Petroleum Engineers.
142. Law, D.-S., Z.-M. Yang, and T. Stone, *Effect of the Presence of Oil on Foam Performance: a Field Simulation Study*. SPE reservoir engineering, 1992. **7**(02): p. 228-236.
143. Chou, S.I., et al., *CO₂ Foam Field Trial at North Ward-Estes*, in *SPE Annual Technical Conference and Exhibition*. 1992, Society of Petroleum Engineers: Washington, D.C.
144. Enick, R.M., Olsen, D.K., *Mobility and Conformance Control for Carbon Dioxide Enhanced Oil Recovery (CO₂-EOR) via Thickeners, Foams, and Gels – A Detailed Literature Review of 40 Years of Research*. 2011, U.S. Dept. of Energy, National Energy Technology Laboratory(NETL): Tulsa.

145. Jonas, T.M., S.I. Chou, and S.L. Vasicek, *Evaluation of a CO₂ Foam Field Trial: Rangely Weber Sand Unit*, in *SPE Annual Technical Conference and Exhibition*. 1990, Society of Petroleum Engineers: New Orleans, Louisiana.
146. Stephenson, D.J., A.G. Graham, and R.W. Luhnig, *Mobility Control Experience in the Joffre Viking Miscible CO₂ Flood*. *SPE Reservoir Engineering*, 1993. **8**(03).
147. Heller, J., D. Boone, and R. Watts. *Testing CO₂-Foam for Mobility Control at Rock Creek*. in *SPE Eastern Regional Meeting*. 1985. Morgantown, West Virginia Society of Petroleum Engineers.
148. Stevens, J., *CO₂ Foam Field Verification Pilot Test at EVGSAU: Phase IIIB--Project Operations and Performance Review*. *SPE Reservoir Engineering*, 1995. **10**(04): p. 266-272.
149. Mukherjee, J., et al. *CO₂ Foam Pilot in Salt Creek Field, Natrona County, WY: Phase III: Analysis of Pilot Performance*. in *SPE improved oil recovery conference*. 2016. Tulsa, Oklahoma, USA: Society of Petroleum Engineers.
150. Sanders, A., et al. *Implementation of a CO₂ Foam Pilot Study in the SACROC Field: Performance Evaluation*. in *SPE annual technical conference and exhibition*. 2012. San Antonio, Texas, USA Society of Petroleum Engineers.
151. Janssen, A. *Enhanced Fluid Separation for Chemical Floods*. in *Proceedings of the SPE Chemical Flooding-EOR Workshop*. Penang, Malaysia, May 2012.
152. Razali, H. *General Requirement of Chemical EOR from HSE Perspectives*. in *Proceedings of the SPE-Chemical Flooding-EOR Workshop*. Penang, Malaysia, May. 2012.
153. Waldman, T. *Design Considerations for Chemical EOR Facilities*. in *Proceedings of the SPE-Advanced Technologies Workshop*. Penang, Malaysia, May. 2012.
154. Zain, T. *Storage, Logistic and Chemical Transferring in Offshore Environment*. in *Proceedings of the SPE-Chemical Flooding-EOR Workshop*. Penang, Malaysia, May. 2012.
155. Henderson, J., Meyer, W., Taber, J., *Miscible Drive Secondary Oil Recovery Process*. 1967, U.S. Patent 3330345.
156. Jianhang, X., *Carbon Dioxide Thickening Agents for Reduced CO₂ Mobility*. 2003, Pittsburgh: University of Pittsburgh.
157. Lee, J., et al. *Development of Small Molecule CO₂ Thickeners for EOR and Fracturing*. in *SPE Improved Oil Recovery Symposium*. 2014. Tulsa, Oklahoma, USA Society of Petroleum Engineers.
158. Kirby, C.F. and M.A. McHugh, *Phase Behavior of Polymers in Supercritical Fluid Solvents*. *Chemical Reviews*, 1999. **99**(2): p. 565-602.
159. Enick, R.M., et al., *Direct Thickeners for Carbon Dioxide*, in *SPE/DOE Improved Oil Recovery Symposium*. 2000, Society of Petroleum Engineers: Tulsa, Oklahoma
160. Enick, R.M., E.J. Beckman, and A. Hamilton, *Novel CO₂-Thickeners for Improved Mobility Control*. 2001, University of Pittsburgh (US): U.S. Department of Energy Office of Scientific and Technical Information
161. Wang, Y., et al., *Design and Evaluation of Nonfluorous CO₂-Soluble Oligomers and Polymers*. *The Journal of Physical Chemistry B*, 2009. **113**(45): p. 14971-14980.
162. Tapriyal, D., *Design of non-Fluorous Carbon Dioxide Soluble Compounds*. 2009, University of Pittsburgh.
163. Zhang, J., et al. *A New Thickener for CO₂ Anhydrous Fracturing Fluid*. in *MATEC Web of Conferences*. 2015. EDP Sciences.
164. DHUWE, A., *Thickeners for Natural Gas Liquids to Improve the Performance in Enhanced Oil Recovery and Dry Hydraulic Fracking*. 2016, University of Pittsburgh.
165. Kilic, S., et al., *Phase Behavior of Oxygen-Containing Polymers in CO₂*. *Macromolecules*, 2007. **40**(4): p. 1332-1341.
166. Shi, C., et al., *Semi-Fluorinated Trialkyltin Fluorides and Fluorinated Telechelic Ionomers as Viscosity-Enhancing Agents for Carbon Dioxide*. *Industrial & Engineering Chemistry Research*, 2001. **40**(3): p. 908-913.
167. O'Brien, M.J., et al., *Anthraquinone Siloxanes as Thickening Agents for Supercritical CO₂*. *Energy & Fuels*, 2016. **30**(7): p. 5990-5998.
168. Enick, R.M. and J. Ammer, *A literature Review of Attempts to Increase the Viscosity of Dense Carbon Dioxide*. 1998: Website of the National Energy Technology Laboratory.
169. Dai, C., et al., *Impairment Mechanism of Thickened Supercritical Carbon Dioxide Fracturing Fluid in Tight Sandstone Gas Reservoirs*. *Fuel*, 2018. **211**: p. 60-66.
170. Huang, Z., et al., *Enhancement of the Viscosity of Carbon Dioxide Using Styrene/Fluoroacrylate Copolymers*. *Macromolecules*, 2000. **33**(15): p. 5437-5442.

171. Martini, A., U.S. Ramasamy, and M. Len, *Review of Viscosity Modifier Lubricant Additives*. Tribology Letters, 2018. **66**(2): p. 58.
172. Lee, J., *Small Molecule Associative CO₂ Thickeners for Improved Mobility Control*. 2017, University of Pittsburgh.
173. Dandge, D., et al., *Kinetics of 1-Hexene Polymerization*. Journal of Applied Polymer Science, 1986. **32**(6): p. 5373-5383.
174. Heller, J., F. Kovarik, and J. Taber, *Improvement of CO₂ Flood Performance-Annual Report 1985*. 1986.
175. Heller, J., F. Kovarik, and J. Taber, *Improvement of CO₂ Flood Performance-Annual Report 1985*. 1986.
176. Heller, J.P., F. Kovarik, and J.J. Taber, *Improvement of CO₂ Flood Performance: Third Annual Report*. 1989, New Mexico Inst. of Mining and Technology, Socorro (USA). New Mexico Petroleum Recovery Research Center.
177. Martin, F. and J. Heller, *Improvement of CO₂ Flood Performance-Quarterly Report Jan.-March 1990*. PRRC, 1990. **2**: p. 90-20.
178. Zhang, S., Y. She, and Y. Gu, *Evaluation of Polymers as Direct Thickeners for CO₂ Enhanced Oil Recovery*. Journal of Chemical & Engineering Data, 2011. **56**(4): p. 1069-1079.
179. Bullen, R.S., J. Mzik, and J.P. Richard, *Novel Compositions Suitable for Treating Deep Wells*, C.F. Ltd, Editor. 1987, U.S Patent 4701270.
180. Sarbu, T., T.J. Styranec, and E.J. Beckman, *Design and Synthesis of Low Cost, Sustainable CO₂-Philes*. Industrial & Engineering Chemistry Research, 2000. **39**(12): p. 4678-4683.
181. Cullick, A.S., *Enhanced Oil Recovery Using Carbon Dioxide*, E.O. Corp, Editor. 1986, U.S.Patent 4609043.
182. Liave, F.M., F.T.H. Chung, and T.E. Burchfield, *Use of Entrainers in Improving Mobility Control of Supercritical CO₂*. SPE Reservoir Engineering, 1990. **5**(01).
183. Holtmyer, M.D. and C.V. Hunt, *Non-Aqueous Viscosified Carbon Dioxide and Method of Use*, D. Halliburton Company, Okla, Editor. 1990, U.S Patent 4964467.
184. Harris, T.V., C.A. Irani, and W.R. Pretzer, *Enhanced Oil Recovery Using CO₂ Flooding*, C.R.a.T. Co, Editor. 1990, U.S Patent 4913235A.
185. Bae, J.H., *Viscosified CO₂ Process: Chemical Transport and other Issues*, in *SPE International Symposium on Oilfield Chemistry*. 1995, Society of Petroleum Engineers: San Antonio, Texas.
186. Williams, L.L., J.B. Rubin, and H.W. Edwards, *Calculation of Hansen Solubility Parameter Values for a Range of Pressure and Temperature Conditions, Including the Supercritical Fluid Region*. Industrial & Engineering Chemistry Research, 2004. **43**(16): p. 4967-4972.
187. Cai, S., *Study of CO₂ Mobility Control Using Cross-linked Gel Conformance Control and CO₂ Viscosifiers in Heterogeneous Media*. 2011, Texas A & M University.
188. Al Yousef, Z., *Study of CO₂ Mobility Control in Heterogeneous Media Using CO₂ Thickening Agents*. 2012, Texas A & M University.
189. Shen, Z., et al., *CO₂-solubility of Oligomers and Polymers that Contain the Carbonyl Group*. Polymer, 2003. **44**(5): p. 1491-1498.
190. McClain, J., et al. *Characterization of Polymers and Amphiphiles in Supercritical CO₂ using Small Angle Neutron Scattering and Viscometry*. in *proceeding of 1996 Spring meeting of ACS, Diveivision of Polymeric materials*. 1996. AMER CHEMICAL SOC 1155 16TH ST, NW, WASHINGTON, DC 20036.
191. Xu, J. and R.M. Enick. *Thickening Carbon Dioxide with the Fluoroacrylate-Styrene Copolymer*. in *SPE Annual Technical Conference and Exhibition*. 2001. New Orleans, Louisiana: Society of Petroleum Engineers.
192. Kilic, S., et al., *Influence of Tert-Amine Groups on the Solubility of Polymers in CO₂*. Polymer, 2009. **50**(11): p. 2436-2444.
193. Potluri, V.K., et al., *The High CO₂-Solubility of Per-acetylated α -, β -, and γ -Cyclodextrin*. Fluid Phase Equilibria, 2003. **211**(2): p. 211-217.
194. Hong, L., M.C. Thies, and R.M. Enick, *Global Phase Behavior for CO₂-Phylic Solids: the CO₂+ β -d-Maltose Octaacetate System*. The Journal of supercritical fluids, 2005. **34**(1): p. 11-16.
195. Potluri, V.K., et al., *Peracetylated Sugar Derivatives Show High Solubility in Liquid and Supercritical Carbon Dioxide*. Organic Letters, 2002. **4**(14): p. 2333-2335.
196. Drohmann, C. and E.J. Beckman, *Phase Behavior of Polymers Containing Ether Groups in Carbon Dioxide*. The Journal of Supercritical Fluids, 2002. **22**(2): p. 103-110.

197. Tapriyal, D., et al., *Poly(Vinyl Acetate), Poly((1-O-(Vinylloxy) Ethyl-2,3,4,6-tetra-O-Acetyl- β -D-Glucopyranoside) and Amorphous Poly(Lactic Acid) are the most CO₂-Soluble Oxygenated Hydrocarbon-Based Polymers*. The Journal of Supercritical Fluids, 2008. **46**(3): p. 252-257.
198. Heller JP, K.F., *Improvement of CO₂ Flood Performance: Fourth Annual Report for the Period of Oct. 1, 1987–Sept. 30, 1988*. 1988, New Mexico Petroleum Recovery Research Centre.
199. Babu, S.S., V.K. Praveen, and A. Ajayaghosh, *Functional π -Gelators and Their Applications*. Chemical Reviews, 2014. **114**(4): p. 1973-2129.
200. Terech, P. and R.G. Weiss, *Low Molecular Mass Gelators of Organic Liquids and the Properties of their Gels*. Chemical reviews, 1997. **97**(8): p. 3133-3160.
201. Escuder, B. and J.F. Miravet, *Silk-Inspired Low-Molecular-Weight Organogelator*. Langmuir, 2006. **22**(18): p. 7793-7797.
202. Terech, P., et al., *Structural Variations in a Family of Orthodialkoxyarenes Organogelators*. Journal of colloid and interface science, 2006. **302**(2): p. 633-642.
203. Trickett, K., et al., *Rod-like micelles thicken CO₂*. Langmuir, 2009. **26**(1): p. 83-88.
204. John, C., *Structure of Cobalt Aerosol-OT Reversed Micelles Studied by Small-Angle Scattering Methods*. Journal of the Chemical Society, Faraday Transactions, 1994. **90**(17): p. 2497-2504.
205. Hirst, A.R., et al., *Low-Molecular-Weight Gelators: Elucidating the Principles of Gelation Based on Gelator Solubility and a Cooperative Self-Assembly Model*. Journal of the American Chemical Society, 2008. **130**(28): p. 9113-9121.
206. Hanabusa, K., et al., *Two-Component, Small Molecule Gelling Agents*. Journal of the Chemical Society, Chemical Communications, 1993(18): p. 1382-1384.
207. Stals, P.J., et al., *The Influence of Oligo (Ethylene Glycol) Side Chains on the Self-Assembly of Benzene-1, 3, 5-Tricarboxamides in the Solid State and in Solution*. Journal of Materials Chemistry, 2009. **19**(1): p. 124-130.
208. Iezzi, A., R. Enick, and J. Brady, *Direct Viscosity Enhancement of Carbon Dioxide*, in *Supercritical Fluid Science and Technology*. 1989, American Chemical Society. p. 122-139.
209. Johnston, K.P. and J.M.L. Penninger, *Supercritical Fluid Science and Technology*. ACS Symposium Series. Vol. 406. 1989: American Chemical Society. 564.
210. Dandge, D.K., et al., *Associative Organotin Polymers. 2. Solution Properties of Symmetric Trialkyltin Fluorides*. Journal of Macromolecular Science: Part A - Chemistry, 1989. **26**(10): p. 1451-1464.
211. Fieser, L.F., et al., *Napalm*. Industrial & Engineering Chemistry, 1946. **38**(8): p. 768-773.
212. Hughes, M., *Book Review: Napalm: An American Biography by Robert M. Neer*. War in History, 2014. **21**(4): p. 560-562.
213. Mysels, K.J., *Napalm. Mixture of Aluminum Disoaps*. Industrial & Engineering Chemistry, 1949. **41**(7): p. 1435-1438.
214. Koide, K., *Latex Composition Comprising a Cross-Linking Agent and Molded Product Thereof*. 2008, U.S. Patent 20080227913A1.
215. Lewis, P., *An Attempt to Increase the Viscosity of CO₂ with Metallic Stearates*. 1990, University of Pittsburgh.
216. Iezzi, A., et al., *'Gel' Formation in Carbon Dioxide-Semifluorinated Alkane Mixtures and Phase Equilibria of a Carbon Dioxide-Perfluorinated Alkane Mixture*. Fluid Phase Equilibria, 1989. **52**: p. 307-317.
217. Gullapalli, P., J.-S. Tsau, and J.P. Heller, *Gelling Behavior of 12-Hydroxystearic Acid in Organic Fluids and Dense CO₂*, in *SPE International Symposium on Oilfield Chemistry*. 1995, Society of Petroleum Engineers: San Antonio, Texas. p. 13.
218. Shi, C., et al., *The Gelation of CO₂ : A Sustainable Route to the Creation of Microcellular Materials*. Science, 1999. **286**(5444): p. 1540-1543.
219. Paik, I.H., et al., *Fiber Formation by Highly CO₂-Soluble Bisureas Containing Peracetylated Carbohydrate Groups*. Angewandte Chemie International Edition, 2007. **46**(18): p. 3284-3287.
220. Eastoe, J., et al., *Variation of Surfactant Counterion and its Effect on the Structure and Properties of Aerosol-OT-Based Water-in-Oil Microemulsions*. Journal of the Chemical Society, Faraday Transactions, 1992. **88**(3): p. 461-471.
221. Eastoe, J., et al., *Structures of Metal Bis (2-Ethylhexylsulfosuccinate) Aggregates in Cyclohexane*. The Journal of Physical Chemistry, 1993. **97**(7): p. 1459-1463.
222. Cummings, S., et al., *Design Principles for Supercritical CO₂ Viscosifiers*. Soft Matter, 2012. **8**(26): p. 7044-7055.
223. Eastoe, J., et al., *Water-in-CO₂ Microemulsions Studied by Small-Angle Neutron Scattering*. Langmuir, 1997. **13**(26): p. 6980-6984.

224. Eastoe, J., S. Gold, and D.C. Steytler, *Surfactants for CO₂*. *Langmuir*, 2006. **22**(24): p. 9832-9842.
225. Eastoe, J., et al., *Effects of Fluorocarbon Surfactant Chain Structure on Stability of Water-in-Carbon Dioxide Microemulsions. Links Between Aqueous Surface Tension and Microemulsion Stability*. *Langmuir*, 2002. **18**(8): p. 3014-3017.
226. Liu, Z.-T. and C. Erkey, *Water in Carbon Dioxide Microemulsions with Fluorinated Analogues of AOT*. *Langmuir*, 2001. **17**(2): p. 274-277.
227. Doherty, M.D., et al., *Small Molecule Cyclic Amide and Urea Based Thickeners for Organic and sc-CO₂/Organic Solutions*. *Energy & Fuels*, 2016. **30**(7): p. 5601-5610.
228. Lee, J.J., et al., *Development of Small Molecule CO₂ Thickeners for EOR and Fracturing*, in *SPE Improved Oil Recovery Symposium*. 2014, Society of Petroleum Engineers: Tulsa, Oklahoma, USA
229. Koottungal, L., *Survey: Miscible CO₂ Continues to Eclipse Steam in US EOR Production*. *Oil Gas J*, 2014. **112**(4): p. 78-91.
230. Jaber, A.K. and M.B. Awang, *Field-Scale Investigation of Different Miscible CO₂-Injection Modes to Improve Oil Recovery in a Clastic Highly Heterogeneous Reservoir*. *Journal of Petroleum Exploration and Production Technology*, 2017. **7**(1): p. 125-146.
231. Dhuwe, A., et al., *Assessment of Solubility and Viscosity of Ultra-High Molecular Weight Polymeric Thickeners in Ethane, Propane and Butane for Miscible EOR*. *Journal of Petroleum Science and Engineering*, 2016. **145**: p. 266-278.
232. Dindar, C., *High-Pressure Viscosity and Density of Polymer Solutions at the Critical Polymer Concentration in Near-Critical and Supercritical Fluids*, in *Chemical Engineering*. 2001, Virginia Polytechnic Institute and State University.
233. Dindar, C. and E. Kiran, *High-Pressure Viscosity and Density of Polymer Solutions at the Critical Polymer Concentration in Near-Critical and Supercritical Fluids*. *Industrial & Engineering Chemistry Research*, 2002. **41**(25): p. 6354-6362.
234. Wu, M.M., *Process for Manufacturing Olefinic Oligomers having Lubricating Properties*. 1989, U.S. Patents 4827073A.
235. Zolper, T., et al., *Lubrication Properties of Polyalphaolefin and Polysiloxane Lubricants: Molecular Structure–Tribology Relationships*. *Tribology Letters*, 2012. **48**(3): p. 355-365.
236. Dunn, P. and D. Oldfield, *Tri-n-Butyltin Fluoride. A Novel Coordination Polymer in Solution*. *Journal of Macromolecular Science: Part A - Chemistry*, 1970. **4**(5): p. 1157-1168.
237. Van Den Berghe, E.V. and G.P. Van Der Kelen, *A Study of the Chemical Bond in (CH₃)_nSn(SCH₃)_{4-n} (n=0, 1, 2, 3) by nmr (1H, 119Sn, 13C) Spectroscopy*. *Journal of Organometallic Chemistry*, 1971. **26**(2): p. 207-213.
238. Smith, K.W. and L.J. Persinski, *Hydrocarbon Gels Useful in Formation Fracturing*, C. Inc, Editor. 1996, U.S Patents 5571315A.
239. Smith, K.W. and L.J. Persinski, *Hydrocarbon Gels Useful in Formation Fracturing*, C. Inc, Editor. 1997, U.S Patent 5614010.
240. Taylor, R.S. and G.P. Funkhouser, *Methods and compositions for treating subterranean formations with gelled hydrocarbon fluids*, H.E.S. Inc, Editor. 2003, U.S. Patent 6511944.
241. Taylor, R.S. and G.P. Funkhouser, *Methods and compositions for treating subterranean formations with gelled hydrocarbon fluids*, H.E.S. Inc, Editor. 2008, U.S. Patent 7314850.
242. Taylor, R.S., et al., *Compositions and methods for treating subterranean formations with liquefied petroleum gas*, C.U.I.E.S. Inc, Editor. 2008, U.S. Patent 7341103.
243. Delgado, E. and B. Keown, *Low Volatile Phosphorous Gelling Agent*. 2013, U.S. Patents 8377854B2.
244. Taylor, R., et al., *Optimized Gas-Well Stimulating Using CO₂-Miscible, Viscosified Hydrocarbon Fracturing Fluids*, in *SPE Gas Technology Symposium*. 2002, Society of Petroleum Engineers: Calgary, Alberta, Canada. p. 8.
245. Taylor, R.S., et al., *Rheological Evaluations of CO Miscible Hydrocarbon Fracturing Fluids*, in *Canadian International Petroleum Conference*. 2005, Petroleum Society of Canada: Calgary, Alberta. p. 8.
246. George, M., G.P. Funkhouser, and R.G. Weiss, *Organogels with Complexes of Ions and Phosphorus-Containing Amphiphiles as Gelators. Spontaneous Gelation by in Situ Complexation*. *Langmuir*, 2008. **24**(7): p. 3537-3544.
247. Gong, Y. and Y. Gu, *Miscible CO₂ Simultaneous Water-and-Gas (CO₂-SWAG) Injection in the Bakken Formation*. *Energy & Fuels*, 2015. **29**(9): p. 5655-5665.
248. Lansangan, R. and J. Smith, *Viscosity, Density, and Composition Measurements of CO₂/West Texas Oil Systems*. *SPE reservoir engineering*, 1993. **8**(03): p. 175-182.

249. Ashcroft, S.J. and M.B. Isa, *Effect of Dissolved Gases on the Densities of Hydrocarbons*. Journal of Chemical & Engineering Data, 1997. **42**(6): p. 1244-1248.
250. Bon, J. and H. Sarma. *Investigation of the Effect of Injection Gas Composition on CO₂-rich Flooding and its Implications in an Onshore Australia Oilfield*. in *Canadian International Petroleum Conference*. 2009. Petroleum Society of Canada.
251. Saryazdi, F., et al., *Density of Hydrocarbon Mixtures and Bitumen Diluted with Solvents and Dissolved Gases*. Energy & Fuels, 2013. **27**(7): p. 3666-3678.
252. Tabasinejad, F., et al. *Density of High Pressure and Temperature Gas Reservoirs: Effect of non-Hydrocarbon Contaminants on Density of Natural Gas Mixtures*. in *SPE Western Regional Meeting*. 2010. California, USA: Society of Petroleum Engineers.
253. Li, H., S. Zheng, and D. Yang, *Enhanced Swelling Effect and Viscosity Reduction of Solvent(s)/CO₂/Heavy-Oil Systems*. SPE Journal. **18**(04): p. 695-707.
254. Abedini, A. and F. Torabi, *On the CO₂ Storage Potential of Cyclic CO₂ Injection Process for Enhanced Oil Recovery*. Fuel, 2014. **124**: p. 14-27.
255. Ding, M., et al., *Mutual Interactions of CO₂/Oil and Natural Gas/Oil Systems and Their Effects on the EOR Process*. Petroleum Science and Technology, 2015. **33**(23-24): p. 1890-1900.
256. Bon, J. and H. Sarma. *A technical Evaluation of a CO₂ Flood for EOR Benefits in the Cooper Basin, South Australia*. in *SPE Asia Pacific Oil and Gas Conference and Exhibition*. 2004. Perth, Australia: Society of Petroleum Engineers.
257. Thomas, S., *Enhanced Oil Recovery-an Overview*. Oil & Gas Science and Technology-Revue de l'IFP, 2008. **63**(1): p. 9-19.
258. Alagorni, A.H., Z.B. Yaacob, and A.H. Nour, *An Overview of Oil Production Stages: Enhanced Oil Recovery Techniques and Nitrogen Injection*. International Journal of Environmental Science and Development, 2015. **6**(9): p. 693.
259. Memon, A.I., et al. *Miscible Gas Injection and Asphaltene Flow Assurance Fluid Characterization: A Laboratory Case Study for Black Oil Reservoir*. in *SPE EOR Conference at Oil and Gas West Asia*. 2012. Muscat, Oman: Society of Petroleum Engineers.
260. Al-Wahaibi, Y.M., *First-Contact-Miscible and Multicontact-Miscible Gas Injection within a Channeling Heterogeneity System*. Energy & Fuels, 2010. **24**(3): p. 1813-1821.
261. Mandel, F., M. McHugh, and J. Don Wang, *Supercritical Fluid Processing of Polymeric Materials*, in *Supercritical Fluid Technology in Materials Science and Engineering*. 2002, CRC Press.
262. Burgers, W., et al., *Worldwide Development Potential for Sour Gas*. Energy Procedia, 2011. **4**: p. 2178-2184.
263. Smith, S.A., et al., *Acid Gas Injection and Monitoring at the Zama Oil Field in Alberta, Canada: A Case Study in Demonstration-Scale Carbon Dioxide Sequestration*. Energy Procedia, 2009. **1**(1): p. 1981-1988.
264. Bedrikov, P. and K. Basniev. *Petroleum Engineering Challenges of the Development of Precaspian Depression Fields (Kazakhstan, Russia)*. in *14th World Petroleum Congress*. 1994. Stavanger, Norway: World Petroleum Congress.
265. Bray, C.L., et al., *High-Throughput Solubility Measurements of Polymer Libraries in Supercritical Carbon Dioxide*. Journal of Materials Chemistry, 2005. **15**(4): p. 456-459.
266. Licence, P., et al., *Large-Aperture Variable-Volume View Cell for the Determination of Phase-Equilibria in High Pressure Systems and Supercritical Fluids*. Review of scientific instruments, 2004. **75**(10): p. 3233-3236.
267. Tan, B., C.L. Bray, and A.I. Cooper, *Fractionation of Poly (Vinyl Acetate) and the Phase Behavior of End-Group Modified Oligo (Vinyl Acetate) s in CO₂*. Macromolecules, 2009. **42**(20): p. 7945-7952.
268. Miller, M.B., et al., *Solid CO₂-philes as Potential Phase-Change Physical Solvents for CO₂*. The Journal of Supercritical Fluids, 2012. **61**: p. 212-220.
269. Economou, I.G., et al., *Solubility of Gases and Solvents in Silicon Polymers: Molecular Simulation and Equation of State Modeling*. Molecular Simulation, 2007. **33**(9-10): p. 851-860.
270. Zeman, L., et al., *Pressure Effects in Polymer Solution Phase Equilibriums. I. Lower Critical Solution Temperature of Poly(isobutylene) and Poly(dimethylSiloxane) in Lower Alkanes*. The Journal of Physical Chemistry, 1972. **76**(8): p. 1206-1213.
271. Small, P., *Some Factors Affecting the Solubility of Polymers*. Journal of Applied Chemistry, 1953. **3**(2): p. 71-80.
272. Rindfleisch, F., T.P. DiNoia, and M.A. McHugh, *Solubility of Polymers and Copolymers in Supercritical CO₂*. The Journal of Physical Chemistry, 1996. **100**(38): p. 15581-15587.

273. Speight, J. and D.I. Exall, *Refining Used Lubricating Oils*. 2014: CRC Press.
274. Hoefling, T., R. Enick, and E. Beckman, *Microemulsions in near-critical and supercritical carbon dioxide*. The Journal of Physical Chemistry, 1991. **95**(19): p. 7127-7129.
275. Dris, G. and S. Barton. *Polymer adsorption from supercritical fluids*. in *ABSTRACTS OF PAPERS OF THE AMERICAN CHEMICAL SOCIETY*. 1996. AMER CHEMICAL SOC 1155 16TH ST, NW, WASHINGTON, DC 20036.
276. Zhao, X., R. Watkins, and S. Barton, *Strategies for supercritical CO₂ fractionation of polydimethylsiloxane*. Journal of applied polymer science, 1995. **55**(5): p. 773-778.
277. Garg, A., E. Gulari, and C.W. Manke, *Thermodynamics of Polymer Melts Swollen with Supercritical Gases*. Macromolecules, 1994. **27**(20): p. 5643-5653.
278. Lee, J.J., et al., *The solubility of Low Molecular Weight Poly(Dimethyl Siloxane) in Dense CO₂ and its use as a CO₂-Philic Segment*. The Journal of Supercritical Fluids, 2017. **119**: p. 17-25.
279. Sagdeev, D.I., et al., *Simultaneous Measurements of the Density and Viscosity of 1-Hexene+ 1-Decene Mixtures at High Temperatures and High Pressures*. Journal of Molecular Liquids, 2014. **197**: p. 160-170.
280. Sagdeev, D.I., et al., *Experimental Study of the Density and Viscosity of 1-Octene and 1-Decene at High Temperatures and High Pressures*. High Temperatures--High Pressures, 2013. **42**(6).
281. Totten, G.E., S.R. Westbrook, and R.J. Shah, *Fuels and Lubricants Handbook: Technology, Properties, Performance, and Testing*. 2003: American Society for Testing & Materials.
282. Selby, T.W., *The Non-Newtonian Characteristics of Lubricating Oils*. A S L E Transactions, 1958. **1**(1): p. 68-81.
283. Ho; Suzzy C., W.M.M., *Process for Improving Thermal Stability of Synthetic Lubes*. 1990, U.S. Patent 4,967,032
284. Wu, M.M., *High Viscosity Index Synthetic Lubricant Compositions*. 1989, U.S. Patent 4,827,064.
285. Dandekar, A.Y., *Petroleum Reservoir Rock and Fluid Properties*. 2006, Boca Raton, FL: Boca Raton, FL : CRC/Taylor & Francis.
286. Larsen, J.K. and I.L. Fabricius, *Interpretation of Water Saturation Above the Transitional Zone in Chalk Reservoirs*. SPE Reservoir Evaluation & Engineering, 2004. **7**(02): p. 155-163.
287. Bloomfield, V.A. and R.K. Dewan, *VISCOSITY OF LIQUID MIXTURES*. Journal of Physical Chemistry, 1971. **75**(20): p. 3113-+.
288. Al Hinai, N.M., et al., *Experimental Study of Miscible Thickened Natural Gas Injection for Enhanced Oil Recovery*. Energy & Fuels, 2017. **31**(5): p. 4951-4965.
289. Gallo, G. and E. Erdmann, *Simulation of Viscosity Enhanced CO₂ Nanofluid Alternating Gas in Light Oil Reservoirs*, in *SPE Latin America and Caribbean Petroleum Engineering Conference*. 2017, Society of Petroleum Engineers: Buenos Aires, Argentina
290. Wang, B., et al., *Effect of Temperature on the Free Volume in Glassy Poly(Ethylene Terephthalate)*. Macromolecules, 2002. **35**(10): p. 3993-3996.
291. Kraska, T., et al., *Correlation of the solubility of low-volatile organic compounds in near- and supercritical fluids. Part 1: applications to adamantane and beta-carotene*. Journal of Supercritical Fluids, 2002. **23**(3): p. 209-224.
292. Seeton, C.J., *Viscosity-temperature correlation for liquids*. Tribology Letters, 2006. **22**(1): p. 67-78.
293. Kumar, J., E. Draoui, and S. Takahashi, *Design of CO₂ Injection Pilot in Offshore Middle East Carbonate Reservoir*, in *SPE EOR Conference at Oil and Gas West Asia*. 2016, Society of Petroleum Engineers: Muscat, Oman.
294. P.J. Linstrom and W.G. Mallard, E. *NIST Chemistry WebBook, NIST Standard Reference Database Number 69*. July 23, 2017 [cited 2018 March 05, 2018]; Available from: doi:10.18434/T4D303.
295. Jelinska, N., et al., *Poly (Vinyl Alcohol)/Poly (Vinyl Acetate) Blend Films*. Sci. J. of Riga Techn. Univ., Mater. Sci. Appl. Chem, 2010. **1**: p. 55-61.
296. Fragiadakis, D. and J. Runt, *Microstructure and Dynamics of Semicrystalline Poly (Ethylene Oxide)- Poly (Vinyl Acetate) Blends*. Macromolecules, 2009. **43**(2): p. 1028-1034.
297. Sato, T. and T. Okaya, *Characterization and Physical Properties of Low Molecular Weight Poly (Vinyl Acetate) and Poly (Vinyl Alcohol)*. Polymer journal, 1992. **24**(9): p. 849-856.
298. Pieliowski, K. and K. Flejtuch, *Differential Scanning Calorimetry Studies on Poly (Ethylene Glycol) with Different Molecular Weights for Thermal Energy Storage Materials*. Polymers for Advanced Technologies, 2002. **13**(10-12): p. 690-696.

299. Kearney, A.S., et al., *Effect of Polyvinylpyrrolidone on the Crystallinity and Dissolution Rate of Solid Dispersions of the Antiinflammatory CI-987*. International journal of pharmaceutics, 1994. **104**(2): p. 169-174.
300. Su, M., et al., *Remarkable Crystallization Morphologies of Poly (4-Vinylpyridine) on Single-Walled Carbon Nanotubes in CO₂-Expanded Liquids*. eXPRESS Polym. Lett., 2011. **5**: p. 1102-1112.
301. Stroupe, J. and R. Hughes, *The Structure of Crystalline Poly-(Methyl Methacrylate)*. Journal of the American Chemical Society, 1958. **80**(9): p. 2341-2342.
302. Wu, B.-G. and J.W. Doane, *Liquid Crystalline-Plastic Material having Submillisecond Switch Times and Extended Memory*. 1987, U.S. Patents 4,671,618.
303. Trivedi, M.K., et al., *Influence of Biofield Treatment on Physicochemical Properties of Hydroxyethyl Cellulose and Hydroxypropyl Cellulose*. Molecular Pharmaceutics & Organic Process Research, 2015. **3**(2).
304. Kamath, P.M. and R.W. Wakefield, *Crystallinity of Ethylene-Vinyl Acetate Copolymers*. Journal of Applied Polymer Science, 1965. **9**(9): p. 3153-3160.
305. Lee, S.H., M. Yoshioka, and N. Shiraishi, *Polymer Blend of Cellulose Acetate Butyrate and Aliphatic Polyestercarbonate*. Journal of applied polymer science, 2000. **77**(13): p. 2908-2914.
306. Rocco, A.M., R.P. Pereira, and M.I. Felisberti, *Miscibility, Crystallinity and Morphological Behavior of Binary Blends of Poly(Ethylene Oxide) and Poly(Methyl Vinyl Ether-Maleic Acid)*. Polymer, 2001. **42**(12): p. 5199-5205.
307. Sandler, S.R., *Polymer Syntheses Volume II Stanley R. Sandler, Wolf Karo*. 2nd ed.. ed. Polymer Syntheses Volume 2, ed. W. Karo. 1997, San Diego, Calif.: San Diego, Calif. : Academic Press.
308. Schildknecht, C., et al., *Polyvinyl Isobutyl Ethers*. Industrial & Engineering Chemistry, 1948. **40**(11): p. 2104-2115.
309. Roch, K.M. and J. Saunders, *Crystalline Polyisobutyl Vinyl Ether*. Journal of Polymer Science, 1959. **38**(134): p. 554-555.
310. Sundararajan, P., *Crystalline Morphology of Poly (Dimethylsiloxane)*. Polymer, 2002. **43**(5): p. 1691-1693.
311. Albouy, P.-A., *The Conformation of Poly (dimethylsiloxane) in the Crystalline State*. Polymer, 2000. **41**(8): p. 3083-3086.
312. Roland, C. and C. Aronson, *Crystallization of Polydimethylsiloxane end-Linked Networks*. Polymer Bulletin, 2000. **45**(4): p. 439-445.
313. Ikehara, T., D. Ito, and T. Kataoka, *Analysis of the degree of crystallinity in interpenetrating spherulites of poly (ethylene succinate) and poly (ethylene oxide) blends using pulsed NMR*. Polymer Journal, 2015. **47**(5): p. 379-384.
314. Qiu, Z., T. Ikehara, and T. Nishi, *Crystallization Behaviour of Biodegradable Poly(Ethylene Succinate) from the Amorphous State*. Polymer, 2003. **44**(18): p. 5429-5437.
315. Qiu, Z., T. Ikehara, and T. Nishi, *Miscibility and Crystallization in Crystalline/Crystalline Blends of Poly (Butylene Succinate)/Poly (Ethylene Oxide)*. Polymer, 2003. **44**(9): p. 2799-2806.
316. Malanga, M. and O. Vogl, *Head to Head Polymers. XXV: Properties of Head to Head Polyisobutylene*. Polymer Engineering & Science, 1983. **23**(10): p. 597-600.
317. Maron, S.H. and C.A. Daniels, *Thermodynamics of Polyisobutylene Solutions. III. Thermal Behavior and Polymer Order*. Journal of Macromolecular Science, Part B: Physics, 1968. **2**(4): p. 591-602.
318. Slowikowska, I., et al., *Studies of the Crystalline Structure of Stretched Polyisobutylene*. Polymer Journal, 1976. **8**(2): p. 221-224.
319. Sant'Angelo, J.G., *Substantially Crystalline Poly (Alkylene Carbonates), Laminate and Methods of Making*. 1996, U.S. Patent 5,536,806.
320. Dimaio, A.J., et al., *Process for Producing Liquid Polyalphaolefin Polymer, Metallocene Catalyst therefore, the Resulting Polymer and Lubricant Containing Same*. 2005, U.S Patent 6,858,767.
321. Fahmy, S.M., *Solubility of Fluorinated Polymers in Supercritical Carbon Dioxide*. 2005, Tesis Doctoral. 2005, Universidad Técnica de Rheinisch-Westfälischen.: Aachen, Alemania.
322. O'Neill, M.L., et al., *Solubility of Homopolymers and Copolymers in Carbon Dioxide*. Industrial & Engineering Chemistry Research, 1998. **37**(8): p. 3067-3079.
323. Kiran, E. and K. Liu, *The Miscibility and Phase Behavior of Polyethylene with Poly(dimethylsiloxane) in Near-Critical Pentane*. Korean Journal of Chemical Engineering, 2002. **19**(1): p. 153-158.

324. Bayraktar, Z. and E. Kiran, *Miscibility, Phase Separation, and Volumetric Properties in Solutions of Poly (dimethylsiloxane) in Supercritical Carbon Dioxide*. Journal of applied polymer science, 2000. **75**(11): p. 1397-1403.
325. Patterson, D., *Free Volume and Polymer Solubility. A Qualitative View*. Macromolecules, 1969. **2**(6): p. 672-677.
326. McHugh, M.A., J. Wang, and F. Mandel, *Supercritical Fluid Processing of Polymeric Materials*. 2002: Marcel Dekker: New York.
327. Watts, R. and C. Komar, *Gas Miscible Displacement Enhanced Oil Recovery: Technology Status Report*. 1989, USDOE Morgantown Energy Technology Center, WV (USA).
328. Bayat, M., et al., *Investigation of Gas Injection Flooding Performance as Enhanced Oil Recovery Method*. Journal of Natural Gas Science and Engineering, 2016. **29**: p. 37-45.
329. Manrique, E.J., et al. *EOR: Current Status and Opportunities*. in *SPE improved oil recovery symposium*. 2010. Tulsa, Oklahoma, USA: Society of Petroleum Engineers.
330. Araktingi, U.G. and F.M. Orr, Jr., *Viscous Fingering, Gravity Segregation, and Reservoir Heterogeneity in Miscible Displacements in Vertical Cross Sections, in SPE/DOE Enhanced Oil Recovery Symposium*. 1990, Society of Petroleum Engineers: Tulsa, Oklahoma
331. Enick, R., et al., *Direct Thickeners for CO₂*. SPE, 2000. **59325**: p. 3-5.
332. Al Hinai, N.M., et al., *Experimental Evaluations of Polymeric Solubility and Thickeners for Supercritical CO₂ at High Temperatures for Enhanced Oil Recovery*. Energy & Fuels, 2018. **32**(2): p. 1600-1611.
333. Heller, J.P. and D.K. Dandge, *Topical Viscosity Control for Light Hydrocarbon Displacing Fluids in Petroleum Recovery and in Fracturing Fluids for Well Stimulation*, N.M.T.R. Foundation, Editor. 1986, U.S. Patent 4607696A
334. Saeedi, A., et al., *Multiphase Flow Behaviour during CO₂ Geo-Sequestration: Emphasis on the Effect of Cyclic CO₂-Brine Flooding*. Journal of Petroleum Science and Engineering, 2011. **79**(3-4): p. 65-85.
335. Bourdet, J., et al., *Evidence for a Palaeo-Oil Column and Alteration of Residual oil in a Gas-Condensate Field: Integrated Oil Inclusion and Experimental Results*. Geochimica et Cosmochimica Acta, 2014. **142**: p. 362-385.
336. Dehaghani, A.H.S. and M.H. Badizad, *Experimental Study of Iranian Heavy Crude Oil Viscosity Reduction by Diluting with Heptane, Methanol, Toluene, Gas Condensate and Naphtha*. Petroleum, 2016. **2**(4): p. 415-424.
337. Golkari, A. and M. Riazi, *Experimental Investigation of Miscibility Conditions of Dead and Live Asphaltenic Crude Oil-CO₂ Systems*. Journal of Petroleum Exploration and Production Technology, 2017. **7**(2): p. 597-609.
338. Jüttner, I., *Oil Displacement in Miscible Condition*. Rudarsko-Geolosko-Naftni Zbornik, 1997. **9**(1): p. 63.
339. Cobanoglu, M., et al. *Improving Ultimate Recovery of Tight Sour Oil Field by Miscible Gas Injection*. in *SPE EOR Conference at Oil and Gas West Asia*. Muscat, Oman.
340. Kioupis, L.I. and E.J. Maginn, *Molecular Simulation of Poly- α -Olefin Synthetic Lubricants: Impact of Molecular Architecture on Performance Properties*. The Journal of Physical Chemistry B, 1999. **103**(49): p. 10781-10790.
341. Kioupis, L.I. and E.J. Maginn, *Impact of Molecular Architecture on the High-Pressure Rheology of Hydrocarbon Fluids*. The Journal of Physical Chemistry B, 2000. **104**(32): p. 7774-7783.
342. Sun, B., et al., *Molecular Simulation Aided Design of Copolymer Thickeners for Supercritical CO₂ as non-Aqueous Tracturing Fluid*. Journal of CO₂ Utilization, 2018. **28**: p. 107-116.
343. Xue, P., et al., *Molecular Dynamics Simulation of Thickening Mechanism of Supercritical CO₂ Thickener*. Chemical Physics Letters, 2018. **706**: p. 658-664.
344. Gu, Y., S. Zhang, and Y. She, *Effects of Polymers as Direct CO₂ Thickeners on the Mutual Interactions between a Light Crude Oil and CO₂*. Journal of Polymer Research, 2013. **20**(2): p. 61.
345. Rao, D.N. and J.I. Lee, *Determination of Gas-Oil Miscibility Conditions by Interfacial Tension Measurements*. Journal of Colloid and Interface Science, 2003. **262**(2): p. 474-482.
346. Cheng, P., et al., *Automation of Axisymmetric Drop Shape Analysis for Measurements of Interfacial Tensions and Contact Angles*. Colloids and Surfaces, 1990. **43**(2): p. 151-167.
347. Rao, D.N., *A New Technique of Vanishing Interfacial Tension for Miscibility Determination*. Fluid Phase Equilibria, 1997. **139**(1): p. 311-324.

348. Charlet, G., R. Ducasse, and G. Delmas, *Thermodynamic Properties of Polyolefin Solutions at High Temperature: 2. Lower Critical Solubility Temperatures for Polybutene-1, Polypentene-1 and Poly (4-methylpentene-1) in Hydrocarbon Solvents and Determination of the Polymer-Solvent Interaction Parameter for PBI and one Ethylene-Propylene Copolymer*. *Polymer*, 1981. **22**(9): p. 1190-1198.
349. Kemmere, M., et al., *A novel Process for the Catalytic Polymerization of Olefins in Supercritical Carbon Dioxide*. *Chemical engineering science*, 2001. **56**(13): p. 4197-4204.
350. Cao, M. and Y. Gu, *Physicochemical Characterization of Produced Oils and Gases in Immiscible and Miscible CO₂ Flooding Processes*. *Energy & Fuels*, 2013. **27**(1): p. 440-453.
351. Yang, Z., et al., *Interfacial Tension of CO₂ and Crude Oils Under High Pressure and Temperature*. *Colloids and Surfaces A: Physicochemical and Engineering Aspects*, 2015. **482**: p. 611-616.
352. Yang, Z., et al., *Dispersion Property of CO₂ in Oil. 1. Volume Expansion of CO₂ + Alkane at near Critical and Supercritical Condition of CO₂*. *Journal of Chemical & Engineering Data*, 2012. **57**(3): p. 882-889.
353. King Jr, A.D. and C. Coan, *Solubility of Water in Compressed Carbon Dioxide, Nitrous Oxide, and Ethane. Evidence for Hydration of Carbon Dioxide and Nitrous Oxide in the Gas Phase*. *Journal of the American Chemical Society*, 1971. **93**(8): p. 1857-1862.
354. Zhang, J., et al., *Molecular Simulation Studies of Hydrocarbon and Carbon Dioxide Adsorption on Coal*. *Petroleum Science*, 2015. **12**(4): p. 692-704.
355. Sequeira, D.S., *Compositional Effects on Gas-Oil Interfacial Tension and Miscibility at Reservoir Conditions*. 2006, Louisiana State University and Agricultural and Mechanical College.
356. Honarvar, B., et al., *Experimental Investigation of Interfacial Tension Measurement and Oil Recovery by Carbonated Water Injection: A Case Study Using Core Samples from an Iranian Carbonate Oil Reservoir*. *Energy & Fuels*, 2017. **31**(3): p. 2740-2748.
357. Hensen, C. and H.S. Parameters, *A user's Handbook*. 2007: CRC Press.
358. Verdier, S. and S.I. Andersen, *Internal Pressure and Solubility Parameter as a Function of Pressure*. *Fluid Phase Equilibria*, 2005. **231**(2): p. 125-137.
359. CROW. *Polymer Properties Database*. 2018 May 7, 2018 [cited 2018 July 30th, 2018]; Available from: <https://polymerdatabase.com/home.html>.
360. Mohammadi, S., S.A. Mousavi-Dehghani, and M. Dinmohammad, *A new Approach for Quality Control of Reservoir Fluid Composition Data using Live Oil Solubility Parameter*. *Journal of Molecular Liquids*, 2016. **223**: p. 943-954.
361. Hutchenson, K.W., A.M. Scurto, and B. Subramaniam, *Gas-Expanded Liquids and Near-Critical Media*. ACS Symposium Series. Vol. 1006. 2009: American Chemical Society. 398.
362. Scurto, A.M., K. Hutchenson, and B. Subramaniam, *Gas-Expanded Liquids: Fundamentals and Applications*, in *Gas-Expanded Liquids and Near-Critical Media*. 2009, American Chemical Society. p. 3-37.
363. Parhi, R. and P. Suresh, *Supercritical Fluid Technology: a Review*. *Journal of Advanced Pharmaceutical Science and Technology*, 2013. **1**(1): p. 13.
364. Kazarian, S., *Polymer Processing with Supercritical Fluids*. *Polymer science series CC/C of vysokomolekuliarnye soedineniia*, 2000. **42**(1): p. 78-101.
365. Sauceau, M., et al., *New Challenges in Polymer Foaming: A Review of Extrusion Processes Assisted by Supercritical Carbon Dioxide*. *Progress in Polymer Science*, 2011. **36**(6): p. 749-766.
366. Shi, W., N.S. Siefert, and B.D. Morreale, *Molecular Simulations of CO₂, H₂, H₂O, and H₂S Gas Absorption into Hydrophobic Poly (dimethylsiloxane)(PDMS) Solvent: Solubility and Surface Tension*. *The Journal of Physical Chemistry C*, 2015. **119**(33): p. 19253-19265.
367. Makrodimitri, Z.A., R. Dohrn, and I.G. Economou, *Atomistic Simulation of Poly (DimethylSiloxane): Force Field Development, Structure, and Thermodynamic Properties of Polymer Melt and Solubility of n-Alkanes, n-Perfluoroalkanes, and Noble and Light Gases*. *Macromolecules*, 2007. **40**(5): p. 1720-1729.
368. Shah, V., B. Hardy, and S. Stern, *Solubility of Carbon Dioxide, Methane, and Propane in Silicone Polymers: Effect of Polymer Side Chains*. *Journal of Polymer Science Part B: Polymer Physics*, 1986. **24**(9): p. 2033-2047.
369. Singh, R., et al., *Fly Ash Nanoparticle-Stabilized CO₂-in-Water Foams for Gas Mobility Control Applications*, in *SPE Annual Technical Conference and Exhibition*. 2015, Society of Petroleum Engineers: Houston, Texas, USA. p. 13.

370. Aroonsri, A., et al., *Conditions for Generating Nanoparticle-Stabilized CO₂ Foams in Fracture and Matrix Flow*, in *SPE Annual Technical Conference and Exhibition*. 2013, Society of Petroleum Engineers: New Orleans, Louisiana, USA. p. 19.
371. Ayirala, S.C. and D.N. Rao, *Solubility, Miscibility and Their Relation to Interfacial Tension in Ternary Liquid Systems*. Fluid phase equilibria, 2006. **249**(1-2): p. 82-91.
372. I. Prigogine, P.D., *Advances in Chemical Physics*. Vol. Volume 1. 1958, University of Brussels, Brussels, Belgium.
373. Huggins, M.L., *The Solubility of Nonelectrolytes*. By Joel H. Hildebrand and Robert S. Scott. The Journal of Physical Chemistry, 1951. **55**(4): p. 619-620.
374. Hildebrand, J.H. and R.L. Scott, *Regular Solutions; International Series of Chemistry*. 1962: Prentice Hall, Englewood Cliffs, New Jersey.
375. Langevin, D. and J. Meunier, *Interfacial Tension: Theory and Experiment*, in *Micelles, Membranes, Microemulsions, and Monolayers*. 1994, Springer. p. 485-519.